UNIVERSITAT POLITÈCNICA DE VALÈNCIA

INSTITUTO UNIVERSITARIO DE INGENIERÍA DE ALIMENTOS PARA EL DESARROLLO

Different strategies to improve the functionality of biodegradable films based on starch and other polymers

DOCTORAL THESIS

Presented by**:**

Amalia I. Cano Embuena

Supervisors:

Chelo Gónzalez Martínez

Amparo Chiralt Boix

Maite Cháfer Nácher

Valencia, September 2015

DEPARTAMENTO DE TECNOLOGÍA DE ALIMENTOS

INSTITUTO UNIVERSITARIO DE INGENIERÍA DE ALIMENTOS PARA EL DESARROLLO

Dª. Chelo Gónzalez Martínez y Dª. Amparo Chiralt Boix, Catedráticas de Universidad y Dª. Maite Cháfer Nácher, profesora titular de Universidad, pertenecientes al Departamento de Tecnología de alimentos de la Universitat Politècnica de València.

CONSIDERAN: que la memoria titulada **"DIFFERENT STRATEGIES TO IMPROVE THE FUNCTIONALITY OF BIODEGRADABLE FILMS BASED ON STARCH AND OTHER POLYMERS"** que presenta **Dª. Amalia Isabel Cano Embuena** para aspirar al grado de Doctor por la Universitat Politècnica de València, reúne las condiciones adecuadas para constituir su tesis doctoral, por lo que **AUTORIZAN** a la interesada para su presentación.

Valencia, 1 de Septiembre de 2015

Fdo. Chelo González Martínez Fdo. Amparo Chiralt Boix Fdo. Maite Cháfer Nácher

Directora de Tesis Directora de Tesis Directora de Tesis

A toda mi familia,

Y en especial a Jorge,

Agradecimientos

A Amparo Chiralt por concederme la oportunidad de formar parte del grupo de “films”. Ha sido un placer poder trabajar junto a un referente internacional en el ámbito de la investigación como tú. Gracias por tus aportes científicos y técnicos, por tu paciencia y dedicación, y por permitirme aprender y trabajar a tu lado.

A Chelo González, tu apoyo durante estos cuatro años, la fuerza que me has transmitido para ir hacia delante, tus conocimientos científicos y las oportunidades que me has brindado para iniciarme en la investigación a nivel nacional e internacional son tan sólo algunas de las cosas que tengo que agradecerte. Gracias también por toda la confianza depositada en mí durante estos años y por el apoyo personal.

A Maite Cháfer por haberme introducido en el área de la investigación dándome la oportunidad de conocer al grupo de “films”. Tu apoyo profesional y personal y tu positividad frente a los problemas han sido de gran ayuda. Gracies!

Al Profesor José María Kenny de la Università degli Studi di Perugia (Italia) y a todo su grupo de investigación. Especialmente a la Dra. Elena Fortunati y a Francesca Luzzi por su ayuda y colaboración durante y después de la estancia. Grazie mille!

Thanks to Dr. Kristberg Kristbersoon for giving me the opportunity to stay at the Innovation Center of Iceland. I also want to thank my colleague Ragnhildur Einarsdóttir for all the help received during those 3 months.

A todos los compañeros del laboratorio con los que he coincidido, vuestros ánimos y consejos han hecho que estos cuatro años hayan sido una gran experiencia. Mª José, Jeannine, Rodrigo, Justine y Raquel, de todos vosotros me llevo algún momento especial. Marco, Marta y María, gracias por ayudarme a aprender a enseñar. Olga, Anna y Emma, gracias por vuestras reflexiones y por ayudarme a desconectar cuando más lo necesitaba. Alberto, gracias por tus explicaciones sobre el mundo de los envases y por

tu colaboración en la Tesis. Clara, gracias por estar siempre a punto para ayudarme y hacerme la vida más fácil con tus consejos. Neus y Ángela, me habéis ayudado tanto con los problemas a nivel experimental como personal, gracias por vuestro apoyo.

A las compañeras de los laboratorios vecinos por la ayudada brindada para poder llevar a cabo la Tesis. En especial a Susana y a Ángela, habéis sido grandes compañeras y mejor amigas, gracias por vuestra confianza, vuestros consejos y por las largas conversaciones por Skype durante las estancias, ¡nunca podré olvidarlas!

A todos mis amigos, Bárbara, Silvia, Jordi, Susana, Ampy, Javi, Ruth, Carol, Gonzalo, Laury, Jose, Chelo, Carlos, Gloria, Marieta, Víctor, María, Paquito y en especial a Lorena, vuestro apoyo continuo y confianza en mí ha sido una de las fuerzas impulsoras de esta Tesis.

A mis dos familias, sin vuestro apoyo esta Tesis no habría sido posible. En especial a Arturo, Mónica, José, Susana, Genaro, Merche y Arturo, nunca habéis puesto objeción a mis decisiones, apoyándome en todas y cada una de ellas. Gracias por la comprensión que habéis tenido conmigo cuando los nervios me han pasado alguna mala jugada.

A mis pequeños, Diego, Josep, Rubén y Amalia, vuestra inocencia y alegría han sido dos cosas muy importantes para poder coger fuerzas para realizar un buen trabajo, os quiero.

A mi madre, por empujarme siempre hacia los sueños, por hacerme creer que puedo y sobre todo por escucharme. Tus esfuerzos para aceptar todas las decisiones, respetar y compartir las idas y venidas que algún disgusto te han costado y acompañarme durante toda esta andadura han sido un pilar fundamental para mí.

A Jorge, su confianza, su apoyo incondicional, sus ánimos, sus reflexiones y su participación activa en este gran proyecto desde que lo inicié, hoy dan su fruto. Sabes que muchas veces te he dicho que esta Tesis ha sido cosa de dos porque sin tu

paciencia, sin el equilibrio y la estabilidad que me transmites y la felicidad que me aportas no hubiera llegado hasta el final. Gracias y mil gracias!

Abstract

In the present Doctoral Thesis, different strategies to improve functional properties of starch films for food packaging applications were analysed: study of the effect of amylose:amylopectin ratio, blend with other polymers poly(vinyl alcohol) (PVA), and incorporation of different fillers (rice bran and cellulose nanocrystals-CNCs) and antimicrobial agents (neem oil-N, oregano essential oil-O and silver nanoparticles-AgNPs). Likewise, a biodegradation study of the films as affected by antimicrobials was carried out.

Among different starches with distinct amylose:amylopectin ratio, pea starch was selected with higher values of this ratio. The high content of amylose gave rise to stiffer and more resistant to fracture films, with lower oxygen permeability, which decreased during storage. Pea starch-PVA (S-PVA) blend films represented a good strategy to improve film properties without a notable increase in cost. The PVA addition led to films which were less water soluble and not as sensitive to water sorption, more extensible and resistant than neat starch films, while they maintained the high oxygen barrier and provided stability to the matrix during ageing. In this sense, S-PVA ratios near to 1:1 are recommendable.

When rice bran with the smallest particle size was used as filler, it improved the elastic modulus of the films, but reduced the film stretchability and barrier properties, due to the enhancement of the water binding capacity and the introduction of discontinuities in the matrix. Incorporation of CNCs into S-PVA films, as a reinforcing material, enhanced phase separation of polymers, did not imply changes in water vapour barrier of the films but improved the film mechanical performance: they became stiffer and more stretchable, while crystallization of PVA was partially inhibited.

Silver loaded S-PVA films exhibited antimicrobial activity against the fungi (*Aspergillus niger* and *Penicillium expansum*) and bacteria (*Listeria innocua* and

Escherichia coli) genera, depending on the silver concentration. Silver nanoparticles provoked notable changes in the film colour and transparency but no relevant changes in the other physical properties. Silver was completely delivered to aqueous simulants within the firsts 60 minutes of contact, but the film release capacity drastically decreased in the non-polar simulant, where the overall migration limit for food contact packaging materials (60 mg/Kg simulant) was accomplished. So, the use of the developed films as food packaging materials should be restricted to fat-rich foodstuffs.

The incorporation of oregano essential oil (O), as antimicrobial agents, into the S-PVA matrix gave rise to active films against bacteria and fungi, whereas films containing neem oil (N) were not effective. Higher O concentration in the films was required to observe antifungal effect with respect to the antibacterial activity. Oils did not notably affect water sensitivity and water barrier properties of the films, but at high ratio, oils implied weaker film networks, affecting their mechanical performance.

Blend of starch with PVA significantly improved PVA biodegradation and disintegration behaviour. Incorporation of silver species to S-PVA films slowed down their biodegradation kinetics while increased their degradation ratio. However, no significant effect of O was observed on the biodegradability indices despite the antimicrobial activity detected for this oil. N even promoted biodegradation of S-PVA films.

Finally, a food application of biopolymer coatings was studied, using chitosan and essential oils (oregano or rosemary) to prevent weight loss and fungal development of semi-hard goat's milk cheeses. Coating were highly effective at reducing fungal growth and cheese weight loss while slightly reduced lipolytic and proteolytic activities in the cheese. Sensory evaluation revealed that the cheeses double coated with chitosan-oregano oil were the best evaluated in terms of aroma and flavour.

Resumen

En la presente Tesis Doctoral, se han analizado diferentes estrategias para mejorar las propiedades funcionales de películas de almidón para aplicaciones de envasado de alimentos: el estudio del ratio amilosa:amilopectina, mezclas con otros polímeros (alcohol de polivinilo-PVA), y la incorporación de diferentes refuerzos (salvado de arroz y nanocristales de celulose-CNCs) y agentes antimicrobianos (aceite de neem-N, aceite esencial de orégano-O y nanopartículas de plata-AgNPs). También se llevó a cabo un estudio de biodegradación de las películas para observar el efecto causado por los diferentes antimicrobianos.

Entre los diferentes almidones con distinto ratio amilosa:amilopectina, se seleccionó el almidón de guisante con altos valores de amilosa. El alto contenido en amilosa dio lugar a películas más rígidas y resistentes a la fractura, con baja permeabilidad al oxígeno, la cual disminuyó durante el almacenamiento. Las películas de mezcla de almidón-PVA (S-PVA) representaron una buena estrategia para mejorar las propiedades de las películas sin incrementar notablemente el precio. La adición de PVA dio lugar a películas menos solubles en agua, menos sensibles a la absorción de esta y más extensible y resistentes que las de almidón puro, mientras mantuvieron alta barrera al oxígeno y dieron estabilidad a la matriz durante el envejecimiento. En este sentido, son recomendables los ratios de S-PVA cercanos a 1:1.

Cuando se utilizó el salvado de arroz con menor tamaño de partícula como material de relleno, mejoró el modulo elástico de las películas, pero su extensibilidad y propiedades barrera empeoraron debido a una mejor capacidad de retención de agua y a la introducción de discontinuidades en la matriz. La incorporación de CNC-s en las películas de S-PVA, como material de refuerzo, incrementó la separación de fases de los polímeros, no implicó cambios en la permeabilidad al vapor de agua de las películas,

y mejoró las prestaciones mecánicas: las películas llegaron a ser más rígidas y extensibles, mientras que se inhibió parcialmente la cristalización del PVA.

Las películas de S-PVA con partículas de plata exhibieron actividad antimicrobiana contra dos géneros de hongos (*Asperguillus niger* y *Penicillium expansum*) y dos de bacterias (*Listeria innocua* y *Escherichia coli*), dependiendo de la concentración de plata incorporada. Las nanopartículas de plata provocaron cambios notables en el color de las películas así como en su transparencia, sin cambios relevantes en el resto de propiedades físicas. La plata fue completamente liberada en los primeros 60 minutos en contacto con simulantes acuosos, sin embargo la capacidad de liberación disminuyó drásticamente en simulantes no polares, donde se cumple el límite de migración global para materiales de envases destinados a entrar en contacto con alimentos (60 mg/Kg simulante). Por lo tanto, el uso de las películas desarrolladas como materiales para envasado de alimentos debe ser restringido a productos alimenticios ricos en grasas.

La incorporación de aceite esencial de orégano (O), como agente antimicrobiano en la matriz de S-PVA dio lugar a películas activas contra bacterias y hongos, mientras que las películas con aceite de neem (N) no fueron efectivas. Fueron necesarias concentraciones más altas de O en las películas para observar un efecto antifúngico respecto a la actividad bactericida. Los aceites no afectaron notablemente la sensibilidad al agua ni las propiedades barrera al agua de las películas, aunque la mayor proporción de aceite dio lugar a películas con una red más débil, afectando sus prestaciones mecánicas.

La mezcla de almidón con PVA mejoró significativamente el comportamiento de biodegradación y desintegración de las películas. La incorporación de partículas de plata a películas de S-PVA disminuyó su cinética de biodegradación mientras aumentó su ratio de degradación. Sin embargo, la adición de O no presentó un efecto significativo

en los índices de biodegradación a pesar de la actividad antimicrobiana detectada para estos aceites. El N incluso mejoró la biodegradación de las películas de S-PVA.

Finalmente, se realizó una aplicación de recubrimientos basados en biopolímeros, usando quitosano y aceites esenciales (orégano y romero) para evitar la pérdida de peso y el desarrollo de hongos en quesos de cabra semi-curados. Los recubrimientos fueron altamente efectivos en la reducción del crecimiento fúngico y la pérdida de peso de los quesos, mientras que la actividad lipolítica y proteolítica en los quesos ligeramente disminuyó. El análisis sensorial reveló que los quesos recubiertos dos veces con quitosano-aceite de orégano fueron los mejor evaluados en términos de aroma y sabor.

Resum

En la present Tesi Doctoral, s'han analitzat diferents estratègies per a millorar les propietats funcionals de pel·lícules de midó per a aplicacions d'envasat d'aliments: l'estudi de la ràtio amilosa:amilopectina, mescles amb altres polímers (alcohol polivinílic-PVA), i la incorporació de diferents reforços (segó d'arròs i nanocristalls de celulosa-CNCs) i agents antimicrobians (oli de neem-N, oli essencial d'orenga-O i nanopartícules de plata). També es va dur a terme un estudi de biodegradació de les pel·lícules per observar l'efecte causat pels diferents antimicrobians.

Entre els diferents midons amb distint ràtio amilosa:amilopectina, es va seleccionar el midó de pèsol amb alts valors d'amilosa. L'alt contingut en amilosa va donar lloc a pel·lícules més rígides i resistents a la fractura, amb baixa permeabilitat a l'oxigen, la qual va disminuir durant l'emmagatzemament. Les pel·lícules de mescla de S-PVA van representar una bona estratègia per a millorar les propietats de les pel·lícules sense incrementar notablement el preu. L'addició de PVA va donar lloc a pel·lícules menys solubles en aigua, menys sensibles a l'absorció d'aquesta i més extensible i resistents que les de midó pur. A més van mantenir l'alta barrera a l'oxigen i van donar estabilitat a la matriu durant l'envelliment. En aquest sentit, són recomanables les ràtios de midó-PVA pròxims a 1:1.

Quan es va utilitzar el segó d'arròs amb menor tamany de partícula com a material de farciment, va millorar el mòdul elàstic de les pel·lícules, però la seua extensibilitat i propietats barrera van empitjorar, a causa d'una millor capacitat de retenció d'aigua i a la introducció de discontinuïtats en la matriu. La incorporació de CNCs en les pel·lícules de S-PVA, com a material de reforç, va incrementar la separació de fases dels polímers, sense implicar canvis en la permeabilitat al vapor d'aigua de les pel·lícules, però millorant les prestacions mecàniques: les pel·lícules van arribar a ser més rígides i extensibles, al mateix temps que es va inhibir parcialment la cristal·lització del PVA.

Les pel·lícules de S-PVA amb partícules de plata van exhibir activitat antimicrobiana front a dos gèneres de fongs (*Asperguillusníger* i *Penicillium expansum*) i dos de bacteris (*Listeria innòcua* i *Escherichia colli*), depenent de la concentració de plata incorporada. Les nanopartícules de plata van provocar canvis notables en el color de les pel·lícules així com en la seua transparència, sense canvis rellevants en la resta de propietats físiques. La plata va ser completament alliberada en els primers 60 minuts en contacte amb simulants aquosos, però la capacitat d'alliberament va disminuir dràsticament en simulants no polars, on es complix el límit de migració global per a materials d'envasos destinats a entrar en contacte amb aliments (60 mg/Kg simulant). Per tant, l'ús de les pel·lícules desenvolupades com a materials per a l'envasat d'aliments ha de ser restringit a productes alimentaris rics en greixos.

La incorporació d'oli essencial d'orenga (O), com a agent antimicrobià en la matriu de S-PVA va donar lloc a pel·lícules actives front a bacteris i fongs. Pel contrari les pel·lícules amb oli de neem (N) no van ser efectives. Van ser necessàries concentracions més elevades d'O en les pel·lícules per a observar un efecte antifúngic respecte a l'activitat bactericida. Els olis no van afectar notablement la sensibilitat a l'aigua ni les propietats barrera a l'aigua de les pel·lícules, però la major proporció d'oli va donar lloc a pel·lícules amb una xarxa més dèbil, afectant les seues prestacions mecàniques.

La mescla de midó amb PVA va millorar significativament el comportament de biodegradació i desintegració. La incorporació de partícules de plata a pel·lícules de S-PVA va disminuir la seua cinètica de biodegradació mentre que va augmentar la seua ràtio de degradació. No obstant això, l'addició d'O no va presentar un efecte significatiu en els índexs de biodegradació a pesar de l'activitat antimicrobiana detectada per a aquests olis. L'N fins i tot va millorar la biodegradació de les pel·lícules de S-PVA.

Finalment, es va realitzar una aplicació de recobriments basats en biopolímers, fent ús de quistosà i olis essencials (orenga i romer) per evitar la pèrdua de pes i el desenvolupament de fongs en formatges de cabra semi-curats. Els recobriments van ser altament efectius en la reducció del creixement fúngic i la pèrdua de pes dels formatges. L'activitat lipolítica i proteolítica en els formatges va disminuir suaument. L'anàlisi sensorial va revelar que els formatges recoberts dues vegades amb quitosà-oli d'orenga van ser els millor avaluats en termes d'aroma i sabor.

Preface

Dissertation Outline

The present Doctoral Thesis is structured in five sections as is highlighted in Figure A. The INTRODUCTION section focuses on the problems associated with biopolymer-based films and the strategies that can be used to overcome them. The OBJECTIVES section presents the general and specific objectives of the Thesis. The CHAPTERS section consists of four chapters, which include the obtained results, presented as a collection of different scientific publications. The GENERAL DISCUSSION section consists of a global discussion about the results obtained in the different chapters. Finally, the most important CONCLUSIONS are compiled in the last section.

I. INTRODUCTION	
II. OBJECTIVES	
III. CHAPTERS	**Chapter I.** Effect of amylose:amylopectin ratio and rice bran addition on starch film properties. **Chapter II.** Study of poly(vinyl alcohol) (PVA)-starch blends. Effect of nano-reinforcements (CNCs). **Chapter III.** Development of starch-PVA active films, containing $AgNO_3$ or essential oils. Effect of antimicrobials on film biodegradability. **Chapter IV.** Active films for fresh cheese preservation.
IV. GENERAL DISCUSSION	
V. CONCLUSIONS	

Figure A. Structure of the present Doctoral Thesis.

It is well known that starch is a good alternative for the development of new food packaging materials because of its great ability to form coatings or edible films at low

cost. Under this premise, **Chapter I**, entitled *Effect of amylose:amylopectin ratio and rice bran addition on starch film properties,* studies the influence of using three different starches (pea, cassava and potato) on the film properties. In the chapter, the amylose:amylopectin ratio of the three starches and the microstructural, mechanical, barrier and optical properties after two storage times of the starch-based films, obtained by casting, are evaluated. Furthermore, it discusses the addition of rice bran of two different particle sizes as a filler material. To this end, the particle sizes and composition of the bran, together with the microstructural, barrier, optical and mechanical properties of composite films are also evaluated.

This study allows us to select the starch matrix which presented the best physical properties and greatest stability over the period of time in question. Thus, pea starch was selected as a film matrix to be used in the rest of the studies of the present Thesis. The addition of bran rice was not further considered because of the scarce improvement of the film's mechanical properties. The use of smaller bran size particles gave better results.

In order to improve the poor barrier and mechanical properties of pure pea starch based films and the changes caused by the ageing, different strategies were considered in **Chapter II**, entitled *Study of poly(vinyl alcohol) (PVA)-starch blends. Effect of nano-reinforcements*. The first strategy was the blending of pure starch with another biopolymer. In spite of its highly hydrophilic nature, PVA was selected because of its low costant biodegradability as well as its adequate mechanical and barrier properties. Firstly, the suitability and compatibility of the blend starch-PVA was studied through the evaluation of their physical properties, including the solubility, barrier, optical and mechanical properties. The positive results obtained encourage us to carry out further analyses in order to optimize the starch:PVA ratio in the blend by means of the evaluation of the microstructural, thermal and physical properties of blend films after two storage

times. From this study, the films incorporating PVA into the starch in a ratio of 1:1 were chosen, where a proper balance was obtained between the functionality and cost of the starch films. Afterwards, the incorporation of nanomaterials as fillers into the starch-PVA film was considered. In this sense, cellulose nanocrystals (CNC) have been reported to be good reinforcing materials. The effect of the incorporation of CNC on the microstructural, thermal and physical properties of starch-PVA blends was evaluated.

The use of natural substances in biopolymer films against food spoilage has been reported to be a good alternative means for developing active films with added value. **Chapter III**, entitled *Development of starch-PVA active films. Effect of antimicrobials on film biodegradability,* details the effect of incorporating different active substances into starch-PVA films in order to obtain active films for the purposes of extending the shelf-life of foodstuffs. In this chapter, three different studies have been included. The first describes a previous screening study among natural substances (Horsetails, Liquid smoke, Equinacea and Neem oil). The best antimicrobials were selected and films containing neem and oregano oils were characterized as to their physical properties and antimicrobial activity against *Listeria innocua* (Gram-positive), *Escherichia coli* (Gram-negative), *Aspergillus niger* and *Penicillium expansum*. In the second study, starch-PVA active films containing silver species were analysed as regards their silver kinetic release to food simulants, as well as their physical properties and antimicrobial power against the same fungus and bacteria genera commented on above. Finally, the current interest in obtaining biodegradable and compostable materials for food packaging is compiled in the third study, which focuses on the processes, of disintegration and biodegradability of the starch-PVA films as affected by the incorporation of the active substances. In this study, S-PVA films containing neem oil, oregano essential oil or silver nitrate were exposed under composting conditions in order to calculate the percentage of biodegradability of the films, as well as their percentage of disintegration.

Thermogravimetric analysis is also discussed, as is the biodegradation kinetics, modelled by applying Hill's model.

Finally, and taking into account the experience acquired from previous studies, a practical application of biopolymer-based films to the preservation of soft ripened cheeses was carried out. Nevertheless, starch and/or PVA coatings were not suitable to be applied to cheese due to the lack of affinity/compatibility between polymer and product surface. The coatings were very heterogeneous, in all likelihood due to the poor adherence between the film forming dispersion and the foodstuff. Thus, **Chapter IV**, entitled *Active films for fresh cheese preservation*, details the application of edible chitosan- essential oil films to cheese manufactured from goat´s milk as an alternative to the conventional preservation methods used in the cheese industry. Coated and uncoated cheeses are analysed in terms of the antifungal and the water vapour barrier effect of coatings during ripening. Likewise, the cheese's main quality parameters, such as weight loss, respiration rate, water activity, pH, content of free fatty acids and free aminoacids and sensory attributes, were evaluated.

DISSEMINATION OF RESULTS

The followed scientific articles published in international peer-reviewed journals were published during the development of this Doctoral Thesis:

- **Cano, A**., Jiménez, A., Cháfer, M., González, C., & Chiralt, A. (2014).Characterization of starch films with different amylose:amylopectin ratio. Effect of rice bran addition. *Carbohydrate Polymers*, 111, 543-555.
- **Cano, A**., Cháfer, M., Chiralt, A., & González-Martínez, C. (2015). Physical and microstructural properties of biodegradable films based on pea starch and PVA. *Journal of Food Engineering*, 167, 59-64.
- **Cano, A**., Fortunati, E., Cháfer, M., Kenny, J. M., Chiralt, A., & González-Martínez, C. (2015). Properties and ageing behaviour of pea starch films as affected by blend with poly(vinyl alcohol). *Food Hydrocolloids*, 48, 84-93.
- **Cano, A**., Fortunati, E., Cháfer, M., González-Martínez, C., Chiralt, A., & Kenny, J. M. (2015). Effect of cellulose nanocrystals on the properties of pea starch- poly(vinyl alcohol) blend films. *Journal of Materials and Science,* 50 (21), 6979-6992*.*

The results were also presented at international conferences:

- **Oral presentation** - **Cano, A**., Jiménez, A., Cháfer, M., González, C., & Chiralt, A. (2013). Rice Bran-filled biodegradable pea starch film. Inside Food Symposium, April, 9-13. Luvem-Belgium.
- **Oral presentation** - **Cano, A**., Jiménez, A., Cháfer, M., González, C., & Chiralt, A. (2014). Efecto de la incorporación de salvado de arroz en las propiedades físicas y microestructurales de films biodegradables basados en diferentes almidones. 9 Congreso Iberoamericano de Ingeniería de Alimentos, CIBIA, Janaury, 13-16. Valencia, Spain.

- **Poster** - **Cano, A**., Cháfer, M., Chiralt, M., Molina, P., Santamarina, P., Borrás, M., Beltran, M. C., Rosello, J., & González-Martínez, C. (2014). Aplicación de recubrimientos a base de quitosano y aceites esenciales en queso tronchón: efecto antifúngico y calidad sensorial. 9 Congreso Iberoamericano de Ingeniería de Alimentos, CIBIA, January, 13-16. Valencia, Spain.
- **Oral presentation** - **Cano, A**., Cháfer, M., Chiralt, M., & González-Martínez, C. (2014). Starch-PVA composite films: towards a new generation of biodegradable packaging material. 3rd International ISEKI_Food Conference, May, 21-23. Athens, Greece.
- **Poster** - **Cano, A**., Cháfer, M., Chiralt, M., Molina, P., Santamarina, P., Borrás, M., Beltran, M. C., Rosello, J., & González-Martínez, C. (2014). Antifungal activity and sensory acceptance of an edible coating based on chitosan and essential oils for cheese. 3rd International ISEKI_Food Conference, May, 21-23. Athens, Greece.
- **Poster** - **Cano, A**., Cháfer, M., Chiralt, M., & González-Martínez, C. (2014). Films compuestos de almidón-PVA: hacia una nueva generación de materiales de envases biodegradables. II Congreso Internacional de Innovación en Ingeniería, Ciencia y Tecnología de Alimentos (IICTA), May, 27-30. Medellin, Colombia.
- **Poster** - **Cano, A**., Fortunati, E., Cháfer, M., Kenny, J. M., Chiralt, A., & González-Martínez, C. (2014). Effect of cellulose nanocrystals addition on physical and microstructure properties of pea starch:PVA composite films. 1st Congress on Food Structure Design, October, 15-17. Porto, Portugal.
- **Poster** - **Cano, A**., Palanca, M., Cháfer, M., Chiralt, M., & González-Martínez, C. (2014). Efectividad antimicrobiana del aceite esencial de orégano y del aceite de neem incorporados en films biodegradabls a base de almidón y PVA. III International

Conference of Food Innovation (Innova), October, 20-23. Concordia, Entre ríos, Argentina.

- **Poster** - **Cano, A**., Cháfer, M., Chiralt, M., & González-Martínez, C. (2015). Efectividad antifúngica de films biodegradables que incorporan aceite esencial de orégano y aceite de neem. VIII Congreso CYTA/CESIA, April, 8-10. Badajoz, Spain.

PREDOCTORAL STAYS AT FOREIGN INSTITUTIONS

Two predoctoral stays were carried out during the development of this Doctoral Thesis at:

- Materials Engineering Centre, UdR INSTM, University of Perugia, (Terni, Italy). From August 2013 to November 2013 under the supervision of Dr. José.M. Kenny and Dr. Elena Fortunati.
- Innovation Center of Iceland – University of Iceland (Reykjavik, Iceland). From March 2015 to June 2015 under the supervision of Dr. Kristberg Kristbergsson.

List of Acronyms

AA: Antimicrobial

AFM: Atomic force microscopy

AgNPs: Silver nanoparticles

ASTM: American Society for Testing and Materials

a_w: Water activity

B: Biodegradation

BS: Burned-out solid

C: Coarse

C_{ab}*: Chroma

CFU: Colony Forming Units

CH: Chitosan

CNCs: Cellulose nanocrystals

CP: Continuous phase

D: Disintegration

$D_{3,2}$: Volume weighted mean diameter

$D_{4,3}$: Surface weighted mean diameter

d.b: dry basis

DM: Dry mass

DP: Dispersed phase

DSC: Differential scanning calorimeter

DTG: Thermal weigh loss derivate

E, %: Percentage of Elongation

E: Equinacea

EM: Elastic modulus

EO: Essential oils

EU: European Union

EVOH: Ethylene(vinyl alcohol) copolymer

F: Fine

FAA: Free aminoacids

FDA: Food and Drugs Administration

FESEM: Field emission scanning electron microscopy

FFA: Free fatty acids

FFD: Films forming dispersion

FT-IR: Fourier transform infrared spectroscopy

Gly: Glycerol

GRAS: Generally Recognized as Safe

h_{ab}*: Hue

HDPE: High Density Poly(ethylene)

HPMC: Hydroxypropilmethylcellulose

HS: Horsetail

L*: Luminosity

LDPE: Low Density Poly(ethylene)

LS: Liquid smoke

LSD: Least significant differences

MC: Moisture content

MCC: Microcrystalline cellulose

N: Neem oil

O: Oregano essential oil

OML: Overall migration limit

OP: Oxygen permeability

PA: Poly(amide)

PBS: Poly(buthylen succinate)

PBSA: Aliphatic copolyesters

PC: Poly(carbonate)

PCL: Poly(ε-caprolactone)

PDA: Potato dextrose agar

PDB: Potato dextrose broth

PE: Poly(ethylene)

PEA: Poly(ester amide)

PEF: Poly(ethylene furanoate)

PES: Poly(ethetersulfone)

PET: Poly(ethylene Terephthalate)

PHA: Poly(hydroxilalkanoates)

PHB: Poly(esters)

PLA: Poly(lactic acid)

PP: Poly(propylene)

PS: Poly(styrene)

PVA or PVOH: Poly(vinyl alcohol)

PVC: Poly(vinyl chloride)

QNM: Quantitative nanomechanics

R: Rosemary

RH: Relative humidity

RR: Respiration rate

SEM: Scanning electron microscopy

Sorb: Sorbitol

t: time

To: Onset temperature

Te: Endset temperature

Tf: Fusion temperature

Tg: Glass transition temperature

TG: Thermal weigh loss

TGA: Thermogravimetrical analysis

Ti: Internal transmittance

Tm: Melting temperature

Tmp: Main peak temperature

Tp: Peak temperature

TPS: Thermoplastic starch

Tr: Transmittance

TS: Tensile strength

TSA: Tryptone soy agar

TSB: Tryptone soy broth

UV: Ultraviolet

UV-VIS: Ultraviolet-visible spectroscopy

WVP: Water vapour permeability

YI: Yellow index

YM: Young modulus

ΔHm: Melting enthalpy

ΔHc: Crystallization enthalpy

ΔH_0: Melting enthalpy of a 100 % crystalline PVA

1W: 1 week

5W: 5 weeks

Justification for the work

Without doubt, plastics are the materials which are most widely used for food packaging purposes (among paper, paperboard, glass or metals) due to their easy application in both rigid and flexible forms. As it is possible to observe in Figure A, the most traditionally used plastics are polyethylene (PE), high density polyethylene (HDPE), polypropylene (PP), polystyrene (PS), polyethylene terephthalate (PET), polyvinyl chloride (PVC) and poly carbonate (PC) and they are selected depending on the final application: bottles, containers, films or coatings. These polymers are not biodegradable (able to disintegrate or degrade themselves), increasing the waste residues and, hence, negatively contributing to the sustainability of our environment. Recycling plays a very important role, but it is not possible to recycle the total amount of plastic waste produced.

Furthermore, one of the main problems in food packaging is the migration or delivery of different substances (the polymer itself or additives) from the package to the foodstuff. These substances should not provoke an unacceptable modification in the food composition. Indeed, the current European legislation established a global limit of migration as well as different specific limits for specific substances.

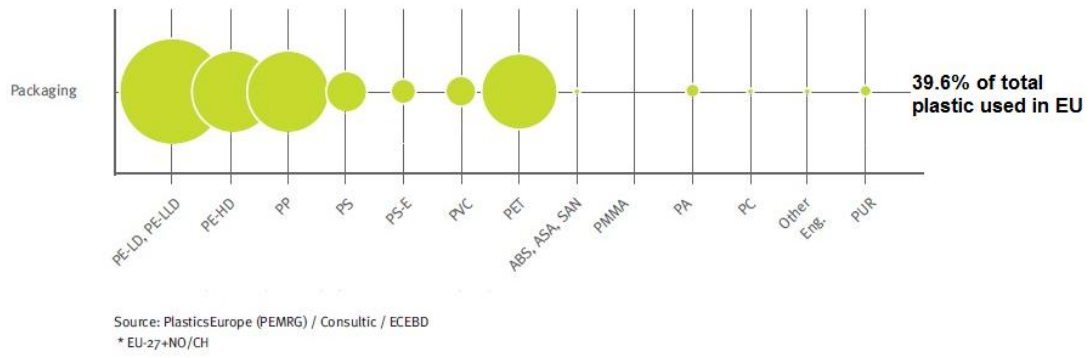

Figure A. Plastic materials used for food packaging in Europe, (Source: PlasticEurope, PEMRG, 2013).

It is a fact that current lifestyles and environmental problems have directly influenced consumer trends and food buying behaviour as well as food processing and packaging technologies. Indeed, consumers are more concerned than ever about environmental protection. Thus, there is ever greater demand for new coatings and food packaging materials to be developed in accordance with these current trends: healthier, free of synthetic chemical substances and sustainably manufactured.

Edible and biodegradable films could be used as an alternative to the conventional fossil-fuel-based plastics in the field of foodstuffs. Coatings or edible films also play an important role in food preservation, extending their shelf life, protecting them from physical and chemical degradation and microbial spoilage. Furthermore, different sustainable polymer materials may be combined in order to obtain a proper coating or biodegradable film with the required properties.

The term “bioplastics” includes two different groups of materials: biopolymers and biodegradable plastics (Figure B). The former are made from biobased resources, such as plants (starch or cellulose) or microbial fermentative processes (chitosan –CH- or polyhydroxialkanoates -PHAs-). Biobased polymers can also be produced by chemical modifications and, therefore, they are not necessarily biodegradable. On the other hand, biodegradable plastics may be obtained from both natural and fossil resources and are degraded by microorganisms in their natural environment. The products of these biodegradation processes are energy, biomass, water and carbon dioxide or methane, depending on the presence or absence of oxygen. If biodegradable plastics are degraded in accordance with standards for compostability, they may be labelled as compostable. Polyvinyl alcohol (PVA) or polycaprolactone (PCL) are examples of these.

Pure biodegradable plastics do not perform as conventional plastics. They usually have poor mechanical and barrier properties. These properties can be enhanced by using different strategies, such as blending different polymers, adding reinforcing

materials, using light and UV stabilizers, incorporating bioactive compounds and cross-linking agents, among others. In this sense, the present study focuses on the development of biodegradable films, mainly based on starch and its blends with other components, to produce proper polymeric matrices for food packaging and preservation, thus also helping to solve environmental problems caused by conventional plastics, using renewable source materials. Different components were incorporated, such as reinforcing materials and bioactive compounds, so as to improve both the film's physicochemical properties and functionality by extending the shelf-life of foods.

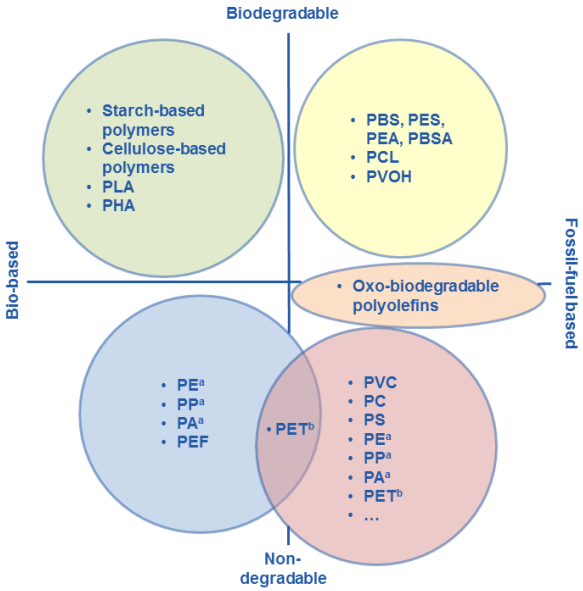

Figure B: Classification of bioplastics according to their origin and biodegradability (Source: Food Packaging Forum, 2014).

I. Introduction

Overall, Europe post-consumer waste plastic for 2010 was estimated at 24.7 million tons; 14.3 million tons (57.9 %) were recovered, 6 million tons were recycled and 8.3 million tons were burned for energy purposes. Nevertheless, 10.4 million tons (42.1 %) were discarded in landfills yet (Plastics Europe, 2012).

Most of the conventional plastics derived from petro-chemicals are non-biodegradable and remain in the environment for decades. In many cases, it is not possible to recover them and the plastics may block the pluvial water draining network and sewers, killing land and sea animals and polluting rivers, beaches and the land, especially the approximately eight million metric tons of waste plastic that enter the earth's ocean every year. Currently, the activities employed to handle the waste plastic include incineration and recycling. Nevertheless, these activities exhibit relevant drawbacks:

- The incineration capacity is not enough
- The gas emission generated during the incineration is highly polluting.
- There is a health crisis due to the saturation of the land and water
- Recycling plays a very important role, but it is not possible to recycle all the waste plastic produced.

Therefore, environmentally degradable plastics have attracted growing attention because of their potential use in the replacement of traditional non-degradable plastic items deriving from fossil fuel feed stocks. Indeed, bioplastics and biodegradable polymers have been the topic of a great deal of research for the last two decades. These polymers represent a significant contribution to sustainable development in view of the wider range of disposal options with a lower environmental impact (Avérous & Pollet, 2012). This is an important reason why the use of biopolymers is becoming more attractive for the purposes of developing new food packaging materials.

1. EDIBLE AND BIODEGRADABLE POLYMER MATRICES USED AS FOOD PACKAGING MATERIALS

There is a wide variety of biopolymers that can be used as packaging material. As commented on above, most of them are obtained from renewable materials (biomass) and others are fossil in origin and both materials can be degraded by microorganisms in their natural environment. Table 1 shows a classification of the biopolymers depending on their origin.

Table 1. Classification of biopolymers (Adapted from Avérous & Pollet, 2002; John & Thomas, 2008).

Biopolymers		
Bioresources	**From chemical synthesis**	**From microorganisms**
Protein: Zein, soy protein, casein, wheat gluten, collagen-gelatine, whey, etc. Carbohydrates: Starch, cellulose, pectin gums, carrageenan, natural fibres; chitin, chitosan, etc. Lipids: Wax, soy bean oil, sunflower oil, fatty acids, beeswax, polyols, etc.	From biomass: Poly (lactic acid) - PLA From petro-chemicals: Poly(ε-caprolactone) - PCL, Poly (vinyl alcohol) - PVA, Poly(butylene succinate) – PBS, Poly(glycodil acid) - PGA, Poly(ester amides) - PEA, Aliphatic copolyesters - PBSA	Polyesters Poly(hydroxyalkanoates) - (PHAs) Carbohydrates: Pullulan, Curdlan

The first family is polymers obtained from bio-resources, such as some proteins, carbohydrates and lipids including starch, cellulose or chitosan. The second family is chemically synthesized polymers, including both those derived from monomers obtained

from biomass, such as poly(lactic acid) (PLA), and those fossil in origin, such as polyvinyl alcohol (PVA) or poly(caprolactone) (PCL), among others. The third family includes biopolymers obtained from the fermentation of the microorganism, or from genetically modified plants, such as poly(hydroxyalkanoates) (PHA) or pullulan. Special emphasis will be placed on starch-based materials due to the ready availability of starch, its low cost and its ability to form films via different methods, including the usual themoprocessing employed in the plastics industry.

2. STARCH: SOURCES AND MAIN USES

Starch is one of the most abundant vegetable polysaccharide raw materials synthesized from plants: the starch content is around 30 to 80 % in cereals (maize, wheat, and rice), 25 to 50 % in legumes (pea and bean) and 60 to 90 % in tubers (potato and cassava). Likewise, the starch content reaches 70 % in the first ripening stage of some fruits, such as banana and mango (Espinosa, 2008).

In the EU, starch production has increased from 8.7 million tons in 2004 to 10 million tons in 2013 and it was mainly obtained from maize, wheat and potatoes (Figure 1), but also from pea, cassava, rice or sorghum, which are widely produced all over the world.

The European starch industry produces over six hundred products, from native starches to physically or chemically modified starches, through to liquid and solid sweeteners. The versatility of starch products is such that they are used as ingredients and functional supplements in a vast array of food, non-food, and feed applications.

The EU consumes 9 million tons of starch (excluding starch by-products, around 5 million tons), of which 61 % is used in food, 1 % in animal feed and 38 % in non- food applications, mainly paper making (29 %), pharma and chemicals (5 %) and other non-food applications (4 %) (Figure 2). Within the last group, the construction and chemical industries have recently increased the uses they put starch to, with particular focus on

detergent applications, fermentations for the production of amino acids, organic acids, enzymes and yeast and the production of surfactants, polyurethanes, resins and biodegradable plastics.

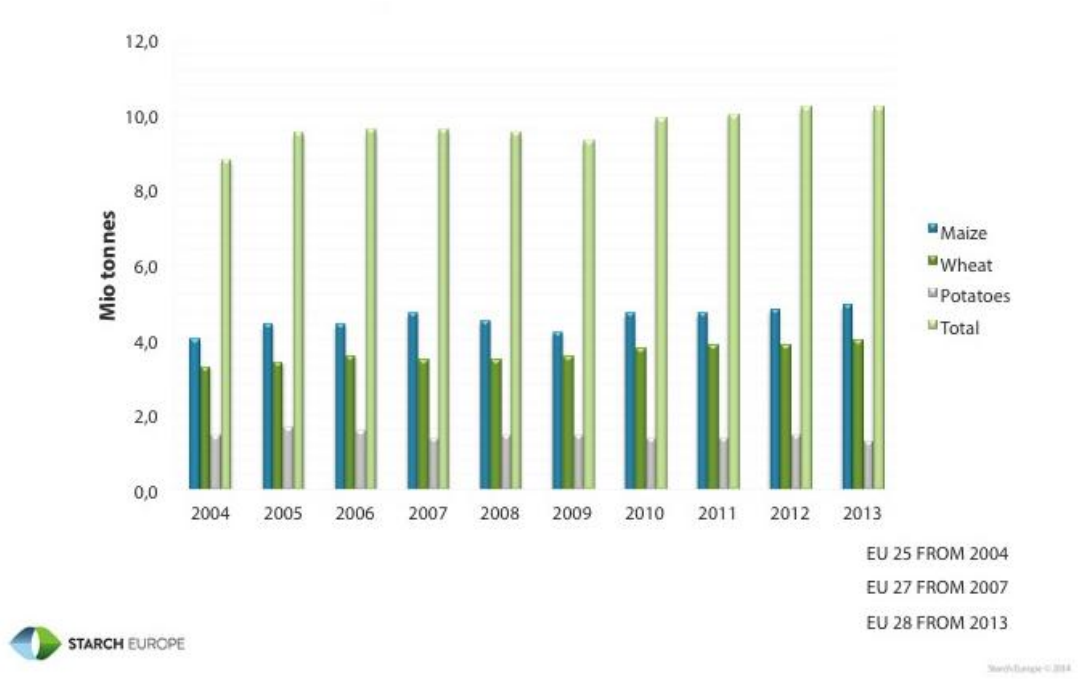

Figure 1. Starch production in the EU (Source: Starch Europe, 2013).

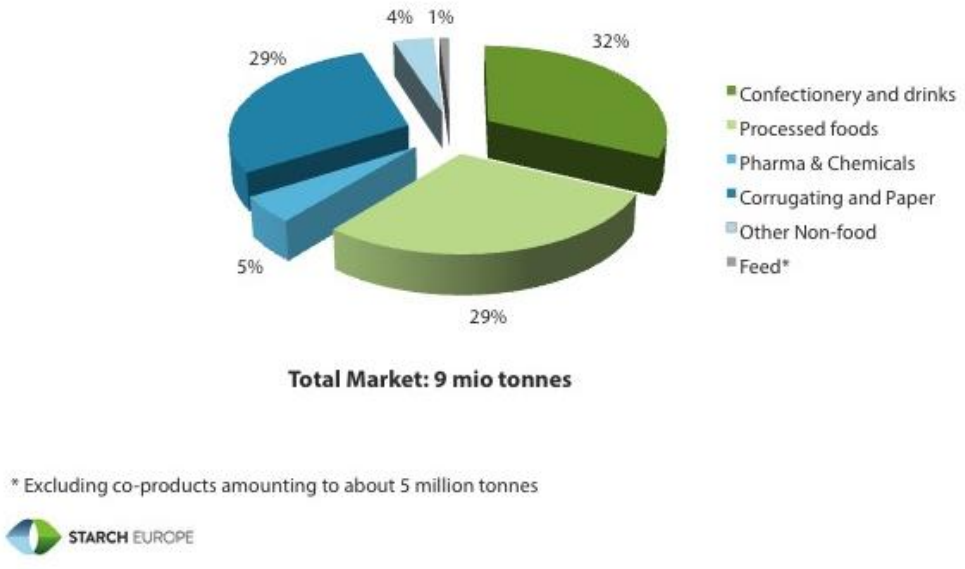

Figure 2. Main starch applications in the EU (Source: Starch Europe, 2013).

Starch has grown in importance as a packaging material due to the fact that it is a renewable resource, inexpensive and widely available (Lourdin *et al*., 1995). In this sense, some starch- based plastics are currently being used in the agricultural sector, in consumer goods and both rigid and flexible packaging, the latter being the most important (Figure 3).

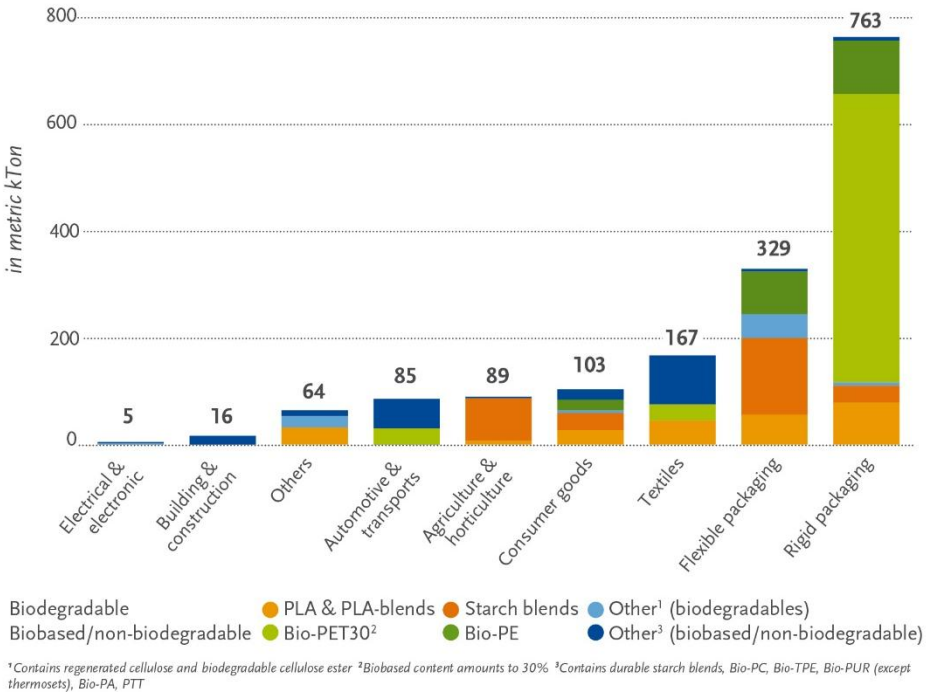

Figure 3. Use of bioplastics in different industrial sectors, 2013. (Source: European Bioplastics, Institute for Bioplastics and Biocomposites, nova-Institute, 2014).

2.1. Starch structure

Starch granules can vary in shape, size, structure, and chemical composition, depending on the origin of the starch (Smith, 2001). Chemically, native starch is composed of two main macromolecular components: amylose and amylopectin. The relative quantity of both polymers and their physical organization within the starch granule confer different physico-chemical and functional properties on the starch films.

Amylose is produced by the condensation of D-glucose by means of α-1,4 glucosidic links which establishes long linear chains with 200-2500 units with a molecular weight of 10^5-10^6 Dalton (Da) (Galliard & Bowler, 1987; Durrani & Donald, 1995). This α-1,4 anhydro-glucose polymer has the ability to acquire a helicoidally tridimensional conformation, in which each helical turn has six molecules of glucose. The interior of the helix is formed by hydrogen atoms which constitute the lipophilic part of the polymer, while hydroxyl groups are located on the outside of the helix. In general, there is about 25 % amylose in a starch granule. Amylose has an excellent film-forming ability, rendering strong, isotropic, odourless, tasteless, and colourless films (Campos *et al*., 2011; Jiménez *et al*., 2012a).

Amylopectin is a highly branched polymer consisting of short α-1,4 chains linked by α-1,6 glucosidic branching points occurring every 25–30 glucose units with very high molecular weight, reaching 10^9 Dalton (Galliard & Bowler, 1987; Durrani & Donald 1995; Liu, 2005). Amylopectin is the main component of the starch, around 75 % in common starches, some of which are exclusively composed of this polymer (waxy starches).

The amylose/amylopectin ratio depends on the source of the starch, as commented on above. For instance, wheat, corn, potato and pea starches contain 20–30 % amylose, while the content in waxy starches is under 5 %; in high-amylose starches, however, the content is as high as 50–80 % (Liu, 2005).

Physically, native starches take the form of granules where both amylose and amylopectin are structured by hydrogen bonding, containing semi-crystalline and amorphous structures with a degree of crystallinity of about 20–45 % (Whistler *et al*., 1984). These semi-crystalline native starch granules exhibit three X-ray diffraction patterns, called A, B and C. In the A-type crystal, the double helices are packed into an orthorhombic unit-cell in an anti-parallel manner, leading to almost hexagonal close-packing (Wu & Sarko, 1978a). In the B-type crystal, the double helices are also packed

in an anti-parallel manner, but into a hexagonal unit cell with two helices per cell leaving an open channel that is filled with water molecules (Wu & Sarko, 1978b). Although the packing of the B-type crystal is less dense than that of the A-type, the similarity in their packing modes suggest that A- and B-type crystals are inter-convertible (Wu & Sarko, 1978a). The C-type polymorph, which is actually a mixture of A- and B-type polymorphs (Bogracheva *et al*., 2002), is usually found in low-amylose starches.

It is well known that starch granules are not soluble in cold water due to the fact that strong hydrogen bonds hold the starch chains together (Jiménez *et al*., 2012a). However, when starch is heated in water, the crystalline structure is disrupted and water molecules interact with the hydroxyl groups of amylose and amylopectin, producing the partial solubilisation of starch (Hoover, 2001). Heating starch suspensions in an excess of water or of another solvent with the ability to form hydrogen bonds and at high temperatures (between 65 and 100 °C approximately, depending on the type of starch) provokes an irreversible gelatinization (de-structuration) process. This process is greatly affected by the kind of solvent and the starch/solvent ratio and it introduces irreversible changes in the starch granules, such as a lixiviation of amylose, the loss of crystallinity, water absorption, and the swelling of the granules (Zhong *et al*., 2009; Carvalho, 2008). According to Ratnayake & Jackson (2007), the gelatinization process initiates at low temperatures and continues until the granules are completely disrupted; there are three steps to the process:

1. The absorption of water by starch granules promotes an increase in starch polymer mobility in the amorphous regions.

2. Starch polymers in the amorphous regions rearrange, often forming new intermolecular interactions.

3. With increasing hydrothermal effects, the polymers become more mobile and lose their intermolecular interactions and overall granular structure.

At the end of the process, low molecular weight amylose chains are highly hydrated, including aggregates, which are also hydrated. After the gelatinization, there is a spontaneous recrystallization process, when the linear chains of amylose and amylopectin re-associate by hydrogen bonds.

2.2. Starch films: development and physical properties

Starch-based films can be obtained by following the wet or dry processes. For the wet or casting process, if native starch is used, the granules have to be disrupted previously through a gelatinization process in an excess of water media (>90 % w/w, Carvalho, 2008) in order to be able to form a film. This is the most commonly used method for obtaining edible films, regardless of the matrix used. The complete process could be divided into several steps: gelatinization and dispersion of the raw material, homogenization of the blends (in the case of emulsions or blends), casting on levelled petry or Teflon® dishes, and drying under controlled conditions (temperature and relative humidity). In this sense, Jiménez *et al*. (2012a) summarized different casting methods employed to obtain starch films and highlighted the differences between the methods used by different authors, concluding that the optimum conditions (temperature vs time) needed to induce a proper starch gelatinization was 95 ºC for 30 min, which have been subsequently used in several studies and also in the present doctoral thesis (Jiménez *et al*., 2012b-c-d, 2013a-b; 2014). Usually, the presence of plasticizers (such as glycerol) is also necessary in order to reduce the brittleness of the pure starch films obtained by casting.

In the dry process, thermoplastic starch is used (TPS) in order to be able to produce a continuous rubbery matrix by extrusion or melt blending and hot pressing. Carvalho (2008) described TPS as an amorphous or semi-crystalline material composed of gelatinized or de-structured starch containing one plasticizer, or a mixture of several.

Thus, TPS is obtained by processing a starch-plasticizer mixture in an extruder at temperatures of between 140-160 ºC, at high pressure and high shear. TPS can be processed thermally by sheet/film extrusion, foaming extrusion, injection moulding, compression moulding, and reactive extrusion (Jiménez *et al*., 2012a).

Starch is used to obtain films because of its ready availability and great ability to form an odourless, colourless and transparent polymer matrix (Vásconez *et al*., 2009) with very low oxygen permeability, which can protect food products by forming an oxygen barrier. It is also especially attractive because of its biodegradability and low cost (Han *et al*., 2006; Chen *et al*., 2008a; Lafargue *et al*., 2007). Nevertheless, starch films present some drawbacks as they present unstable mechanical properties due to the phenomenon of recrystallization and a relatively high water vapour permeability and poor water resistance (Lafargue *et al*., 2007; Chen *et al*., 2008a; Phan The *et al*., 2009; Wu *et al*., 2010).

In order to develop optimized starch films, several authors have studied the effect of starch composition (amylose/amylopectin ratio, presence of plasticizers), film formation conditions (drying temperature and air humidity) and structural factors (crystallinity and glass transition temperature) on the film properties. The main conclusions have been summarized below.

Similarly to starch granules, the structure of the starch films is often semi-crystalline, containing both amorphous and crystalline phases. The amorphous and crystalline phases are characterized by the glass transition temperature and the degree of crystallinity, respectively, both of which will affect the major properties of starch films. The partial crystalline structure of the starch-based film is mainly attributed to the spontaneous recrystallization of amylose molecules after gelatinization (Myllärinen *et al*., 2002; Forssell *et al*., 1999; Rindlav-Westling *et al*., 1998). During the ageing of the films, starch molecules are re-associated into more ordered structures by forming simple

juncture points and entanglements, helices, and crystal structures (Vázquez & Álvarez 2009). This process mainly occurs during film drying when the chain is still highly mobile due to the greater water content. Several authors (Rindlav-Westling *et al*., 1998) reported that drying at high relative humidity, or long drying times, greatly promote amylose crystallization, whereas amylopectin exhibited a retarded crystallization. This phenomenon of chain reorientation is one of the main drawbacks of using starch to obtain films due to the fact that the phenomenon takes place over time, greatly affecting the mechanical properties. In general, the increased crystallinity associated with the re-arrangement of the starch molecules throughout time (or ageing) provokes the development of stiffer and less flexible films, which becomes a mechanical problem.

Moreover, the crystallinity of starch films also depends on several factors, such as drying and storage conditions (temperature and relative humidity), as well as the plasticizer content (Rindlav *et al*., 1997). Plasticizers seem to retard and decrease the crystallinity (Talja *et al*., 2008) and to limit crystal growth due to the interactions with the polymer chains (Jiménez *et al*., 2012a)

Finally, the crystallization process of the starch-based matrix is promoted if the storage temperature is greater than the Tg, which in turn, decreases in line with the increase in the moisture content or the amount of plasticizer added (García *et al*., 2009).

This highlights the importance of carrying out ageing studies when working with starch- based films so as to ensure their functionality after processing. In fact, several works have focused on the development of time-stable starch-based films in recent years, usually blended with other materials, so as to avoid changes in the film´s physical properties throughout time.

Generally, plasticizers are added to the starch-based film-forming dispersions to decrease the attractive intermolecular forces generated among the film's polymer molecules, which can lead to the undesirable property of brittleness. Polyhydric alcohols

are the most commonly-used types of plasticizers, including propylene glycol, glycerin, sorbitol and other polyols. The incorporation of plasticizers into the starch matrix normally increases the distance that the film is stretched prior to the failure point. This parameter is well known as stretchability. Finally, the main drawback of incorporating plasticizers into starch-based films is the increase in the film´s permeability to water vapour, oxygen, and aroma compounds due to the fact that the hydroxyl-absorbed molecules (-OH) cause weakening and/or the disruption of the intra- and inter-molecular hydrogen bonds of starch (Rankin *et al*., 1958).

As regards the mechanical properties, it has been demonstrated that the mechanical response of the film depends on the moisture content of the film. In turn, the water sorption capacity of starch films was found to be influenced by the relative humidity and the storage temperature (Chang *et al*., 2000). In this sense, a nearly linear region in the range of intermediate humidity (20-70 %) suggests that a slight fluctuation in the environmental RH could cause a significant change in the water content of starch films, which could consequently affect the Tg, and the degree of crystallinity of the film (Bizot *et al*., 1997).

As expected, starch films are less resistant to $C0_2$ (polar molecule) than to O_2 (non-polar) because of the greater solubility of $C0_2$ in starch films (Arvanitoyannis *et al*., 1994). The addition of plasticizers and increase in the degree of crystallinity of starch films significantly reduces the $C0_2$ and 0_2 permeability (García *et al*., 2000; Liu, 2005; Talja *et al*., 2008) as crystallites can be considered to be impermeable to oxygen/gas transfer.

3. STRATEGIES TO IMPROVE THE FUNCTIONALITY OF BIOPOLYMER-BASED FILMS

The potential for the widespread use of starch-based films is enormous as they are totally biodegradable and also inexpensive when compared to other available

biodegradable polymers (Galliard, 1987; Reis *et al*., 1997; Yu *et al*., 2006). However, pure starch-based films present some limitations, such as ageing and poor water barrier, water resistance and mechanical properties, as commented on above.

These limitations have encouraged the search for new strategies as a means of improving the physical properties and stability throughout time. These strategies usually involve blending different biopolymers or the incorporation of particles in order to mitigate some of the current problems, or additives that confer an additional functionality which was not in the previous film. The modification of the initial polymer structure (by using plasma technologies for example) to modify its properties (to make it more hydrophobic, i.e.) have also been explored (Andrade *et al*., 2005).

The main strategies carried out by different authors in order to enhance the starch film properties are explained in detail below:

3.1. Blends of starch with different biopolymers

Many scientists have blended the starch with other polymers, in order to modulate the properties of the films, to limit the ageing process and/or to improve their functional properties. The blended polymers should be at least partially compatible in order to be able to obtain a proper continuous network during the coating or film formation.

Several authors have examined the films obtained by blending gelatinized starch with other polymers, in terms of their structural, physical and barrier properties. To summarize the information found, and taking into account the focus/interest of the present doctoral thesis, the biopolymers blended with starch have been divided into Poly(vinyl alcohol) and other polymers.

Poly(vinyl alcohol)

Poly(vinyl alcohol) (PVA or PVOH) is a synthetic water soluble and biodegradable polymer; which has been used since the early 1930s in a wide range of industrial,

commercial, medical, pharmaceutical and food applications, including resins, lacquers, surgical threads and food-contact applications (Barrera *et al.*, 2007; DeMerlis & Schoneker, 2003; Massey, 2004; Lin & Kub, 2008; Zhang *et al*., 2011).

PVA is a polymer made by the hydrolysis of polyvinyl acetate in the presence of an alkaline catalyst, its chemical and physical characteristics being dependent on its method of preparation. Varying the length of the initial vinyl acetate polymer and the degree of hydrolysis under alkaline or acidic conditions yields PVA products of differing molecular weights (20,000–400,000), solubility, flexibility, tensile strength and adhesiveness (Figure 4), among other things (Barrera *et al.*, 2007; DeMerlis & Schoneker, 2003; Tang & Alavi, 2011).

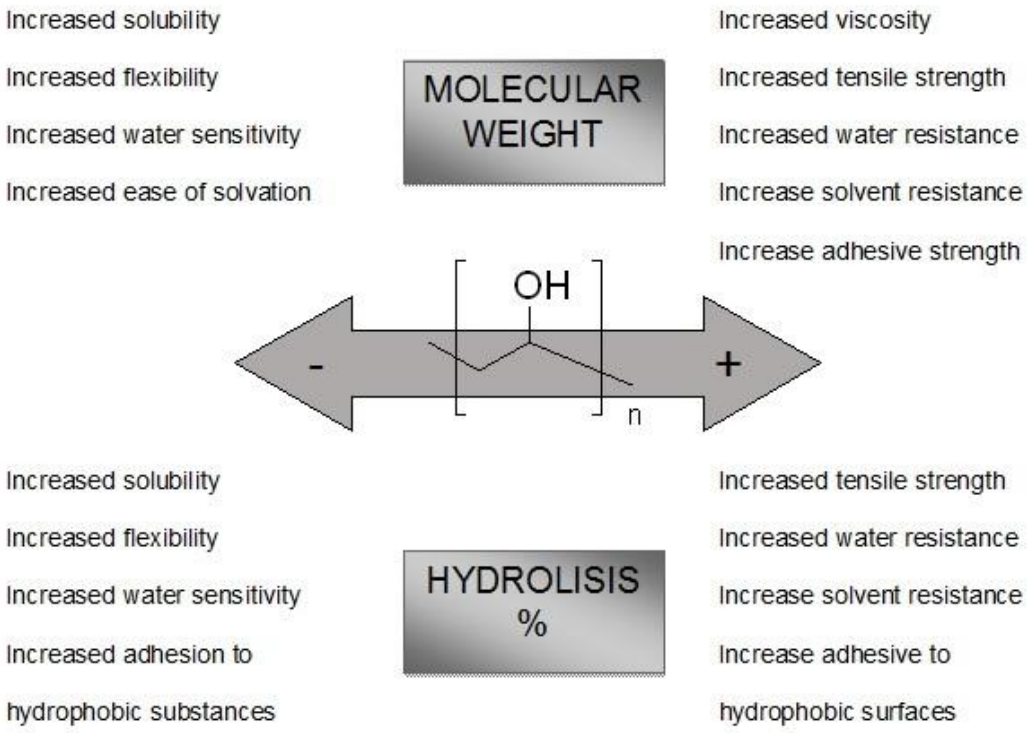

Figure 4. The chemical structure and the effect of molecular weight and level of hydrolysis on the physical properties of PVA. (Source: Modification of Tang & Alavi, 2011).

In general, PVA offers excellent hydrophilic, film-forming, emulsifying and adhesive properties. Films made from PVA can be obtained by casting or dry methods, including compression moulding, extrusion, blown and melting methods. However, their low degree of thermoplasticity at the melting temperature where decomposition occurs quickly makes it difficult to use the drying method. In order to improve the thermo-process capability of PVA (and similarly to the TPS), glycerol was adopted as a plasticizer to reduce the melting temperature and enhance the flow performance by reducing the intra- and intermolecular interaction of the hydroxyl groups of PVA (Lin & Kub, 2008).

On the other hand, PVA is water soluble, as commented on above, but it slowly dissolves in cool water. Temperatures of 90 to 95 °C are generally required for complete dissolution (Hu *et al*., 2013; Jiang *et al*., 2012; Luo *et al*., 2012). Water is the only practical solvent for PVA, but small amounts of alcohols can be added to water solutions without causing precipitation.

PVA films obtained by casting are transparent with high tensile strength and flexibility (in comparison with starch films for example), exhibiting excellent adhesive properties, chemical resistance and low permeability to oxygen (Chen *et al*., 2007; Massey, 2004; Zhang *et al*., 2011). As is common in hydrophilic films, its mechanical properties also depend on the moisture and plasticizer content.

One of the main advantages of PVA films is their biodegradability and biocompatibility with the environment. PVA films totally biodegrade when composted and, when solubilized, they are degraded and assimilated by a number of acclimated microorganisms in waste water streams. However, the degradation process of pure PVA films is slow, and the degradation rate is heavily dependent on the residual acetate groups (Corti *et al*., 2002; Pšeja *et al*., 2006; Ramaraj, 2006).

A simple way to enhance the biodegradability and to decrease the cost of PVA films is to prepare composites with a more biodegradable, cheaper and easily processable

material such as starch. In fact, Zhang *et al*. (2011) reported that PVA is well suited for composites with natural polymeric materials because both of them are highly polar.

In recent years, there has been a growing number of studies into starch-PVA blends due to the fact that this blend could become an alternative means of producing edible films or biodegradable packaging materials. So far, different studies involving starch-PVA films obtained via casting have been carried out with the following objectives:

- to evaluate the effect of the incorporation of native starch and pea-starch nanocrystals (Chen *et al*., 2008a),
- to study the plasticizing mechanism and effect of calcium chloride (Jiang *et al*., 2012) and sorbitol addition (Valencia *et al*., 2013),
- to analyse the effect of glycerol and urea addition on the morphology and thermal properties of ungelatinized and gelatinized starch films (Luo *et al*., 2012),
- to compare the physical properties of starch-PVA blends with and without crosslinking agents (Ramaraj *et al*., 2007; Zhou *et al*., 2009),
- to study the effect of citric acid on the structural properties and cytotoxicity of the blended films (Shi *et al*., 2008),
- to evaluate the compatibility of different blend ratios in terms of mechanical, optical and thermal properties (Siddaramaiah *et al*., 2004; Sreekumar *et al*., 2012),
- to analyse the addition of nano-size poly(methyl methacrylate-co-acrylamide) particles (S-D-Yoon *et al*., 2012)
- and to evaluate the incorporation of different additives, such as glycerol, succinic acid, malic acid and tartaric acid (S-D-Yoon *et al*., 2006).

Table 2 summarizes the main results obtained in the above mentioned studies. Clearly, both the starch-PVA ratio used and the presence of plasticizer affected the physical properties of the blend films. The film thickness significantly increased in line with the PVA content, which ranged between 0.1 and 1.5 mm. Furthermore, the melting point was greatly affected by the ratio of starch: PVA used in the blend, ranging from 168 to 230 ºC. In addition, films became significantly more transparent and mechanically more resistant when the content of PVA rose in the blend.

As regards the current legislation, different American Institutions (Joint FAO/WHO Expert Committee on Food Additives, US Food and Drug Administration) have approved the use of PVA as a coating, food packaging material, and as an indirect additive in products which are in contact with food. In Europe, the European Food Safety Authority (EFSA) authorized its use as a food additive (E1203) in 2005 (European Directive 2010/67/UE).

Table 2: Physical properties of Starch-PVA blends films obtained by csting technique.

Matrix	S:PVA	Plasticizer	WC	M Uptake	Thickness	Thermal properties	S	Optical properties	Mechanical properties	References
		(poly:plas)	(%d.b.)	(%)	(mm)	(ºC)	(%)	(%)	TS, YM (MPa) and E (%)	
(PE)S-PVA	1:1(8wt%) 5%:95%	Gly - 4:1		75±5 (98%RH)	0.2			Tr (800nm) = 74.7±1.07	TS=35.03±1.96 // E=600±30	Chen *et al*., 2008a
	1:1(8wt%) 25%:75%	Gly - 4:1		72±5 (98%RH)	0.2			Tr (800nm) = 46.43±2.14	TS=19.64±3.57 // E=445±20	
	1:1(8wt%) 40%:60%	Gly - 4:1		67±4 (98%RH)	0.2			Tr (800nm) = 31.1±2.32	TS=15±1.25 // E=350±23	

(PO)S-PVA	1:1 (2.5 wt%)		13.56 (54%RH)		0.2	Tg=11.6 // TGA=296			TS=28 // E=8 // YM=1680
									TS=12 // E=282// YM=300
										Jiang *et al*., 2012

	1:1 (2.5 wt%)	$CaCl_2$-1:4	29.61 (54%RH)		0.2	Tg=20.3 // TGA=234-190-172			TS=12 // E=282// YM=300	
(C)S-PVA	1:1 (16.8 wt%)					Tm=231.32 // ΔH=36.80				Luo *et al*., 2012
	1:1 (16.8 wt%)	Gly - 1:0,4				Tm=219.86 // ΔH=39.96				
	1:1 (16.8 wt%)	Urea - 1:0,4				Tm=208.96 // ΔH=15.09				
(PO)S-PVA	9:1 90%:10%		12.02			Tg=124.62 // Tm=191.65	37.65		TS=12.8 // E=230	Ramaraj, 2007
	1:1 50%:50%		11.13			Tg=110.55 // Tm=186.95	36.67		TS=8.02 // E=94.32	
(C)S-PVA	3:01	Gly 20 wt%			0.1	Tg=11.7 // Tf=240/357/456 // TGA=218/298/415			TS=39 // E=81.2	Shi *et al*., 2008
(C)S-PVA	5.6:2.4 70%:30%	Gly 3.78 wt%				Tm=184 // ΔH=8 // Cry=19			TS=7.5±1 // E=45.8±3 // YM=50±3	Sreekumar *et al*., 2012
	4:4 50%:50%	Gly 3.78 wt%				Tm=190 // ΔH=16 // Cry=22			TS=7.5±1 // E=60±3 // YM=54.17±4	
	2.4:5.6 (30%:70%)	Gly 3.78 wt%				Tm=197 // ΔH=23 // Cry=23			TS=10±1 // E=70.83±4// YM=13±1.5	

Matrix	S:PVA	Plasticizer	WC	M Uptake	Thickness	Thermal properties	S	Optical properties	Mechanical properties	References
		(poly:plas)	(%d.b.)	(%)	(mm)	(ºC)	(%)	(%)	TS, YM (MPa) and E (%)	
(C)S-PVA	0.02:1.98 (2 wt%)				1.5			Tr (480nm) = 90	TS=26.5 // E=204	Siddaramaiah *et al*., 2004
	0.05:1.95 (2 wt%)				1.5			Tr (480nm) = 90	TS=26 // E=220	
	0.1:1.9 (2 wt%)				1.5			Tr (480nm) = 82	TS=26.5 // E=208	
	0.15:1.85 (2 wt%)				1.5			Tr (480nm) = 75	TS=26.1 // E=212	
	0.2:1.8 (2 wt%)				1.5			Tr (480nm) = 72	TS=27.4 // E=230	
(C)S-PVA	1:1 (5%w/w)			75±5 (51%RH)	1.0		20±1		TS=55±5 // E=20±10	S-D. Yoon *et al*., 2012
(C)S-PVA	1:1 (5 wt%)	Gly 10.8 mmol			0.25		21.86		TS=23.33 // E=42.11	S-D. Yoon *et al*., 2006
		Gly 54.29 mmol			0.25		35.0		TS=3.33 // E=157.89	
(CAS)S-PVA	10:90 (%w/w)	Sorb 6 %w/w				Tg=41.9 // Tm=168.3 // ΔH=0.9 // TGA=204.7				Valencia *et al*., 2013
	25:75 (%w/w)	Sorb 6 %w/w				Tg=40.2 // Tm=171.9 // ΔH=2.9 // TGA = 217.0				
	40:60 (%w/w)	Sorb 6 %w/w				Tg=48.6 // Tm=168.4 // ΔH=5.9 //TGA=228.4				
	55:45 (%w/w)	Sorb 6 %w/w				Tg=53.7 // Tm=169.5 // ΔH=2.0 // TGA = 232				
(C)S-PVA	7:1.5 (7wt%)	Gly 7:1.5:1.5	48.64 (93%RH		0.22		23.8		TS=5.5±1 // E=14.7±3.3// YM=50±25	Zhou *et al*., 2009

S: starch; PE: pea; C: corn; .CAS: cassava; PO: potato; Gly; glycerol; sorb: sorbitol; PVA: poly (vinyl alcohol); Tg: glass transition temperature; Tm: melting temperature; Tf: fusion temperature; ΔH: fusion enthalpy; Tr: transmittance; TS; tensile strength; E: elongation; YM: Young's Modulus.

Other biopolymers

There are a great deal of compounds that may be blended with starch. They are also wide-ranging in nature, from proteins such as caseinates and gelatine to polysaccharides (HPMC, pullulan, chitosan, etc.), gums and polyesters (PHB), among others. The response was dependent on the type and content of the polymer added, and it has been summarized below.

In this sense, Moreno *et al*. (2014) analysed the effect of the incorporation of buttermilk proteins on the properties of the film-forming dispersions and the physical and microstructural characteristics of corn starch films. Microstructural analysis revealed a reduced compatibility between the starch and milk proteins, leading to phase separation and a heterogeneous structure where lipid droplets can also be observed. As a consequence, blended films exhibited poor stiffness and resistance to break. Water vapour permeability was promoted and a more saturated yellowness was observed in the composite films.

Acosta, (2014) studied the incorporation of gelatin into cassava starch matrix containing glycerol as a plasticizer and concluded that the blended films exhibited a significantly higher degree of hardness, resistance to break and extensibility than pure starch films, especially in the case of films which have incorporated 50 % gelatin.Han *et al*. (2006) identified the effects of the addition of lipids (beeswax) on the pea- starch based film properties. The results showed that the addition of a high concentration of beeswax in pea-starch films negatively affected their mechanical and thermal properties. Moreover, the addition of 30 % beeswax was not an effective means of increasing their water resistance. Da Matta *et al*. (2011) concluded that the mechanical properties of plasticized pea-starch films blended with xanthan gum were not significantly affected.

Jiménez *et al*. (2014) evaluated the influence of the incorporation of different raw materials, such as fatty acids and sodium caseinate and hydroxypropylmethylcellulose

(HPMC), on the microstructural, physico-chemical properties and aging behaviour of the glycerol-plasticized corn starch films. The addition of sodium caseinate to plasticized starch matrices reduced the degree of crystallinity of the films. Mixtures of both hydrocolloids provided films which were less stiff and resistant to fracture but more flexible and deformable than pure starch films, with similar water vapour permeability (WVP) values. In addition, the incorporation of sodium caseinate provoked a slight increase in transparency, but a loss of gloss (Jiménez *et al*., 2012c). When fatty acids were introduced into a plasticized corn starch matrix, the glass transition at low moisture contents decreased, except when incorporating oleic acid. Microstructural observations corroborated the formation of complex structures between both materials, starch and fatty acids. The film´s mechanical behaviour depended on the moisture content, the plasticization effects and the presence of structural discontinuities in the polymer matrices (Jiménez *et al*., 2013a). The incorporation of HPMC into the corn starch matrix gave rise to a more amorphous structure, as was observed by X-ray diffraction. However, SEM micrographs revealed a polymer phase separation which provoked a loss of gloss in the films. The elastic modulus of composite films decreased as compared to pure starch and HPMC films, although tensile strength and deformation at break were slightly improved with respect to pure starch films. Composite films showed similar WVP but slightly higher oxygen permeability (OP) due to the contribution of the HPMC, which had high OP values (Jiménez *et al*., 2012d).

Blend edible films from wheat starch and chitosan with glycerol as plasticizer were prepared by Bonilla *et al*. (2013) and their structural, mechanical, optical and barrier properties and antimicrobial activity were studied. The blend film exhibited a compact, ordered and homogeneous structure, without pores. The extent to which the properties were affected depended on the amount of chitosan added. With a higher chitosan content, the tensile strength and elastic modulus of the films were improved and the

oxygen and WVP slightly increased. Films showed a significant bactericidal activity when the chitosan–starch ratio in the film was 50 %.

Blends of gelatinized and non- gelatinized corn starch plasticizer with glycerol and poly (lactic acid) (PLA) were studied by Park *et al*. (2000), who concluded that the presence of gelatinized starch in the blend decreased the crystallization temperature and increased the degree of crystallinity in PLA-starch blends, and acted as a nucleating agent with respect to PLA films. The mechanical properties of gelatinized starch-PLA blends were superior to the non-gelatinized.

Kim *et al*. (2014) obtained tapioca starch and pullulan blends for the preparation of edible films, and studied the mechanical strength and stability of the composite films in low and high relative humidity environments (23 and 85 %RH, respectively). The mechanical properties and the storage stability were effectively improved when using the low RH environment during the storage period. However, starch tended to decrease the water solubility of blended films. Polyhydroxybutyrate-hydroxyvalerate (PHB-HV)/maize starch blend films were obtained by Reis *et al*. (2008). Films showed a decrease in the Young's modulus, tensile strength and puncture force values when the starch content rose. FT-IR measurements indicated that no intermolecular interactions existed between the two polymers as no shift in the absorption peaks of the PHB-HV or starch in the blends was observed, which suggests that PHB-HV and starch were immiscible. The blend also exhibited low crystallinity (< 4 %). However, blends of PHB-HV with maize starch have the potential to offer a low cost alternative to pure PHB-HV.

3.2. Reinforcement materials: fibres and nano-reinforcements

The main role of the reinforcement material in composite films is for the purposes of enhancing their mechanical properties. In addition, the resistance to water can also be

improved. From reviewing the literature, it can be seen that the most commonly used reinforcement materials have been fibres and nanoparticles, as commented on below.

Fibres are continuous filament materials or discrete elongated pieces. They can be divided into two types: natural fibres, which are subdivided according to their origins (from plants, animals or minerals), and synthetic fibres.

Plant fibres are composed of cellulose, hemicellulose, lignin, pectins, and waxes, while animal fibres mainly consist of proteins (hair, silk, and wool). Plant fibres include bast (or stem or soft sclerenchyma) fibres, leaf or hard fibres, seed, fruit, wood, cereal straw, and other grass fibres obtained from flax, hemp, jute, sisal, kenaf, coir, kapok, banana, henequen and many others (Ku *et al*., 2011; Li *et al*., 2009). The use of such materials in composite films has increased due to their relatively low cost and density, their ability to recycle, being renewable and biodegradable, and for the fact that they can compete well in terms of specific tensile properties (John &Thomas, 2008; Mondragon *et al.*, 2008). Moreover, they are non-abrasive and pose no health risks (Ku *et al*., 2011; Malkapuram *et al*., 2008).

All of the different fibres used in composites have different properties and so affect the properties of the composite in different ways (Carvalho *et al*., 2001; Jiménez *et al*., 2012a; Tang *et al*., 2009). For example, the cellulose fibrils are aligned along the length of the fibre, rendering maximum tensile strength and flexibility, in addition to providing rigidity. The reinforcing efficiency of natural fibre is related to the nature of cellulose and its crystallinity.

Bearing in mind the good interactions established between cellulose derivatives and starch, several authors have introduced fibres from different natural sources (husk of corncobs, cotton, wheat bran, cassava, potato pulp, decolorized hsian-tsao leaf gum, pea hull fibre and pea hull fibre derived from nanowhiskers) into the starch-based films obtained via casting. They concluded that the mechanical properties (TS, E and EM) and

water vapour permeability of starch composites improved when the fibre content rose (Famá *et al*., 2009) due to their hydrophobic nature and to the development of good interactions between the starch matrix and fibres. These interactions promoted, in some cases, a lower degree of mobility of the amylopectin molecules and a synergistic effect of the cellulose fibres and the amylose complexes, which hindered the retrogradation of starch (Mondragón *et al*., 2008). The effect of its incorporation on the glass transition temperature (Tg) is not clear; Zhang *et al*. (2011) did not find any effect, but Chen *et al*. (2009a-b) found that the Tg values rose when pea hull fibre nano-whiskers were incorporated.

The influence of the size of the fibres was studied by Chen *et al*. (2009a-b). They concluded that the smaller fibre size presented better mechanical and barrier results as they became dispersed more homogeneously within the polymer matrix, resulting in larger interface areas and stronger interactions with the starch.

To summarize, it is possible to conclude that fibres significantly enhanced the mechanical properties of starch films, but they also influenced their crystallinity, thermal stability and barrier properties. These changes depended on the natural source and the particle size of the fibre, and to the use of the smallest possible size is recommended due to the fact that macroscopic reinforcing components usually contain defects, which become less important as the particles of the reinforcing component grow smaller (Azeredo, 2009; Chen *et al*., 2008a; Ludueña *et al*., 2007). In this sense, there is increasing interest being shown in the application of nanotechnology for the purposes of reinforcing films and this may open up new possibilities for the improvement not only of the properties but also of the cost-price-efficiency (Sorrentino *et al*., 2007).

Nanoparticles, are considered to be fillers which have at least one dimension in the nanometric range (particles between 1-100nm in size) (Alexandre & Dubois, 2000). Three types of fillers can be distinguished, depending on how many dimensions are in

the nanometric range: isodimensional (3 nanometric dimensions), nanotubes or whiskers (2 dimensions) and polymer-layered crystal nanocomposites (only one dimension) (Azeredo, 2009; Alexandre & Dubois, 2000). These prominent nanoparticles used as a reinforcement for the purposes of producing composite films via casting are also obtained from different natural resources, the most common being:

- Clay and silicates; the most widely used being montmorillonite. Potato starch (Cryas *et al*., 2008), cassava starch (Kampeerapappun *et al*., 2007), corn starch (Romero-Bastida *et al*., 2015) methyl cellulose (Tunc & Duman, 2010) and cellulose (Mahmoundian *et al*., 2012) are examples of matrices reinforced with montmorillonite.

Other authors have developed nanoparticles from:

- Carbon (nanotubes), incorporated into PVA (Bin *et al*., 2006) and polyamide films (Zeng *et al*., 2006).
- Silica (SiO_2), in starch/PVA films by Tang *et al*. (2008).
- Starch nanocrystals (Shi *et al*., 2013).
- Chitin and chitosan, incorporated into gelatin films (Fakhreddin *et al*., 2015).
- Cellulose nanocrystals or whiskers into PVA and PLA films (Lee *et al*., 2009; Fortunati *et al*., 2012a-c; 2013a-b).

By using these nanoparticles, a uniform dispersion was formed, which led to a very large matrix/filler interfacial area, which affected the molecular mobility thus improving the thermal, barrier and mechanical properties of the material. Fillers with a high aspect ratio, defined as the length-to- width (L/w), are particularly interesting because of their high specific surface area, providing better reinforcement (Azeredo, 2009; Azizi Samir *et al*., 2005; Dalmas *et al*., 2007; Dubief *et al*., 1999, Habbibi *et al*., 2010).

In addition to the effects of the nano-reinforcements themselves, their use resulted in a percolating interphase network in the composite, which plays an important role in improving the nanocomposite properties (Habbibi *et al*., 2010; Qiao & Brinson, 2009).

4. BIOACTIVE COMPOUNDS WITH ANTIMICROBIAL ACTIVITY

In recent years there has been considerable consumer pressure to reduce or eliminate chemically synthesized additives in foods. Following this trend, there has been a notable increase in the interest shown in the possible use of natural alternatives as food additives as a means of preventing bacterial, fungal and yeast growth (Lanciotti *et al*., 2004).

Packaging materials, edible films and coatings can be fortified with these antimicrobials in order to create a protective barrier to help to control the growth of pathogenic and spoilage microorganisms and to prevent post-contamination of foods (Kristo *et al*., 2008; Azeredo, 2009). These antimicrobials can be released in an effective manner into the food product through controlled release strategies so as to prolong its shelf life, quality and safety.

Various techniques have been developed to incorporate these compounds into packaging materials: (a) by means of using inherently antimicrobial polymers, such as chitosan, and (b) by means of the direct incorporation of the antimicrobials into the packaging films via coating, adsorption or direct blend with the polymer (Sadaka *et al*., 2014).

The sources of most of these antimicrobials are mineral or plant extracts, but different peptides and proteins have also been used. Some of them are commented on in detail below, divided up according to their origin.

Table 3 summarizes different studies about the antimicrobial effect of films containing active compounds from mineral and plant origin.

Table 3. Summary of different antimicrobial studies using AgNPs and oregano essential oil (O).

Antimicrobial Agent	Film material	Microorganisms	Method	Inoculum (CFU/ml)	Effectiveness	Reference
AgNPs-Synthesized	PVA	*Staphiloccocus aureus* ATCC3953 (+) *Escherichia coli* ATCC3954I (-) *Pseudomona aeruginosa* ATCC3955 (-) *Klebsiella pneumoniae* (-)	Agar disc diffusion and viable cell count	10^8	I (better against *S. aureus*)	Sedlarik, *et al*., 2010
AgNPs-Synthetised	PVA- TEOS tetreethylorthosi-licate	*Staphiloccocus aureus* ATCC25923(+) *Escherichia coli* ATC25922(-) *Pseudomona aeruginosa* ATCC27853 (-)	Agar disc diffusion	10^8	I (bactericidal)	Bryaskova *et al*., 2010
AgNPs-Synthetised	Agar-Agar	*Staphiloccocus aureus* ATCC25923 (+) *Escherichia coli* ATCC1302 (-)	Agar disc diffusion	10^8	I (better against *E. coli*)	Ghos *et al*., 2010
AgNPs-Synthetised	CH-PEGs-Glutaraldehide	*Bacillus* (+) *Escherichia coli* (-) *Klebsiella pneumoniae* (-)	Agar disc diffusion and viable cell count	10^8	I (good inhibition)	Vimala *et al*., 2010
AgNPs-Synthetised	CH-starch	*Staphiloccocus aureus* (+) *Bacillus cereus* (+) *Escherichia coli* (-)	Agar disc diffusion	10^5	I (better against *E. coli*)	Yoksan & Chirachanchai, 2010
AgNPs-Synthetised	CH-PVA-Glutaraldehide	*Staphylococcus* (+) *Micrococcus* (+) *Escherichia coli* (-) *Pseudomona aeruginosa* (-) *Pseudomonas* (-) *Candida albacian*	Agar disc diffusion and viable cell count	10^8	I (good inhibition)	Vimala *et al*., 2011
AgNPs-commercial	PVA	*Staphiloccocus aureus* 8325-4 (+) *Escherichia coli* RB (-)	Viable cell count	10^3	I (better against *E. coli*)	Fortunati *et al*., 2012b
AgNPs-Synthetised	HPMC	*Staphiloccocus aureus ATCC 25923 (+)* *Escherichia coli ATC 25922 (-)*	Agar disc diffusion		I (better against Gram+)	De Moura *et al*., 2012
AgNPs-Synthetised	Agar-Gly	*Listeria monocytonges ATCC 19111 (+)* *Escherichia coli ATCC 11775 (-)*	Viable cell count	10^4	I (better against Gram-)	Rhim *et al*., 2013

Antimicrobial Agent	Film material	Microorganisms	Method	Inoculum (CFU/ml)	Effectiveness	Reference
AgNPs-Synthetised	Poly(hydroxy alkanoates)	*Salmonella enterica* CECT554 (-)	Viable cell count	10^5	I (bactericidal). *aureus*)	Castro-Mayorga *et al*., 2014
AgNPs-Synthetised	Gelatin-Sorbitol	*Staphiloccocus aureus 8325-4 (+)* *Listeria monocytonges (+)* *Escherichia coli (-)* *Salmonella typhimurium (-)* *Bacillus cereus (+)*	Viable cell count	10^6	I	Kanmani & Rhim, 2014
AgNPs-Synthesized	Starch-clay	*Staphiloccocus aureus CECT4210 (+)* *Escherichia coli CECT 4210 (-)* *Candida albicans ATCC 90028*	Agar disc diffusion	10^5	I (microbiostatic effect)	Abreu *et al*., 2015
AgNPs-Synthesized	CH-cellulose	*Staphiloccocus aureus* ATCC 25923 (+) *Escherichia coli* ATCC25922 (-)	Agar disc diffusion	10^2	I (better against *E. coli*)	Lin *et al*., 2015
O	Chitosan	*Listeria monocytonges* (+) *Escherichia coli* O157:H7 (-)	Agar disc diffusion	10^6	I (both Gram+ and Gram-)	Zinanovic *et al*., 2005
O	Whey protein-Glycerol	*Staphiloccocus aureus* ATCC 43300 (+) Listeria monocytogenes NCTC 2167 (+) *Escherichia coli* O157:H7 ATCC 35218 (-) *Salmonella enteriditis* ATTCC 13076 (-) *Lactobacillus plantarum* (+)	Agar disc diffusion	10^8	I	Seydim & Sarikus, 2006
O	PP Polypropylene PE/EVOH Polyethylene/ethylene vinyl alcohol copolymer	*Staphiloccocus aureus* (+) *Listeria monocytogenes* (+) *Bacillus cereus (+)* *Enterococcus faecalis* (+) *Escherichia coli* (-) *Salmonella choleraesuis* (-) *Yersinia enterocolitica* (-) *Pseudomona aeruginosa* (-) *Eurotium repens* *Aspergillus flavus* *Penicillium islandicum* *Penicillium roqueforti* *Penicillium nalgiovense*	Viable cell count	10^4- 10^7	I (Fungi > Gram+> Gram-)	López *et al*., 2007

Antimicrobial Agent	Film material	Microorganisms	Method	Inoculum (CFU/ml)	Effectiveness	Reference
O	Tomato	*Listeria monocytogenes* RM 2199 (+) *Escherichia coli* O157:H7 RMI 1484 (-) *Salmonella enteriditis* RM 1309 (-)	Agar disc diffusion	10^4	I	Rojas-Graü *et al*., 2007
O	Starch-Glycerol Amaranth-Glycerol Chitosa-Tween20	*Aspergillus niger* *Penicillium spp.*	Agar disc diffusion	10^4	I except Amaranth films	Avila-Sosa *et al*., 2009
O	Soy	*Staphiloccocus aureus* (+) *Lactobacillus plantarum* (+) *Escherichia coli* O157:H7 (-), *Pseudomona aeruginosa* (-)	Agar disc diffusion	10^5- 10^6	I	Emiroğlu *et al*., 2010
O	Amaranth flour-Glycerol CH-Glycerol	*Aspergillus niger* *Penicillium digitatum*	Agar disc diffusion	10^4	I	Avila-Sosa *et al*., 2012
O	Corn starh-Glycerol Alginate	*Staphiloccocus aureus* (+) *Listeria monocytogenes* (+) *Escherichia coli* (-) *Salmonella enteriditis* (-)	Agar disc diffusion	10^5- 10^6	I (Gram+ better than Gram-)	Benavides *et al*., 2012
O	Triticale protein	*Staphiloccocus aureus* ATGG 29737 (+) *Escherichia coli* ATGG 25923 (-) *Pseudomona aeruginosa* ATGG 27853 (-)	Agar disc diffusion	10^8	I (Gram+ better than Gram-)	Aguirre *et al*., 2013

Antimicrobial Agent	Film material	Microorganisms	Method	Inoculum (CFU/ml)	Effectiveness	Reference
O	potato processing waste	*Listeria monocytogenes* CWD1002, CWD1157, CWD1198, V7	Agar disc diffusion		I	Tammineni *et al*., 2013
O	Pectin	*Staphiloccocus aureus* ATCC 6538 (+) *Listeria monocytogenes* (+) *Escherichia coli* O157:H7 ATCC 43890 (-) *Salmonella enteriditis* ATTCC 7001 (-)	Agar disc diffusion	10^8	I (Gram+ better than Gram-)	Alvarez *et al*., 2014
O	Quince seed mucilage	*Staphiloccocus aureus* (+) *Listeria monocytogenes* (+) *Bacillus cereus* (+) *Escherichia coli* (-) *Salmonella* thyphimurium (-) *Pseudomona aeruginosa* (-) *Shewanella putrefaciens* (-) *Yersinia enterocolitica*(-) *Vibrio Cholera* (-)	Agar disc diffusion	10^7	I except *P. aeruginosa* and *S. thyphymurium*	Jouki *et al*., 2014
O	Fish gelatin -CH	*Staphylococcus aureus* (+) *Bacillus subtilis* (+) *Escherichia coli* (-) *Salmonella enteriditis* (-) *Shiga bacillus* (-) *Escherichia coli* O157:H7 (-), *Pseudomona aeruginosa* (-)	Agar disc diffusion	10^8	I concentration higher than 1%(Gram+ better than Gram-)	Wu *et al*., 2014
O	Fish gelatin -CH	*Staphylococcus aureus* (+) *Listeria monocytogenes* (+) *Escherichia coli* (-) *Salmonella enteriditis* (-)	Agar disc diffusion	10^5	I (Gram+ better than Gram-)	Hosseini *et al*., 2015
O	Gelatin-propylene glycerol	*Staphylococcus aureus* ATCC 25923 (+) *Escherichia coli* O157:H7 ATCC 32158 (-)	Agar disc diffusion	10^4- 10^5	I (Gram+ better than Gram-)	Martucci *et al*., 2015
O	EVOH er	*Escherichia coli* ATCC 25922 (-) *Penicillium expansum*	Agar disc diffusion and viable cell	10^4	Total I	Muriel-Galet *et al*., 2015

I: Inhibition; (+):Gram-positive and (-): Gram-negative.

4.1. Substances from mineral sources

Metals have been used for their antimicrobial properties for thousands of years. For example, vessels made of Cu and Ag have been used for water disinfection and food preservation since the time of the Persian kings, and historically there were many medical applications of Ag (Lemire *et al*., 2013).

Certain heavy metals are antimicrobial in the form of salts, oxides, and colloids. These metals can be incorporated into food-contact polymers and surfaces to enhance the mechanical and barrier properties and to extend the shelf-life of foods (Pal *et al*., 2007). The most commonly used metal and metal oxides are silver (Ag), gold (Au), copper (Cu), zinc oxide (ZnO), silica (SiO_2), titanium dioxide (TiO_2), alumina (Al_2O_3), and iron oxides (Fe_3O_4, Fe_2O_3) (Corrales *et al*., 2014; Sharma *et al*., 2009).

Recently, some of these metals have been used as nanoparticles because their high surface area/volume ratio enhances the antimicrobial potential and broadens the prospects of these particles being used in the food industry (Chaudhry *et al*., 2008; Emamifar *et al*., 2010).

Silver and its compounds have been known to exert strong inhibitory and bactericidal effects as well as a broad spectrum of antimicrobial activities against bacteria, fungi, and viruses (Ghosh *et al*., 2010; Mohanty *et al*., 2012; Li *et al*., 2010; Silver 2003). Compared with other metals, silver exhibits higher degrees of toxicity to microorganisms while being less toxic to mammalian cells in minute concentrations (Pal *et al*., 2007; Rai *et al*., 2009; Zhao & Stevens 1998); also remarkable is its great thermal stability and low volatility and cost of production (Duran *et al*., 2007, Martínez-Abad, 2014a).

The antimicrobial and antiviral actions of silver are related to the amount of silver and the rate of its release. In its metallic state, silver is inert, but it reacts with the environmental moisture according to the following reaction:

$$4Ag^0 + 4H^+ + O_2 \rightarrow Ag^+ + 2H_2O$$

The exact mechanism of action of silver on the microbes is still not known but the possible mechanism of action of metallic silver, silver ions and silver nanoparticles has been suggested based on the morphological and structural changes found in the bacterial cells (Rai *et al*., 2009). This mechanism of action is linked with the interactions with both the thiol group (-SH) compounds found in the respiratory enzymes of bacterial cells, which inhibit the respiration process, (Klasen, 2000) and with L-Cysteine residues, which cause denaturation and loss of enzymatic functions (Feng *et al*., 2000; Martínez-Abad, 2014a; Liau *et al*., 1997). It is suggested that when DNA molecules are in a relaxed state, the replication of DNA can be effectively conducted whereas when DNA is in a condensed form, it loses its ability to replicate. Hence, when the silver ions penetrate the bacterial cell, the DNA molecule condenses and loses its ability to replicate leading to cell death. It has also been reported that heavy metals react with proteins by attaching themselves to the thiol group, inactivating the proteins (Liau *et al*., 1997; Feng *et al*., 2000). The antimicrobial action mode of silver nanoparticles is probably similar to that of silver ions (Mohanty *et al*., 2012). However, the silver nanoparticles showed greater antimicrobial activity compared to other salts due to their extremely large surface area, which results in more significant interactions with the vital component of the cells, leading to unbalanced respiratory functions, an increase in reactive oxygen species and a depletion of ATP levels, and also intercalating between DNA bases and, in consequence, interfering with replication (Martínez-Abad, 2014a; Rai *et al*., 2014). In addition, the physicochemical conditions promoting the release of silver ions from silver nanoparticles enhanced their bactericidal activity (Feng *et al*., 2000; Sondi & Salopek-Sondi, 2004; Morones *et al*., 2005; Song *et al*., 2006).

The bactericidal effect of silver nanoparticles (AgNPs) is both size and shape - dependent (Ghosh *et al*., 2010; Morones *et al*., 2005 Rai *et al*., 2009; Raimondi *et al*.,

2005). The size of the nanoparticle implies that a large surface area comes into contact with the bacterial cell components and hence, the interactions will be more significant than in the case of bigger particles (Castro-Mayorga *et al*., 2014; Morones *et al*., 2005; Pal *et al*., 2007; Rai *et al*., 2009). As regards the shape, truncated triangular nanoparticles exhibited a high degree of bacterial inhibition with a silver content of 1 µg, while in spherical nanoparticles, a total silver content of 12.5 µg was needed (Pal *et al*., 2007).

Silver nanoparticles (AgNPs) can be purchased from commercial companies or synthetized on a laboratory scale. In this case, wet chemical reduction is the most frequently applied method for the synthesis of AgNPs. When silver nitrate ($AgNO_3$) is dissolved, it splits into a positive silver ion (Ag^+) and a negative nitrate ion (NO^{-3}). In order to turn the silver ions into solid silver, the ions have to be reduced by receiving an electron from a donator, according to the following reaction:

$$Ag^+(aq) + e^- \rightarrow Ag^0(s)$$

In literature, various methodologies (Table 4) have been described for the synthesis of AgNPs from silver nitrate using different radiation sources, such as laser, ultraviolet light and gamma rays, and a combination of different strong reducing agents, such as sodium dodecyl sulphate, polyacrylic acid, sodium borohydride, citrate, ascorbate, and elemental hydrogen (Ahmadi *et al*., 1996; Khanna *et al*., 2005; Lee & Meisel, 1982; Mohanty *et al*., 2012; Neto *et al*., 2008; Sharma *et al*., 2009). Moreover, the synthesis of nanoparticles by chemical reduction is often performed in the presence of stabilizers in order to prevent the unwanted agglomeration of the colloidal particles.

An alternative to the use of these strong chemical agents is to follow the green synthesis of AgNPs, which involves three main steps: (1) the selection of solvent medium, (2) the selection of an environmentally being reducing agent, and (3) the selection of non-toxic substances for the AgNPs' stability (Raveendran *et al*., 2003;

Sharma *et al*., 2009). In this sense, some researchers synthesized the nanoparticles by using biopolymer matrices as the stabilizing and reducing agents shown in Table 4. Nanoparticle preparation with biopolymers has several advantages over conventional synthetic chemical agents. For example, the macromolecular chains of these biopolymers have a large number of hydroxyl groups that can complex with the metal ion well, favouring a good control of the size, shape and dispersion of nanoparticles, increasing the biocompatibility and biodegradability, having a less toxic effect on mammalian cells (Mohanty *et al*., 2010).

The reduction of silver ions (Ag^+) in an aqueous solution generally yields colloidal silver with particle diameters of several nanometers (Wiley *et al*., 2005). When the silver ions are reduced, the colloidal particles are much smaller than the wavelength of visible light and, consequently, the solution takes on a brown-yellow colour due to the excitation of Surface Plasmon Resonance (SPR) vibrations of the SNPs, giving rise to an intense band located in the 400–458 nm range (Table 4) and other less intense or smaller bands at a longer wavelength in the absorption spectrum (Ahmed *et al*., 2015; Darrouri *et al*., 2011; Kanmani & Lim 2013; Sharma *et al*., 2009; Shukla *et al*., 2012; Torres-Castro *et al*., 2011).

Table 4. Different methods used in AgNPs synthesis, by using strong or green reduction processes.

Method	Solvent medium	Reducing Agent	Stabilizing Agent	[Ag+] (mM)	T (ºC)	Time (min)	Catalyst	Absorbance (nm)	Diameter size (nm)	Reference
Strong	Water	hydrazine hydrate / sodium formaldehyde sulfoxylate	PVA	10		25	Stirring	418	from 2 to 15	Khanna *et al*., 2005
Green	Water		Starch	100	121	5		420	22.85±12.94	Vigneshwaran *et al*., 2006
Strong	Water	Sodium borohydride	PVA	0.5			Stirring	400		Neto *et al*., 2008
Green	Water	Ethylene glycol	PVP	150-250	125-140-150		Stirring	408-432	from 18 to 41	Morales *et al*., 2009
Strong	Water	Sodium borohydride	PVA	79		5	Stirring (500-1000 rpm)	405	40 and 100	De Moura *et al*., 2009
Green	Water		PVA	5.7-11.5-23.1	100	60	Stirring			Bryaskova *et al*., 2010
Green	Water	PVP-ethanol	agar-agar	1	90	120		410	from 15 to 25	Ghos *et al*., 2010
Strong	Water	Sodium-citrate	b-chitin		High			435	from 4 to 8	Sudheesh-Kumar *et al*., 2010
Green	Water	PEG	PEG	24	60 and 80	60		433 and 416		Vimala *et al*.,2010
Green	Water	γ-ray irradiation	CH	50				411	46.7±3.5	Yoksan &Chirachanchai, 2010
Green	Water	Glucose	Geltin	1000			Stirring	430 (48h)	from 5 to 20	Darroudi *et al*., 2011
Green	Water	Sunlight-UV	Gelatin	30-6-0-120-240		120	Stirring		from 10 to 22	Pourjavadi & Soleyman, 2011
Green	Water	Sodium borohydride	Starch	10					from 10 to20	Torres-Castro *et al*., 2011
Strong		Gelatinized Starch	Starch	28	55-85	120-1440		430	from 55 to 80	

Method	Solvent medium	Reducing Agent	Stabilizing Agent	[Ag+] (mM)	T (ºC)	Time (min)	Catalyst	Absorbance (nm)	Diameter size (nm)	Reference
Green	Water	Sunlight	CH-PVA	12		60			from 413 to 421	Vimala *et al*., 2011
Green	Water		Starch	1	121	5-10		401	from 5 to 40	Ernest *et al*., 2012
Green	Water		Starch	1	121	5		420 (90days)	20	Mohanty *et al*., 2012
Green	Water	Agar	Agar	2.5-5	25-60-100	60-240-2880	Stirring (200rpm)	421	6±2	Shukla *et al*., 2012
	Water	Pullulan		1-3-5-7-9-12	121	15		from 405 to 410	from 2 to 40	Kanmani & Lim, 2013
Strong	Water	Trisodium citrate		0.032-0.8-1.6-3.2	High boiling	60				Rhim *et al*., 2013
Green	Water	D(+)-Glucose	Starch	15	85	60-4320	Stirring (700 rpm)	from 422 to 450	from 10 to 30	Cheviron *et al*., 2014
Green	Water	Gelatin and Sorbitol	Gelatin	300	Boiling	60	Stirring	from 400 to 450		Kanmani *et al*., 2014
Green	Water	pectin/sodium hydroxide		100	1 to 60		Stirring	from 400 to 450	5 and 10	Zharan et al., 2014
Strong	Water	Sodium borohydride	Starch/clay	0.3-0.5-0.8-1		5	5			Abreu *et al*., 2015
Green	Water	*S. laureda* leaf extract		10	Room		Stirring	460	46	Ahmed *et al*., 2015
Green	Water	*C. officinalis* seed extract		1	Room			440	7.5	Baghizadeh *et al*., 2015
Green	Water	D-glucose	CP, CMC and MCC	5		360	Sonicator (10 min)	from 407 to 419		Hassabo *et al*., 2015
Green	Water	*H. indicus* leaf extract		0.75	Room			430	from 19.91 to 47.60	Latha *et al*., 2015
Green	DEG	DEG and PAA		200			Stirring		9	Lin *et al*., 2015

Method	Solvent medium	Reducing Agent	Stabilizing Agent	[Ag+] (mM)	T (ºC)	Time (min)	Catalyst	Absorbance (nm)	Diameter size (nm)	Reference
Green	Water	Sun light and *P. nigrum* seed extract		0.625-1.25-2.5		5-20		from 453 to 458	from 23.8 to 32.2	Mohapatra *et al*., 2015
Green	Water	*E. helioscopia Linn* leaf extract		0.0177	80	180	Stirring	440		Nasrollahzadeh *et al*., 2015
Green	Water	*Areca catechunut* extract		1.17	27 and 100	3	Stirring	from 414 to 440	from 18.2 to 24.3	Rajan *et al*., 2015
Green	Water	*S. tuberosum* (potato) extract		10	Room	1440		430	from 10 to 12	Roy *et al*., 2015

As far as the actual regulation of the European Union governing packaging materials (EU n. 10/2011 commission 14 January 2011) is concerned, there is no particular indication for the use of silver compounds in a packaging application and, consequently, the established specific migration limit is set at 60 mg/Kg for foodstuffs. On the other hand, The Food and Drug Administration/Centre for Food Safety and Applied Nutrition (FDA/ CFSAN – USA) accepted the use of silver nitrate as a food additive in bottled waters and silver zeolites to be used in all types of food-contact polymers (FDA, 2010), while in the European Regulation, silver is accepted under Directive 94/36/EC as a coloring agent (E-174) with no restrictions.

4.2. Substances from plant extracts

The most prominent of these , are a wide range of substances, such as alkaloids, tannins, flavonoids and phenolic and volatile compounds extracted from plants (Shihabudeen *et al*., 2010; Utama *et al*., 2002).These products have been widely used as food flavouring agents and most of them are generally recognized as safe (GRAS) (Lanciotti *et al*., 2004; Newberne *et al*., 2000). In Europe, extracts from natural resources are regulated under Regulation 1334/2008 on natural flavorings.

Of the plant-extract substances used, one of the most bioactive is the essential oils, which are composed of high amounts of hydrophobic and volatile compounds (85-99 %). The aromatic compounds include terpenes, terpenoids, and aromatic constituents and aliphatic constituents, all characterized by their low molecular weight (Sánchez-González *et al*., 2011). Both essential oils and pure substances obtained from them are commonly used as flavouring in the food industry, and their antibacterial, antifungal and antioxidant properties have also been reported in numerous studies (Sánchez-González *et al*., 2011).

Their antimicrobial activity cannot be explained by a single specific mechanism but rather by the combined effect of different substances (Burt, 2004; Corrales *et al*., 2014) and the chemical structure of the individual compounds of the essential oil. Gram-positive bacteria have been reported to be slightly more sensitive to essential oil than Gram-negative (Aguirre *et al*., 2013; Burt, 2004; Corrales *et al*., 2014; Martucci *et al*., 2015; Smith-Palmer *et al*., 2001). This difference is related to the presence of an additional, relatively impermeable, outer membrane surrounding the cell wall in Gram-negative bacteria, which restricts the diffusion of hydrophobic compounds through its lipopolysaccharide covering (Burt, 2004; Sánchez-González *et al*., 2011). Phenolic compounds of EOs, such as carvacrol, eugenol and thymol, can attack the phospholipid cell membrane leading to an increase in both the permeability and leakage of the cytoplasm, or an interaction with enzymes located on the cell wall (Burt, 2004; Campos *et al*., 2011; Zivanovic *et al*., 2005; Matan *et al*., 2006).

The USFDA (1997) classified some essential oils, such as clove, oregano, thyme, nutmeg, basil, mustard, and cinnamon, as a GRAS. The antimicrobial activity of essential oils occurs when the volatile antimicrobials entrapped in the polymeric matrices are released either into the headspace or by direct contact. The main constraint against the use of essential oils in food products is their strong flavour and aroma, which may affect the sensory acceptance of the product (Burt & Reinders, 2004; Corrales *et al*., 2014).

Of the essential oils, oregano has been found to be one of the most effective. Its antimicrobial properties have been demonstrated in numerous studies (Aguirre *et al*., 2013; Emiroğlu *et al*., 2010; Zivanovic *et al*., 2005). Carvacrol, thymol, γ-therpinene and p-cymene are its principal constituents (Benavides *et al*., 2010; Burt, 2004; Jouki *et al*., 2014; Kuorwel *et al*., 2011; Sadaka *et al*., 2014; Sánchez-González *et al*., 2011) and the antimicrobial activity is related to the synergic effect established among them. The carvacrol mode of action was explained by Burt in 2004. Carvacrol disintegrates the outer

membrane of gram-negative bacteria, releasing lipopolysaccharides and increasing the permeability of the cytoplasmic membrane to ATP.

The antimicrobial properties of rosemary essential oil have also been extensively studied by several authors (Aguirre *et al*., 2013). This essential oil has been reported to be active against a wide spectrum of microorganisms, derived from high polyphenol content, the most abundant of which are carvacrol, eugenol and thymol (Lambert *et al.*, 2001).

Some other plant extracts have also been found to exert antimicrobial activity. For example, plant extracts from *Tussilago farfara*, *Equisetum arvense, Sambucus nigra* and *Aesculus hippocastanum* have exhibited antimicrobial activity against *Escherichia coli* and *Pseudomonas aeruginosa* (Hleba *et al*., 2014). Farjana *et al*. (2014) determined the antimicrobial activity of some leaf extracts of common plants, such as guava (*Psidium guajava*), green tea (*Camellia sinensis*), neem (*Azadirachta indica*) and marigold (*Calendula officinalis*) leaves, against some Gram negative bacteria, such as *Pseudomonas*, *Escherichia coli* and *Staphylococcus aureus*, among others.

Significant antimicrobial activity has been attributed to of Echinacea (*E. purpurea*) extracts in a series of in vitro experiments testing against *Saccharomyces cerevisiae,* various *Candida* species, *Listeria monocytogenes and Staphylococcus (*Barret, 2003; Stanisavljević *et al*., 2009*).* Besides, the alkamides content in Echinacea can be exploited as an alternative means of controlling fungi that are pathogens or involved in food spoilage. However, the antimicrobial mode of action of compounds in Echinacea has not been well characterized (Cruz, 2014).

Field horsetail (*Equisetum)* has also been described as an herb with antioxidant and antimicrobial properties (García *et al*., 2013). Some research studies have shown that extract of horsetail has an inhibitory effect on *Aspergillus* spp. and *Fusarium* spp. growth and toxin production (Mahoney & Molyneux, 2004; Radulovic *et al*., 2006; Samapundo

et al., 2007). García *et al*., (2012) used an *Equisetum arvense* hydro-alcoholic extract to control the growth of *A. flavus* and *F. verticillioides*. Their results confirmed that the extract was effective against the growth of both fungi, especially at high water activity levels.

For centuries, traditional wood smoke has been used as a food quality preservation technique due to its antioxidant and antimicrobial properties (Lingbeck *et al*., 2014; Saloko *et al*., 2014). Nowadays, the use of condensates or "liquid smoke" requires less time than traditional smoking, is more environmentally friendly, and eliminates potentially toxic compounds while still imparting the desired flavours and aromas of traditional smoking. Different authors have shown that different woods generate different levels of phenols, carbonyls and organic acids upon pyrolysis, which affect the antimicrobial properties against *Staphylococcus aureus*, *Aeromonas hydrophila, Salmonella, Listeria monocytogenes* and *Escherichia coli* (Boyle *et al*., 1988; Linbeck *et al*., 2014; Sofos *et al*., 1988). Volatile compounds present in liquid smoke lead to a lower pH, thus affecting the functionality of the bacterial cell walls (Pszczola, 1995). Commercially manufactured liquid smoke extracts have been approved as GRAS and are being used as antimicrobial agents (Martin *et al*., 2010).

Neem oil extracted from the seeds of *Azadirachta indica* has versatile properties, such as ovicidal, antifungal, antibacterial, immunostimulant, and acaricidal activities (Abdel-Ghaffar & SemmLer, 2007; Divakar *et al*., 2001; Du *et al*., 2008, 2009; Jahan *et al*., 2007; Pu *et al*., 2010; Xu *et al*., 2010). In fact, Baswa *et al*. (2001) revealed that the neem oil exhibits bactericidal activity against 14 strains of pathogenic bacteria, such as *Staphylococcus aureus* (Rao *et al*., 1986), *Staphylococcus typhus* (Patel &Trivedi, 1962), and *Escherichia coli*, *Streptococcus mutans* and *lactobacilli* (Vanka *et al*., 2001). In addition, Hoque *et al*. (2007) determined the antibacterial activity of neem extracts against 21 strains of foodborne pathogens: *Listeria monocytogenes*, *Staphylococcus*

aureus, *Escherichia coli* O157:H7, *Salmonella enteritidis*, *Vibrio parahaemolyticus*, and *Bacillus cereus*, and five food spoilage bacteria: *Pseudomonas aeroginosa*, *P. putida*, *Alcaligenes faecalis*, and *Aeromonas hydrophila*. They concluded that neem extracts generally showed higher antimicrobial activity against Gram-positive bacteria than Gram-negative and none of the extracts exhibited antimicrobial activity against *E. coli* O157:H7 and *Salmonella Enteritidis*. The action mechanism of the extract of neem is attributed mainly to the inhibition of cell-membrane synthesis in the bacteria (Baswa *et al*., 2001).

References

- Abdel-Ghaffar, F., & SemmLer, M. (2007). Efficacy of neem seed extract shampoo on head lice of naturally infected humans in Egypt. *Parasitology Research*, 100, 329-332.
- Abreu, A. S., Olivera, M., Rodeigues, M., Cerqueira, A., Vicente, A. A., & Machado, A.V. (2015). Antimicrobial nanostructured starch based films for packaging. *Carbohydrate Polymers*, accepted date: 8-4-2015 http://dx.doi.org/10.1016/j.carbpol.2015.04.021
- Acosta, S. (2014). Propiedades de films de almidón de yuca y gelatina. Incorporación de aceites esenciales con efecto antifúngico, Doctoral Thesis. Supervised by: C. González-Martínez, & M. Cháfer. Universitat Politècnica de València, Spain.
- Aguirre, A., Borneo, R., & León, A. E. (2013). Antimicrobial, mechanical and barrier properties of triticale protein in films incorporated with oregano essential oil. *Food Bioscience*, 1, 2-9.
- Ahmadi, T. S., Wang, Z. L., Green, T. C., Henglein, A., & El-Sayed, M. (1996). Shape-Controlled synthesis of colloidal platinum nanoparticles, Science, 272, 19241926.
- Ahmed, M. J., Murtaza, G., Mehmood, A., & Bhatti, T. M. (2015). Green synthesis of silver nanoparticles using leaves extract of *Skimmia laureola*: Characterization and antibacterial activity. *Materials Letters*, 153, 10–13.
- Alexandre, M., & Dubois, P. (2000). Polymer-layered silicate nanocomposites: preparation, properties and uses of a new class of materials. *Materials Science and Engineering*, 28, 1–63.

- Alvarez, M. V., Ortega-Ramirez, L., Gutierrez-Pacheco, M. M., Bernal-Mercado, A. T., Rodriguez-Garcia, I., Gonzalez-Aguilar, G. A., Ponce, A., Moreira, M. R., Roura, S. I., & Ayala-Zavala, J. F., (2014). Oregano essential oil-pectin edible films as anti-quorum sensing and food antimicrobial agents. *Frontiers in Microbiology*, 5, 699-1, 699-7. doi: 10.3389/fmicb.2014.00699.

- Andradea, C.T., Simão, R.A., Thire, R.M.S.M., & Achete, C.A. (2005). Surface modification of maize starch films by low-pressure glow 1-butene plasma. *Carbohydrate Polymers*, 61, 407–413.

- Arvanitoyannis, I., Kalichevsky, M., Blanshard, J. M. V., & Psomiadou, E. (1994). Study of diffusion and permeation of gases in undrawn and uniaxially drawn films made from potato and rice starch conditioned at different relative humidities. *Carbohydrate Polymer*, 24, 1-15.

- Avérous, L., & Pollet, E. (2012). Biodegradable polymers. In L. Avérous & E. Pollet (Eds), Environmental Silicate Nano-Biocomposites (pp. 13-39). *Springer-Verlag*, London. ISBN: 978-1-4471-4101-3. DOI: 10.1007/978-1-4471-4108-2_2.

- Avila-Sosa, R., Hernández-Zamoran, E., López-Mendoza, I., Palou, E., Jiménez Munguía, M. T., Nevárez-Moorillón, G. V., & López-Malo, A. (2009). Fungal Inactivation by Mexican Oregano (*Lippia berlandieri Schauer*) Essential Oil Added to Amaranth, Chitosan, or Starch Edible Films. *Journal of Food Sicience*, 75, (3), M127-M133.

- Avila-Sosa, R., Palou, E., Jiménez Munguía, M. T., Nevárez-Moorillón, G. V., Navarro Cruz, A. R., & López-Malo, A. (2012). Antifungal activity by vapor contact of essential oils added to amaranth, chitosan, or starch edible films. *International Journal of Food Microbiology*, 153, 66-72.

- Azeredo, H.M.C. (2009). Nanocomposites for food packaging applications, Review. *Food Research International*, 42, 1240–1253.

- Azizi Samir, M. A. S.; Chazeau, L.; Alloin, F.; Cavaille, J. Y.; Dufresne, A.; & Sanchez, J. Y. (2005). POE–based nanocomposite polymer electrolytes reinforced with cellulose whiskers. *Electrochimica Acta*, 50 (19), 3897-3903.

- Baghizadeh, A., Ranjbar, S., Kumar, V., Asif, M., Pourseyedi, S., Karimi, M. J., & Mohammadinejad, R. (2015). Green synthesis of silver nanoparticles using seed extract of *Calendula officinalis* in liquid phase. *Journal of Molecular Liquids*, 207, 159-163.

- Barrera, J.E., Rodríguez, J.A., Perilla, J. E., & Algecira, N. A. (2007). A study of poly(vinyl alcohol) thermal degradation by thermogravimetry and differential thermogravimetry. *Revista de Ingeniería e Investigación*, 27(2), 100-105.

- Barret, B. (2003). Medicinal properties of Echinacea: A critical review. *Phytomedicine*, 10, 66–86.

- Baswa, M., Rath, C. C., Dash, S. K., & Mishra, R. K. (2001). Antibacterial activity of Karanj (*Pongamia pinnata*) and Neem (*Azadirachta indica*) seed oil: a preliminary report. *Microbiology*, 105, 183-189.

- Benavides, S., Villalobos-Carvajal, R., & Reyes, J.E. (2012). Physical, mechanical and antibacterial properties of alginate films: Effect of the crosslinking degree and oregano essential oil concentration. *Journal of food engineering*, 110, 232-239.

- Bin, Y., Mine, M., Koganemaru, A., Jiang, X., & Matsuo, M. (2006). Morphology and mechanical and electrical properties of oriented PVA–VGCF and PVA–MWNT composites. *Polymer*, 47, 1308-1317.

- Bizot, H., Le Bail, P., Leroux, B., Roger, P. & Bulkon, A. (1997). Calorimetric evaluation of the glass transition in hydrated, linear and branched polyanhydroglucose compounds. *Carbohydx Polym*. 32, 33-50.

- Bogracheva, T. Y., Wang, Y. L., Wang, T. L. & Hedley, C. L. (2002). Structural studies of starches with different water contents. *Biopolymers*, 64,268-281.

- Boyle, D. L., Sofos, J. N., & Maga, J. A. (1988). Inhibition of spoilage and pathogenic microorganisms by liquid smoke from various woods. *Lebensmittel-Wissenschaft & Technologie*, 21, 54–58.

- Bonilla, J., Aratés, L., Vargas, M., & Chiralt, A. (2013). Properties of wheat starch film-forming dispersions and films as affected by chitosan addition. *Journal of Food Engineering*, 114, 303-312.

- Bryaskova, R., Pencheva, D., Kale, G. M., Lad, U., & Kantardjiev, T. (2010) Synthesis, characterisation and antibacterial activity of PVA/TEOS/Ag-Np hybrid thin films. *Journal of Colloid and Interface Science*, 349, 77–85.

- Burt, S. (2004). Essential oils: their antibacterial properties and potential applications in foods—a review. *International Journal of Food Microbiology*, 94, 223– 253.

- Burt, S.A., & Reinders, R.D. (2003). Antibacterial activity of selected plant essential oils against Escherichia coli O157:H7. *Letters in Applied Microbiology*, 36 (3), 162- 167.

- Campos, C. A., Gerschenson, L. N., & Flores, S. K. (2011). Development of edible films and coatings with antimicrobial activity. *Food and Bioprocess Technology*, 4(6), 849–875.

- Carvalho, A. J. F. (2008). Starch: major sources, properties and applications as thermoplastic materials. In M. N. Belgacem & A. Gandini (Eds.), Monomers, polymers and composites from renewable resources (pp. 321–342). Elsevier, Amsterdam.

- Carvalho, A. J. F., Curvelo, A. A. S., & Agnelli, J. A. M. (2001). A first insight on composites of thermoplastic starch and kaolin. *Carbohydrate Polymers*, 45(2), 189-194.

- Castro-Mayorga, J. L., Martínez-Abad, A., Fabra, M. J., Olivera, C., Reis, M., & Lagarón, J. M. (2014). Stabilization of antimicrobial silver nanoparticles by apolyhydroxyalkanoate obtained from mixed bacterial culture. *International Journal of Biological Macromolecules*, 71, 103–110.

- Chang, Y. P., Cheah, P. B., & Seow, C. C. (2000). Plasticizing-antiplasticizing effects of water on physical properties of tapioca starch films in the glassy state. *Journal of Food Science*, 65, 445-451.

- Chaudhry, Q., Scotter, M., Blackburn, J., Ross, B., Boxall, A., Castle, L., *et al*., (2008). Applications and implications of nanotechnologies for the food sector. *Food Additives and Contaminants*, 25, 241-258.

- Chen, Y., Cao, X., Chang, P.R., & Huneault, M.A. (2008a). Comparative study on the films of poly(vinyl alcohol)/pea starch nanocrystals and poly(vinyl alcohol)/native pea starch. *Carbohydrate Polymers*, 73, 8–17.

- Chen, J., Liu Ch Chen, Y., Chen, Y., & Chang, P. R. (2008b). Structural characterization and properties of starch/konjac glucomannan blend films. *Carbohydrate Polymers*, 74, 946–952.

- Chen, Y., Liu Ch., Chang, P. R., Cao, X., & Anderson, D. P. (2009a). Bionanocomposites based on pea starch and cellulose nanowhiskers hydrolyzed from pea hull fibre: Effect of hydrolysis time. *Carbohydrate Polymers*, 76, 607–615.

- Chen, Y., Liu Ch., Chang, P. R., Anderson, D.P., & Huneault, M.A. (2009b). Pea starch-based composite films with pea hull fibers and pea hull fiber-derived nanowhiskers. *Polymer engineering and Science*, 369-378. DOI 10.1002/pen.21290.

- Chen, N., Li, L., & Wang, Q. (2007). New technology for thermal processing of poly(vinyl alcohol). *Plastics, Rubber and Composites*, 36, 283-290.

- Cheviron, P., Gouanvé, F., & Espuche, E., (2014). Green synthesis of colloid silver nanoparticles and resulting biodegradable starch/silver nanocomposites *Carbohydrate Polymers*, 108, 291-298.

- Corrales, M., Fernández, A., & Han, J.H. (2014). Chapter 7, Antimicrobial packaging systems. In J. H. Han (Ed.), Innovations in food packaging (second edition) (pp. 133-170). *Academia Press: San Diego*, CA, USA.

- Corti, A., Cinelli, P., D'Antone, S., Kenawy, E-R., & Solaro, R. (2002). Biodegradation of poly(vinyl alcohol) in soil environment: influence of natural organic fillers and structural parameters. *Macromolecular Chemistry and Physics*, 203, 1526-1531.

- Cruz, I., Cheetham, J. J., Arnason, J. T., Yack, J. E., & Smith, M. L. (2014). Alkamides from *Echinacea* disrupt the fungal cell wall-membranecomplexI. *Phytomedicine*, 21, 435-442.

- Cyras, V. P., Manfredi, L. B., Ton-That, M. T., & Vazquez, A. (2008). Physical and mechanical properties of thermoplastic starch/montmorillonite nanocomposite films. *Carbohydrate Polymers*, 73, 55–63.

- Da Matta, M. D., Silveira, S. B., de Oliveira, L. M., & Sandoval, S. (2011). Mechanical properties of pea starch films associated with xanthan gum and glycerol. *Starch*, 63, 274-282.
- Dalmas, F., Cavaille, J. Y., Gauthier, C., Chazeau, L., & Dendievel, R. (2007). Viscoelastic behavior and electrical properties of flexible nanofiber filled polymer nanocomposites. Influence of processing conditions. *Composites Science and Technology*, 67, 829–839.
- Darroudi, M., Ahmad, M. B., Zamiri, R., Zak, AK., Abdullah, A. H., & Ibrahim, N. A. (2011). Time-dependent effect in green synthesis of silver nanoparticles. *International Journal of Nanomedicine*, 6, 677-681.
- DeMerlis, C.C., & Schoneker, D.R. (2003). Review of the oral toxicity of polyvinyl alcohol (PVA). *Food and and Chemical Toxicology*, 41, 319–326.
- De Moura, M. R., Mattoso, L. H. C., & Zucolotto, V. (2012). Development of cellulose-based bactericidal nanocomposites containing silver nanoparticles and their use as active food packaging. *Journal of Food Engineering*, 109, 520-524.
- Divakar, M. C., Rao, S. B., Nair, G. R. N., & Hisham, A. (2001). The role of fatty acids on the ulcer healing property of the nimbidin fraction of the neem oil. *Journal of Medical Aromatic Plant Science*, 23, 404-408.
- Du, Y. H., Jia, Y., Yin, Z. Q., Pu, Z. H., Chen, J., Yang, F., Zhang, Y. Q., & Lu, Y. (2008). Acaricidal activity of extracts of neem (*Azadirachta indica*) oil against the larvae of the rabbit mite *Sarcoptes scabiei* var. cuniculi *in vitro*. *Veterinary Parasitology*, 157, 144-148.
- Du, Y. H., Li, J. L., Jia, R. Y., Yin, Z. Q., Li, X. T., Lv, C., Ye, G., Zhang, L., & Zhang, Y. Q. (2009). Acaricidal activity of four fractions and octadecanoic acid-tetrahydrofuran-3,4-diyl ester isolated from chloroform extracts of neem (*Azadirachta indica*) oil against *Sarcoptes scabiei* var. cuniculi larvae *in vitro*. *Veterinary Parasitology*, 163, 175-178.
- Dubief, D.; Samain, E.; & Dufresne, A. (1999). Polysaccharide microcrystals reinforced amorphous poly (hydroxyloctanoate) nanocomposite materials. *Macromolecules*, 1999, 32, 5765.

- Duran, N., Marcarto, P. D., De Souza, G. I. H., Alves, O. L., & Esposito, E. (2007). Antibacterial effect of silver nanoparticles produced by fungal process on textile fabrics and their effluent treatment. *Journal of Biomedical Nanotechnology*, 3, 203-208.

- Durrani, C. M., & Donald, A. M. (1995). Physical characterisation of amylopectin gels. *Polym. Gels Networlrs*, 3, l-27.

- Elsabee, M. Z., & Abdou, E.S. (2013).Chitosan based edible films and coatings: A review. *Materials Science and Engineering C*, 33, 1819-1841.

- Emamifar, A., Kadivar, M., Shahedi, M., & Solaimanianzad, S., (2010). Evaluation of nanocomposite packaging containing Ag and ZnO on the shelf life of fresh orange juice. *Innovative Food Science and Emergin Technology*, 11, 742-748.

- Emiroğlu, Z. K., Yemiş, G. P., Coşkun, B. K., & Candoğan, K. (2010). Antimicrobial activity of soy edible films incorporated with thyme and oregano essential oils on fresh ground beef patties. *Meat Science*, 86, 283–288.

- Ernest, V., Shiny, P.J., Mukherjee, A., & Chandrasekaran, N. (2012). Silver nanoparticles: a potential nanocatalyst for the rapid degradation of starch hydrolysis by a-amylase. *Carbohydrate Research*, 352, 60-64.

- Espinosa Solís, V. (2008). Thesis: Estudios estructurales de almidón de fuentes no convencionales: Mango (*Mangifera indica L.*) y plátano (*Musa paradisiaca L.*). (2008). Director: Bello Pérez, L.A. Instituto Politécnico Nacional, Yartepec, Morelos.

- European Commission. (2010). COMMISSION DIRECTIVE (EU). Nº 2010/67/EU of 20 October 2010 on laying down specific purity criteria on food additives other than colours and sweeteners. L277, 17-26.

- European Commission. (1994). European parliament and council directive 94/36/EC of 30th June 1994 on colours for use in foodstuffs.

- European Parliament. (2008). Regulation 1334/2008 of the European Parliament and of the Council of 16 December 2008 on flavourings and certain food ingredients with flavouring

properties for use in and on foods and amending Council Regulation 1601/91, Regulations 2232/96 and 110/2008 and Directive 2000/13/EC. Off. J. Eur. Comm. L354, 34_50.

- European Standard EN 1186-1:2002. Materials and articles in contact with foodstuffs. Plastics. Guide to the selection of conditions and test methods for overall migration.
- Farjana, A., Zerin, N., & Kabir, Md. S. (2014). Antimicrobial activity of medicinal plant leaf extracts against pathogenic bacteria. *Asian Pacific Journal of Tropical Disease*, 4(2), S920-S923.
- FDA. (1997). USFDA, Grape Seed Extract GSE Notification Generally Recognized As Safe Exemption Claim from the Requirement for Premarket Approval Pursuant to Proposed, 21 CFR 170.36.
- FDA. (2004). Agency Response Letter GRAS Notice No. GRN 000141 (Polyvinyl Alcohol). U.S. Food and Drug Administration (FDA). April 28, 2004.
- FDA/CFSAN (2010). Listing of food additive status: Silver nitrate-172.167, U. FDA/CFSAN, Editor.
- Famá, L., Gerschenson, L., & Goyanes, S. (2009). Starch-vegetable fibre composites to protect food products. *Carbohydrate Polymers*, 75, 230-235.
- Forssell, P. M., Helleman, S. H. D., Myllärinen, P. J., Moates, G. K., & Parker, R. (1999). Ageing of rubbery thermoplastic barley and oat starches. *Carbohydrate Polymers*, 39, 43–51.
- Feng, Q. L., Wu, J., Chen, G. Q., Cui, F. Z., Kim, T. N., & Kim, J. O. (2000). A mechanistic study of the antibacterial effect of silver ions on Escherichia coli and *Staphylococcus aureus*. *Journal of Biomedical Materials Research*, 52(4), 662-668.
- Fakhreddin, S., *, Rezaei, M., Zandi, M., & Farahmandghavi, F. (2015). Fabrication of bio-nanocomposite films based on fish gelatin reinforced with chitosan nanoparticles. *Food Hydrocolloids*, 44, 172-182.
- Fortunati, E., Armentano, I., Zhou, Q., Puglia, D., Terenzi, A., Berglund, L.A. & Kenny, J.M. (2012a). Microstructure and nanoisothermal cold crystallization of PLA composites based on

silver nanoparticles and nanocrystalline cellulose. *Polymer Degradation and Stability*, 97, 2027-2036.

- Fortunati, E., Armentano, I., Zhou, Q., Iannoni, A., Saino, E., Visai, L. & Berglund, L.A. (2012b). Multifunctional bionanocomposite films of poly(lactic acid), cellulose nanocrystals and silver nanoparticles. *Carbohydrate polymers*, 87, 1596-1605.

- Fortunati, E., Peltzer, M., Armentano, I., Torre, L., Jiménez, A., & Kenny, J.M. (2012c). Effects of modified cellulose nanocrystals on the barrier and migration properties of PLA nano-biocomposites. *Carbohydrate Polymers*, 90, 948-956.

- Fortunati, E., Peltzer, M., Armentano, I., Jiménez, A. & Kenny, J.M. (2013a). Combined effects of cellulose nanocrystals and silver nanoparticles on the barrier and migration properties of PLA nano-biocomposites. *Journal of Food Engineering*, 118, 117-124.

- Fortunati, E., Puglia, D., Luzi, F., Santulli, C., Kenny, J.M. & Torre, L. (2013b). Binary PVA bio-nanocomposites containing cellulose nanocrystals extracted from different natural sources: Part I. *Carbohydrate Polymers*, 97, 825-836.

- Galliard, T., & Bowler, P. (1987). Morphology and composition of starch. In: T. Galliard (Ed.), Starch: Properties and Potential (pp. 55-78). *John Wiley & Sons*, New York, NY.

- García, D., Ramos, A. J., Sanchis, V., & Marín, S. (2012). Effect of *Equisetum arvense* and *Stevia rebaudiana* extracts on growth and mycotoxin production by *Aspergillus flavus* and *Fusarium verticillioides* in maize seeds as affected by water activity. *International Journal of Food Microbiology*, 153, 21–27.

- García, D., Ramos, A. J., Sanchis, V., & Marín, S. (2013). *Equisetum arvense* hydro-alcoholic extract: phenolic composition and antifungal and antimycotoxigenic effect against *Aspergillus flavus* and *Fusarium verticillioides* in stored maize. *Journal of the Science of Food and Agriculture*, 93, 2248–2253.

- García, M. A., Pinotti, A., Martimo, M. N., & Zaritzky, E. (2009). Characterization of starch and composite edible films and coating. In M.E. Embuscado & K.C. Huber (Eds.), Edible Films and

Coatings for Food Applications (pp. 169-209). *Springer Science + Business Media*, *LLC*, London. ISBN 978-0-387-92823-4. DOI 10.1007/978-0-387-92824-1_6.

- García, M. A., Martino, M. N., & Zaritzky, N. E. (2000). Microstructural characterization of plasticized starch-based films. *Starch/Starke*, 52, 118–124.

- Ghosh, S., Kaushik, R., Nagalakshmi, K., Hoti, S. L., Menezes, G.A., Harish, B. N. & Vasan, H. N. (2010). Antimicrobial activity of highly stable silver nanoparticles embedded in agar–agar matrix as a thin film. *Carbohydrate Research*, 345, 2220-2227.

- Habibi, Y., Lucia, L.A. & Rojas, O.J. (2010). Cellulose Nanocrystals: Chemistry, self-assembly, and applications. *Chemical Reviews*, 110(6), 3479-3500.

- Han, J. H., Seo, G. H., Park, I. M., Kim, G. N., & Lee, D. S. (2006). Physical and mechanical properties of pea starch edible films containing beeswax emulsions. *Journal of Food Science*, 71(6), 290–296.

- Hassabo, A. G., Nada, A. A., Ibrahim, H. M., & Abou-Zeid, N. H. (2015). Impregnation of silver nanoparticles into polysaccharide substrates and their properties. *Carbohydrate Polymers*, 122, 343-350.

- Hleba, L., Vuković, N., Horská, E., Petrová, J., Sukdolak, S., & Kačániová, M. (2014). Phenolic profile and antimicrobial activities to selected microorganisms of some wild medical plant from Slovakia. Asian Pacific Journal of Tropical Disease, 4(4), 269-274.

- Hoover, R. (2001). Composition, molecular structure, and physicochemical properties of tuber and root starches: a review. *Carbohydrate Polymers*, 45, 253-267.

- Hoque, M.D. M., Bari, M.L., Inatsu, Y., Juneja, V.K., & Kawamoto, S. (2007). Antimbacterial activity of Guava (*Psidium guajava L.*) and Neem (*Azadirachta indica A. Juss*.). Extracts against foodborne pathogens and spoilage bacteria. *Foodborne Pathogens and Disease*, 2007, 4(4), 481-488. doi:10.1089/fpd.2007.0040.

- Hosseini, S.F., Rezaei, M., Zandi, M., & Farahmandghavi, F. (2015). Fabrication of bio-nanocomposite films based on fish gelatin reinforced with chitosan nanoparticles. *Food Hydrocolloids*, 44, 172-182.

- Hu, Y., Wang, Q., & Tang, M. (2013). Preparation and properties of Starch-g-PLA/poly (vinyl alcohol) composite film. *Carbohydrate Polymers*, 96, 384-388.

- Jahan, T., Begum, Z.A., & Sultana, S. (2007). Effect of neem oil on some pathogenic bacteria. *Bangladesh Journal Pharmacology*, 2, 71-72.

- JECFA (2004). The Joint FAO/WHO Expert Committee on Food Additives (JECFA). Polyvinyl alcohol (PVA). Chemical and Technical Assessment (CTA). 61st JECFA meeting, Rome, 10-19 June 2003.

- Jiang, X., Jiang, T., Gan, L., Zhang, X., Dai, H., & Zhang, X. (2012). The plasticizing mechanism and effect of calcium chloride on starch/poly(vinyl alcohol) films. *Carbohydrate Polymers*, 90, 1677e1684.

- Jiménez, A. (2014). Propiedades de films de almidón de maíz. Influencia de la incorporación de lípidos, biopolímeros y compuestos bioactivos, Thesis. Directors: Chiralt, A., Talens, P., & Fabra, M.J. Universitat Politècnica de València, Spain.

- Jiménez, A., Fabra, M.J., Talens, P., & Chiralt, A. (2012a). Edible and Biodegradable Starch Films: A Review. *Food Bioprocess Technology*, 5, 2058–2076. DOI 10.1007/s11947-012-0835-4.

- Jiménez, A., Fabra, M. J., Talens, P., & Chiralt, A. (2012b). Effect of re-crystallization on tensile, optical and water vapour barrier properties of corn starch films containing fatty acids. *Food Hydrocolloids*, 26, 302–310.

- Jiménez, A., Fabra, M. J., Talens, P., & Chiralt, A. (2012c). Effect of sodium caseinate on properties and ageing behaviour of corn starch based films. *Food Hydrocolloids*, 29(2), 265–271.

- Jiménez, A., Fabra, M. J., Talens, P., & Chiralt, A. (2012d). Influence of hydroxypropylmethylcellulose addition and homogenization conditions on properties and ageing of corn starch based films. *Carbohydrates Polymers*, 89, 676-686.

- Jiménez, A., Sánchez-González, L., Desorbry, S., Chiralt, A., & Tehrany, E. A. (2014). Influence of nanoliposomes incorporation on properties of film forming dispersions and films based on corn starch and sodium caseinate. *Food Hydrocolloids*, 35, 159-169.
- Jiménez, A., Fabra, M. J., Talens, P., & Chiralt, A. (2013a). Phase transitions in starch based films containing fatty acids. Effect on water sorption and mechanical behaviour. *Food Hydrocolloids*, 30, 408-418.
- Jiménez, A., Fabra, M. J., Talens, P., & Chiralt, A. (2013b). Physical properties and antioxidant capacity of starch–sodium caseinate films containing lipids. *Journal of Food Engineering*, 116, 695–702.
- John, M.J., & Thomas S. (2008). Review: Biofibres and biocomposites. *Carbohydrate Polymers*, 71, 343-364.
- Jouki, M., Yazdi, F.T., Mortazavi, S.A., & Koocheki, A. (2014). Quince seed mucilage films incorporated with oregano essential oil: physical, thermal, barrier, antioxidant and antibacterial properties. *Food Hydrocolloids*, 36, 9-19.
- Kampeerapappun, P., Aht-ong, D., Pentrakoon, D., & Srikulkit, K. (2007). Preparation of cassava starch/montmorillonite composite film. *Carbohydrate Polymers*, 67, 155–163.
- Kanmani, P., & Rhim, J-W. (2014). Physicochemical properties of gelatin/silver nanoparticle antimicrobial composite films. *Food Chemistry*, 148, 162-169.
- Kanmani, P., & Lim, S. T. (2013). Synthesis and characterization of pullulan-mediated silver nanoparticles and its antimicrobial activities. *Carbohydrate Polymers*, 97, 421– 428.
- Khanna, P. K., Singh, N., Charan, S., Subbarao, V. V. V. S., Gokhale, R., & Mulik, U. P. (2005). Synthesis and characterization of Ag/PVA nanocomposite by chemical reduction method. *Materials Chemistry and Physics*, 93, 117–121.
- Kim, J-H., Choi, Y-G., Kim, S.R.B., & Lim, S-T. (2014). Humidity stability of tapioca starch e pullulan composite films. *Food Hydrocolloids*, 41, 140-145.
- Klasen, H.J. (2000) A historical review of the use of silver in the treatment of burns. II. Renewed interest for silver. *Burns*, 26, 131-138.

- Kristo, E., Koutsoumanis, K. P., & Biliaderis, C.G. (2008). Thermal, mechanical and water vapor barrier properties of sodium caseinate films containing antimicrobials and their inhibitory action on *Listeria monocytogenes*. *Food Hydrocolloids*, 22, 373–386

- Ku, H., Wang, H., Pattarachaiyakoop, N., & Trada, M. (2011). A review on the tensile properties of natural fiber reinforced polymer composites. *Composites*: Part B, 42, 856-873.

- Kuorwel, K. K., Cran, M. J., S., Sonneveld, K., Miltz, J., & Bigger, S. W. (2011). Essential Oils and Their Principal Constituents as Antimicrobial Agents for Synthetic Packaging Films. *Journal of Food Science*, 76 (9), R164-R177.

- Lafargue, D., Lourdin, D., & Doublier, J. L. (2007). Film-forming properties of a modified starch/k-carrageenan mixture in relation to its rheological behavior. *Carbohydrate Polymers*, 70, 101–111.

- Lambert, R. J. W., Skandamis, P. N., Coote, P. J., & Nychas, G-J. E. (2001). A study of the minimum inhibitory concentration and mode of action of oregano essential oil, thymol and carvacrol. *Journal of Applied Microbiology*, 91, 453-462.

- Lanciotti, R., Gianotti, A., Patrignani, F., Belletti, N., Guerzoni, M.E., & Gardini, F. (2004). Use of natural aroma compounds to improve shelflife and safety of minimally processed fruits. *Trends in Food Science & Technology*, 15, 201–208.

- Latha, m., Sumathi, M., Manikandan, R., Arumugam, A., & Prabhu, N. M. (2015). Biocatalytic and antibacterial visualization of green synthesized silver nanoparticles using *Hemidesmus indicus. Microbial Pathogenesis*, 82, 43-49.

- Lee, P. C., & Meisel, D. J. (1982). Adsorption and Surface-Enhanced Raman of Dyes on Silver and Gold Sols. *Journal of Physical Chemestry*, 86, 3391-3395.

- Lee, S-Y., Mohan, D.J., Kang, I-A., Doh, G-H., Lee, S., & Han, S.O. (2009). Nanocellulose Reinforced PVA Composite Films: Effects of Acid Treatment and Filler Loading. *Fibers and Polymers*, 10(1), 77-82.

- Lemire, J.A., Harrison, J.J. & Turner, J. (2013). Antimicrobial activity of metals: mechanisms, molecular targets and applications. *Nature Reviews Microbiology*, 11, 371–384. doi:10.1038/nrmicro3028

- Li, X., Tabil, L.G., Panigrahi, S., & Crerar, W.J. (2009). The influence of fiber content on properties of injection molded flax fiber-HDPE biocomposites. *Can Biosyst Eng* 148, 1–10.

- Li, W-R., Xie, X-B., Shi, Q-S., Zeng, H-Y., OU-Yang, Y-S., & Chen, Y-B. (2010). Antibacterial activity and mechanism of silver nanoparticles on Escherichia coli. *Applied Microbiology and Biotechnology*, 85, 1115-1122.

- Liau, S. Y., Read, D. C., Pugh, W. J., Furr, J. R., & Russell, A. D. (1997). Interaction of silver nitrate with readily identifiable groups: Relationship to the antibacterial action of silver ions. *Letters in Applied Microbiology*, 25(4), 279-283.

- Lin, C-A., & Kub, T-H. (2008). Shear and elongational flow properties of thermoplastic polyvinyl alcohol melts with different plasticizer contents and degrees of polymerization. *Journal of materials processing technology*, 200, 331–338.

- Lin, S., Chen, L., Huang, L., Cao, S., Luo, X., & Liu, K. (2015). Novel antimicrobial chitosan–cellulose composite films bioconjugated with silver nanoparticles. *College Industrial Crops and Products*, 70, 395-403.

- Lingbeck, J. M., Cordero, P., O'Bryan, C. A., Johnson, M. G., Ricke, S. C., & Crandall, P. G. (2014). Review, Functionality of liquid smoke as an all-natural antimicrobial in food preservation. *Meat Science*, 97, 197–206.

- Liu, H., Du, Y., Wang, X., & Sun, L. (2004). Chitosan kills bacteria through cell membrane damage. *International Journal of Food Microbiology*, 95 (2), 147-155.

- López, P., Sánchez, C., Batlle, R., & Nerin, C. (2007). Development of Flexible Antimicrobial Films Using Essential Oils as Active Agents. *J. Agric. Food Chem*., 55 (21), 8814-8824.

- Lourdin, D., Della Valle, G., & Colonna, P. (1995). Influence of amylose content on starch films and foams. *Carbohydrate Polymers*, 27(4), 261–270.

- Ludueña, L. N., Alvarez, V. A., & Vasquez, A. (2007). Processing and microstructure of PCL/clay nanocomposites. *Materials Science and Engineering*: A, 121–129.

- Luo, X., Li, J., & Lin, X. (2012). Effect of gelatinization and additives on morphology and thermal behavior of cornstarch/PVA blend films. *Carbohydrate Polymers*, 90, 1595-1600.

- Mahmoudian, S., Wahit, M. U., Ismail, A. F., & Yussuf, A. A. (2012). Preparation of regenerated cellulose/montmorillonite nanocomposite films via ionic liquids. *Carbohydrate Polymers*, 88, 1251-1257.

- Mahoney, N. & Molyneux, R. J., (2004). Phytochemical inhibition of aflatoxigenicity in *Aspergillus flavus* by constituents of walnut (*Juglans regia*). *Journal of Agriculture and Food Chemestry*, 52, 1882-1889.

- Malkapuram, R., Kumar, V., & Yuvraj, S. N. (2008). Recent development in natural fibre reinforced polypropylene composites. *Journal of Reinforced Plastics and Composites*, 28, 1169–1189.

- Martín, E. M., O'Bryan, C. A., Lary Jr., R. Y., Griffis, C. L., Vaughn, K. L. S., Marcy, J. A., Ricke, S. C., & Crandall, P. G. (2010). Spray application of liquid smoke to reduce or eliminate Listeria monocytogenes surface inoculated on frankfurters. *Meat Science*, 85, 640–644.

- Martínez-Abad, A. (2014a). Development of Silver Based Antimicrobial Films for Coating and Food Packaging Applications, Doctoral Thesis. Supervised by: M. J. Ocio, & J. M. Lagarón. Universitat Politècnica de València, Spain.

- Martucci, J. F., Gende, L. B., Neira, L. M., & Ruseckaite, R. A. (2015). Oregano and lavender essential oils as antioxidant and antimicrobialadditives of biogenic gelatin films. *Industrial Crops and Products*, 71, 205–213.

- Massey, L.K. (2004). Polyvinyl alcohol-PVOH. In L.K. Massey (Ed.), Films properties of plastics and elastomers, 2nd edition (pp. 149-152). *Plastics Design Library*, United State of America, USA.

- Matan, N., Rimkeeree, H., Mawson, A.J., Chompreeda, P., Haruthaithanasan, V., & Parker, M., (2006). Antimicrobial activity of cinnamon and clove oils under modified atmosphere conditions. *International Journal of Food Microbiology*. 107, 180-185.

- Mohanty, S., Mishra, S., Jena, P., Jacob, B., Sarkar, B., & Sonawane, A. (2012). An investigation on the antibacterial, cytotoxic, and antibiofilm efficacy of starch-stabilized silver nanoparticles. *Nanomedicine: Nanotechnology, Biology, and Medicine*, 8, 916–924.

- Mohapatra, B., Kuriakose, S., & Mohapatra, S. (2015). Rapid green synthesis of silver nanoparticles and nanorods using *Piper nigrum* extract. *Journal of Alloys and Compounds*, 637, 119-126.

- Mondragón, M., Arroyo, K., & Romero-García, J. (2008). Biocomposites of thermoplastic starch with surfactant. *Carbohydrate Polymers*, 74, 201–208.

- Morales, J., Morán, J., Quintana, M., & Estrada, W. (2009). Synthesis and characterization of silver nanoparticles by Sol-Gel route from silver nitrate. *Rev Soc Quim Peru*, 75 (2), 177-184.

- Moreno, O., Pastor, C., Muller, J., Atarés, L., González, C., & Chiralt, A. (2014). Physical and bioactive properties of corn starch – Buttermilk edible films. *Journal of Food Engineering*, 141, 27–36.

- Morones, J. R., Elechiguerra, J. L., Camacho, A., & Ramirez, J. T. (2005). The bactericidal effect of silver nanoparticles. *Nanotechnology*, 16, 2346-53.

- Muriel-Galet, V., Cran, M. J., Bigger, S. W., Hernández-Muñoz, P., & Gavara, R. (2015). Antioxidant and antimicrobial properties of ethylene vinyl alcohol copolymer films based on the release of oregano essential oil and green tea extract components. *Journal of Food Engineering*, 149, 9-16.

- Myllärinen, P., Buleon, A., Lahtinen, R., & Forssell, P. (2002). The crystallinity of amylose and amylopectin films. *Carbohydrate Polymers*, 48, 41–48.

- Nasrollahzadeh, M., Sajadi, S. M., Babaei, F., & Mahamd, M. (2015). *Euphorbia helioscopia Linn* as a green source for synthesis of silver nanoparticles and their optical and catalytic properties. *Journal of Colloid and Interface Science*, 450, 374-380.

- Neto, E. A. B., Ribeiro, C., & Zucolotto, V. (2008). Síntese de Nanopartículas de Prata para Aplicação na Sanitização de Embalagens. Comunicadp técnico, 99. Sao Pablo, SP. ISSN 1517-4786.

- Newberne, P., Smith, R. L., Doull, J., Feron, V. J., Goodman, J. I., Murno, I. C., Portoghese, P. S., Waddel, W. J., Wagner, B. M., Weil, C. S., Adams, T. B., & Hallagan, J. B. (2000). GRAS flavouring substances. *Food Technology*, 54, 66–83.

- Pal, S., Tak, Y. K., & Song, J. M. (2007). Does the antibacterial activity of silver nanoparticles depend on the shape of the nanoparticle? A study of the Gram-negative bacterium Escherichia coli. *Applied and Environmetal Microbiology*, 73, 1712-1720.

- Park, J. W., Im, S.S., Kim, S. H., & Kim, Y.H. (2000). Biodegradable Polymer Blends of Poly(L-lactic acid) and Gelatinized Starch. *Polymer Engineering and Science*, 40 (12), 2593-2550.

- Patel, R. P., & Trivedi, B. M. (1962). The *in vitro* antibacterial activity of some medicinal oils. *Indian Journal of Medical Research*, 8, 218-222.

- Phan The, D., Debeaufort, F., Voilley, A., & Luu, D. (2009). Biopolymer interactionsaffect the functional properties of edible films based on agar, cassava starch and arabinoxylan blends. *Journal of Food Engineering*, 90, 548–558.

- Pourjavadi, A., & Soleyman, R. (2011). Silver nanoparticles with gelatin nanoshells: photochemical facile green synthesis and their antimicrobial activity. *Journal of Nanoparticles Research*, 13, 4647-4658.

- Pszczola, D.E. (1995). Tour highlight production and uses of smoke based flavors. Food Technology, 49, 70–74.

- Pšeja, J., Charvátová, H., Hruzík, P., Hrnčiřík, J., & Kupec, J. (2006). Anaerobic Biodegradation of Blends Based on Polyvinyl Alcohol. *Journal of Polymers and the Environment*, 14,185-190.

- Pu, Z-h., Zhang, Y-q., Yin, Z-q., Xu, J., Jia, R-y., Lu, Y., & Yang, F. (2010). Antibacterial Activity of 9-Octadecanoic Acid-Hexadecanoic Acid- Tetrahydrofuran-3,4-Diyl Ester from Neem Oil. *Agricultural Sciences in China*, 9(8), 1236-1240.

- Qiao, R., & Brinson, C. (2009). Simulation of interphase percolation and gradients in polymers nanocomposites. *Composite Science and Technology*, 69, 491-499.

- Radulovic, N., Stojanovic, G., & Palic, R. (2006). Composition and antimicrobial activity of *Equisetum arvense L*, essential oil. *Phytotherapy Research,* 20, 85-88.

- Rai, M., Yadav, A., & Gade, A. (2009). Silver nanoparticles as a new generation of antimicrobials. *Biotechnology Advances*, 27, 76–83.

- Raimondi, F., Scherer, G. G., Kotz, R., & Wokaun, A. (2005). Nanoparticles in energy technology: examples from electochemistry and catalysis. Angewandte Chemmie International Edition, 44, 2190-209.

- Rajan, A., Vilas, V., & Philip, D. (2015). Catalytic and antioxidant properties of biogenic silver nanoparticles synthesized using *Areca catechu* nut. *Journal of Molecular Liquids*, 207, 231–236.

- Ramaraj, B. (2007). Crosslinked Poly(vinyl alcohol) and Starch Composite Films. II. Physicomechanical, Thermal Properties and Swelling Studies. *Journal of Applied Polymer Science*, 103, 909-916.

- Rankin, J. C., Wolff, I. A., Davis, H. A., & Rist, C. E. (1958). Permeability of amylose film to moisture vapor, selected organic vapors, and the common gasses. *Industrial, Engineering and Chemistry*, 3,120-123.

- Rao, D. V. K., Singh, I., & Chopra, P. (1986). *In vitro* antibacterial activity of neem oil. *Indian Journal of Medical Research*, 6, 314-316.

- Ratnayake, W. S., & Jackson, D. S. (2007). A new insight into the gelatinization process of native starches. *Carbohydrate Polymers*, 67, 511–529.

- Raveendran, P., Fu, J., & Wallen, S.L. (2003). Completely “green” synthesis and stabilization of metal nanoparticles. *Journal of the American Chemical Society*, 125 (46), 13940-13941.

- Reis, R.L., Cunha, A.M., Allan, P.S., & Bevis, M.L. (1997). Mechanical behaviour of injection moulded starch-based polymers. *Polymer for Advanced Technology*, 16, 263–77.

- Reis, K.C., Pereira, J., Smith, A.C., Carvalho, C.W.P., Wellner, N., & Yakimets, I. (2008). Characterization of polyhydroxybutyrate-hydroxyvalerate (PHB-HV)/maize starch blend films. Journal of Food Engineering, 89, 361-369.

- Rhim, J. W., Wang, L. F., & Hong, S. I. (2013). Preparation and characterization of agar/silver nanoparticles composite films with antimicrobial activity. *Food Hydrocolloids*, 33, 327-335.

- Rindlav, A., Hulleman, S. H. D., & Gatenholm, P. (1997). Formation of starch films with varying crystallinity. *Carbohydrate Polymers*, 34, 25–30.

- Rindlav-Westling, A., Stading, M., Hermansson, A. M., & Gatenholm, P. (1998). Structure, mechanical and barrier properties of amylose and amylopectin films. *Carbohydrate Polymers*, 36, 217–224.

- Rojas-Graü, M. A., Avena-Bustillos, R. J., Olsen, C., Friedman, M., Henika, P. R., Martín-Belloso, O., Pan, Z., & McHugh, T. H. (2007). Effects of plant essential oils and oil compounds on mechanical, barrier and antimicrobial properties of alginate–apple puree edible films. *Journal of Food Engineering*, 81, 634-641.

- Romero-Bastida, C.A., Bello-Pérez, L.A., Velázquez, G., & Álvarez-Ramírez, J. (2015). Effect of the addition order and amylose content on mechanical, barrier and structural properties of films made with starch and montmorillonite. *Carbohydrate Polymers*, 127, 195–201.

- Roller, S., & Covill, N. (1999). The antifungal properties of chitosan in laboratory media and apple juice. *International Journal of Food Microbiology*, 47, 67–77.

- Roy, K., Sarkar, C. K., & Ghosh, C. K. (2015). Photocatalytic activity of biogenic silver nanoparticles synthesized using potato (*Solanum tuberosum*) infusion. *Spectrochimica Acta*, Part A: Molecular and Biomolecular Spectroscopy, 146, 286-291.

- Sadaka, F., Nguimjeu, C., Brachais, C-H., Vroman, I., Tighzert, L., & Couvercelle, J-P. (2014). Review on antimicrobial packaging containing essential oils and their active biomolecules. *Innovative Food Science and Emerging Technologies*, http://dx.doi.org/10.1016/j.ifset.2014.03.002.

- Saloko, S., Darmadji, P., Setiajic, B., & Pranoto, Y. (2014). Antioxidative and antimicrobial activities of liquid smoke nanocapsules using chitosan and maltodextrin and its application on tuna fish preservation. *Food Bioscience*, 7, 71-79.

- Samapundo, S., De Meulenaer, B., Osei-Nimoh, D., Lamboni, Y., Debevere, J. & Devlieghere, F. (2007). Can phenolic compounds be used for the protection of corn from fungal invasion and mycotoxin contamination during storage? *Food Microbiology*, 24, 465-473.

- Sánchez-González, L., González-Martínez, C., Chiralt, A., & Cháfer, M. (2011). Use of Essential Oils in Bioactive Edible Coatings. *Food Engineering Review*, 3, 1–16.

- Sedlarik, V., Galya, T., Sedlarikova, J., Valasek, P., & Saha, P. (2010). The effect of preparation temperature on the mechanical and antibacterial properties of poly(vinyl alcohol)/silver nitrate films. *Polymer Degradation and Stability*, 95, 399-404.

- Seydim, A. C., & Sarikus, G. (2006). Antimicrobial activity of whey protein based edible films incorporated with oregano, rosemary and garlic essential oils. *Food Research International*, 39, 639-644.

- Sharma, V.K., Yngard, R.A., & Lin, Y. (2009). Silver nanoparticles: Green synthesis and their antimicrobial activities. *Advances in Colloid and Interface Science*, 145, 83–96.

- Shi, R., Bi, J., Zhang, Z., Zhu, A., Chen, D., Zhou, X., Zhang, L., & Tian, W. (2008). The effect of citric acid on the structural properties and cytotoxicity of the polyvinylalcohol/starch films when molding at high temperature. *Carbohydrate Polymer*, 74, 763–770.

- Shi, A., Wang, L., Li, D., & Adjikari, B. (2013): Characterization of starch films containing starch nanoparticles Part 1: Physical and mechanical properties. *Carbohydrate Polymers*, 96, 593–601.

- Shihabudeen, M. H., Priscilla, D. H., & Thirumurugan, K. (2010). Antimicrobial activity and phytochemical analysis of selected Indian folk medicinal plants. *International Journal Pharmaceutical Science and Research*, 1, 430-434.

- Shukla, M. K., Singh, R. P., Reddy, C. R. K., & Jha, B. (2012). Synthesis and characterization of agar-based silver nanoparticles and nanocomposite film with antibacterial applications. *Bioresource Technology*, 107, 295–300.

- Siddaramaiah, Raj, B., & Somashekar, R. (2004). Structureeproperty relation in polyvinyl alcohol/starch composites. *Journal of Applied Polymer Science*, 9, 630-635.

- Silver, S. (2003). Bacterial silver resistance: molecular biology and uses and misuses of silver compounds. *FEMS Microbiology Reviews*, 27, 341-353.

- Smith, A. M. (2001). The biosynthesis of starch granules. *Biomacromolecules*, 2(2), 335–341.

- Smith-Palmer, A., Stewart, J., & Fyfe, L. (2001). The potential application of plant essential oils as natural food preservatives in soft cheese. *Food Microbiology*, 18, 463-470.

- Sofos, J. N., Maga, J. A., & Boyle, D. L. (1988). Effect of ether extracts from condensed wood smokes on the growth of *Aeromonas* hydrophila and *Staphylococcus aureus*. *Journal of Food Science*, 53, 1840–1843.

- Sondi, I., & Salopek-Sondi, B. (2007). Silver nanoparticles as antimicrobial agent: a case study on *E. coli* as a model for gram-negative bacteria. *Journal of Colloid and Interface*, 275, 177-82.

- Song, H. Y., Ko, K. K., Oh, L. H., & Lee, B. T. (2006). Fabrication of silver nanoparticles and their antimicrobial mechanisms. *European Cells and Materials*, 2006, 11-58.

- Sorrentino, A., Gorrasi, G., & Vittoria, V. (2007). Potential perspectives of bionanocomposites for food packaging applications. *Trends in Food Science & Technology*, 18(2), 84-95.

- Sreekumar, P. A., Al-Harthi, M. A., & De, S. K. (2012). Studies on compatibility of biodegradable starch/polyvinyl alcohol blends. *Polymer Engineering and Science*, 52(10), 2167-2172.

- Stanisavljević, I., Stojičević, S., Veličković, V., & Lazić, M. (2009). Antioxidant and Antimicrobial Activities of Echinacea (*Echinacea purpurea L.*) Extracts Obtained by Classical and Ultrasound Extraction. *Chinese Journal of Chemical Engineering*, 17(3), 478-483.

- Sudheesh-Kumar, P. T., Abhilash, S., Manzoor, K., Nair, S.V., Tamura, H., & Jayakumar, R. (2010).Preparation and characterization of novel b-chitin/nanosilver composite scaffolds for wound dressing applications. *Carbohydrate Polymers*, 80, 761–767.

- Tammineni, N., Ünlü, G., & Min, S. C. (2013). Development of antimicrobial potato peel waste-based edible films with oregano essential oil to inhibit Listeria monocytogenes on cold-smoked salmon, short communication. *International Journal of Food Science and Technology*, 48, 211–214.

- Tang, H., Xiong, H., Tang, S., & Zou, P. (2009). A starch-based biodegradable film modified by nano silicon dioxide. *Journal of Applied Polymer Science*, 113(1), 34-40.

- Tang, S., Zou, P., Xiong, H., & Tang, H. (2008). Effect of nano-SiO2 on the performance of starch/polyvinyl alcohol blend films. *Carbohydrate Polymers*, 72, 521-526.

- Tang, X., & Alavi, S. (2011). Review, Recent advances in starch, polyvinyl alcohol based polymer blends, nanocomposites and their biodegradability. *Carbohydrate Polymers*, 85, 7–16.

- Talja, R. A., Peura, M., Serimaa, R., & Jouppila, K. (2008). Effect of amylose con-tent on physical and mechanical properties of potato-starch-based edible films. *Biomacromolecules*, 9, 658–663.

- Torres-Castro, A., González, V. A., Garza, M., & Gauna, E. (2011). Síntesis de nanocompósitos de plata con almidón. *Ingenierías*, 50 (14), 34-41.

- Tunc, S., & Duman, O. (2010). Preparation and characterization of biodegradable methyl cellulose/montmorillonite nanocomposite films. *Applied Clay Science*, 48, 414-424.

- Utama, I. M. S., Willis, R. B. H., Ben-Yehoshua, S., & Kuek, C. (2002). In vitro efficacy of plant volatiles for inhibiting the growth of fruit and vegetable decay microorganisms. *Journal of Agricultural and Food Chemistry*, 50, 6371–6377.

- Valencia, A., Rivera, C., & Murillo, E.A. (2013). Estudio de las propiedades de mezclas de alcohol polivinílico-almidón de yuca-sorbitol obtenidas por casting. *Revista Colombiana de Materiales*, 4, 41-55.

- Vanka, A., Tandon, S., Rao, S. R., Udupa, N., & Ramkumar, P. (2001). The effect of indigenous Neem (*Adirachtaindica*) mouth wash on *Streptococcus mutans* and *lactobacilli* growth. *Indian Journal of Dental Research*, 12, 133-144.

- Vásconez, M. B., Flores, S. K., Campos, C. A., Alvarado, J., & Gerschenson, L. N. (2009). Antimicrobial activity and physical properties of chitosan–tapioca starch based edible films and coatings. *Food Research International*, 42,762–769.

- Vázquez, A., & Álvarez, V. A. (2009). Starch-cellulose fiber composites. In L. Yu (Ed.), Biodegradable polymer blends and composites from renewable resources (pp. 241–286). *Wiley*, New York.

- Vigneshwaran, N., Nachane, R. P., Balasubramanya, R. H., & Varadarajan, P. V. (2006). A novel one-pot 'green' synthesis of stable silver nanoparticles using soluble starch. *Carbohydrate Research*, 341, 2012-2018.

- Vimala, K., Murali, Y., Varaprasad, K., Narayana, N., Ravindra, S., Sudhakar, N., & Mohona, K. (2011). Fabrication of Curcumin Encapsulated Chitosan-PVA Silver Nanocomposite Films for Improved Antimicrobial Activity. *Journal of Biomaterials and Nanobiotechnology*, 2, 55-64.

- Vimala, K., Mohan, M., Sivudu, S., Varaprasad, K, Ravinadra, S., Narayana Reddya, N., Padmab, Y., Sreedharc, B., & MohanaRajua, K. (2010). Fabrication of porous chitosan films impregnated with silver nanoparticles: A facile approach for superior antibacterial application. *Colloids and Surfaces B: Biointerfaces*, 76, 248-258.

- Whistler, R. L. (1984). History and future expectation of starch use. In R. L. Whistler, J. N. BeMiller & E. F. Paschall (Eds), Starch: Chemistry and Technology (pp. 1-9). *Academic Press*, New York, NY.

- Wiley, B., Sun, Y., Mayers, B., & Xi, Y. (2005). Shape-Controlled Synthesis of Metal Nanostructures: The Case of Silver. *Chemestry, a European Journal*, 11, 454-463.

- Wu, H.-C. H. & Sarko, A. (1978a). The double-helical molecular structure of crystalline B-amylose. *Carbohydrate Research*, 61, 27-40.

- Wu, H.-C. H. & Sarko, A. (1978b). The double-helical molecular structure of crystalline B-amylose. *Carbohydrate Research*, 61, 7-25.

- Wu, H., Liu, Ch., Chen, J., Chen, Y., Anderson, D. P., & Chang, P. R. (2010). Oxidized pea starch/chitosan composite films: Structural characterization and properties. *Journal of Applied Polymer Science*, 118, 3082–3088.

- Wu, J., Ge, S., Liu, H., Wang, S., Chen, S., Wang, J., Li, J., & Zhang, Q. (2014). Properties and antimicrobial activity of silver carp (Hypophthalmichthys molitrix) skin gelatin-chitosan films incorporated with oregano essential oil for fish preservation. *Food packaging and shelf life*, 2, 7-16.

- Xu, J., Du, Y. H., Yin, Z. Q., Li, X. T., Jia, R. Y., Wang, K. Y., Lv, C., Fan, Q. J., Ye, G., Geng, Y., *et al*. (2010). The preparation of neem oil microemulsion (*Azadirachta indica*) and the comparison of acaricidal time between neem oil microemulsion and other formulations *in vitro*. *Veterinary Parasitology*, 164 (3-4), 399-403.

- Yoksan, R., & Chirachanchai, S. (2010). Silver nanoparticle-loaded chitosan–starch based films: Fabrication and evaluation of tensile, barrier and antimicrobial properties. *Materials Science and Engineering*, C 30, 891-897.

- Yoon, S-D., Chough, S-H., & Park, M-H. (2006). Effects of Additives with Different Functional Groups on the Physical Properties of Starch/PVA Blend Film. *Journal of Applied Polymer Science*, 100, 3733–3740.

- Yoon, S-D., Park, M-H., & Byun, H-S. (2012). Mechanical and water barrier properties of starch/PVA composite films by adding nano-sized poly(methyl methacrylate-co-acrylamide) particles. *Carbohydrate Polymers*, 87, 676- 686.

- Yu, L., Deana, K., & Lib, L. (2006). Polymer blends and composites from renewable resources. *Progress in Polymer Science*, 31, 576–602.

- Zahran, M.K., Ahmed, B., & El-Rafie, M. H. (2014). Facile size-regulated synthesis of silver nanoparticles using pectin. *Carbohydrate Polymers*, 111, 971-978.

- Zeng, H., Gao, C., Wang, Y., Watts, P. C. P., Kong, H., Cui, X., *et al*. (2006). In situ polymerization approach to multiwalled carbon nanotubes-reinforced nylon 1010 composites: mechanical properties and crystallization behavior. *Polymer*, 47, 113–122.

- Zhang, W., Yang, X., Li, C., Liang, M., Lu, C., & Deng, Y. (2011). Mechanochemical activation of cellulose and its thermoplastic polyvinyl alcohol ecocomposites with enhanced physicochemical properties. *Carbohydrate Polymers*, 83, 257–263.

- Zhao, G. J., & Stevens, S. E. (1998). Multiple parameters for the comprehensive evaluation of the susceptibility of Escherichia coli to the silver ion. *Biometals*, 11, 27–32.

- Zhong, F., Li, Y., Ibanz, A. M., Oh, M. H., Mckenzie, K. S., & Shoemaker, C. (2009). The effect of rice variety and starch isolation method on the pasting and rheological properties of rice starch pastes. *Food Hydrocolloids*, 23, 406–414.

- Zhou, J., Ma, Y., Ren, L., Tong, J., Liu, Z., & Xie, L. (2009). Preparation and characterization of surface crosslinked TPS/PVA blend films. *Carbohydrate Polymers*, 76, 632–638.

- Zinanovic, S., Chi, S., & Draughon, A.F. (2005). Antimicrobial activity of Chitosan films enriched with essential oils. *Journal of Food Science*, 70 (1), M45–M51.

Visited websites:

- European Bioplastics, Institute for Bioplastics and Biocomposites, nova-Institute, 2014, http://en.european-bioplastics.org

- Federal Food, Drug and Consmetic Act (FDA). (2011). GRAS Notice No. GRN 000397. http://www.fda.gov

- Plastics Europe. (2014). Plastics-the Facts 2014/2015. An analysis of European plastics production, demand and waste data. http://www.plasticseurope.org

- Starch Europe, 2013, http://www.starch.eu

II. Objectives

OBJECTIVES

General objective

The main objective of the Thesis was to improve the functional properties of starch based films by using different strategies: blends with other polymers (PVA), the incorporation of different kinds of fillers (rice brand, different nanoparticles) and antimicrobial compounds to provide the starch materials with active properties. The application of biopolymer coatings to a food product was also considered as an objective of the Thesis.

Specific objectives

- To analyse the influence of the different amylose:amylopectin ratios on the properties of films obtained from three different starches (pea, potato and cassava) after different storage times in order to compare their structure and physical behaviour.
- To analyse the effect of blending different ratios of PVA and pea starch on the structure, thermal behaviour, physical properties and ageing of blend films, in order to elucidate possible beneficial effects on the starch film properties.
- To study the incorporation of filler materials in terms of their structure, thermal behaviour and physical properties after different ageing times in order to improve the physical behaviour of starch or starch-PVA films. On the one hand, the addition of rice bran of two different particle sizes, as a film filler in pea, potato and cassava films was studied and, on the other hand, the incorporation of cellulose nanocrystals into pea starch-PVA blend films was considered.

- To evaluate the effect of the incorporation of bioactive substances from natural source (silver nanoparticles, neem oil and oregano essential oil) into starch-PVA-based films in order to develop new biodegradable active films.
- To elucidate the effect of the different bioactive substances on the disintegration and biodegradability processes of starch-PVA films.
- To study the effect of chitosan coatings containing rosemary and oregano essential oils on the quality and shelf-life of semi-hard goat's milk cheeses.

III. Chapters

Chapter I: Effect of amylose:amylopectin ratio and rice bran addition on starch film properties.

Amalia I. Cano, Alberto Jiménez, Maite Cháfer, Chelo González-Martínez, Amparo Chiralt. **Characterization of starch films with different amylose:amylopectin ratio. Effect of rice bran addition.** *Carbohydrate Polymers*, 111, **2014**, 543-555.

Abstract

The influence of the amylose:amylopectin ratio on the properties of pea, potato and cassava starch (with a high, intermediate and low amylose-amylopectin ratio, respectively) films and the effect of the incorporation of rice bran of two different particle sizes were studied. The structural, mechanical (elastic modulus, tensile strength and percentage of elongation at break), optical (gloss and internal transmittance) and barrier (water vapour permeability and oxygen permeability) properties of the films were analysed after 1 and 5 weeks under controlled storage conditions (25 ºC and 53 %RH). The properties of the films were affected by both amylose-amylopectin ratio and storage time. The high content of amylose gave rise to stiffer, more resistant to fracture, but less stretchable films, with lower oxygen permeability and greater water binding capacity. Although no changes in the water vapour permeability values of the films were observed during storage, their oxygen permeability decreased. Throughout storage, films became stiffer, more resistant to break, but less stretchable. Rice bran with the smallest particles improved the elastic modulus of the films, especially in high amylose content films, but reduced the film stretchability and its barrier properties, due to the enhancement of the water binding capacity and the introduction of discontinuities (fibre particles) in the matrix.

Keywords: Pea, potato, cassava, rice bran, storage, microstructure.

1. INTRODUCTION

Conventional plastics are synthetic polymers derived from petroleum whose residues are not easily assimilated in the environment. This fact has led to the increasing use of biodegradable raw materials to obtain biodegradable plastics as an alternative to petroleum-derived polymers in different sectors, such as agricultural, medical or pharmaceutical. Nowadays, the use of films or edible coatings based on biodegradable polymers is increasing because these materials are environmentally friendly (Chen, *et al.*, 2008, Mehyar & Han, 2004) and exhibit properties which can become similar to those observed in conventional plastics (Jiménez *et al*., 2012a; Famá *et al*., 2007; Rindlav-Westling *et al*., 1998).

Materials for biodegradable packaging are classified according to their molecular structure; polysaccharides, proteins and fats are the most widely used (Falguera *et al*., 2011; Adebiyi *et al.*, 2008; Nam *et al*., 2007; Mehyar & Han, 2004; Gnanasambandam, *et al*., 1997). Of the polysaccharides, starch, cellulose and their derivates are very commonly studied as film-forming compounds (Jiménez *et al*., 2012a; Chen *et al*., 2009a).

Starch is a polysaccharide from cereals (corn, wheat or rice), legumes (pea) and tubers (potato or cassava). It has a granular structure and is composed of two macromolecules: amylose and amylopectin. Amylose is a lineal polymer formed by glucose units linked by α-(1,4) whereas amylopectin is a highly branched polymer of glucose units with ramifications in α-(1,6). The amylose:amylopectin ratio depends on the source of starch and this ranges from 15:85 to 35:65, except in waxy starch and high amylose corn starch whose amylose content is about 5 % and 50-80 % respectively (Liu, 2005) . It is known that both polymers are responsible for the starch crystallization which

leads to changes in the mechanical response (increased stiffness) of starch products (Talja *et al*., 2007).

Starch is used to obtain films because of its high availability and great ability to form an odourless, colourless and transparent (Vásconez *et al*., 2009) polymer matrix with low oxygen permeability, which is very interesting for food preservation (Jiménez *et al*., 2012a; Dole *et al*., 2004; Han *et al*., 2006; Liu, 2005). It is also especially attractive because of its biodegradability and low cost (Han *et al*., 2006; Chen *et al*., 2008; Lafargue *et al*., 2007). Nevertheless, starch films present some drawbacks: unstable mechanical properties due to the retrogradation phenomenon and a relatively high water vapour permeability (Lafargue *et al*., 2007; Chen *et al*., 2008; Phan The *et al*., 2009; Wu *et al*., 2010).

In starch films, the retrogradation phenomenon over time, can greatly affect not only their mechanical properties but also their barrier capacity. So, the study of changes occurring during their storage is necessary to ensure their functionality at different times after processing. Different authors have studied the development of properties of starch films. Jiménez *et al*. (2012b) studied the effect of re-crystallization on physical properties of corn starch films containing fatty acids and concluded that fatty acid incorporation did not notably improve water vapour permeability while the degree of crystallinity of the matrix increased during storage time. In order to improve properties of the starch films different strategies are used by different authors. Da Matta *et al*. (2011) evaluated mechanical properties of edible films made from wrinkled pea starch rich in amylose combined with xanthan gum and glycerol and they observed that the increase in xanthan gum concentration did not affect the physical and mechanical properties of the films. For potato starch films, Zhang *et al*. (2011) studied how cellulose fibre and potato pulp affected the properties of thermoplastic starch. The addition of fibre did not affect the film glass transition. Nevertheless, moisture content, surface tension and the hydrophilic

character of films increased in line with the fibre content. Souza *et al*. (2011) stated that films based on glycerol and clay nanoparticles as reinforcement are an interesting biodegradable alternative as packaging material. Famá *et al*. (2009) also studied the influence of wheat bran on physicochemical characteristics of cassava starch films and concluded that the mechanical properties and water vapour permeability of starch-wheat bran composites improved when the fibre content rose.

One of the means of improving the barrier and mechanical properties of starch films is through the incorporation of natural fibres from plant origin as fillers. In this sense, Chen *et al*. (2009a) used pea hull fibre nanoparticles in pea starch films, which improved film transparency, tensile strength, elongation at break and water barrier properties due to the high content of cellulose crystalline regions and the interactions between the nanofibre and the starch matrix. Famá *et al*. (2009) introduced wheat bran as filler in cassava starch matrices, thus improving their mechanical and water vapour permeability.

Bran rice is a by-product of rice which is obtained from rice bleaching and it represents about 10% of the grain weight. Rice bran contains good quality biological proteins, fats and starch. Depending on the variety of rice and the type of processing, rice bran contains about 15-20 % fat, 12-16 % protein, 23-28 % fibre and 7-10 % ash (Sánchez *et al*., 2004). In addition, bran has a high vitamin B and E complex (as α-tocopherol) content (Carroll, 1990).

Despite its interesting composition, rice bran is not given the importance it deserves since it is only used in animal food. Nevertheless, in recent years, attempts have been to reappraise it by studying applications in different areas. In this way, rice bran has been evaluated as a source of oil (Nikolosi *et al*., 1990), protein concentrates (Gnanasambandam & Hettiarachache, 1995) and as a matrix of edible films (Dias *et al*., 2010; Adebiyi *et al*., 2008; Gnanasambandam *et al*., 1997).

The aim of this work was to analyse the influence of the amylose:amylopectin ratio on the properties of films obtained from three different (pea, potato and cassava) starches, with different ratios of both polymers and the effect of the addition of rice bran with two different particle sizes, as a film filler. Structural, mechanical, optical and barrier properties of the films were analysed at different storage times (1 and 5 weeks) in order to compare their behaviour and functionality.

2. MATERIALS AND METHODS

2.1. Materials

Pea (PE) and potato (PO) starch were purchased from Roquette (Lestrem, France) and cassava starch (CAS) obtained from Asia Modified Starch CO; LDT (Kalasin, Thailand). Rice bran obtained from Arrocería Antonio Tomás, S.L. (Sollana, Valencia, Spain). Glycerol, used as plasticizer, was provided by Panreac Química S.A. (Castellar de Vallès, Barcelona, Spain).

2.2. Amylose-amylopectin ratio

Amylose-amylopectin ratio in each starch (pea, potato and cassava) was determined in triplicate, by using an Amylose/Amylopectin Assay Procedure enzymatic kit which was purchased from Megazyme (Wicklow, Ireland).

2.3. Rice bran particle size

To select particle size, rice bran was sieved to obtain two different bran fractions. The smallest particle size fraction that pass through the 100 μm mesh and the coarse fraction contained between mesh 250 and 100 μm were obtained and used for film preparation. The smallest particle bran is named “Fine” (F) and the other bran fraction is called “Coarse” (C).

The rice bran particle size, surface weighted mean diameter ($D_{3,2}$, Eq. 1) and volume weighted mean diameter ($D_{4,3}$, Eq. 2) were determined in bran aqueous dispersions, in triplicate, with a laser light scattering instrument (Malvern Instruments Ltd, Worcestershire, U.K.). Particle size measurements were taken for two different fractions. To this end, bran fraction was dispersed in aqueous medium and measurements were taken with ultrasonic homogenization to maintain the sample homogeneity.

$$D_{4,3} = \frac{\sum n_i d_i^4}{\sum n_i d_i^3} \quad (1)$$

$$D_{3,2} = \frac{\sum n_i d_i^3}{\sum n_i d_i^2} \quad (2)$$

2.4. Compositional analysis of rice bran

Moisture content (MC) was determined from sample weight loss when samples were introduced into a convection oven at 100 ºC for 24 h and, afterwards, equilibrated in desiccators with P_2O_5 for 2 weeks until constant weight.

Ash content was obtained by applying the gravimetric method 104/1 of the International Association for Cereal Science and Technology (ICC, 1990). The rice bran was introduced into a muffle "Select-Horn" (J.P. Selecta; Abrera, Barcelona, Spain) at 910ºC for 15 min.

Protein content was obtained by means of the method of analysis 105/2 (ICC, 1994). The crude protein content was obtained by multiplying the nitrogen content, determined by the Kjeldahl procedure, using the factor F=5.95. A digestion unit “Bloc-digest” (J.P. Selecta; Abrera, Barcelona, Spain) and a Kjeldahl distiller “Pro-Nitro M” (J.P. Selecta; Abrera, Barcelona, Spain) were used.

Fat content was obtained by using the Soxhlet method 30-20 (ICC, 1967). Samples were firstly dried at 103 ºC and then the fat was extracted by an oil extractor "Det-GrasasN" (J.P. Selecta; Abrera, Barcelona, Spain).

Starch content of the rice bran was determined using the enzymatic Kit "Starch Assay Kit", which was supplied by Sigma (Saint Louis, Missouri, USA).

Fibre percentage was estimated from the difference between the total percentage of the rest of the analysed components and 100, assuming that starch is the only carbohydrate.

2.5. Preparation of films

For preparation of starch films, three formulations based on distilled water, starch (pea, potato or cassava) and glycerol were prepared. The dispersions contained 2 % w/w of starch whereas the plasticizer was added considering a starch:glycerol ratio of 1:0.25, on the basis of previous studies (Jimenez *et al*., 2012a). In the preparation of starch films containing rice bran as filler, six formulations were obtained by using fine (F) or coarse (C) rice bran and starch (pea, potato or cassava) and glycerol. The film forming dispersions were prepared in the same way and with the same glycerol ratio and bran was afterwards incorporated in a starch:rice bran ratio of 1:0.1.

Starch aqueous dispersions were maintained at 95 ºC for 30 min to induce starch gelatinization. Then, glycerol was added and the dispersion was homogenized using a rotor-stator homogenizer (Ultraturrax D125, Janke and Kunkel, Germany) at 13,500 rpm for 1min and 20,500 rpm for 3 min at 95 ºC under vacuum. For starch films containing rice bran, this was incorporated prior to the homogenization step. The film-forming aqueous dispersions were cast into a levelled Teflon casting plates (15 cm diameter) and each film contained 1.5 g of total solids. Films were formed by drying at 25 ºC and 45 % RH for 48 h. Then, they were peeled intact from the plates and were conditioned

at 53 % RH using magnesium nitrate-6-hydrate saturated solution (Panreac química, S.A., Castellar del Vallés, Barcelona, Spain) at 25 ºC until analysis. Their thickness was measured at six random positions with a Palmer digital micrometer to the nearest 0.0025 mm. All films were analysed after one or five storage weeks.

2.6. Characterization of films

2.6.1. X-ray diffraction spectra

X-ray diffraction spectra were obtained using a Diffractometer D8 Advance (Bruker AXS, 230 V, 50 Hz and 6.5 KVA, Karlsruhe, Germany). For this analysis conditioned samples were cut into squares of 4 cm and mounted on a carbon base. Spectra were obtained at 2θ between 5 and 30, using Kα Cu radiation (λ: 1,542 Å), 40 kV and 40 mA with a step size of 0.04982.

2.6.2. Microstructural properties

Microstructural analysis of films was carried out using a scanning electron microscope (SEM) (JEOL®, model JSM-5410, Japan) and an atomic force microscope (AFM) (Multimode 8, Bruker AXS, Inc. Santa Barbara, California, USA) with a NanoScope® V controller electronics. To this end, films were equilibrated in desiccators with P_2O_5 for two weeks to ensure that no water was present in the samples.

SEM observations were carried out on the film surface and in their cross section. To prepare the samples, films were frozen in liquid N_2 and cryofractured to observe the cross section. Samples were fixed on copper stubs, gold coated, and observed using an accelerating voltage of 11 kV. Three replicates per formulation were observed.

AFM with the PeakForce QNM (Quantitative NanoMechanics) was used to analyse surface film nanostructure. Measurements were taken from small areas of the film surface (20x20 µm) and the resulting data were transformed into 2D image of the Log

DMT modulus. Three images were captured per formulation, for samples stored for 1 and 5 weeks.

2.6.3. Moisture Content

To determine film moisture content, five replicates by formulation were dried in a convection oven at 60 ºC for 24 h, and then they were equilibrated with P_2O_5 until constant weight.

2.6.4. Water Vapour Permeability

The water vapour permeability (WVP) of films was determined following the gravimetric method ASTM E96-95 (1995) by using Payne permeability cups (Payne, elcometer SPRL, Hermelle/sd Argenteau, Belgium) of 3.5 cm diameter. The temperature was 25 ºC and the relative humidity gradient was 53-100 %, which was obtained using magnesium nitrate-6-hydrate and pure water, respectively. Cups were introduced into desiccators and these into a temperature-controlled chamber at 25 ºC. Control of cup weights was performed every 2 h using an analytical balance (±0.00001 g). The water vapour transmission (WVTR) was determined from the slope obtained from the regression analysis of weight loss data versus time, once the steady state had been reached, divided by the film areas. For each type of film, WVP measurements were replicated four times.

2.6.5. Oxygen Permeability

The oxygen permeability (OP) was obtained by using an Oxtran System (Mocon, Minneapolis, USA) which determined the oxygen permeation. Measurements were taken at 25 ºC following the standard method (ASTM D3985-05, 2005) at 53 % RH. Film samples (50 cm^2) were introduced into the equipment to perform the assay. Films were exposed to pure oxygen flow on one side and pure nitrogen flow on the other side. An

oxygen sensor read permeation through the film and the rate of oxygen transmission was calculated taking into account the amount of oxygen and the area of sample. Oxygen permeability was calculated by dividing the oxygen transmission by the difference in oxygen partial pressure between the two sides of the film, and multiplying by the average film thickness. At least two replicates per formulation were considered.

2.6.6. Mechanical properties

Mechanical properties were measured with a Universal Test Machine (TA.XT plus, Stable Micro Systems, Haslemere, England) following the ASTM standard method D882 (ASTM, 2001). Force-distance curves were obtained and transformed into stress-strain curves which allowed tensile strength at break (TS), percentage of elongation at break (E, %) and elastic modulus (EM) to be obtained. Eight replicates carried out per formulation. Equilibrated film specimens (2.5 cm wide and 10 cm long) were mounted in the film-extension grips (A/TG model) which were set 50 mm apart. The speed of the testing machine during stretching was 50 mm min^{-1} until breaking.

2.6.7. Optical properties

The opacity of films was determined by applying the Kubelka-Munk theory of multiple dispersion to the reflection spectra (Judd & Wyszecki, 1975; Hutchings, 1999). Internal transmittance (Ti) of the films was quantified using Eq. (3). In this equation R_0 is the reflectance of the film on an ideal black background. Parameters a and b were calculated by Eqs. (4) and (5), where R is the reflectance of the sample layer backed by a known reflectance Rg. The reflection spectrum on the white and black background was determined from 400 to 700 nm with a MINOLTA spectrocolorimeter CM.36000d (Minolta Co. Tokyo, Japan). Measurements were performed in the side of film which was in contact with air during drying and each formulation was analysed in triplicate.

$$T_i = \sqrt{(a - R_0)^2 - b^2} \quad (3)$$

$$a = \frac{1}{2}\left(R + \frac{R_0 - R + R_g}{R_0 R_g}\right) \quad (4)$$

$$b = (a^2 - 1) \quad (5)$$

Gloss measurements were obtained according to the ASTM standard D523 method (ASTM, 1999), using a flat surface gloss meter (Multi-Gloss 268, MINOLTA) at an angle of 60º with respect to the normal to the film surface. Three films of each formulation were measured over a black matte standard plate. Results were expressed as gloss units, relative to a highly polished surface of standard black glass with a value close to 100.

2.7. Statistical Analysis

The analysis of data was performed through variance analysis (ANOVA) using the Statgraphics Plus 5.1. software (Manugistics Corp., Rockville, MD). To discern between samples the Fisher least significant difference (LSD) at the 95 % confidence level was used.

3. RESULTS AND DISCUSSION

3.1. Properties of the starches. Amylose:amylopectin ratio

Properties of starch films, such as mechanical behaviour, depend on the amylose:amylopectin ratio since the different behaviour of amylose and amylopectin molecules contributes to film properties (da Matta *et al*., 2011). The amylose content of pea, potato and cassava starches were 24.9 ± 0.9, 17.9 ± 1.9 and 9 ± 2, respectively with an amylose/amylopectin ratio of 1/3.0, 1/4.6 and 1/9.9, respectively. These values reflect an important difference between these starches, pea starch being the richest in amylose and cassava starch the poorest. Although the obtained values are in the

reported range for the different starches, differences associated to origin or cultivar could be observed. Mehyar & Han (2004); Chen *et al.* (2008); Ma *et al*. (2008) and Zhang & Han (2006) reported amylose contents of between 30 and 40 % in pea starch, which is higher than the values obtained. For potato starch the value obtained coincides with the result reported by Talja *et al*. (2008) whereas it was lower than that reported by Alvani *et al*. (2011). (25.2-29.1 %). For cassava starch, higher amylose contents (19.7 % and 22.5 %) were found by Souza *et al.* (2011). The amylose content will affect the film properties since the phenomenon of recrystallization, which occurs during film formation and storage, has been mainly related with this polymer (Myllärinen *et al*., 2002; Rindlav-Westling *et al*., 1998). This phenomenon is mainly responsible for changes in the mechanical behaviour (increase in the elastic modulus and decrease in the film stretchability) which make the films excessively brittle (Jiménez *et al*., 2012a).

3.2. X-ray diffraction

Figure 1 shows the X-ray diffraction spectra of pure starch films, which were equilibrated at 53 % RH and 25 ºC for 1 and 5 weeks in order to analyse the re-crystallization progress in the films. For starch matrices, the crystalline structure was mainly attributed to the spontaneous recrystallization of amylose molecules after gelatinization (Myllärinen *et al*., 2002; Forssell *et al*., 1999; Rindlav-Westling *et al*., 1998). This process occurs mainly during film drying when the chain mobility is still high due to the water content. Several authors (Rindlav-Westling *et al.*, 1998) report that drying conditions at high relative humidity, or long drying times, greatly promote amylose crystallization, whereas amylopectin shows a retarded crystallization when the molecular mobility in the system is high enough.

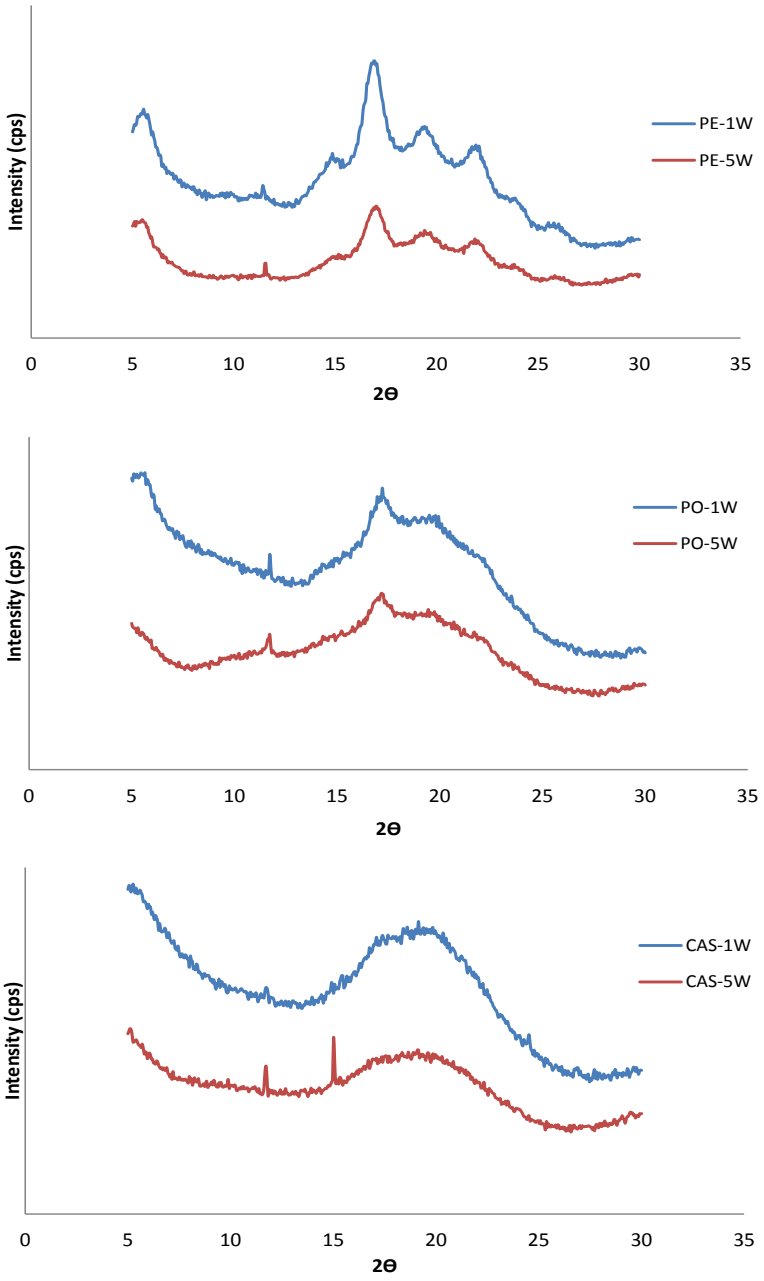

Figure 1. X-Ray diffraction pattern of pea (PE), potato (PO) and cassava (CAS) starch films at one (1W) and five (5W) storage weeks.

After both 1 and 5 weeks of storage, pea starch films exhibited the highest crystallinity, as deduced from the greater intensity of its sharp peaks. On the contrary, the lowest crystallinity was found in cassava starch films, where an amorphous X-Ray diffraction pattern was observed after both storage times. This behaviour can be related

with the different amylose:amylopectin ratio and confirms that the crystallization progress in the films was faster as the amylose content increased. This was also observed by other authors in gelatinized starch (García *et al*., 2000), whereas for native starch the higher crystallinity in granules is associated with a greater content of amylopectin (Cheetham & Tao, 1998).

A typical C-type crystallinity pattern was found in pea starch films. This type of crystallinity is an intermediate form between A and B types, as reported by Carvalho (2008). In this sense, pea starch films showed peaks at 2θ 5.4º (characteristic of B-type polymorphs), 14.8º (characteristic of A-type polymorphs), 16.8º (characteristic of both A and B-type polymorphs) and 19.0º and 21.8º (characteristic of B-type polymorphs). Similar results have been observed by da Matta *et al*. (2011), Wu *et al*. (2010) and Chen *et al*. (2009a). In the case of potato starch films, a typical C-type pattern can also be observed, with peaks at 5.1º, 11.7º and 17.2º of Bragg angle. Nevertheless, the peaks are smaller and less sharp as compared with those obtained in pea starch films, which indicates that the film exhibited a more amorphous character with smaller crystallites (Talja *et al*., 2008). Cassava starch films were mainly amorphous since no sharp peaks were found, as previously observed by other authors (Chen *et al*., 2009b).

Comparisons of difractogrames after 1 and 5 storage weeks allow us to conclude that no significant changes in the crystallinity occur throughout the storage period, probably due to the low moisture content of the films which inhibits the chain mobility to form crystalline associations for both amylose and amylopectin polymers. Different authors (Myllärinen *et al*., 2002) have pointed out that amylose crystallizes very fast during the film formation, whereas the crystallization of amylopectin is a slower process. In the richest amylose starch (pea starch), crystallization had occurred at the first control time (1 week) and probably during the drying period, as reported by other authors (Myllärinen *et al*., 2002; Forssell, *et al*., 1999; Rindlav-Westling *et al*., 1998; Rindlav, *et*

al., 1997). During storage, no notable changes in the X-ray diffraction pattern were observed in any case.

3.3. Microstructural features

SEM and AFM microstructure analyses provide information about the surface morphology and internal microstructure of the films. Figure 2 shows SEM micrographs of the surface and cross section of the different starch films. In general, starch films showed a homogeneous aspect, thus indicating that the gelatinization step was enough to disrupt all the starch granules. Smooth film surfaces were also previously observed by other authors for starch films obtained by casting (Wu *et al*., 2010; Chen *et al*., 2009a; Chen *et al*., 2009b). Nevertheless, in the cross section image, the presence of a heterogeneously-fractured layer on the film surface in the pea starch sample reveals the progress of crystallization in this zone, probably due to the greater molecular mobility associated to the water vapour diffusion near the film surface. The presence of microcracks in cassava starch films is remarkable. This may be due to the electron impact during observation as explained by Jiménez *et al.* (2012c), as a result of the lower mechanical resistance of this sample.

Figure 3 shows AFM images of pea, potato and cassava starch films, obtained by using PeakForce QNM. Raw data were converted into 2D images and their scale is expressed as Log DMT modulus. Differences in the surface mechanical resistance can be observed in the samples at both 1 and 5 storage weeks. The surfaces of pea and potato starch films are rougher, which indicates the co-existence of crystalline (harder) and amorphous (softer) zones. It is remarkable that these zones are wider in pea starch than in potato starch samples, in agreement with the sharper peaks reflected in the X-ray spectra, associated with bigger crystals. No notable differences were appreciated between 1 and 5 storage weeks.

In cassava starch samples, more homogenous, but lower, values of DMT modulus can be observed, due to the more amorphous character of the films. It is remarkable that in these films, a harder surface was detected at 5 storage weeks which reveals that films were significantly hardened (higher values of Modulus) during storage, although no crystallization was detected since the surface appears homogenous. The different behaviour of the starch matrices was coherent with the different amylose:amylopectin ratio, which is associated with a different recrystallization progress during film formation.

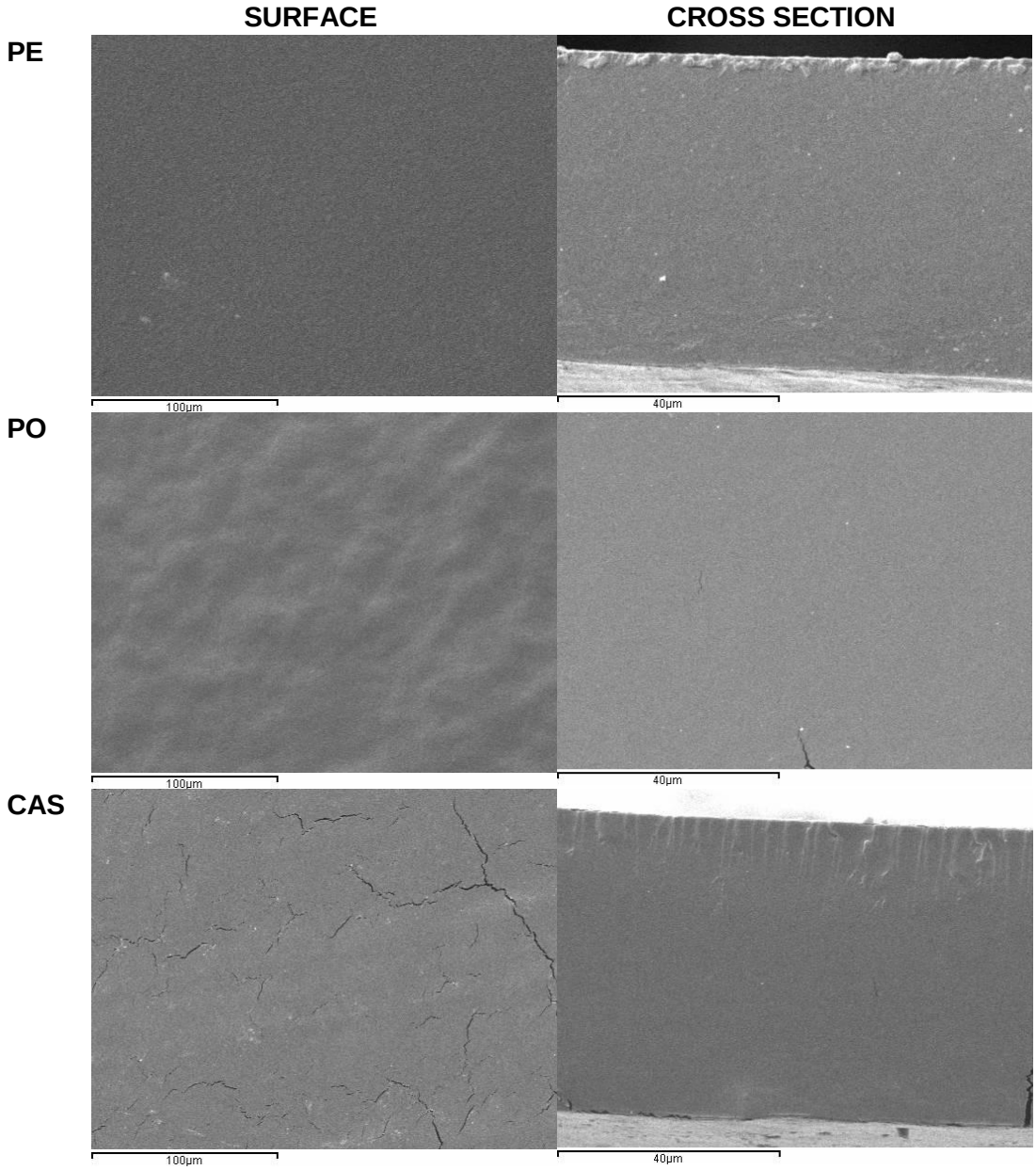

Figure 2. SEM micrographs of surface and cross section of pea, potato and cassava starch films.

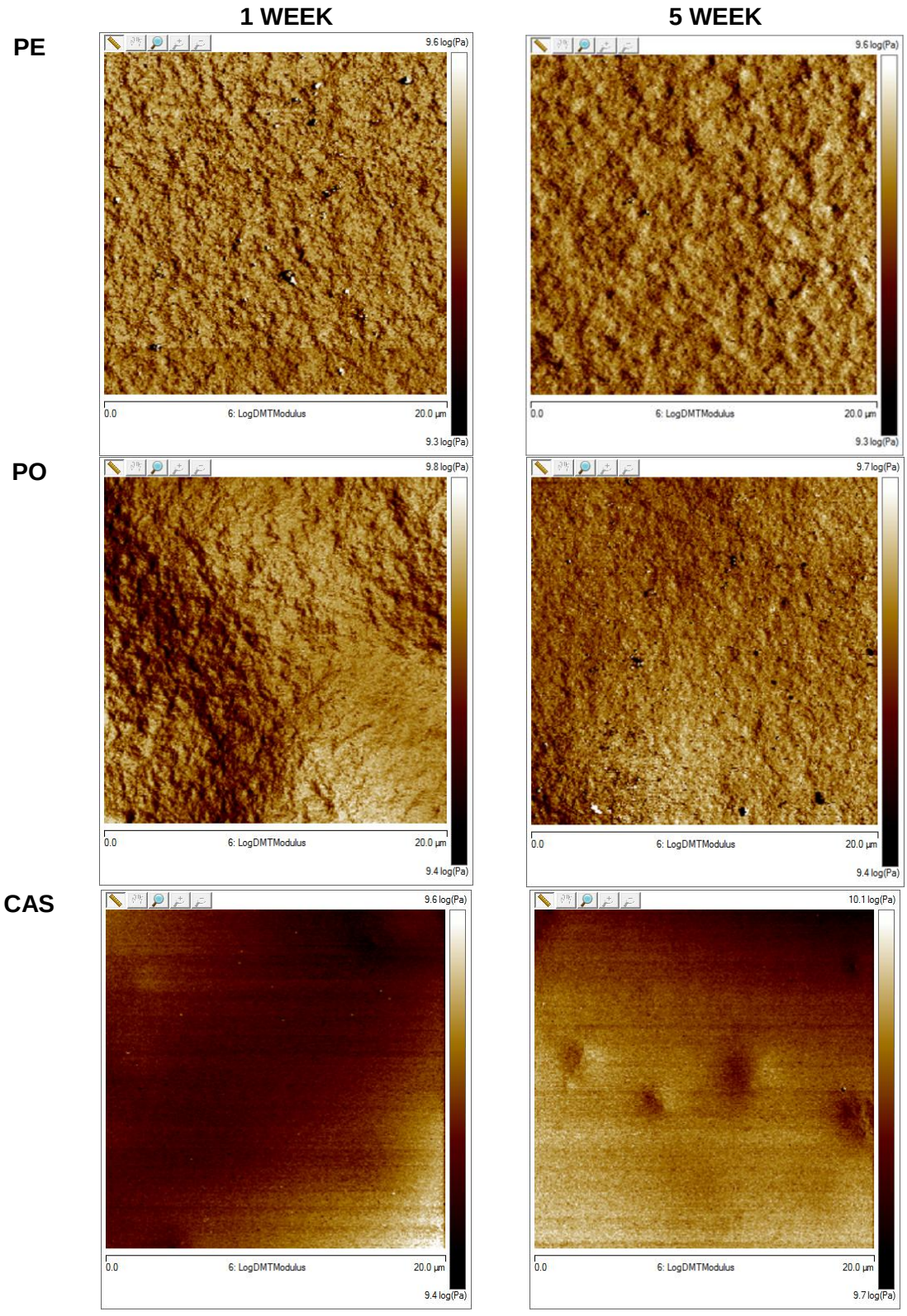

Figure 3. Maps of Log DTM modulus obtained from AFM in surface of pea, potato and cassava starch films for samples stored for 1 and 5 weeks.

3.4. Moisture content and barrier properties

Table 1 shows the moisture content values of the studied films, stored for 1 and 5 weeks at 25 ºC and 53 % RH. The values ranged between 9.9 and 11.4% and pea and potato starch films were the samples which exhibited the highest moisture content, as reported in previous studies (Mehyar & Han, 2004; Kaisangsti, *et al*., 2012). This can be associated with the higher degree of crystallization, since crystalline zones bond a greater amount of water than amorphous zones (Myllärinen *et al.*, 2002; Forssell *et al*., 1999 and Rindlav-Westling *et al*., 1998). Nevertheless, moisture content significantly ($p<0.05$) decreased after 5 storage weeks, when more homogeneous values of moisture content were obtained for the different films. This development indicates that films equilibrate slowly with the conditioning relative humidity, reaching a value closer to the equilibrium by losing water during storage. The water loss will provoke a greater chain aggregation in the amorphous region which will imply an increase in the film compactness that will affect barrier and mechanical properties.

Water vapour permeability (WVP) values define the final application of a film in contact with food systems and they must be as low as possible to avoid water transfer (Ma *et al*., 2008). Table 1 shows WVP values of starch films analysed at 25 ºC and a 53-100 % RH gradient. No significant differences between WVP values of the different films were found at the different storage times, in agreement with results found by other authors (Han *et al*., 2006; Ma *et al*., 2008). The small changes in sample moisture content and the subsequent increase in the matrix compactness did not affect the water vapour barrier properties of the films.

Table 1: Moisture content (MC), water vapour permeability (WVP) and oxygen permeability (OP) of pea (PE), potato (PO) and cassava (CAS) starch films at 1 (1W) and 5 (5W) storage weeks. Films with fine (F) and coarse (C) fractions incorporated to starch films were also included. Mean values and standard deviation.

	MC d.b. (%)		WVP ($g.mm.kPa^{-1}h^{-1}m^{-2}$)		OP($10^{-14}cm^3m^{-1}s^{-1}kPa^{-1}$)	
Film	1W	5W	1W	5W	1W	5W
PE	11.4 ± 0.4^{a1}	8.7 ± 0.4^{a2}	6.0 ± 0.3^{a1}	6.7 ± 0.7^{a1}	3.8 ± 0.3^{a1}	2.7 ± 0.2^{ab2}
PO	11.4 ± 0.7^{a1}	8.5 ± 0.3^{a2}	6.1 ± 0.5^{a1}	7.2 ± 0.2^{a1}	4.55 ± 0.07^{b1}	3.4 ± 0.3^{a2}
CAS	9.9 ± 0.9^{b1}	8.2 ± 0.3^{a2}	5.4 ± 0.4^{a1}	6.8 ± 0.5^{a2}	4.2 ± 0.4^{b1}	2.45 ± 0.12^{b2}
			WITH BRAN			
PE-F	9.99 ± 0.08^{a1}	9.53 ± 0.19^{b2}	6.35 ± 0.18^{a1}	6.3 ± 0.4^{a1}	4.5 ± 0.2^{1}	1.84 ± 0.08^{2}
PE-C	13.1 ± 0.9^{b1}	10.9 ± 0.8^{c2}	7.5 ± 0.9^{b1}	8.6 ± 0.4^{b2}		
PO-F	14.9 ± 1.4^{a1}	10.1 ± 0.9^{b2}	8.1 ± 0.9^{a1}	6.5 ± 0.7^{a2}	4.9 ± 0.2^{1}	3.06 ± 0.19^{2}
PO-C	16.1 ± 0.9^{a1}	11.4 ± 0.8^{c2}	10.3 ± 1.2^{b1}	9.2 ± 0.6^{b2}		
CAS-F	10.3 ± 0.5^{a1}	8.78 ± 1.09^{a2}	7.5 ± 0.4^{a1}	5.1 ± 0.8^{a2}	5.46 ± 0.07^{1}	3.56 ± 0^{2}
CAS-C	12.9 ± 1.2^{b1}	8.1 ± 0.3^{a2}	7.3 ± 0.9^{a1}	8.3 ± 0.2^{b2}		

[a, b, c] Different superscripts within a column indicate significant differences between starch matrix and fine or coarse rice bran in the same matrix. ($p<0.05$).

[1, 2] Different superscripts within the same file indicate significant differences between storage times for the same formulation. ($p<0.05$).

The oxygen permeability (OP) was analysed at 25 ºC and 53% RH in films equilibrated under these conditions for 1 and 5 weeks. Table 1 shows the mean values of OP after the different storage times. For pea starch films, similar values have been reported by Mehyar & Han (2004). After one week, the OP values were significantly lower for films with the highest content of amylose (PE), which indicates that this polymer is mostly responsible for the oxygen barrier ability of the films. This coincides with that reported by García *et al*. (2000) for plasticized corn and amylomaize starch films.

Likewise, Forssell *et al*. (2002) report that unplasticized amylose films exhibited lower oxygen permeability than amylopectin films, regardless of their equilibration at different relative humidities. Nevertheless, the plasticizer content, in combination with the water content, had a great influence on the oxygen permeability values of starch films. After 5 storage weeks, the oxygen permeability values of every film were significantly reduced, coherently with the increase in the matrix compactness, as commented on above. In general, the OP values are very low and, as reported by Wu, *et al*. (2010), one great advantage of starch films is their ability to protect food products by forming an oxygen barrier.

3.5. Mechanical properties

Film properties related to easy film-handling, their fragility or their stretchability, are very interesting from a technological point of view (Jiménez *et al*., 2009). Elastic modulus (EM), tensile strength at break (TS) and percentage of elongation at break (%E) are the usual parameters with which to describe the mechanical behaviour of films, and they are closely related to the film microstructure (McHugh & Krochta, 1994). TS and %E represent the film's resistance to elongation and its stretching capacity, respectively, whereas EM is a measure of the stiffness of films. Table 2 shows the mean values of these mechanical parameters for the films after 1 and 5 storage weeks at 25 ºC and 53% RH. The mechanical behaviour of starch films was similar to that reported by other authors for pea starch films (Chen *et al*., 2008; Da Matta *et al*., 2011), potato starch films (Cyras, *et al*., 2008) and cassava starch films (Famá, *et al*., 2005; Souza *et al*., 2011).

After one week of storage, the mechanical parameter values were significantly different ($p<0.05$) for the three matrices. The pea starch films (with the highest amylose content) have the highest values in break strength and stiffness and the lowest in

stretchability. On the contrary, cassava starch films (with the lowest amylose content) exhibited the lowest break strength values and the highest in stretchability. This indicates the important role played by crystal formation in the mechanical behaviour of the matrix.

Table 2: Elastic modulus (EM), tensile strength at break (TS) and percentage of elongation at break (E, %) of pea (PE), potato (PO) and cassava (CAS) starch films at 1 (1W) and 5 (5W) storage weeks. Films with fine (F) and coarse (C) fractions incorporated to starch films were also included. Mean values and standard deviation.

	EM (MPa)		TS (MPa)		E (%)	
Film	1W	5W	1W	5W	1W	5W
PE	417 ± 41^{a1}	964 ± 88^{a2}	14.2 ± 1.3^{a1}	24 ± 2^{a2}	10 ± 2^{a1}	4.7 ± 0.9^{a2}
PO	40 ± 24^{b1}	430 ± 44^{b2}	3.0 ± 0.8^{b1}	11.6 ± 1.5^{b2}	29 ± 3^{b1}	9.4 ± 1.8^{b2}
CAS	20 ± 7^{b1}	771 ± 171^{c2}	1.7 ± 0.4^{c1}	12.5 ± 1.7^{b2}	48 ± 9^{c1}	1.8 ± 0.5^{c2}
			WITH BRAN			
PE-F	663 ± 229^{a1}	610 ± 72^{a1}	16 ± 7^{a1}	6.5 ± 0.9^{a2}	3.1 ± 0.9^{1a}	1.3 ± 0.2^{2a}
PE-C	618 ± 38^{a1}	579 ± 61^{a1}	13.7 ± 1.5^{a1}	6 ± 3^{a2}	4.3 ± 0.8^{1b}	1.2 ± 0.6^{2a}
PO-F	36 ± 9^{a1}	460 ± 98^{a2}	1.6 ± 0.4^{a1}	5.8 ± 1.4^{a2}	25 ± 13^{1a}	1.6 ± 0.6^{2a}
PO-C	108 ± 49^{b1}	478 ± 94^{a2}	1.8 ± 0.7^{a1}	5.9 ± 1.9^{a2}	9 ± 3^{1b}	1.5 ± 0.3^{2a}
CAS-F	33 ± 9^{a1}	543 ± 137^{a2}	1.2 ± 0.5^{a1}	6 ± 4^{a2}	42 ± 24^{1a}	1.2 ± 0.7^{2a}
CAS-C	43 ± 15^{a1}	387 ± 94^{a2}	1.5 ± 0.7^{a1}	3.57 ± 1.07^{a2}	16 ± 4^{1a}	1.1 ± 0.4^{2a}

[a, b, c] Different superscripts within a column indicate significant differences between starch matrix and fine or coarse rice bran in the same matrix. ($p<0.05$).

[1, 2] Different superscripts within the same file indicate significant differences between storage times for the same formulation. ($p<0.05$).

After 5 weeks of storage, film stiffness and resistance to break increased for all the films, coinciding with the increase in the matrix compactness promoted by water loss. Nevertheless, the highest relative increase occurs for cassava starch films, which could

indicate the formation of very small association zones of amylopectin chains between 1 and 5 weeks. In the same sense, although all the films lost stretchability during storage, it was cassava starch films which experienced the greatest losses due to the greater extent of amylopectin association during the storage period. As previously commented on, amylose rich starch crystallizes very fast during film drying and subsequent conditioning, whereas amylopectin rich films crystallize more slowly, which is reflected in the way that the different films develop mechanical behaviour. Nevertheless, it is remarkable that the films that are richest in amylose (pea starch) showed the highest values of stiffness and resistance to break after long storage times, whereas intermediate amylose films (from potato starch) showed the greatest stretchability after 5 storage weeks.

3.6. Optical properties

The optical properties of the films, gloss and transparency, are directly related with the film microstructure (previously described) and are affected by the surface and internal heterogeneity of the structure (Jiménez *et al*., 2012b). According to Hutchings (1999), the above-mentioned parameters are the best optical properties with which to evaluate the appearance of the films. Table 3 shows the mean values of the internal transmittance (Ti) of films measured at 450 nm. The Ti of films is related to their degree of transparency and structural homogeneity: low Ti values are related to a high structural heterogeneity with a greater opacity. Analyses were carried out in films previously equilibrated at 53 % RH and 25 ºC. After one week of storage, different starch based films did not show any significant differences ($p<0.05$) as regards the Ti values, these being about 85 %. These coincide with those reported in the case of corn starch films by Jiménez *et al*. (2012b). After five weeks, no significant changes in transparency occurred in the films.

Table 3 also shows the mean gloss values of starch films, which were measured at after 1 or 5 weeks' storage at 53 %RH and at an incidence angle of 60º with respect to the normal to the film surface. At initial time, the gloss values of pea starch films were higher than those corresponding with cassava and potato starch films. The differences observed in the film gloss at initial time remained after 5 weeks of storage, since in no case did any significant changes in gloss occur during storage. The higher gloss of pea starch films could be due to the presence of crystalline structures at surface level, as deduced from the SEM micrographs and the higher surface modulus obtained by AFM.

Table 3: Gloss values at 60º and internal transmittance (Ti) of pea (PE), potato (PO),and cassava (CAS) starch films at 1 (1W) and 5 (5W) storage weeks. Films with fine (F) and coarse (C) fractions incorporated to starch films were also included. Mean values and standard deviation.

	60º		Ti (450nm)	
Film	1W	5W	1W	5W
PE	47±17^{a1}	33±8^{a1}	85.4±1.6^{a1}	87.09±0.12^{a1}
PO	9.9±0.9^{b1}	9.7±1.9^{b1}	85.9±0.4^{a1}	85.09±0.54^{a1}
CAS	18±4^{c1}	16±5^{c1}	84.9±0.4^{a1}	86.6±0.4^{b1}
		WITH BRAN		
PE-F	30±4^{b1}	20±5^{a2}	81.7±0.2^{a1}	82.3±0.5^{a1}
PE-C	14±5^{a1}	13.5±1.6^{b1}	81.8±0.5^{a1}	81.5±0.2^{a1}
PO-F	6.5±1.0^{a1}	8.2±0.7^{a2}	79.1±1.4^{a1}	81.35±1.02^{a1}
PO-C	8.75±1.04^{b1}	6.9±0.8^{b2}	80.8±0.4^{a1}	80.6±0.7^{a1}
CAS-F	16±3^{a1}	11±3^{a2}	81.7±0.7^{a1}	82.0±0.3^{a1}
CAS-C	13.5±1.6^{a1}	15.4±1.7^{a2}	81.3±0.5^{a1}	81.09±0.19^{a1}

$^{a, b, c}$ Different superscripts within a column indicate significant differences between starch matrix and fine or coarse rice bran in the same matrix. ($p<0.05$).

$^{1, 2}$ Different superscripts within the same file indicate significant differences between storage times for the same formulation. ($p<0.05$).

In conclusion, films obtained from pea starch, richer in amylose, are stiffer, more resistant to fracture and glossier and less permeable to oxygen, although less extensible, than starch films with a lower amylose content. All the films become harder and more resistant during storage, and those richer in amylopectin become shorter (less stretchable). The oxygen permeability slightly decreased throughout storage time in every case.

3.7. Effect of rice bran addition

The two rice bran fractions obtained by sieving were analysed as to the particle size distribution by dispersing them in water to the adequate obscuration rate in the laser diffraction equipment. The bran particle size distribution curves are shown in Figure 4 for both the smaller particle fraction (F) and the bigger particle fraction (C). Differences between the particle size distribution of two fractions (F and C) can be observed, although a certain degree of curve overlapping was obtained, since sieving only partially separates the particles by size. In Figure 4, the mean values of the bran particle size in terms of $D_{3,2}$ and $D_{4,3}$ are also shown. The differences between these diameters in a given sample indicate that particle size distributions are wide or that they are irregularly-shaped. On the contrary, similar values are associated with narrow particle size distributions and more spherical particles. As expected, significant differences ($p < 0.05$) between $D_{3,2}$ and $D_{4,3}$ were found for both fine and coarse fractions, thus indicating the presence of irregular particles of very different sizes.

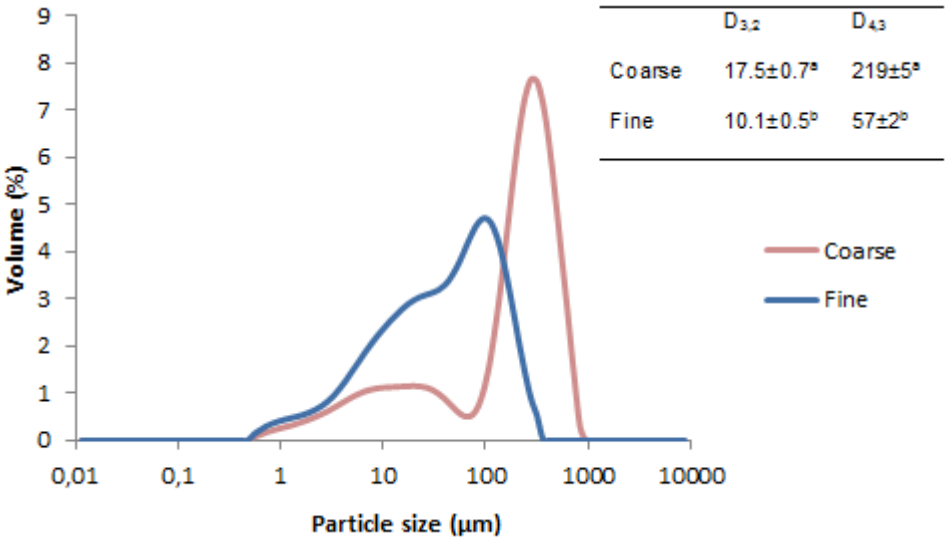

	$D_{3,2}$	$D_{4,3}$
Coarse	17.5±0.7ª	219±5ª
Fine	10.1±0.5ᵇ	57±2ᵇ

Figure 4. Typical particle size distributions of the different bran fractions. $D_{3,2}$ and $D_{4,3}$, mean values and standard deviation.

Figure 5 shows the SEM micrographs of the powder of both bran fractions. Fraction F contains more spherical particles than fraction C which, in turn, contain composite particles (where components are not released). The composition of both fractions is shown in Table 4. The mean values of the moisture, protein, fat and ash contents were very similar for F and C fractions, but significant differences were found for starch and fibre contents; the fine fraction was richer in starch (twice) whereas the coarse fraction contained more fibre. The obtained composition of the two rice bran fractions coincides with data previously reported by Sánchez *et al*. (2004). The protein content is similar to that reported by Rodríguez (2007), Gnanasambandam *et al*. (1997), whereas Pacheco, *et al*. (2002) obtained a similar fat content. These authors observed that the varietal effect and smoothening method may cause significant differences in the ash, fat, protein, starch and fibre content of rice bran.

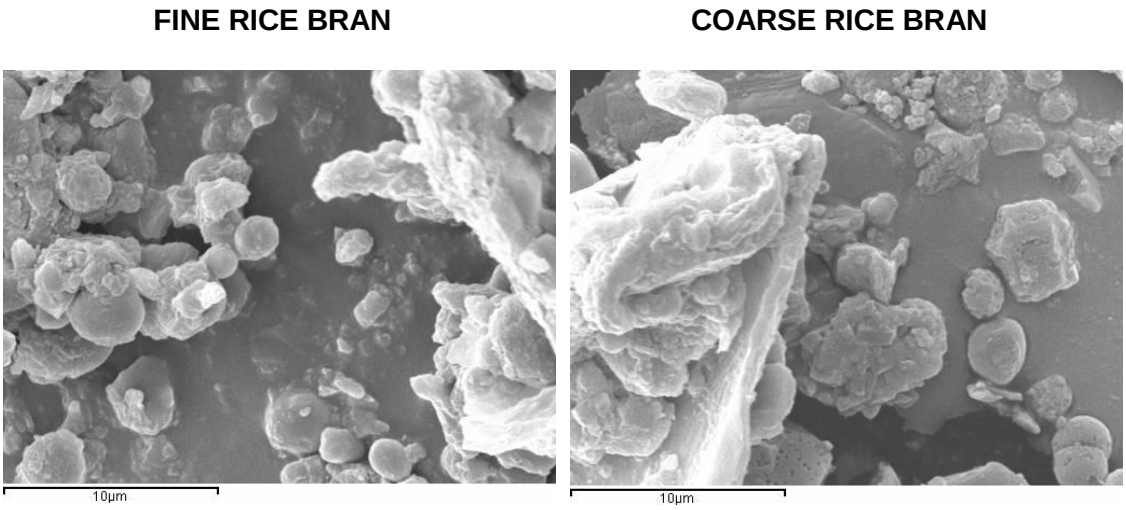

Figure 5. SEM micrographs of fine and coarse rice bran fractions.

Table 4: Chemical composition of rice bran, % dry basis. Mean values and standard deviation.

	Moisture	Protein	Fat	Ashes	Starch	Fibre
Fine	7.2±0.2	15.3±0.5	16.2±0.9	9.84±0.05	27±3	24.23
Coarse	6.9±0.2	15.56	17.1±1.3	10.04±0.02	12.6±0.8	37.8

3.7.1. Effect of bran addition on microstructural properties

The microstructure analysis allows us to identify the arrangement of some components of the film (mainly those non-miscible with the polymer) and the characteristics of the polymer matrix. The microstructural features are also directly related with the film's physical (mechanical, barrier and optical) properties. Figures 6 and 7 show the surface and cross section micrographs of starch films containing rice bran obtained by SEM. The cross section micrographs of films containing bran fractions show a continuous matrix with similar characteristics to those described for bran-free films, but with some dispersed particles, corresponding to proteins, lipid particles and fibres, incorporated by bran. Dispersed particles also appear at surface level in the film, thus indicating that flocculation and creaming occurred during film drying, leading particles to

the film surface. It is remarkable that no starch granules were appreciated in the observed fields, which could be due to their gelatinization during the 4 minutes of hot homogenization with the gelatinized starch dispersions. Fat and proteins could also be well integrated in the matrix as a result of the thermal homogenization. In this sense, the particles observed will be mainly fibre. Large composite particles are sometimes observed (Figure 6), although in relatively low numbers for the fine fraction.

The presence of the large particles affected the film thickness. Incorporating bran particles led to some irregularities in the film thickness related with the presence of these very large particles. The mean thickness value of bran-films was 75.2 ± 1.1 μm, whereas for films with F and C fractions the values were 75.8 ± 0.8, and 98 ± 4 μm, respectively. The variation coefficients were 1.5, 1.1 and 4.1 %, respectively. This indicates that while no differences were observed between bran-free films and those containing the F bran fraction, the C fraction is, not suitable to be incorporated into the films since it causes an irregular film formation with a non-constant thickness.

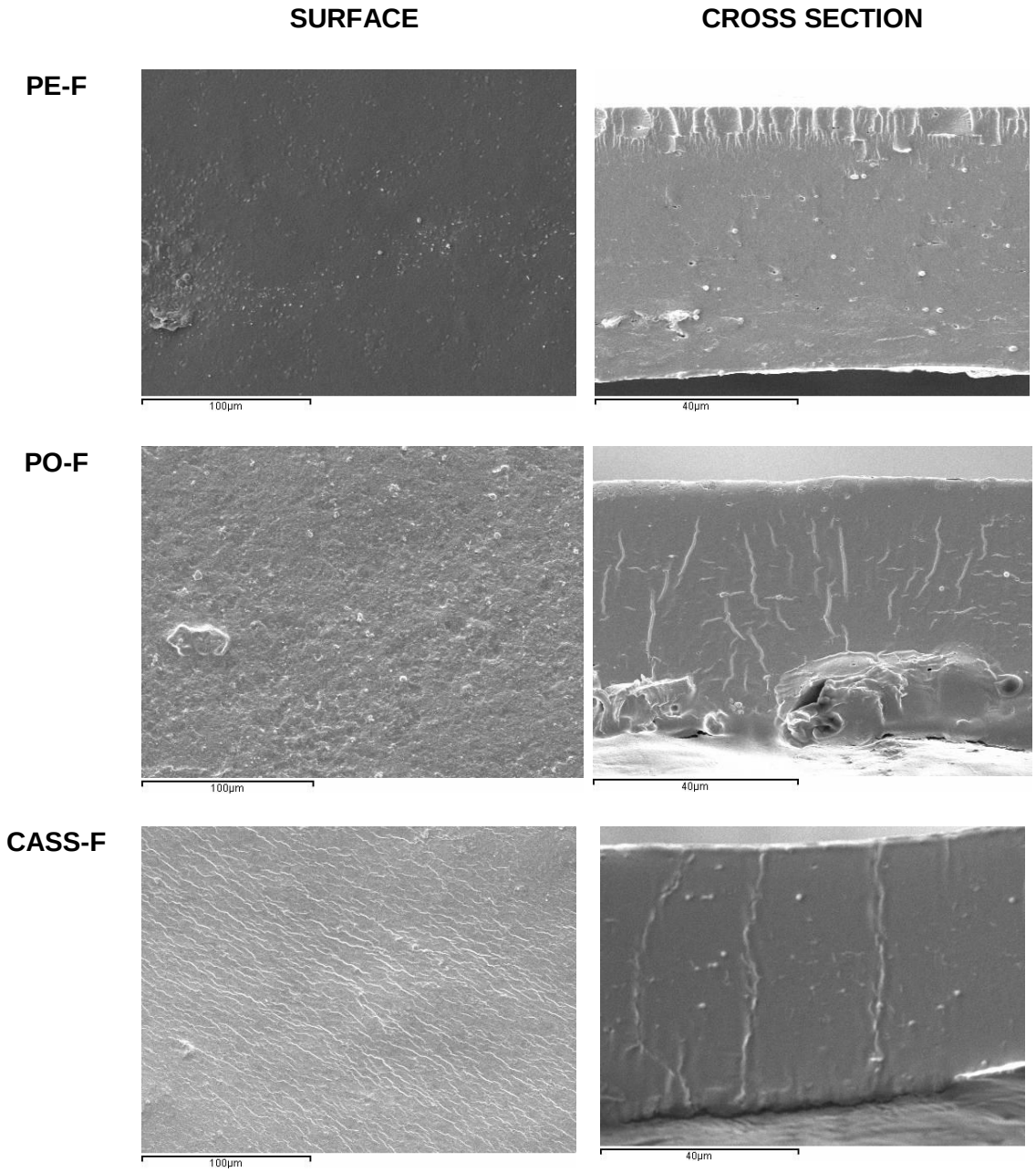

Figure 6. SEM micrographs of surface and cross section of pea (PE), potato (PO) and cassava (CAS) starch films containing fine (F) rice bran.

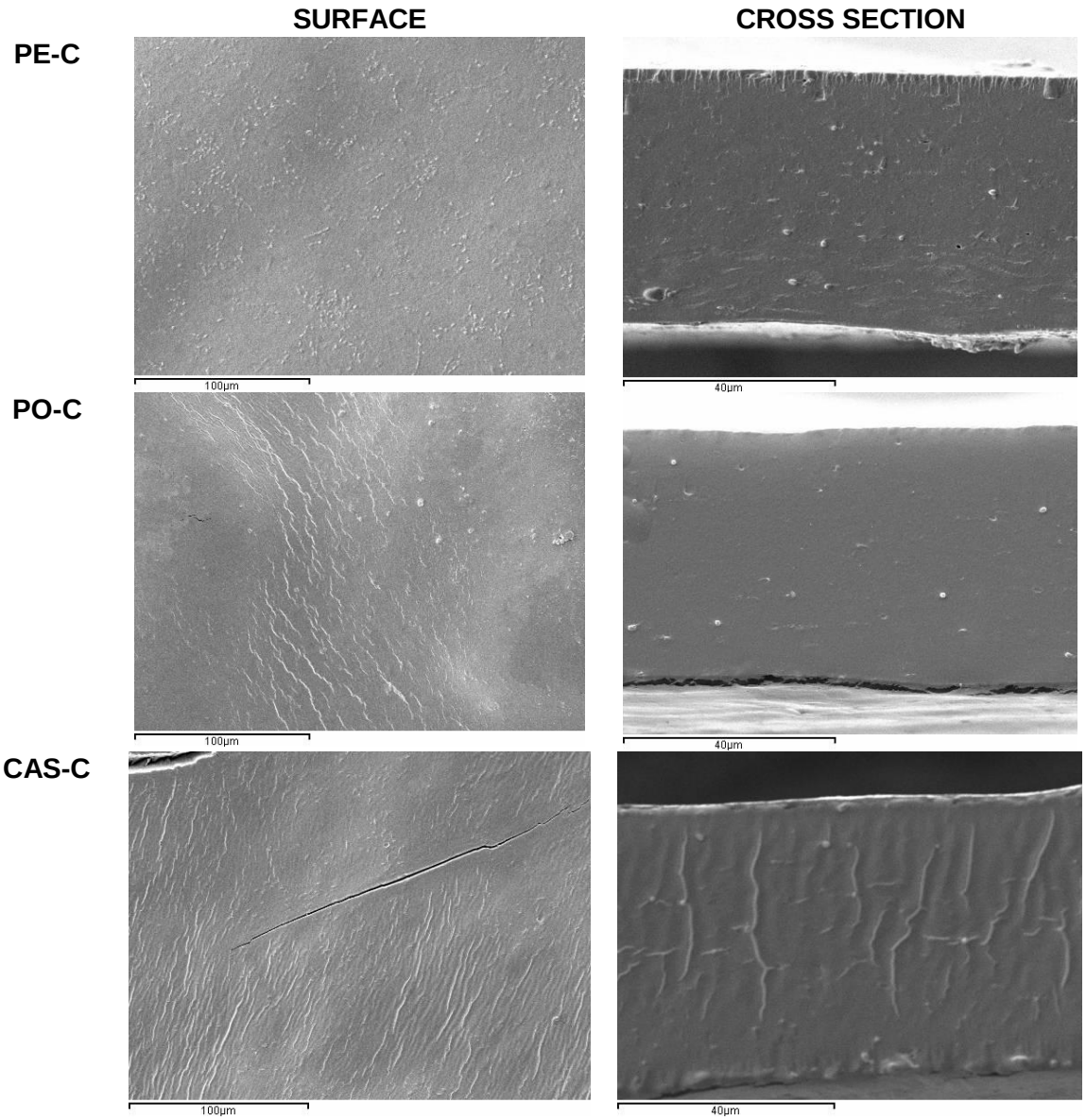

Figure 7. SEM micrographs of surface and cross section of pea (PE), potato (PO) and cassava (CAS) starch films containing coarse (C) rice bran.

Figure 8 shows the surface micrographs of films containing rice bran obtained by AFM using PeakForce QNM. The data were converted into 2D images in terms of Log DMT modulus maps, where the darker colour means lower DMT modulus or soft areas. As can be observed, the incorporation of bran filler implied the appearance of a great number of hard particles on the film surface (white spots), as compared with the polymer

background, which indicates that the dispersed material which migrates to the film's surface during the drying step is stiffer than the polymer matrix. The surface characteristics of the continuous matrix remain as in the bran-free films with notable differences between pea, potato and cassava films due to the differing extent of amylose crystallization. Crystalline zones appear lighter, whereas amorphous zones are darker. Differences can be observed between the ratio and size of the hard particles on the film surface of the three different starch films. In pea starch films, smaller, free particles can be observed, whereas bigger aggregates appear in the potato starch films. In cassava starch films, the bran particles are not aggregated, but some very soft small spots appeared, which could be attributed to discontinuities on the film surface probably produced by the loss of particles, generating a surface void. This can also occur in the other films, but due to the natural surface roughness it was not easily appreciated.

The fact that there are differences in the particle distribution at surface level indicates that differing degrees of flocculation and creaming occurred during film drying, which depends on the viscosity of the aqueous medium induced by starch. In this sense, pea starch, which has the highest amylose ratio, can form gel during film drying, thus inhibiting the particle migration. Cassava starch did not form gel, but the solutions exhibit very high viscosity. The potato starch film-forming dispersion is probably the one that shows the poorest stabilizing properties, thus promoting particle flocculation and migration towards the film surface.

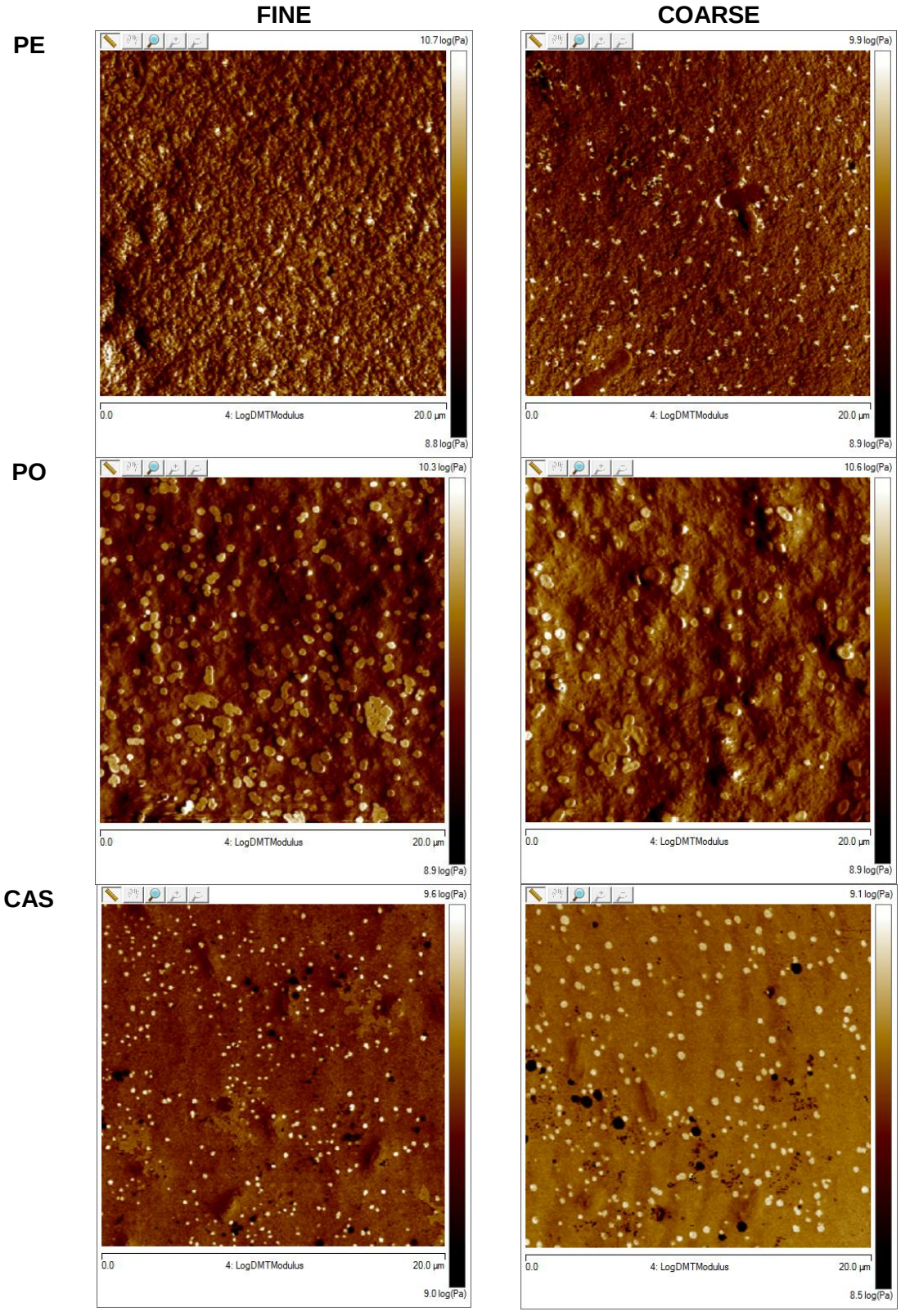

Figure 8. Maps of Log DTM modulus obtained from AFM in surface of pea, potato and cassava starch films containing Fine (F) and coarse (C) rice bran.

3.7.2. Effect on barrier properties

The moisture content of pure starch films ranged from 9.9 to 11.4 (Table 1). The incorporation of rice bran provoked an increase in the film's moisture content as can be observed in Table 1, mainly in films containing coarse fraction. This not only indicates that the addition of fibre leads to an increase in the water retention capacity of the films, as suggested by Zhang *et al.* (2011), but also that the introduction of mineral content (ashes) implies an increase in the water retention capacity of the matrix, especially from intermediate relative humidity. After 5 storage weeks, the moisture content significantly decreased ($p < 0.05$) in all the films, as was observed for bran-free films, which suggests their slow equilibration with the storage chamber relative humidity.

WVP, analysed at 25 ºC and a relative humidity gradient 53 – 100 %, are shown in Table 1. Whereas these values at initial time ranged between 5-6 g mm kPa^{-1} h^{-1} m^{-2} for starch films without bran, in films containing rice bran these were significantly higher ($p < 0.05$), mainly for the films with the largest particles. This can be explained by the greater water content in the films, which plasticizes the matrix, as well as by the presence of large particles whose induced tension in the matrix can provoke associated channels that constitute preferential paths for mass transport. On the contrary, Famá *et al*. (2009) reported that wheat bran incorporation in cassava starch significantly reduced the WVP, although they use particles with a lower size range: between 75 and125 µm. The low particle size is essential as a means of improving the film matrix properties.

The influence of particle size on WVP values can be clearly observed in Table 1. Coarse fibres significantly increased WVP as compared with fine fibres, regardless of the type of starch. In this case, large particles seriously interrupt the continuity of the films, thus creating large channels for water diffusion. After 5 weeks of storage, the values of WVP slightly changed, but without any clear tendencies, depending on the starch type and bran fraction. Nevertheless, whereas WVP values tend to decrease with

time in films with fine particles, in line with the moisture content reduction in the matrix, they tend to increase in films with the largest particles and a greater fibre content.

The OP of films containing bran (Table 1) follows the same tendency as observed for bran-free films, increasing when the amylose content in the starch decreases. Nevertheless, for fine bran, fibres provoked a slight increase in the oxygen permeability of starch films, which can be due to increases in the films' water content. The incorporation of coarse rice bran gives rise to films with micro-cracks, associated to the tension in the dried film provoked by the largest particles. In these cases, it was not possible to measure the OP and this also contributed to the anomalous values of the WVP. After 5 storage weeks, the mean values of OP significantly decreased, as observed in bran-free matrices, due to the reduction in moisture content.

3.7.3. Effect on mechanical properties

Table 2 shows the values of the mechanical parameters of the films with bran fractions after 1 and 5 weeks of storage. The incorporation of rice bran did not significantly affect the elastic modulus of potato and cassava starch films, but significantly increased the elastic modulus of pea starch films. The film resistance to fracture was not significantly affected by the addition of bran, although film extensibility was notably reduced, mainly for the coarse fraction in potato and cassava starch films. In pea starch films, the stretchability reduction is less appreciable due to their very low initial values. These results are coherent with those reported by Famá *et al*. (2009) for cassava starch films reinforced with wheat bran.

The effect of storage time is quite similar to that observed for bran-free films. The elastic modulus increased in all cases, except pea starch films, where bran particles partially inhibit the increase in the elastic modulus that occurred in bran-free films. This may be due to the smaller water loss which occurred during storage when the films

contained bran. Film resistance to break increased in every case during storage, except pea starch films where it diminishes, in agreement with that commented on above. Film stretchability also decreases in all cases, the values being very similar for all the films after 5 storage weeks. The presence of discontinuities in the matrix, associated to bran particles, affected the matrix cohesion forces, giving rise to very brittle matrices.

3.7.4. Effect on optical properties

Ti values of starch films containing bran fibres are shown in Table 3. As expected, bran addition contributed to reduce film transparency due to the presence of a dispersed phase that leads to light scattering. Nevertheless, as observed in bran-free films, the transparency of films containing bran particles was not affected ($p > 0.05$) by the type of starch, nor by the bran particle size. Similar results were found by Famá *et al*. (2009). These authors also compared the yellow index (YI) of cassava starch samples with different wheat bran contents and observed that YI values rose as the bran content increased.

Table 3 also shows mean gloss values of starch films containing rice bran. Bran addition decreased the film gloss with respect to the bran-free ones, except in potato starch based films, where gloss was very low, even without added bran. The effect of bran addition on gloss values was greater when coarse particles were added, in agreement with their greater particle size which largely contributes to the increase in the surface roughness and the subsequent gloss loss.

4. CONCLUSIONS

Properties of starch films were greatly affected by the amylose-amylopectin ratio. Amylose-rich films form amylose crystalline regions during film drying which give rise to stiffer, more resistant to fracture, but less stretchable films, with lower oxygen

permeability and more water binding capacity. All the films develop throughout storage time, mainly due to water loss which leads to more compact matrices: stiffer, more resistant to fracture and less extensible, with lower oxygen permeability, but without changes in water vapour permeability. Rice bran with lower particle size ($D_{4,3}$= 57 μm) improved the elastic modulus of the films, especially in high amylose content films (pea starch), but reduced the film stretchability and worsened barrier properties, due to the enhancement of the water binding capacity of the films and the introduction of fibre discontinuities in the matrix. So, the hygroscopic character of the filler was a drawback to the improvement of the film properties. The reduction of the filler particle size is necessary to minimize the negative effect of large particles.

Acknowledgment

The authors acknowledge the financial support from the Spanish Ministerio de Economía y Competitividad throughout the project AGL2010-20694, con-financed with FEDER founds. Amalia Cano also thanks Spanish Ministerio de Educación, Cultura y Deporte for the FPU grant.

References

- Adebiyi, A.P., Adebiyi, A.O., Jin, D., Ogawa, T., & Muramoto, K. (2008). Rice bran protein-besed edible films. *International Journal of Food Science and Techonology*, 43, 476-483.
- Alvani, K., Qi, X., Tester, R.F., & Snape, C.E. (2011). Physico-chemical properties of potato starches. *Food Chemistry*, 125, 958-965.
- ASTM (1992). Standard methods for tensile properties of thin plastic sheeting. In: Annualbook of American Standard Testing Methods. Designation (D882-91). Philadelphia, Pa:ASTM
- ASTM. (1995). Standard test methods for water vapour transmission of materials. Standard designations: E96-95 Annual book of ASTM standards. Philadelphia, PA: American Society for Testing and Materials. (pp. 406e413).

- ASTM. (1999). Standard test methods for specular gloss. Designation (D523). In Annual book of ASTM standards, Vol. 06.01. Philadelphia, PA: American Society for Testing and Materials.
- ASTM. (2001). Standard test method for tensile properties of thin plastic sheeting. Standard D882 Annual book of American standard testing methods. Philadelphia, PA: American Society for Testing and Materials. (pp. 162e170).
- ASTM. (2005). Standard test method for oxygen gas transmission rate through plastic film and sheeting using a Coloumetric sensor. Standard Designation: D3985-05 Annual book of American society for testing materials, West Conshohocken, PA, USA.
- Carroll. 1990. Functional properties and applications of stabilized rice bran in bakery products. *Food Technology*. Abril 74-76.
- Carvalho, A. J. F. (2008). Starch: major sources, properties and applications as thermoplastic materials. In M. N. Belgacem & A. Gandini (Eds.), *Monomers, polymers and composites from renewable resources* (pp. 321–342). Amsterdam: Elsevier.
- Cheetham, N. W. H., & Tao, L. (1998). Variation in crystalline type with amylose content in maize starch granules: an X-ray powder diffraction study. *Carbohydrate Polymers*, 36 (4), 277–284.
- Chen, Y., Liu, Ch., Chang, P.R., Cao, X., & Anderson, D.P. (2009a). Bionanocomposites based on pea starch and cellulose nanowhiskers hydrolyzed from pea hull fibre: Effect of hydrolysis time. *Carbohydrate Polymers*, 76, 607-615.
- Chen, C.H., Kuo, W.S., & Lai, L.S. (2009b). Rheological and physical characterization of film-forming and edible films from tapioca starch/decolorized hsian-tsao leaf gum. *Food Hydrocolloids*, 23, 2132-2140.
- Chen, J., Liu, Ch., Chen, Y., Chen Y., & Chang, P.R. (2008). Structural characterization and properties of starch/konjac glucomannan blend films. *Carbohydrate Polymers*, 74, 946-952.
- Cyras. V.P., Manfredi, L., Ton-That, M., & Vázquez, A. (2008). Physical and mechanical properties of thermoplastic starch/montmorillonite nanocomposite films. *Carbohydrate Polymers,* 73, 55-63.

- Da Matta, M.D., Silveira, S.B., de Oliveira, L.M., & Sandoval, S. (2011). Mechanical properties of pea starch films associated with xanthan gum and glycerol. *Starch*, 63, 274-282.

- Dias, A.B., Müller, C.M.O., Larotonda, F.D.S., & Laurindo, J.B. (2010). Biodegradable films based on rice starch and rice flour. *Journal of Cereal Science*, 51, 213-219.

- Dole, P., Joly, C., Espuche, E., Alric, I., & Gontard, N. (2004). Gas transport properties of starch based films*. Carbohydrate Polymers*, 58, 335–343.

- Falguera, V., Quintero, J. P., Jiménez, A., Muñoz, J. A., & Ibarz, A. (2011). Edible films and coatings: structures, active functions and trends in their use. *Trends in Food Science & Technology*, 22 (6), 292–303.

- Famá, L., Gerschenson, L., & Goyanes, S. (2009). Starch-vegetable fibre composites to protect food products. *Carbohydrate Polymers*, 75, 230-235.

- Famá L., Goyanes, S., & Gerchenson, L. (2007). Influence of storage time at room temperature on the physicochemical properties of cassava starch films. *Carbohydrate Polymers, 70, 265-273.*

- Famá, L., Flores, S.K., Gerschenson, L., & Goyanes, S. (2006). Physical characterization of cassava starch biofilms with special reference to dynamic mechanical properties at low temperatures. *Carbohydrates Polymers*, 66, 8-15.

- Famá, L., Rojas, A.M., Goyanes, S., & Gerschenson, L. (2005). Mechanical properties of tapioca-starch edible films containing sorbates. *Swiss Society of Food Science and Technology.*631-639.

- Forssell, P. M., Helleman, S. H. D., Myllärinen,P. J., Moates, G.K., & Parker, R. (1999). Ageing of rubbery thermoplastic barley and oat starches. *Carbohydrate Polymers,* 39, 43-51.

- García, M. A., Martino, M. N., & Zaritzky, N. E. (2000). Microstructural characterization of plasticized starch-based films. *Starch/Stärke*, 52 (4), 118–124.

- Gnanasambandam, R., Hettiarachchy, N.S., & Coleman, M. (1997). Mechanical and barrier properties of rice bran films. *Journal of Food Science*, 62 (2), 395-398.

- Gnanasambandam, R., & Hettiarachchy, N.S. (1995). Protein concentrates from unstabilized and stabilized rice bran: Preparation and properties. *Journal Food Science*, 60, 1066-1069.
- Han, J.H., Seo, G.H., Park, I.M., Kim, G.N., & Lee, D.S. (2006). Physical and mechanical properties of pea starch edible films containing beeswax emulsions. *Journal of Food Science*, 71 (6), 290-296.
- Hutchings, J.B. (1999). Food and Colour Appearance, Second Edition. Gaithersburg, Maryland: Chapman and Hall Food Science Book, Aspen Publication.
- Jiménez, A. (2009). Efecto de la incorporación de ácidos grasos en las propiedades físicas de films a base de hidroxipropil-metilcelulosa (HPMC). Master thesis. Universitat Politècnica de València.
- Jiménez, A., Fabra, M.J., Talens, P., & Chiralt, A. (2012a). Edible and biodegradable starch films: A review. *Food and Bioprocess Technology*, 5 (6), 2058-2076.
- Jiménez, A., Fabra, M.J., Talens, P., & Chiralt, A. (2012b). Effect of re-crystallization on tensile, optical and wáter vapour barrier properties of corn starch films containing fatty acids. *Food Hydrocolloids*, 26, 302-310.
- Jiménez, A., Fabra, M.J., Talens, P., & Chiralt, A. (2012c). Effect of sodium caseinate on properties and ageing behaviour of corn starch based films. *Food Hydrocolloids*, 29 (2), 265-271.
- Judd, D. B. & Wyszecki, G. (1975). Colour in Business, Science and Industry. New York: John Wiley and Sons, Inc. ISBN. 0471452122.
- Kaisangsti, N., Kerdchoechuen, O., & Laohakunjit, N. (2012). Biodegradable foam tray from cassava starch blended with natural fiber and chitosan. *Industrial Crops and Products,* 37, 542-546.
- Koskinen, M., Suortti, T., Autio, K., Myllärinen, P., & Poutanen, K. (1996). Effect of pretreatment on the film forming properties of potato and barley starch dispersions. *Industrial Crops Products*, 5, 23-34.

- Lafargue, D., Lourdin, D., & Doublier, J.L. (2007). Film-forming properties of a modified starch/k-carrageenan mixture in relation to its rheological behavior. *Carbohydrate Polymers*, 70, 101-111.

- Liu, Z. (2005). Edible films and coatings from starch. In J. H. Han (Ed.), Innovations in food packaging (pp. 318–332). London: Elsevier Academic Press.

- Lu, Y., Weng, L., & Cao, X. (2006). Morphological, thermal and mechanical properties of ramie crystallites-reinforced plasticized starch biocomposites. *Carbohydrate Polymers*, 63, 198-204.

- Ma, X., Chang, P.R., & Yu, J. (2008). Properties of biodegradable thermoplastic pea starch/carboxymethyl cellulose and pea starch/microcrystalline cellulose composites. *Carbohydrate Polymers*, 72, 369-375.

- Mc Hugh, T. H. & Krochta, J. M. (1994).Water vapour permeability properties of edible whey protein-lipid emulsion films. *Journal of the American Oil Chemists Society,* 71, 307-312.

- Mehyar, G.F. & Han, J.H. (2004). Physical and mechanical properties of high-amylose rice and pea starch films as affected by relative humidity and plasticizer. *Journal of Food Science*, 69 (9), 449-454).

- Myllärinen, P., Buleon, A., Lahtinen, R., & Forssell, P. (2002). The crystallinity of amylose and amylopectin films. *Carbohydrate Polymers,* 48, 41-48.

- Nam, S., Scanlon, M.G., Han, J.H., & Izydorczyk, M.S. (2007). Extrusion of pea starch containing lysozyme and determination of antimicrobial activity. *Journal of Food Science*, 72 (9), 477-484.

- Nikolosi, R.J., Ausman, L.M., & Hegstead, D.M. (1990). Lipoprotein levels in monkeys fed a diet containing rice bran oil. Presented at USA Rice Council Rice Bran Technical Meeting Houston, TX. March 23-25, 1996.

- Pacheco E., Peña, J. & Ortiz, A. (2002). Composición físico-química del aceite y salvado de arroz estabilizado por calor. *Agronomía Tropical*, 52 (2), 173-185.

- Phan The, D., Debeaufort, F., Voilley, A., & Luu, D. (2009). Biopolymer interactions affect the functional properties of edible films based on agar, cassava starch and arabinoxylan blends. *Journal of Food Engineering*, 90, 548-558.

- Rindlav, A., Hulleman, S.H.D., & Gatenholm, P. (1997). Formation of starch films with varying crystallinity. *Carbohydrate Polymers,* 34, 25-30.

- Rindlav-Westling, A., Stading, M., Hermansson, A.M., & Gatenholm, P. (1998). Structure, mechanical and barrier properties of amylose and amylopectin films. *Carbohydrate Polymers,* 36, 217-224.

- Rodríguez, M.B. (2007) .Determinación de la composición química y propiedades físicas y químicas del pulido de arroz (*Oryza sativa L.*). Tesis Doctoral Valdivia, Chile.

- Sánchez, J., Quintero, A.G., & González, G. (2004). El salvado de arroz en la elaboración de alimentos de alto valor nutricional. *Hypatia*, 8, Visited 01/23/2014. (http://hypatia.morelos.gob.mx/index.php?option=com_content&task=view&id=94&Itemid=65).

- Shen, X.L., Wu, J.M., Chen, Y., & Zhao, G. (2010). Antimicrobial and physical properties of sweet potato starch films incorporated with potassium sorbate or chitosan. *Food Hydrocolloids*, 24, 285-290.

- Souza, A.C., Benze, R., Ferrao, E.S., Ditchfield, C., Coelho, A.C.V., & Tadini, C.C. (2011). Cassava starch biodegradable films: influence of glycerol and clay nanoparticles content on tensile and barrier properties and glass transition temperature. *Food Science and Technology*, doi: 10.1016/j.lwt.2011.10.018.

- Talja, R. A., Peura, M., Serimaa, R., & Jouppila, K. (2008). Effect of amylose content on physical and mechanical properties of potato-satch-besed edible films. *Biomacromolecules*, 9, 658-663.

- Talja, R. A., Helén, H., Roos, Y. H., & Jouppila, K. (2007). Effect of various polyols and polyol contents on physical and mechanical properties of potato starch-based films. *Carbohydrate Polymers*, 67(3), 288e295.

- Vásconez, M.B., Flores, S.K., Campos, C.A., Alvarado, J., & Gerschenson, L.N. (2009). Antimicrobial activity and physical properties of chitosan-tapioca starch based edible films and coatings. *Food Research International*, 42, 762-769.

- Wu, H., Liu, Ch., Chen, J., Chen, Y., Anderson, D.P., & Chang, P.R. (2010). Oxidized pea starch/chitosan composite films: Structural characterization and properties. *Journal of Applied Polymer Science*, 118, 3082-3088.

- Zhang, Y., Thompson, M., & Liu, Q. (2011). The effect of pea fiber and potato pulp on thermal property, surface tension, and hydrophilicity of extruded starch thermoplastics. *Carbohydrate Polymers*, 86, 700-707.

- Zhang, Y. and Han, & J.H. (2006). Mechanical and thermal characteristics of pea starch films plasticized with monosaccharides and polyols. *Journal of Food Science*, 71 (2), 109-118.

- 104/1: Determination of Ash in Cereals and Cereal Products. (1990). International Association for Cereal Science and Technology (I.C.C.).

- 105/2: Determination of Crude Protein in Cereals and Cereal Products for Food and Feed (1994). International Association for Cereal Science and Technology (I.C.C.).

- 30-20: Determination of Fat in Cereals and Cereal Products for Food and Feed (1967). American Association of Cereal Chemist. Cereal Laboratory.

Chapter II: Study of poly(vinyl alcohol) (PVA)- starch blends. Effect of nano-reinforcements (CNCs).

Part A: Study of poly(vinyl alcohol) (PVA) - starch blends.

Amalia I. Cano, Maite Cháfer, Amparo Chiralt, Chelo González-Martínez. **Physical and microstructural properties of biodegradable films based on pea starch and PVA.** *Journal of Food Engineering*, **2015**, 167, 59-64.

Amalia I. Cano, Elena Fortunati, Maite Cháfer, José M. Kenny, Amparo Chiralt, Chelo González-Martínez. **Properties and ageing behaviour of pea starch films as affected by blend with poly(vinyl alcohol).** *Food Hydrocolloids*, **2015**, 48, 84-93.

This part of the Chapter II summarizes the results of the two articles which include the complete study in order to avoid repetitions of some common aspects.

Abstract

Pea starch (S) and poly(vinyl alcohol) (PVA) blends with different ratios were produced in order to elucidate the possible advantages of blend films to overcome the common drawbacks of starch films. Starch, poly(vinyl alcohol) and blends were obtained by casting, and microstructure and thermal behaviour were characterized. Moreover, barrier, mechanical and optical properties were evaluated after 1 and 5 storage weeks at 25 ºC and 53 % relative humidity in order to study the effect of poly(vinyl alcohol) on the ageing process of starch. The incorporation of PVA into pea starch films implied the formation of interpenetrated networks of both incompatible polymers with partial solubilisation. S-PVA blend films were much more extensible and stable during storage, with improved water barrier properties and reduced water sorption capacity. Starch-poly(vinyl alcohol) blend films are environmentally friendly, low cost materials, with good functional properties.

Key words: blend films, barrier, crystallization, glass transitions, mechanical, microstructure, optical

1. INTRODUCTION

The reduction in petroleum reserves and the great environmental impact of petroleum-derived plastics have led to the development of biodegradable materials that may be used in packaging applications. Bioplastics are biodegradable or compostable products, from renewable sources or synthesis, whose global production has increased considerably in the last few years. They have hydrolytically or enzymatically labile bonds or groups (Lu *et al*., 2009). These biodegradable materials provide opportunities to reduce the waste through biological recycling in order to achieve a sustainable ecosystem.

Starch is considered as a bioplastic and is one of the most abundantly-occurring natural polymers, second only to cellulose (Ramaraj, 2007). It is also especially attractive because of its biodegradability and low cost (Chen *et al.*, 2008; Han, *et al.,* 2006; Lafargue *et al.,* 2007). Starch has the ability to form films that are odourless, colourless, transparent, and with very low oxygen permeability (Jiménez *et al.,* 2012a; Vásconez *et al.,* 2009). Native starch has a granular structure and presents different properties depending on its amylose/amylopectin ratio. Gelatinized starch shows a great film-forming capacity and, as is well known, its two macromolecules are responsible for starch recrystallization, which leads to changes in the mechanical response of starch-based films (Cano *et al.,* 2014; Jiménez *et al.,* 2012a; Talja *et al.,* 2007). Besides their poor mechanical properties, starch films are highly hydrophilic in nature, which confers a great water vapour sensitivity and poor water barrier properties. Some authors have tried to overcome these aspects by blending starch with other compounds, such as sodium caseinate (Jiménez *et al.,* 2012c), sorbitan esters of fatty acids (Ortega-Toro *et al.,* 2014), soy protein isolate (Galus *et al.,* 2012; Galus *et al.,* 2013) or biodegradable synthetic polymers (Arvanitoyannis, 1999).

Poly(vinyl alcohol) (PVA) is a synthetic water-soluble polymer, widely used in different industrial, commercial, medical and food applications (Ramaraj, 2007). PVA has been extensively studied because of its biocompatibility and interesting physical properties, which are due to the presence of OH groups and the hydrogen bond formation (Alexy *et al.,* 2003; Bonilla *et al.,* 2014). Films obtained from PVA are fully biodegradable, odourless, transparent, non-toxic and have useful physical properties, such as high tensile strength and flexibility, good oxygen and aroma barrier properties and transparency (Ramaraj, 2007).

Different studies into starch-PVA blends have been carried out, focusing on biodegradability studies (Gupta *et al.,* 2014; Lu *et al.,* 2009; Siddaramajah *et al.,* 2004) or the effect of the incorporation of different additives to the blends, such as citric acid, glutaraldehyde or urea (Gupta *et al.,* 2014; Luo *et al.,* 2012; Shi *et al.,* 2008; Ramaraj *et al.,* 2006), calcium chloride (Jiang *et al.,* 2012), poly(methyl methacrylate-co-acrylamide) nanoparticles (Yoon *et al.,* 2012) for different purposes (compatibility enhancement or development of biomedical and packaging materials).

Chen *et al.* (2008) studied the effect of pea-starch nanocrystals (PSN) and native pea starch (NPS) on the structure and physicochemical properties of the PVA films. They found that PSN were more homogeneously dispersed in the PVA matrix than the NPS, resulting in stronger interactions with PVA and better mechanical behaviour. Sreekumar *et al.* (2012) found a partial miscibility of the polymers in blends of corn starch and PVA, by analysing X-ray diffraction and thermal and mechanical response. Polymer compatibility and PVA crystallinity greatly decreased when the starch content rose, which affected the mechanical response of the films.

Mechanical and optical properties, wide-angle X-ray scattering, and biodegradation of PVA films containing a small ratio of corn starch (0-10 %) were analysed by Siddaramaiah *et al.* (2004). Although they report an increase in the haze and diffusion of

light, there was only a slight change associated with the tensile behaviour of PVA films, which could be explained in terms of the changes in the crystalline structural parameters.

Pea starch is highly available and one of its advantage is its high amylose content about 24 % to 65 %, depending on variety (Hoover & Sosulski, 1991; Han *et al.,* 2006). In most of the cases the amylose/amylopectin ratio is higher than in corn starch. The high amylose content contributes to improve the tensile strength and gas barrier properties of starch based films (Wolff *et al.,* 1951; Lourdin *et al.,* 1995; Palviainen, *et al.,* 2001; Cano *et al*., 2014). The very low oxygen permeability of high amylose starch films make them very useful for preservation of foods sensitive to oxidation process, such as meat and fish products or nuts. No studies have been found into the effect of PVA on the properties of gelatinized pea- starch films and on their ageing behaviour, which is one of the main drawbacks to the practical use of starch films as food packaging material. Although it could be expected a relatively close behaviour of pea-starch-PVA blend films to that obtained for corn starch blends, differences in starch sources (tubercles, cereals or legumes) can imply notable changes in the film's properties (Fredriksson *et al.,* 1998; Hoover & Ratnayake, 2000).

This study has planned with two aims:

- First, to analyse how PVA affects the physical properties starch films and their development throughout the storage. To this end, only a blend with a S:PVA ratio of 2:1 was characterized as to its physical properties and compared with those of neat polymers.
- On the basis of the obtained results, a wider range of S:PVA ratios was considered in order to identify the best proportion in terms of the film functionality and stability. A deeper study was carried out to know the structure, thermal behaviour, physical properties and ageing development of blend films. This second experimental series was partially carried in the Materials Engineering

Centre UdR INSTM, (University of Perugia, Terni, Italy), and some differences in the used methods are explained in the corresponding section.

2. MATERIALS AND METHODS

2.1. Materials

Pea starch (S) was purchased from Roquette Laisa España S.A. (Benifaió, Valencia, Spain), poly(vinyl alcohol) (PVA)(M_w: 89,000-98,000, degree of hydrolysis > 99 %, and viscosity: 11.6-15.4cP) was obtained from Sigma Aldrich Química S.L. (Madrid, Spain) and glycerol and magnesium nitrate-6-hydrate were provided by Panreac Química S.A. (Castellar de Vallès, Barcelona, Spain).

2.2. Preparation of film- forming dispersions and S:PVA blend films

Films were obtained by solvent casting procedure after the preparation of film-forming dispersions (FFDs).

Starch (1 % w/w) was dispersed in an aqueous solution at 95 ºC for 30 min and, while stirred, to induce starch gelatinization. Thereafter, the dispersion was homogenized using a rotor-stator homogenizer (Ultraturrax D125, Janke and Kunkel, Germany) at 13,500 rpm for 1min and 20,500 rpm for 3 min. Finally, glycerol was added at a starch:glycerol ratio of 1:0.25, on the basis of previous studies (Jiménez *et al*., 2012b). PVA (2 % w/w) was dispersed in an aqueous solution and maintained at 90 ºC for 30 min until complete dissolution. For S-PVA blends, PVA was incorporated into the previously gelatinized starch dispersion by using S:PVA ratios of 2:1 (S-PVA) for the first experimented series and 1:2, 1:1 and 2:1 for the second (named as S1:PVA2, S1:PVA1 and S2:PVA1, respectively). Afterwards, glycerol was also added (ratio starch:glycerol, 1:0.25).

To obtain the films, the FFDs were stirred for 30 minutes and poured into Teflon (first experimental series) or petri casting plates (second experimental series), in the amount which would provide a density of solid of 84 and 145 $g.m^{-2}$, respectively. Films were dried at 40 ºC in a convection oven for 48 h and afterwards, peeled off the casting surface. After the drying process, films were conditioned in desiccators at 25 ºC and 53 %RH by using magnesium nitrate-6-hydrate oversaturated solution for one week when the first series of analysis were carried out. One part of the samples was stored under the same conditions for five weeks in order to perform the second series of analysis of stored films (Cano *et al*., 2014).

The film thickness of every sample was measured after these two times at six random positions with a Palmer digital micrometre to the nearest 0.0025 mm.

2.3. Characterization of S:PVA films

2.3.1. Fourier transform infrared spectroscopy (FT-IR)

Structural analysis was carried out by using the Fourier transform infrared spectra (FT-IR, Jasco FT-IR 615 spectrometer, Easton MD, USA). For the measurement, a few drops of solution were cast on a silicon plate for each formulation and investigated in transmission mode over the 400-4000 cm^{-1} range. Two replicates per formulation were measured.

2.3.2. Microstructure of films

The microstructural analysis of the cross-section and surface of the films was carried out using field emission scanning electron microscopy (FESEM) (Supra™ 25-Zeiss, Germany). To this end, films were equilibrated at 53 % RH in desiccators by using $Mn(NO_3)_2$ solution. Two replicates per formulation were fixed on copper stubs, gold

coated, and observed using an accelerating voltage of 2 and 5 kV, for the surface and cross-section observations, respectively.

2.3.3. Thermogravimetric analysis (TGA)

A thermogravimetric analyzer (Seiko Exstar 6300, Italy) was used to obtain the thermal weight loss (TG), and the derivate (DTG), of samples. To this end, the samples were heated from 30 ºC to 600 ºC at 10 ºC/min, using a nitrogen flow (250 ml/min). Prior to the analyses, the samples were conditioned at 25 ºC and 53 % RH. The thermal degradation temperature was obtained at the maximum of the DTG curves (T_{max}). The measurements were taken in triplicate.

2.3.4. Differential scanning calorimeter (DSC)

Differential scanning calorimeter (TA Instrument, Q200, USA) measurements were carried out in triplicate under nitrogen flow in the temperature range of −25 to 250 ºC, at 10 ºC min^{-1}, by performing two heating and one cooling scan. Firstly, samples were heated from room temperature to 250 ºC at the selected heating rate and maintained for 5 min at 250 ºC. Then, samples were cooled down to -25 ºC and heated again until 250 ºC. Data were recorded during both the cooling and second heating steps. From the cooling step thermograms (heat flux vs. temperature), the crystallization temperatures (Tc) and enthalpy (∆Hc) values were obtained. Likewise, from the second heating step, the glass transition temperatures (Tg) and melting temperatures (Tm) and enthalpy values (∆Hm) were obtained. Prior to the analyses, the samples were conditioned at 25 ºC -53 % RH.

The crystallinity degree of PVA was calculated as shown in equation 1:

$$X = \frac{1}{X_{PVA}}\left[\frac{\Delta H}{\Delta H_0}\right] * 100 \quad (1)$$

where ΔH, is the melting enthalpy of the sample, ΔH_0 , the melting enthalpy of a 100 % crystalline PVA sample (161.6 $J.g^{-1}$; Roohani *et al*., 2008) and X_{PVA}, the mass fraction of PVA in the film.

2.3.5. Solubility

The solubility of films), equilibrated at 53 % RH and 25 ºC for 1 and 5 weeks, was determined by means of a gravimetric method previously described by Ortega-Toro *et al*. (2014b). For this purpose, the samples were kept in distilled water in a film: water ratio of 1:10 for 48 h, and later on, they were transferred to a convection oven (J.P. Selecta, S.A., Barcelona, Spain) for 24 h at 60 ºC to remove the free water, and afterwards, they were completely dried in a desiccator with P_2O_5 until constant weight. Three replicates were analysed for each formulation, and results were expressed in $g_{of\ dissolved\ film}\ g_{dry\ film}^{-1}$.

2.3.6. Moisture content

The moisture content of the films (MC), equilibrated at 53 % RH and 25 ºC, was analysed by drying the samples in a vacuum oven at 60 ºC for 24 h. Later on, the pre-dried samples were placed in desiccators containing P_2O_5 until reaching constant weight. Five replicates were analysed per film formulation.

2.3.7. Barrier properties

Water vapour permeability (WVP) was evaluated in films equilibrated at 25 ºC and 53 % RH after 1 and 5 storage weeks, following the ASTM E96-95 gravimetric method by using Payne permeability cups (Payne, elcometer SPRL, Hermelle/sd Argenteau, Belgium) 3.5 cm in diameter. Deionised water was used inside the testing cup to reach 100 % RH on one side of the film, while an oversaturated magnesium nitrate solution was used to control the RH on the other side of the film. The top surface of the film during

drying was exposed to 100 % RH. A fan placed on the top of the cup was used to reduce resistance to water vapour transport. Water vapour transmission rate measurements (WVTR) were performed at 25 ºC. These conditions were chosen to simulate the storage conditions of intermediate moisture foods exposed at high relative humidity and at room temperature. To calculate WVTR, the slopes of the steady state period of the curves of weight loss as a function of time were determined by linear regression. For each type of film, WVP measurements were replicated four times and WVP was calculated according to Cano *et al*. (2014).

The oxygen permeation rate of the films was determined at 53 % RH and 25 ºC by an OX-TRAN (Model 2/21 ML Mocon Lippke,Neuwied, Germany) following the standard method (ASTM D3985-05, 2005). The samples were placed into the equipment to perform the permeation assay: an oxygen sensor read the permeation through the film and the rate of oxygen transmission was calculated taking into account the amount of oxygen and the sample area (50 cm^2). Oxygen permeability (OP) was calculated by dividing the oxygen transmission by the difference in oxygen partial pressure between the two sides of the film, and multiplying it by the average film thickness. Measurements were taken in triplicate.

2.3.8. Mechanical properties

In the first experimental series, mechanical properties were measured by means of a Universal Machine (TA.XT plus, Stable Micro Systems, Haslemere, England). Equilibrated specimens at 25 ºC and 53 % RH (1 and 5 storage weeks) were mounted in the film-extension grips of the testing machine and stretched at 50 mm min^{-1} until breaking, following the ASTM standard method D882 (ASTM, 2001).

In the second experimental series, mechanical properties were measured using a Universal Test Machine (Digital Lloyd instrument, West Sussex, UK), following UNI ISO

527-1 (ISO, 2012), by using 5 cm min^{-1} and a load cell of 1.5 N. The film samples (1 x 5 cm) equilibrated at 25 ºC and 53 % RH (1 and 5 storage weeks) were analysed. These conditions were chosen to simulate the storage conditions of intermediate moisture foods exposed at high relative humidity and at room temperature. Film samples were mounted in the film-extension grips (A/TG model), which were set 20 mm apart.

In both cases, Stress-Hencky strain curves were obtained and the tensile strength at break (TS), percentage of elongation at break (E, %) and elastic modulus (EM) were calculated. The measurements were taken at room temperature and eight replicates carried out per formulation.

2.3.9. Optical properties

Film samples (1 x 1 cm) equilibrated at 25 ºC and 53 % RH were analysed by means of a UV–VIS spectrophotometer (Perkin Elmer Instruments, Lambda 35, Waltham, USA), by using a wavelength range between 250 and 1000 nm.

Internal transmittance, as a measure of the film transparency, was determined by applying the Kubelka–Munk theory for multiple scattering to the reflection spectra obtained in a spectrocolorimeter CM-3600d (Minolta Co., Tokyo, Japan) with a 30 mm illuminated sample area. This theory assumes that each light flux which passes through the film is partially absorbed and scattered, which is quantified by the absorption (K) and the scattering (S) coefficients. Transparency (K/S) was calculated, as indicated by Hutchings (1999), from the reflectance of the sample layer on a white background of known reflectance and on an ideal black background. Measurements were taken triplicate in samples equilibrated at 25 ºC and 53 % RH for one and five weeks, using both a white and a black background.

Gloss was measured using a flat surface gloss meter (Multi- Gloss 268, Minolta, Langenhagen, Germany) at an angle of 60 º with respect to the normal to the film surface,

according to the ASTM standard D523 (ASTM, 1999). Prior to gloss measurements, films were conditioned at 25 ºC and 53 % RH for one and five weeks. Gloss measurements were carried out over a black matte standard plate and were taken in triplicate. Results were expressed as gloss units, relative to a highly polished surface of standard black glass with a value close to 100.

2.4. Statistical analysis

The results were analysed by means of analysis of variance (ANOVA), using the Statgraphics Plus 5.1. Program (Manugistics Corp., Rockville, MD). Fisher's least significant difference (LSD) was used at the 95 % confidence level to distinguish the samples.

3. RESULTS AND DISCUSSION

3.1. Physical properties and ageing behaviour of pea starch-PVA blend film

3.1.1. Solubility and moisture content

Table 1 shows the solubility and moisture content mean values and the standard deviation of the films. The water solubility values of films are relatively high, concordant with the hydrophilic nature of the polymers. Nevertheless, blend films exhibited significantly lower solubility ($p<0.05$) than pure polymers. This fact suggested that a decrease in the hydrophilic nature of the matrix occurred in the blend, probably due to the establishment of polymer interactions, leading to decreased water affinity. In this sense, hydrogen bonds between hydroxyl groups of PVA and starch have been reported by Valencia *et al.* (2013) and Chaléat *et al.* (2012). The formation of hydrogen bonds between PVA hydroxyls and those of amylose or amylopectin would imply the re-

orientation of the hydrophobic side of the PVA chain, generating hydrophobic regions in the matrix, which would reduce the water affinity of the blend films.

Table 1 also shows the moisture content (MC) of S, PVA and blend films equilibrated at 53 % RH at the beginning (1W) and the end (5W) of the storage time. At the beginning of the storage, significant differences ($p<0.05$) were found between the water content of the three matrices. S and PVA films exhibited a higher moisture content than blend films. This decrease is coherent with the loss of water solubility and has been attributed to the formation of hydrogen bonds between the two polymers, which reduced their water sorption capacity (Chaléat *et al*., 2012; Chen *et al*., 2008).

At the end of the storage time (5W), the moisture content tended to decrease, but becoming significantly different only for S films. This could be attributed to progressive chain aggregations through hydrogen bonds, limiting the water sorption capacity of the films. The water loss could provoke a greater chain aggregation in the amorphous region, which will imply an increase in the film compactness that will affect the mechanical, optical and barrier properties (Cano *et al*., 2014).

Table 1: Solubility (S), moisture content (MC), water vapour permeability (WVP) of pea starch (S), PVA and composite (S:PVA) films at the beginning (1W) and the end (5W) of the storage time. Mean values and standard deviation.

	S ($g_{dissolved}\ g_{dry\ film}^{-1}$)	MC (% d.b.)	
Films		1W	5W
S	0.21 ± 0.02^{a}	11.4 ± 0.4^{a1}	8.7 ± 0.4^{a2}
PVA	0.19 ± 0.05^{b}	12.8 ± 1.2^{b1}	11.9 ± 1.3^{b1}
S:PVA	0.1157 ± 0.0008^{c}	8.0 ± 0.5^{c1}	7.1 ± 1.7^{a1}

[a, b, c] Different superscripts within a column indicate significant differences among formulations. ($p<0.05$).

[1, 2] Different superscripts within the same file indicate significant differences among storage times for the same formulation. ($p<0.05$).

The thickness values of the films were 0.087 ± 0.017 mm, 0.107 ± 0.019 mm and 0.123 ± 0.013 mm, for pure S, PVA and blend films, respectively. Blend films presented the greater values. This result suggests that the chains in the blend matrix were less tightly packaged, giving rise to a more open network, probably due to steric hindrances caused by the different polymers.

3.1.2. Mechanical properties

Figure 1 shows the typical stress-strain curves obtained for all the films after one and five storage weeks under controlled conditions (53 % RH and 25 ºC), where the different mechanical behaviour of the matrices and the effect of ageing can be observed. Starch films exhibited the typical mechanical behaviour of a brittle material, without plastic deformation and with very low extensibility at break. On the other hand, the great resistance to break of PVA is highlighted.

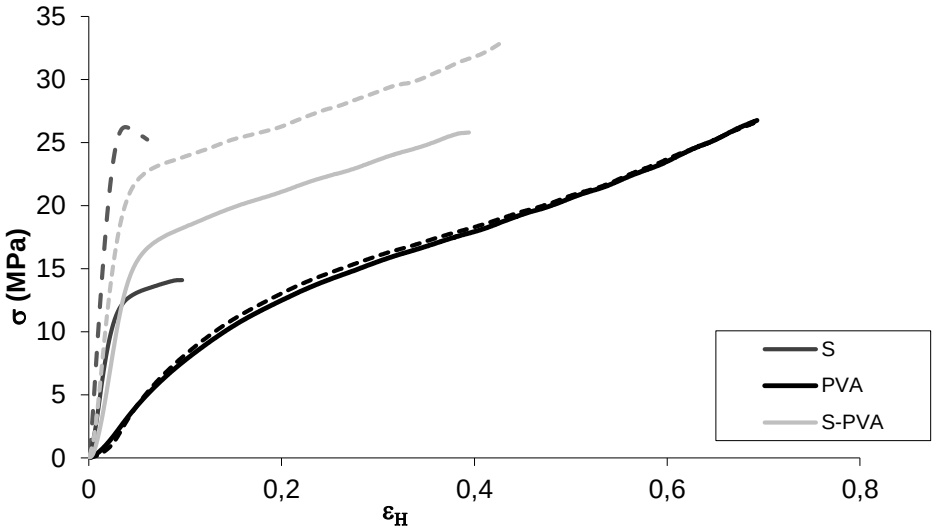

Figure 1. Strain-Stress curves of pea starch (S), PVA and composite (S:PVA) films at the beginning (solid lines) and the end (dashed lines) of the storage time.

The mechanical behaviour of films was analysed in terms of elastic modulus (EM), tensile strength at break (TS) and percentage of elongation at break (E, %). EM

represents the stiffness of the material, TS the resistance to elongation at break and E is a measure of the films' capacity for stretching. In Table 2, the mean values of the mechanical parameters and the standard deviation of the studied films throughout the storage time are shown. The values obtained are similar to those reported by other authors for pea starch films (Cano *et al*., 2014; Da Matta *et al*., 2011) and PVA films (Chen *et al*., 2008; Fortunati *et al*., 2013).

Table 2: Elastic modulus (EM), tensile strength at break (TS) and percentage of elongation at break (E, %) of pea starch (S), PVA and composite (S:PVA) films at the beginning (1W) and the end (5W) of the storage time. Mean values and standard deviation.

	1W			5W		
Films	EM (MPa)	TS (MPa)	E (%)	EM (MPa)	TS (MPa)	E (%)
S	417 ± 41^{a1}	14.2 ± 1.3^{a1}	10 ± 2^{a1}	964 ± 88^{a2}	24 ± 2^{a2}	4.7 ± 0.9^{a2}
PVA	95 ± 22^{b1}	27 ± 2^{b1}	69.1 ± 0.4^{b1}	103 ± 20^{b1}	27.2 ± 0.9^{b1}	69.296 ± 0.013^{b1}
S:PVA	506 ± 62^{c1}	26.9 ± 1.4^{b1}	40 ± 4^{c1}	689 ± 44^{c2}	32.3 ± 1.6^{c2}	41 ± 3^{c1}

$^{a, b, c}$ Different superscripts within a column indicate significant differences among formulations. ($p<0.05$).

$^{1, 2}$ Different superscripts within the same file indicate significant differences among storage times for the same formulation. ($p<0.05$).

Significant differences ($p<0.05$) were found between the mechanical parameters of the different films. At the beginning of the storage time (1W), PS films exhibited the poorest mechanical properties because of their lower resistance and stretchability (lower TS and % E). This may be explained by the strong interchain interactions of starch polymers through hydrogen bonds, which increases the cohesion forces of the matrix but makes it difficult for the chains to shift during the tensile test. On the contrary, although PVA films were very resistant and stretchable, they were not as stiff as S films. Blend films exhibited better mechanical properties than pure starch films; these being stiffer,

more resistant and stretchable. Thus, PVA can be used to enhance the poor mechanical features of starch-based films.

After the storage period (5W), S films significantly ($p<0.05$) increased in rigidity, becoming more resistant and brittle; this was due to the greater compactness of the matrix associated with water loss (Table 1), coinciding with what was found by other authors (Cano *et al*., 2014; Jiménez *et al*., 2012b). On the contrary, the mechanical behaviour of PVA films did not change throughout the ageing process ($p>0.05$).

The rigidity and resistance (high EM and TS) of blend films significantly increased ($p<0.05$) through storage, following the same, but less pronounced, pathway as S films. However, film stretchability was not significantly affected by the storage time in blend films, these maintaining their high extensibility. The greater stability PVA provided to blend films could be attributed to the inhibition of the re-arrangement of the starch polymer chains throughout time due to interactions between the chains of both polymers.

These satisfactory results indicate that the blend of both polymers improved the mechanical response of pure starch films. These blend films behaved similarly to some commercial plastics very flexible and resistant, such as the typical black low density polyethylene bag used for trash, whose values obtained using the same experimental conditions and equipment were: thickness = 0.02 mm, EM = 370 ± 74 MPa, TS = 27 ± 7 MPa and % E = 39.7 ± 0.2 %.

3.1.3. Optical properties

According to Hutchings (1999), the gloss and internal transmittance (Ti) parameters are the best optical properties with which to evaluate the appearance of the films. Ti is related to the transparency of films and their structural homogeneity: high values of Ti are associated with structural homogeneity and high transparency. The main Ti differences among the films occurred at 450 nm; so, at 450 nm, Ti is taken to evaluate

differences in the films' transparency. These values are shown in Table 3. At the initial storage time (1W), the Ti values of PVA and blend films were slightly higher than those of S films, but these small differences disappeared the longer they were stored. The different transparency level is linked to the internal structure developed in each film.

Table 3: Gloss values at 60º and internal transmittance (Ti) of pea starch (S), PVA and composite (S:PVA) films at the beginning (1W) and the end (5W) of the storage time. Mean values and standard deviation.

	Gloss 60º		Ti (450nm)	
Films	1W	5W	1W	5W
S	47±17^{a1}	33±8^{a2}	85.4±1.6^{a1}	87.09±0.12^{a1}
PVA	53±23^{a1}	32±11^{a1}	88.2±0.2^{b1}	85.7±0.9^{a1}
S:PVA	13.2±1.6^{b1}	12.9±1.2^{b1}	86.2±0.5^{b1}	85.2±0.9^{a1}

$^{a, b, c}$ Different superscripts within a column indicate significant differences among formulations. ($p<0.05$).

$^{1, 2}$ Different superscripts within the same file indicate significant differences among storage times for the same formulation. ($p<0.05$).

Table 3 also shows the mean gloss values of studied films at an incidence angle of 60º. The gloss of the films is related with the surface morphology achieved during film drying. In general, the smoother the surface, the glossier the film (Ward & Nussinovitch, 1996). In this sense, the decrease in the gloss values of the blend films may be explained by an increase in the surface roughness of these films provoked by the blend effect. After the storage period (5W), the gloss values of pure starch films decreased ($p<0.05$) while those of pure PVA and blend films did not change. Changes in the gloss of starch films have been observed by different authors (Jimenez *et al*., 2012b) and related with the progress of surface level crystallization.

3.1.4. Barrier properties

Table 4 shows the WVP values of films analysed at 25 ºC and a RH gradient of 53-100 %. PVA films exhibited slightly lower WVP values than starch films, in accordance

with their less marked hydrophilic nature and, coherently with this, blend films had an intermediate WVP value. The values obtained for S and PVA films agree with those found by other authors (Cano *et al*., 2014; Mehyar & Han, 2004). In no case were the WVP values significantly affected by the storage time.

Table 4: Water vapour permeability (WVP) and oxygen permeability (OP) of pea starch (S), PVA and composite (S:PVA) films at the beginning (1W) and the end (5W) of the storage time. Mean values and standard deviation.

	WVP ($gmmh^{-1}m^{-2}KPa^{-1}$)		OP ($cm^3m\ h^{-1}mm^{-2}KPa^{-1}$)	
Films	1W	5W	1W	5W
S	6.0 ± 0.3^{a1}	6.7 ± 0.7^{a1}	1.39 ± 0.09^{a1}	1.01 ± 0.06^{a2}
PVA	4.74 ± 1.05^{b1}	4.8 ± 0.8^{b1}	0.623 ± 0.009^{b1}	0.71 ± 0.06^{b1}
S:PVA	5.09 ± 1.17^{ab1}	5.1 ± 0.4^{b1}	0.53 ± 0.02^{b1}	0.609 ± 0.018^{c2}

[a, b, c] Different superscripts within a column indicate significant differences among formulations. ($p<0.05$).

[1, 2] Different superscripts within the same file indicate significant differences among storage times for the same formulation. ($p<0.05$).

The mean oxygen permeability (OP) values of the films after the different storage times are also shown in Table 1. In the case of S films, similar values have been reported by Mehyar & Han (2004). The OP values were significantly lower for blend films, which can be due to a decrease in the oxygen solubility of the matrix. The OP values were greatly ($p<0.05$) reduced in S films after 5 storage weeks, coinciding with the increased matrix compactness as a result of water content reduction. The incorporation of PVA into the starch matrix seems to inhibit these changes in the starch phase, thus also inhibiting changes in the barrier properties.

On the basis of these results, the incorporation of PVA into starch-based films appears to be a successful alternative means of improving the mechanical and barrier properties of these films, while providing enough stability to the matrix to inhibit physical

changes provoked by ageing. The blend led to films which were less water soluble and not as sensitive to water sorption, more stretchable and resistant than starch films while maintaining the low oxygen barrier property of starch films. These promising films could be used to prevent oxidative reactions in food packaging, although more studies considering different ratios of starch and PVA are needed to optimize their ratio in terms of the film functionality. In the next section, this aspect has been considered and a deeper structural and thermal analysis of the films, a part from their physical properties characterization, was performed.

3.2. Properties and ageing behaviour of pea starch films as affected by blend with poly(vinyl alcohol)

3.2.1. Structure of the films

Polymer interactions in the blends lead to nano and microstructural features which are relevant in the final functional properties of the films. FT-IR analyses of the samples were carried out in order to analyse particular interactions between the chains' functional groups through the shift of their specific IR bands. In this sense, hydroxyl groups of both starch and PVA chains can form hydrogen bonds, as reported by Ramaraj (2006).

Figure 2 shows FT-IR spectra for S, PVA and S:PVA blends, showing the wavenumber values corresponding to the main peaks in each sample. For every film, the broad band located between 3200-3400 cm^{-1} corresponds to the stretching vibration mode of hydroxyl groups from the absorbed water and from the polymers themselves (Chen *et al*., 2008; Fortunati, *et al*., 2013; Jiménez, *et al*., 2013). In S and PVA films, the peak wavenumber was higher than for blend films, which showed a significant peak shift (about 40 cm^{-1}), in agreement with the promotion of hydrogen bond formation between the hydroxyl groups of both polymers. The peak associated with the bending vibration

mode of hydroxyl group appears between 1400-1460 cm^{-1} and was slightly displaced for S and PVA (1455 and 1420 cm^{-1}, respectively).

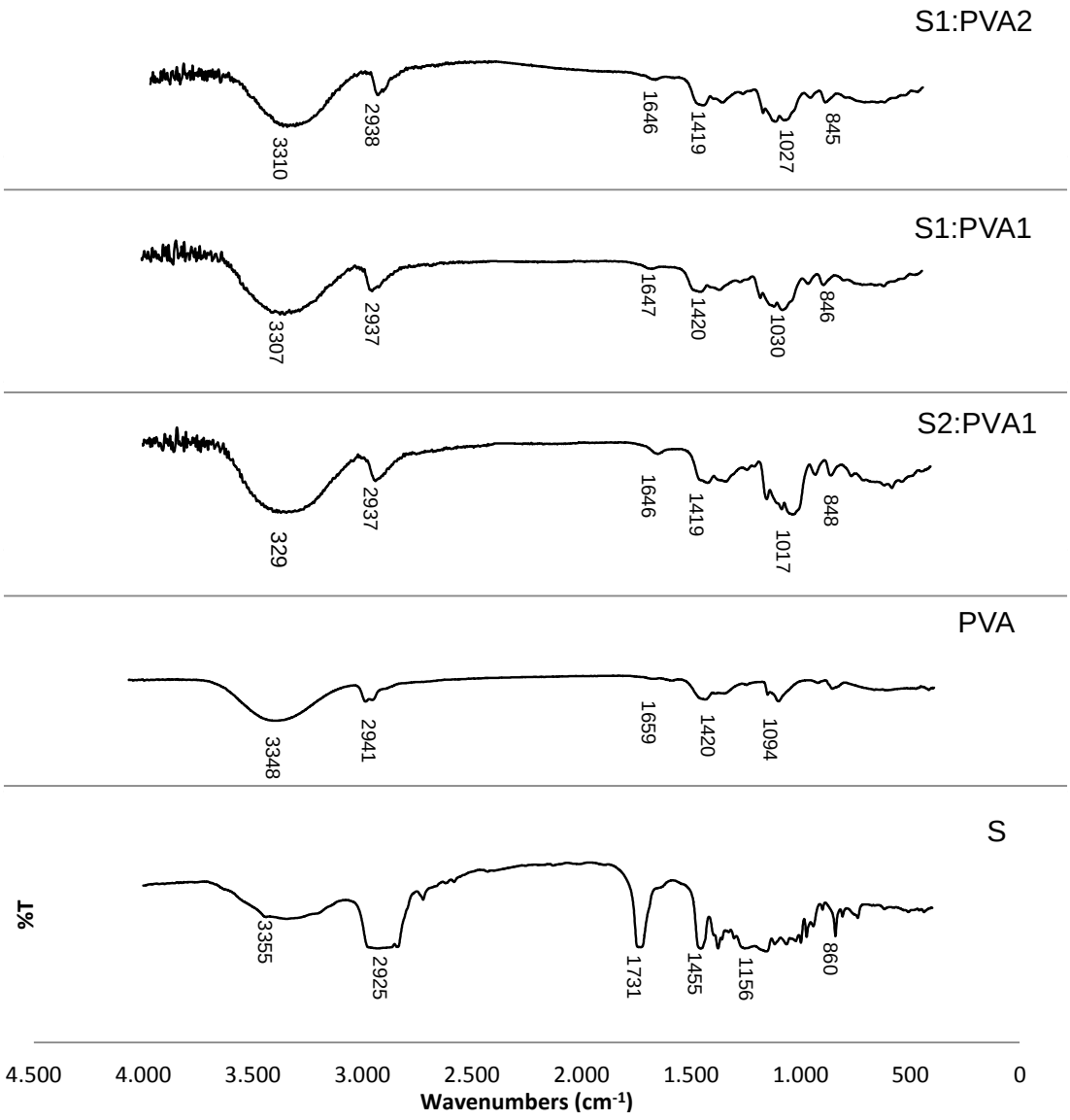

Figure 2. FT-IR spectra for S, PVA and S:PVA blend films.

In blend films, this peak was also shifted towards a lower wavenumber in agreement with the formation of hydrogen bonds, as mentioned above. The peak located between 2910-2935 cm^{-1} is related with C-H stretching (Fortunati *et al*., 2013; Jagadish & Raj., 2011; Jiménez *et al*., 2013) and appeared with different intensities for S and PVA films. In the blends, this peak was shifted to a higher wavenumber. The peak at 1731 cm^{-1} has

been assigned to the C-C-O stretching in starch films (Jagadish & Raj., 2011). In PVA and blend films, this peak greatly decreased in intensity despite the high ratio of starch in the S2:PVA1 film. Moreover, this peak shifts to a lower wavenumber in blend films. The stretching vibration of C-O in C-C-O and in the glucose ring in starch corresponds to the peaks at 1024 and 860 cm^{-1}, respectively, and also appeared with lesser intensity and a slight shift in the blend films. For PVA films, C-O stretching vibration appeared at 1094 cm^{-1}, according to Chen *et al*. (2008). These results highlight the formation of hydrogen bonds to some extent between the hydroxyl groups of the starch polymers and PVA chains, and point to a certain degree of polymer miscibility.

Figures 3 and 4 show the FESEM images of the surface and cross section of the different films. S films had a smooth surface and a homogeneous internal structure, typical of gelatinized starch, as was found in other studies (Cano *et al*., 2014; Chen, *et al*., 2009; Wu, *et al*., 2010). Nevertheless, the presence of a heterogeneously-fractured layer near the film surface reveals the progress of crystallization in this zone, probably due to the greater molecular mobility associated with the diffusion of water vapour to the film surface (Cano *et al*., 2014).

PVA films also exhibited a smooth surface. Nevertheless, the cross section images revealed the presence of zones with different morphology which could be attributed to the coexistence of amorphous and crystalline regions in the film. The chain associations in crystalline regions will define a different morphology from that of the amorphous zones, coinciding with that reported by other authors (Bonilla *et al*., 2014; Chen *et al*., 2008; Fortunati *et al*., 2013).

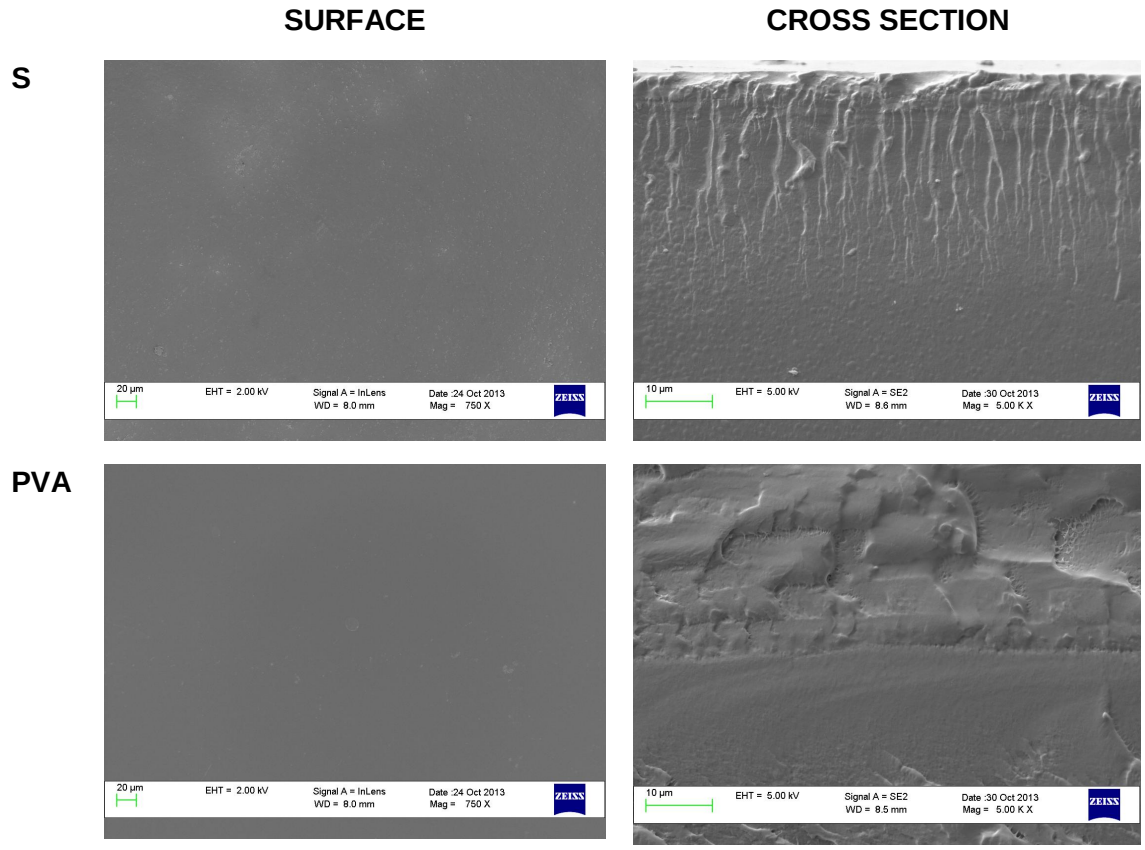

Figure 3. FESEM micrographs of the surface and cross section of S and PVA films.

Blend films (Figure 3) showed rougher, irregular surfaces, especially when the proportion of PVA in the blend was equal or higher than that of the starch. This indicates polymer incompatibility and the formation of two phases: one PVA-rich phase and another starch-rich phase, which emerge to the surface in a differentiated way when starch is present at equal or lower ratio than PVA. For the highest starch ratio, this polymer forms a more continuous phase and no particles were observed at the film surface. The cross section images of blend films also exhibit this phase separation, which gives rise to two interpenetrated networks of both polymers where the zones with different morphology for PVA can also be appreciated. The phase separation of both polymers in corn starch and PVA blend films has also been reported by Sreekumar *et al.* (2012).

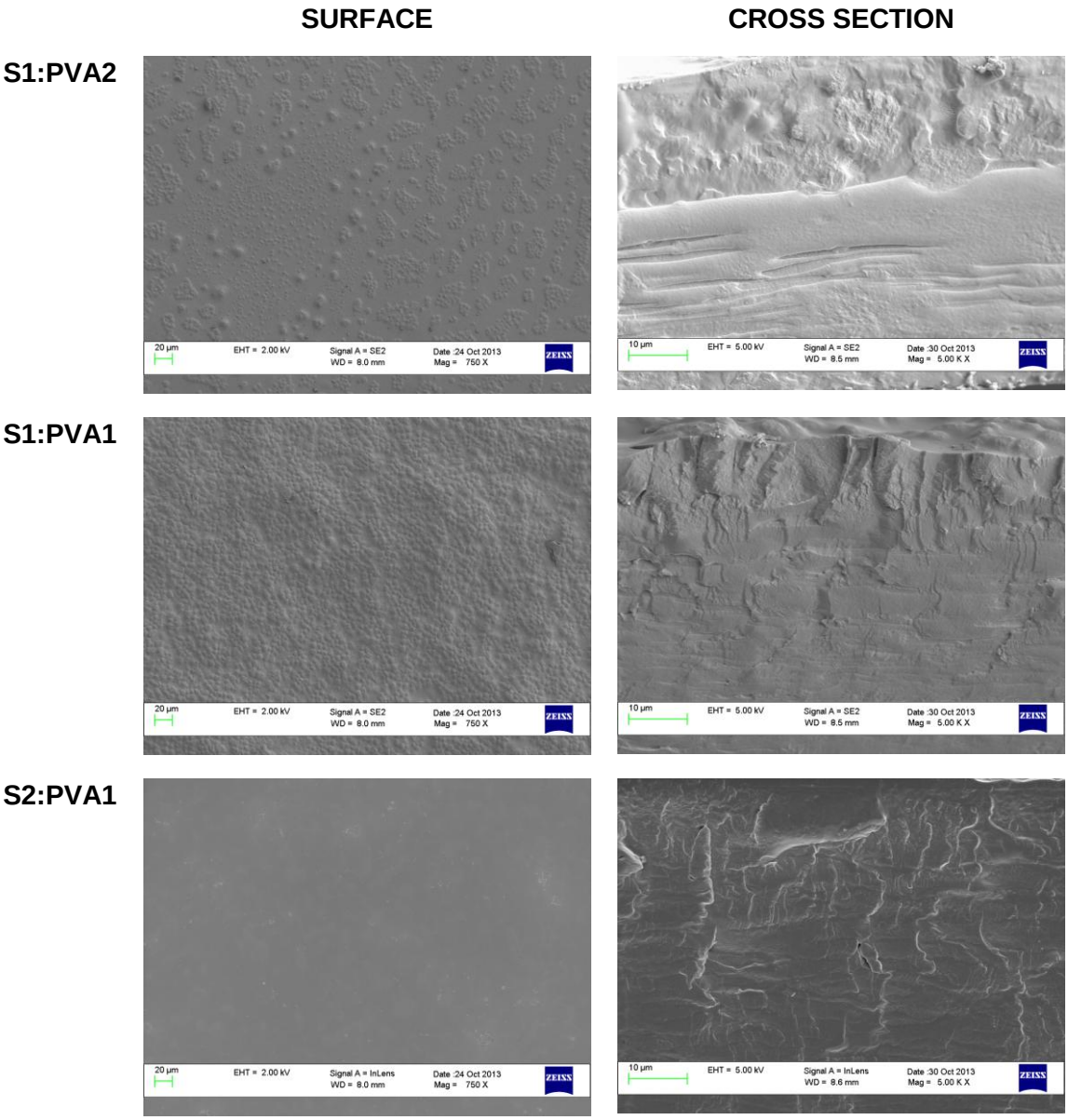

Figure 4. FESEM micrographs of the surface and cross section of S:PVA blend films.

3.2.2. Thermal behaviour

The thermal behaviour of the films was analysed by TGA and DSC measurements, in order to find out the thermal stability of polymers (Adbelrazek *et al*., 2010) and to highlight the effect of the different S:PVA ratios on the thermal degradation pattern, as well as the phase transitions in the films in the processing/handling temperature range.

Figure 5 shows the weight loss (TG) and derivate (DTG) curves for S, PVA and S:PVA blend films obtained by thermogravimetric analysis while the temperatures for the main degradation step of the films are summarized in Table 5. For pure starch films, two weight loss steps were observed. The initial weight loss (first peak) up to about 100 ºC, can be attributed to the loss of bonded water in the film (Luo, *et al*., 2012). In the second step, between 170-450 ºC, about 70 % of the sample weight was lost, which is related to the main degradation process (peak temperature: 315 ºC). For PVA films, three weight loss steps were observed in Figure 5. As in the S films, the initial step, up to about 100 ºC, can be attributed to the loss of adsorbed and bound water (Bonilla *et al*., 2014). The second step occurs between 200-400 ºC, in which the dehydration of the PVA takes place, followed by chain scission and decomposition (Frone *et al*., 2011; Li *et al*., 2012). The third step occurs between 400 – 500 ºC and it can be attributed to the degradation of the by-products generated by PVA during the thermal process (Bonilla *et al*., 2014; Lewandowska, 2009). Similar three-step weight loss behaviour was observed for the S:PVA blends, except for the film with the lowest PVA ratio (S2:PVA1), where a second weight loss step was observed after the first water loss, at relatively low temperature (150-200 ºC). This could indicate either that PVA starts to degrade at very low temperatures when it is present in the blend at the lowest ratio, or that the PVA hydroxyl groups react with those of starch chains through the formation of oxi (-O-) groups with subsequent water loss. Sreekumar *et al*. (2012) also observed similar behaviour when analysing corn starch PVA blend films obtained by casting.

Mean values exhibit significant differences ($p<0.05$) for the different formulations, indicating that PVA films degrade at the lowest temperature (279 ºC), although S:PVA blends with the highest PVA ratio showed slightly greater thermal stability, with higher values of the degradation temperature, similar to that of the starch (Table 5). The blend

with the lowest ratio of PVA exhibited anomalous thermal behaviour, showing the first small degradation peak at 172 ºC.

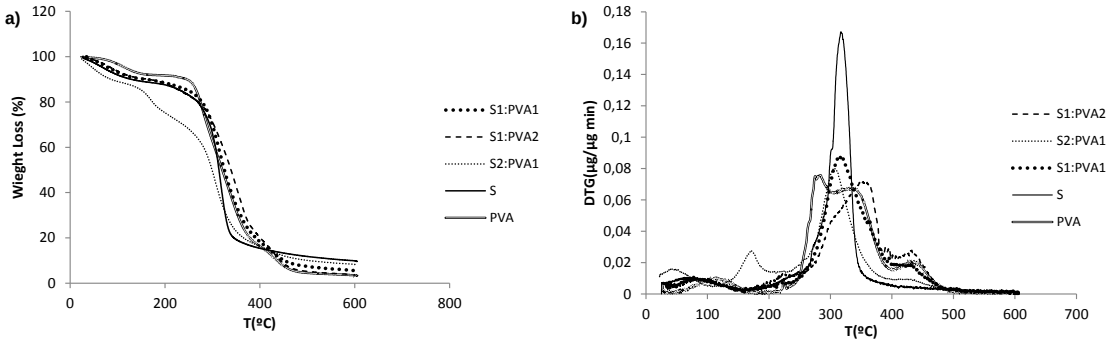

Figure 5. a) TG and b) DTG curves of S, PVA and S:PVA blend films.

Tables 5 and 6 show the results obtained from the DSC analysis, in terms of glass transition (Tg), crystallization (Tc) and melting temperatures (Tm), enthalpy of crystallization (ΔHc) and melting (ΔHm) and percentage of crystallinity (X) of PVA.

The cooling scan of the samples showed different peaks associated with the crystallization of PVA. Starch films do not show crystallization peaks or crystallite melting. The crystallization temperature (Tc) values for the different crystallization peaks of PVA are shown in Table 5. Two peaks at 140 (secondary peak) and 201 ºC (main peak) were observed for PVA films, which could be due to the fact that the crystallization of some molecules is delayed by steric hindrances at the end of the crystallization process. This usually occurred in complex mixtures, when the molecular mobility of the polymer chain segments was limited. Likewise, some trends were observed in the crystallization behaviour of PVA, due to the incorporation of starch. As in PVA, two crystallization peaks were observed for the blend films with the highest PVA ratio, but at a higher temperature for the secondary peak (178 ºC). For the greatest PVA ratio in the blend, three crystallization peaks were observed. The greater the starch ratio in the blend, the higher the Tc values of the main peak (at 209 ºC), with two secondary peaks at 200 and 178

ºC. These results suggest that starch enhanced the crystallization rate of PVA, since less undercooling was required.

The melting temperature of PVA is 227 ºC, without the split observed in crystallization. This value coincides with those reported by other authors (Bonilla *et al*., 2014; Mailo *et al*., 2011). No differences in the Tm of PVA were observed for blend films with the lowest PVA ratio. However, in the other blends with a higher ratio of PVA, two melting peaks were observed at 226 and at about 210 ºC. This suggests that PVA polymorphism was promoted when a high proportion of starch was present in the film, thus showing two melting intervals. The differences between crystallization and melting behaviour are explained in terms of kinetic hindrances which take place during the crystallization process. In this sense, notable differences can be found between the obtained Tc and Tm temperatures; the latter is the equilibrium value and the former is affected by crystallization kinetics.

The crystallization and melting enthalpies of PVA in the different films are shown in Table 6, expressed as $J.g^{-1}$ of sample and $J.g^{-1}$ of PVA in the film, and deduced from the additive integration of all the melting peaks in the thermogram. As expected, the greater the PVA content in the film, the higher the enthalpy value. No significant differences were observed between the ΔHm and ΔHc values, which indicates that no undercooling occurred during the cooling step. The crystallinity of PVA was obtained from the ΔHm values ($J.g^{-1}$ PVA), taking the ΔHm reported (Roohani *et al*., 2008) for 100 % crystallized PVA (161.6 $J.g^{-1}$ PVA) into account. The crystallinity values are shown in Table 6, where the inhibition of PVA crystallization brought about by the starch blend can be observed for films containing the same ratio of starch and PVA. An increased variability in the values can also be observed in blend films, which can be attributed to a kinetic control of the polymer chain interactions during crystallization. Taking the variability into account,

it is remarkable that no significant inhibition of PVA crystallization occurs in the other blend films with different ratios of PVA and S.

As far as glass transition is concerned, starch films showed the highest Tg value (160 ºC), which was similar to that reported by other authors for starch films (Ortega-Toro, *et al*., 2014b), while the PVA amorphous phase showed lower Tg values (79 ºC) in agreement with that previously reported (Fortunati *et al*., 2013). Two glass transitions were observed in thermograms of blend films, one for each polymer phase, in agreement with the phase separation of the polymers commented on above. The Tg of the PVA rich phase did not significantly change with respect to the pure PVA, except for the S1:PVA1 blend, where an increase in the Tg value can be observed. This indicates that starch (with a higher molecular weight) partially solubilises in the PVA phase, thus promoting an increase in the Tg in the blend with the same ratio of polymers. On the contrary, the Tg values of the starch rich phase decreased when the PVA (lower molecular weight) was solubilised in this phase, and this effect was more intense at the highest ratio of starch in the film. So, the partial compatibility of the polymer was dependent on the polymer ratio, as reported by Sreekumar *et al*. (2012); the highest degree of starch miscibility in PVA films occurred at the ratio of 1:1, while the PVA solubilizes in the starch phase at all the tested starch ratios.

Table 5: Crystallization, glass transition and melting temperatures of S, PVA and S:PVA blend films obtained by DSC and the degradation temperatures (Tmax) obtained from TGA analysis.

	Cooling scan			Second heating scan				
Films	Tc_1 (ºC)	Tc_2 (ºC)	Tc_3 (ºC)	Tm_1 (ºC)	Tm_2 (ºC)	Tg_1 (ºC)	Tg_2 (ºC)	Tmax (ºC) *
S							160±3[a]	315±2[a]
PVA	140.7±1.7[a]	201.52±0.06[a]			227.3±0.4[a]	79.3±0.2[a]		279±3[b]
S1:PVA2	178.4±1.2[bc]	196.9±1.3[b]			226.4±1.3[a]	76±4[a]	124±2[a]	374.3±0.4[c]
S1:PVA1	179±3[b]	200±2[ab]	209.1±0.2[b]	212.2±1.9[a]	226.2±1.4[a]	89±11[b]	124±10[a]	307±5[d]
S2:PVA1	175±2[c]	199.8±0.7[a]	209.2±0.2[b]	207±4[a]	226.43±0.06[a]	78±3[a]	113.1±0.8[b]	304.6±1.6[d]

(*) A previous peak with smaller weight loss at 172.09±0.54 ºC was observed.

Tg: glass transition temperature; Tc: crystallization temperature; Tm: melting temperature and Tmax: temperature at maximum decomposition rate.

[a, b, c, d] different letters in the same column indicate significant differences among formulations ($p<0.05$).

Table 6: The crystallization and melting enthalpy of S, PVA and S:PVA blend films obtained by DSC.

	Cooling scan		Second heating scan		
Films	ΔHc (J g^{-1})	ΔHc (J g^{-1})	ΔHm (J g^{-1})	ΔHm (J g^{-1})	X (%)
PVA	72±2[a]	77±2[ab]	73.8±0.2[a]	78.6±0.3[ab]	49.7±0.3[a]
S1:PVA2	30±3[b]	49±4[c]	49±7[b]	79±11[b]	49±7[a]
S1:PVA1	31±8[b]	69±19[c]	21±1[c]	47±2[c]	29.2±1.4[b]
S2:PVA1	27±5[a]	87±16[b]	18±5[c]	61±19[c]	43±4[a]

ΔHc: enthalpy of crystallization; ΔHm: enthalpy of fusion and X: crystallinity.

[a, b, c] different letters in the same column indicate significant differences among formulations ($p<0.05$).

An analysis of the thermal behaviour of S:PVA blends, as compared with non-blend polymers, indicates that both polymers show partial miscibility, which depended on the polymer ratio, and which affected the behaviour of PVA crystallization and the glass transition of the different phases in the films. In blends with the S1:PVA1 ratio, PVA crystallization was significantly inhibited while the Tg of amorphous PVA significantly increased with respect to pure PVA. This indicates that, at this ratio, interactions of starch molecules in the PVA phase were enhanced, and the blend effects were intense. However, the starch rich phase is affected by PVA molecules (lower Tg), especially at the highest S ratio.

3.2.3. Water vapour barrier properties of the films

Table 7 shows the water vapour permeability values (WVP) of the films at 25 ºC and a 53-100 % RH gradient, together with their equilibrium moisture content and thickness. The moisture content of the films ranged between 5 and 8 %, the S films exhibiting higher values ($p<0.05$) than the PVA films, coherent with their more hydrophilic nature (a higher ratio of hydroxyl groups). PVA is water-soluble and starch is water-sensitive, which leads to their blends being water sensitive (Chen *et al*., 2008). S:PVA blends had moisture contents that were more similar to S than to PVA films, showing significant differences ($p<0.05$) with respect to the latter. The higher the starch contents in the films, the greater their equilibrium moisture content. The moisture content of the samples tends to increase throughout 5 storage weeks, but only S and PVA films showed significant differences ($p<0.05$) after the storage time. This fact indicate that films equilibrate slowly with the conditioning relative humidity, approaching equilibrium value after 5 weeks' storage.

Table 7: Moisture content (MC), water vapour permeability (WVP) and thickness of S, PVA and S:PVA blend films after 1 (1W) and 5 (5W) storage weeks. Mean values and standard deviation.

	MC (%d.b.)		WVP (g.mm.kPa^{-1}h^{-1}m^{-2})		Thickness(mm)	
Films	1W	5W	1W	5W	1W	5W
S	6.9±0.2^{a1}	8.0±0.3^{a2}	5.3±0.3^{a1}	6.77 ±0.09^{a2}	0.078±0.008^{a1}	0.081±0.007^{a1}
PVA	5.03±0.06^{b1}	5.3±0.2^{b2}	2.2±0.2^{b1}	2.32±0.15^{b1}	0.13±0.03^{b1}	0.13±0.03^{b1}
S1:PVA2	6.6±0.8^{a1}	6.7±0.3^{c1}	3.5±0.3^{c1}	3.4±0.2^{c1}	0.11±0.03^{cd1}	0.104±0.014^{c1}
S1:PVA1	6.7±0.8^{a1}	7.3±0.4^{d1}	4.97±0.10^{d1}	4.7±0.2^{d1}	0.124±0.015^{bc1}	0.12±0.02^{d1}
S2:PVA1	6.9±0.5^{a1}	8.2±0.9^{a1}	5.7±0.4^{e1}	5.2±0.2^{e1}	0.11±0.03^{d1}	0.10±0.03^{c1}

$^{a, b, c, d, e}$ different letters in the same column indicate significant differences among formulations ($p<0.05$).

$^{1, 2}$ different numbers in the same row indicate significant differences between storage times ($p<0.05$).

The WVP values define the final application of a film in contact with food systems and they must be as low as possible so as to avoid water transfer (Ma *et al*., 2008). Significant differences between the WVP values of the different films are found after the two different storage times, which coincides with results found by other authors studying pea starch films (Cano *et al*., 2014; Han *et al*., 2006; Ma *et al*., 2008) and PVA films (Bonilla *et al*., 2014). Pea starch films showed the highest WVP (5.03 g mm kPa^{-1} h^{-1} m^{-2}), while PVA films were less permeable (2.2 g mm kPa^{-1} h^{-1} m^{-2}) and S:PVA blends had intermediate WVP values. The higher the starch content, the more permeable the films are to water vapour. After five storage weeks, the WVP only significantly changed for S films, a fact which could be related with the increase in moisture content and the structural changes which occurred in the starch matrix. Several authors reported that starch microstructure changes throughout storage time in line with the progress of the recrystallization process or chain aggregation, thus giving rise to changes in barrier and mechanical properties (Cano *et al*., 2014; Jiménez *et al*. 2012b). In this sense, PVA

incorporation into the starch matrix seems to limit structural changes, as deduced from the stability of water vapour permeability values.

The differences in the WVP values of S and PVA films are related with the different hydrophilic nature of the polymers. In both, hydroxyl groups favour water affinity but their distribution and density in the chains establish relevant differences in the water sorption capacity and the mass transfer rate of water molecules. As previously commented, RH gradient used was chosen to simulate the storage conditions of intermediate moisture foods exposed at high relative humidity and at room temperature. In this sense, it is remarkable that, due to the water sensitivity of polymer blend, at lower RH conditions better water vapour barrier of the films can be expected, in line with the reduced mean water content of the film and the subsequent diminution of molecular mobility and diffusion properties.

The different polymer and water interactions also affected the film thickness. Table 7 shows these values, where the lower thickness values for starch films than for PVA films can be observed. This indicates that a best chain packaging occurs in starch matrix, whereas PVA chains are less densely packed. For blend films, intermediate thickness values were obtained, regardless of the polymer ratio. No significant changes ($p>0.05$) in film thickness were observed throughout storage time, despite the increase in moisture content in some cases. The small differences in the film thickness could affect the obtained values of barrier and mechanical properties of the films, although this parameter is included in the models used to determine these properties. In fact Yeun *et al*. (2005) found that oxygen permeability tend to decreased when the film thickness increased in PVA hybrid films.

3.2.4. Mechanical properties

Figure 6 shows the typical stress-strain curves obtained for all the films after one and five storage weeks under controlled conditions (53 % RH and 25 ºC), where the different mechanical behaviour of the matrices and the effect of ageing can be observed. Although starch films exhibited the typical mechanical behaviour of a brittle material, without plastic deformation and with very low extensibility at break, the great resistance to break of PVA is highlighted.

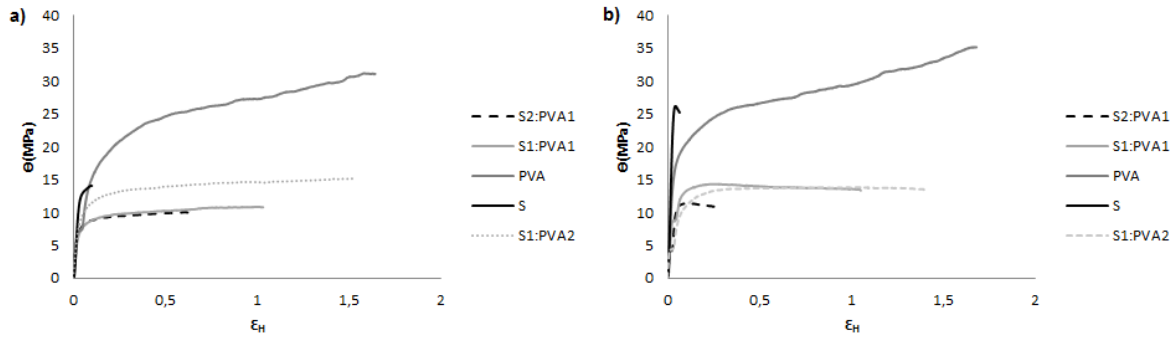

Figure 6. Typical strain-stress curves of S, PVA and S:PVA blend films at different storage times: a) one and b) five weeks.

Elastic modulus (EM), tensile strength at break (TS) and percentage of elongation at break (E, %) are the parameters used to describe the mechanical behaviour of films. Table 8 shows the mean values of these parameters for the S films, PVA films and S:PVA blend films. The obtained values are coherent with those reported by other authors working on pea starch films (Cano *et al*., 2014; Da Matta *et al*., 2011), PVA films (Chen *et al*., 2008; Fortunati *et al*., 2013) and S:PVA blend films (Shi *et al*., 2008; Yoon *et al*., 2012). The S films were stiffer than the PVA films, but the latter showed highest break strength and stretchability values.

Table 8: The elastic modulus (EM), tensile strength at break (TS) and percentage of elongation at break (E, %) of S, PVA and S:PVA blend films after 1 (1W) and 5 (5W) storage weeks. Mean values and standard deviation.

	EM (MPa)		TS (MPa)		E (%)	
Films	1W	5W	1W	5W	1W	5W
S	420 ± 40^{a1}	940 ± 90^{a2}	14.2 ± 1.3^{a1}	24 ± 3^{a2}	11 ± 2^{a1}	5.7 ± 1.9^{a2}
PVA	430 ± 90^{b1}	580 ± 80^{b2}	31 ± 5^{b1}	33 ± 3^{b1}	170 ± 50^{b1}	168 ± 19^{b1}
S1:PVA2	210 ± 60^{c1}	340 ± 50^{c2}	14 ± 2^{a1}	16 ± 3^{c1}	161 ± 16^{b1}	151 ± 30^{b1}
S1:PVA1	280 ± 60^{c1}	340 ± 70^{c2}	10.5 ± 1.9^{c1}	13 ± 3^{cd1}	80 ± 20^{c1}	93 ± 23^{1c}
S2:PVA1	272 ± 13^{c1}	420 ± 80^{d2}	9.5 ± 0.9^{c1}	10 ± 2^{d1}	58 ± 9^{c1}	33 ± 8^{a2}

$^{a, b, c, d}$ different letters in the same column indicate significant differences among formulations ($p<0.05$).

$^{1, 2}$ different numbers in the same row indicate significant differences between storage times ($p<0.05$).

In the case of the S films, every parameter significantly changes during storage. The films become harder, more resistant to break, but more brittle and less stretchable, as previously reported by Cano *et al*. (2014). The stiffness of the PVA films also slightly increased, but their resistance to break and extensibility did not change, the latter being much higher for PVA than for the S films. The blend films were the least stiff, with no significant differences between blends; the elastic modulus slightly increased during storage, especially when the S ratio was the greatest. These films also exhibited the lowest resistance to break, while maintaining high values of stretchability. Both resistance and extensibility decreased when the S ratio increased in the blend.

The effect of storage time on these parameters was only appreciated at the highest S ratio where the films underwent a significant loss in extensibility. The changes in mechanical behaviour during storage are related with the structural changes in the film associated with the progressive formation of hydrogen bonds, reinforcing the interchain

forces (Myllärinen *et al*., 2002; Rindlav *et al*., 1997). This increase in the interchain forces could be related with a potential glycerol migration throughout the storage time, which would lead to the establishment of the hydrogen bonds between chains, thus increasing the film toughness and reducing their extensibility. However, these effects were observed in all samples, included the neat PVA films which do not contain glycerol. So, the progressive chain aggregation throughout storage time occurred in all cases, thus affecting mechanical behaviour. Nevertheless, the incorporation of PVA into starch films seems to limit these changes, giving rise to more stable films from the mechanical point of view, while conferring better flexibility and extensibility to the blend films, with high values of hardness and mechanical resistance.

The mechanical behaviour of blend films is coherent with the formation of two interpenetrated networks of both polymer phases with partial chain miscibility, as deduced from the microstructural and phase transition analyses.

3.2.5. Optical properties

The optical properties, UV-VIS spectra, transparency (Ti) and gloss of the films are also directly related with their microstructure, respectively and are affected by the surface and internal heterogeneity of the structure (Jiménez *et al*., 2012a).

The UV-VIS spectra of the pea starch, PVA and S:PVA blend films are shown in Figure 7. The S, PVA and the blend with the ratio of 1:2 S:PVA exhibit higher values of transmittance (T) in the visible light range (400-800 nm) than in the UV range (200-400 nm), according to what is reported by Chen *et al*., (2008) for PVA films. In the range of visible light, the T values are over 90 %, indicating a good transparency. The blend films with S:PVA ratios of 1:1 and 2:1 showed the highest values of T, while the S and PVA films and 1:2 blend films exhibited lower T values, especially in the UV range. Therefore, in terms of light transmission no additive behaviour of the polymer contents in the blends

can be inferred from visible spectra. In the UV range, differences between the spectra grew and the blends with S:PVA ratios of 1:1 and 2:1 had the highest transmittance values. These results confirm the interactions between the PVA and S chains that greatly modify the UV-light interactions of the blends, as compared with the PVA or S films. 1:1 and 2:1 S:PVA blends were more transparent to UV radiation, which represents a drawback in terms of the protection of food against oxidative processes or other UV induced reactions.

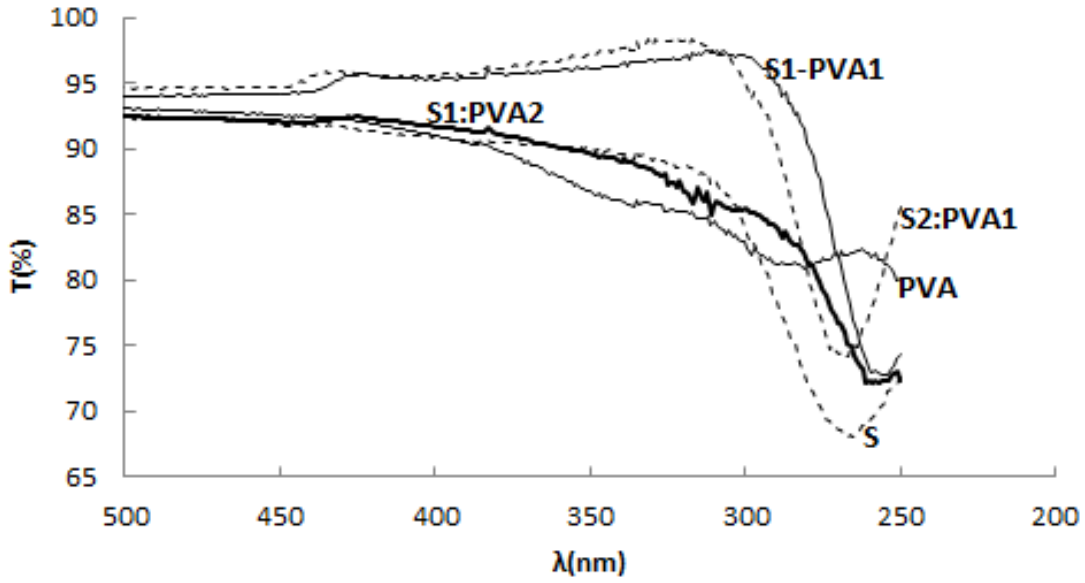

Figure 7. UV-VIS spectra for S, PVA and S:PVA blend films

In terms of internal transmittance at 450 (Ti) nm (Table 9), all the films showed a similar degree of transparency which did not significantly change during storage time and the differences in the film structure did not notably affect the film appearance. As for the film gloss, the PVA films are the glossiest, while the blend films exhibit the lowest gloss values due to the appearance of surface roughness associated with the presence of the two polymer phases, as commented on above. In general, except for the S films, the gloss values were quite stable during storage (Table 9). A reduction of the gloss in starch films during storage was previously reported and attributed to crystalline formation at

surface level, where water sorption occurs, inducing molecular mobility (Cano, *et al*. 2014; Jiménez *et* al., 2012b).

Table 9: The internal transmittance (Ti) at 450 nm and gloss values at 60º of S, PVA and S:PVA blend films after 1 (1W) and 5 (5W) storage weeks. Mean values and standard deviation.

	Ti (450 nm)		Gloss 60 º	
Films	1W	5W	1W	5W
S	84.38±0.14^{a1}	83.9±0.2^{a1}	27±12^{a1}	18.9±1.4^{a1}
PVA	85.9±0.7^{b1}	85.1±1.0^{b1}	153.9±0.9^{b1}	145±8^{b2}
S1:PVA2	85.27±0.03^{b1}	85.4±0.3^{b1}	18±3^{c1}	20±3^{a1}
S1:PVA1	85.5±0.2^{b1}	85.09±0.14^{b1}	14.0±1.4^{c1}	17±2^{a2}
S2:PVA1	85.53±0.09^{b1}	85.77±0.06^{b1}	13.2±1.6^{c1}	12.9±1.2^{a1}

$^{a, b, c}$ different letters in the same column indicate significant differences among formulations ($p<0.05$).

$^{1, 2}$ different numbers in the same row indicate significant differences between storage times ($p<0.05$).

4. CONCLUSIONS

The incorporation of PVA into pea starch blends implied the formation of interpenetrated networks of both incompatible polymers with the partial solubilisation of each one in the other polymer phase, depending on the polymer ratio. This has beneficial effects on the mechanical properties of the films, these becoming much more extensible and stable during storage. The water barrier properties were also improved by PVA blending at a S:PVA ratio of under 50 %, when films also reduced their water content as compared to the S films. The blends did not lead to a notable loss of transparency or gloss as compared to starch films and maintained their optical characteristics during storage, which did not occur in pure starch films. So, incorporating PVA to the S films at a ratio of around 1:1 represents a good strategy for improving the functionality of starch films without a notable increase in cost.

Acknowledgments

The authors acknowledge the financial support from the Spanish Ministerio de Economía y Competitividad throughout the projects AGL2010-20694. Amalia Cano also thanks the Spanish Ministerio de Educación, Cultura y Deporte for the FPU grant and COST-STSM-FA1001-14253 for the financial support for the collaboration.

References

- Abdelrazek, E. M., Elashmawi, I. S., & Labeeb, S. (2010). Chitosan filler effects on the experimental characterization, spectroscopic investigation and thermal studies of PVA/PVP blend films. *Physica B*, 405, 2021-2027.
- Alexy, P., Bakos, D., Hanzelova, S., Kukolíkova, L., Kupec, J., Charvátová, K., Chiellini, E. & Cinelli, P. (2003). Poly(vinyl alcohol)-collagen hydrolysate thermoplastic blends: I. Experimental design optimisation and biodegradation behaviour. *Polymer Testing,* 22, 801-809.
- Arvanitoyannins I.S. (1999). Totally and partially biodegradable polymer blends based on natural and synthetic macromolecules: preparation, physical properties and potential as food packaging materials. *Journal of Macromolecular Science-Reviews in Macromolecular Chemestry & Physics*, 39, 205-271.
- ASTM. (1995). Standard test methods for water vapour transmission of materials. Standard designations: E96-95 Annual book of ASTM standards. Philadelphia, PA: American Society for Testing and Materials. (pp. 406 e 413).
- ASTM. (1999). Standard test methods for specular gloss. Designation (D523). In Annual book of ASTM standards, Vol. 06.01. Philadelphia, PA: American Society for Testing and Materials.
- ASTM (2001). Standard test method for tensile properties of thin plastic sheeting. Standard D882 Annual book of American standard testing methods. Philadelphia, PA: American Society for Testing and Materials. (162-170).

- ASTM (2005). Standard test method for oxygen gas transmission rate through plastic film and sheeting using a Coloumetric sensor. Standard Designation: D3985-05 Annual book of American society for testing materials, West Conshohocken, PA, USA.

- Bonilla, J., Fortunati, E., Atarés, L., Chiral, A., & Kenny, J.M. (2014). Physical, structural and antimicrobial properties of poly vinyl alcohol-chitosan biodegradable films. *Food Hydrocolloids*, 35, 463-470.

- Cano, A., Jiménez, A., Cháfer, M., González, C., & Chiralt, A. (2014). Effect of amylose:amylopectin ratio and rice bran addition on starch films properties. *Carbohydrate Polymers*, 111, 543-555.

- Chaléat, C. M., Halley, P. J. H., & Truss, R. W. (2012). Study on the phase separation of plasticized starch/ poly(vinylalcohol) blends. *Polymer Degradation and Stability*, 97, 1930-1939.

- Chen, J., Liu, Ch., Chen, Y., Chen Y., & Chang, P.R. (2008). Comparative study on the films of poly(vinyl alcohol)/pea starch nanocrystals and poly(vinyl alcohol)/native pea starch. *Carbohydrate Polymers*, 73, 8-17.

- Chen, Y., Liu, Ch., Chang, P.R., Cao, X., & Anderson, D.P. (2009). Bionanocomposites based on pea starch and cellulose nanowhiskers hydrolyzed from pea hull fibre: Effect of hydrolysis time. *Carbohydrate Polymers*, 76, 607-615.

- Da Matta, M.D., Silveira, S.B., de Oliveira, L.M., & Sandoval, S. (2011). Mechanical properties of pea starch films associated with xanthan gum and glycerol. *Starch*, 63, 274-282.

- Fortunati, E., Puglia, D., Luzi, F., Santulli, C., Kenny, J.M., & Torre, L. (2013). Binary PVA bio-nanocomposites containing cellulose nanocrystals extracted from different natural sources: Part I. *Carbohydrates Polymers,* 97, 825-836.

- Fredriksson, H., Silverio, J., Andersson, R., & Eliasson, P. (1998). The influence of amylose and amylopectin characteristics on gelatinization and retrogradation properties of different starch. *Carbohydrate Polymers*, 35, 119-134.

- Frone, A. N., Panaitescu, D. M., Donescu, D., Spataru, C. I., Radovici, C., & Trusca, R., (2011). Preparation and characterization of PVA composites with cellulose nanofibers obtained by ultrasonication. *BioResources*, 6, 487–512.
- Galus S., Mathieu H., Lenart A., & Debeaufort F. (2012). Effect of modified starch or maltodextrines incorporation on the barrier and mechanical properties, moisture sensitivity and appearance of soy protein isolate-based edible films. *Innovative Food Science and Emerging Technologies*, 16, 148-154.
- Galus S., Lenart A., Voilley A., & Debeaufort, F. (2013). Effect of oxidized potato starch on the physicochemical properties of soy protein isolate-based edible films. *Food Technology and Biotechnology*, 5 (3), 403-409.
- Gupta, V. K., Priya, B., Pathania, D. & Singh, A. (2014). Synthesis, characterization and antibacterial activity of biodegradables Starch/PVA composite films reinforced with cellulosic fibre, *Carbohydrate Polymer*, http://dx.doi.org/10.1016/j.carbpol.2014.03.044.
- Han, J.H., Seo, G.H., Park, I.I., Kim, G.N., & Lee, D.S. (2006). Physical and mechanical properties of pea starch edible films containing beeswax emulsions. *Food engineering and physical properties*, 71 (6), 290-296.
- Hoover, R., & Sosulski, F.W. (1991).Composition, structure, functionality and chemical modification of legume starches*. Canadian Journal Physiology and Pharmacology, 69, 79–92.*
- Hoover, R., & Ratnayake, W.S. (2002). Starch characteristics of black bean, chick pea, lentil, navy bean and pinto bean cultivars grown in Canada. *Food Chemestry*, 78(4), 489-498.
- Hutchings, J.B. (1999). Food and Colour Appearance, Second Edition. Gaithersburg, Maryland: Chapman and Hall Food Science Book, Aspen Publication.
- ISO 527-1. (2012). Plastics and determination of tensile properties. Part 1: General principles.
- Jagadish, R.S., & Raj, B. (2011). Properties and sorption studies of polyethylene oxide-starch blended films. *Food Hydrocolloids,* 25, 1572-1580.

- Jiang, X., Jiang, T., Gana, L., Zhang, X., Daia, H., & Zhang, X. (2012). The plasticizing mechanism and effect of calcium chloride on starch/poly(vinyl alcohol) films. *Carbohydrate Polymers*, 90, 1677-1684.

- Jiménez, A., Fabra, M.J., Talens, P., & Chiralt, A. (2012a). Edible and biodegradable starch films: A review. *Food Bioprocess Technol*, 5(6), 2058-2076.

- Jiménez, A., Fabra, M.J., Talens, P., & Chiralt, A. (2012b). Effect of re-crystallization on tensile, optical and water vapour barrier properties of corn starch films containing fatty acids. *Food Hydrocolloids*, 26, 302-310.

- Jiménez, A., Fabra, M.J., Talens, P., & Chiralt, A. (2012c). Effect of sodium caseinate on properties and ageing behaviour of corn starch based films. *Food Hydrocolloids*, 29 (2), 265-271.

- Jiménez, A., Sánchez-González, L., Desorby, S., Chiralt, A. & Tehrany, E.A. (2013). Influence of nanoliposomes incorporation on properties of film forming dispersions and films based on corn starch and sodium caseinate. *Food Hydrocolloids,* 35, 159-169.

- Lafargue, D., Lourdin, D., & Doublier, J.L. (2007). Film-forming properties of a modified starch/k-carrageenan mixture in relation to its rheological behavior. *Carbohydrate Polymers*, 70, 101-111.

- Lewandowska, K. (2009). Miscibility and thermal stability of poly(vinyl alcohol)/ chitosan mixtures. *Thermochimica Acta*, 493, 42-48.

- Lourdin, D., Della Valle, G., & Colonna, P. (1995). Influence of amylose content on starch films and foams. *Carbohydrate Polymers*, 27, 261–70.

- Li, W., Yue, J., & Liu, S. (2012). Preparation of nanocrystalline cellulose via ultrasound and its reinforcement capability for poly(vinil alcohol) composites. *Ultrasonics Sonochemistry*, 19, 479–485.

- Lu, D.R., Xiao, C.M. & Xu, S.J., (2009). Starch-based completely biodegradable polymer materials. *–eXPRESS Polymer Letters*, 3, 366-375.

- Luo, X., Li, J. & Lin, X. (2012). Effect of gelatinization and additives on morphology and thermal behavior of cornstarch/PVA blend films. *Carbohydrates Polymers*, 90, 1595-1600.

- Mailo, S.A., Gonzalez, J.S., Hoppe, C & Alvarez, V.A. (2011). Geles compuestos basados en poli(vinil alcohol) para su uso en biomedicina. 11º Congreso Binacional de Metalurgia y Materiales SAM / CONAMET 2011.

- Mehyar, G.F. & Han, J.H. (2004). Physical and mechanical properties of high-amylose rice and pea starch films as affected by relative humidity and plasticizer. *Journal of Food Science*, 69 (9), 449-454.

- Myllärinen, P., Buleon, A., Lahtinen, R., & Forssell, P. (2002). The crystallinity of amylose and amylopectin films. *Carbohydrate Polymers,* 48, 41-48.

- Ortega, R., Jiménez, A., Talens, P., & Chiralt, A., (2014b). Properties of starch–hydroxypropyl methylcellulose based films obtained by compression molding. *Carbohydrate Polymers,* 109, 155–165.

- Ortega-Toro, R., Jiménez, A., Talens, P & Chiralt, A. (2014a). Effect of the incorporation of surfactants on the physical properties of corn starch films. *Food Hydrocolloids,* 38, 66-75.

- Palviainen, P., Heinämäki, J., Myllärinen, P., Lahtinen, R., Yliruusi, J., & Forssell, P. 2001. Corn starches as film formers in aqueous-based film coating. *Pharmaceutical, Development and Technology*, 6,353–61.

- Ramaraj, B. (2007). Crosslinked poly(vinyl alcohol) and starch composite films. II. Physicomechanical, thermal properties and swelling studies. *Journal of Applied Polymer Science,* 103, 909-916.

- Ramaraj, B. (2006). Mechanical, thermal and morphological properties of environmentally degradable ABS and poly(vinyl alcohol) blends. *Journal of Applied Polymer Science,* 106, 1048-1052.

- Rindlav, A., Hulleman, S.H.D., & Gatenholm, P. (1997). Formation of starch films with varying crystallinity. *Carbohydrate Polymers,* 34, 25-30.

- Roohani, M., Habibi, Y., Belgacem, N.M., Ebrahim, G., NaghiKarimi, A., & Dufresne, A. (2008). Cellulose whiskers reinforced polyvinyl alcohol copolymers Nanocomposites. *European Polymer Journal*, 44, 2489–2498.

- Shi, R., Bi, J., Zhang, Z., Zhu, A., Chen, D., Zhou, X., Zhang, L., & Tian, W. (2008). The effect of citric acid on the structural properties and cytotoxicity of the polyvinylalcohol/starch films when molding at high temperature. *Carbohydrate Polymers*, 74, 763–770.

- Siddaramaiah, Raj, B., & Somashekar, R. (2004). Structure–property relation in polyvinyl alcohol/starch composites. *Journal of Applied Polymer Science*, 9, 630–635.

- Sreekumar, P.A., Al-Harthi, M. A., & De, S.K. (2012). Studies on compatibility of biodegradable starch/polyvinyl alcohol blends. *Polymer engineering and science*, 52(10), 2167-2172.

- Talja, R. A., Helén, H., Roos, Y. H., & Jouppila, K. (2007). Effect of various polyols and polyol contents on physical and mechanical properties of potato starch-based films. *Carbohydrate Polymers*, 67(3), 288-295.

- Ward, G., & Nussinovitch, A. (1996). Peel gloss as a potential indicator of banana ripeness. *LWT – Food Science and Technology*, 29, 289-294.

- Valencia, A., Rivera, C., & Murillo, E.A. (2013). Estudio de las propiedades de mezclas de alcohol polivinílico-almidón de yuca-sorbitol obtenidas por casting. *Revista Colombiana de Materiales*, 4, 41-55.

- Vásconez, M.B., Flores, S.K., Campos, C.A., Alvarado, J., & Gerschenson, L.N. (2009). Antimicrobial activity and physical properties of chitosan-tapioca starch based edible films and coatings. *Food Research International*, 42, 762-769.

- Wolff, I.A., Davis, H.A., Cluskey, J.E., Gundrum, L.J., & Rist, C.E. (1951). Preparation of films from amylose. *Industrial & Engineering Chemestry Research*, 43, 915–9.

- Wu, H., Liu, Ch., Chen, J., Chen, Y., Anderson, D.P., & Chang, P.R. (2010). Oxidized pea starch/chitosan composite films: Structural characterization and properties. *Journal of Applied Polymer Science*, 118, 3082-3088.

- Yoon, S., Park, M. & Byun, H. (2012). Mechanical and water barrier properties of starch/PVA composite films by adding nano-sized poly(methylmethacrylate-co-acrylamide) particles. *Carbohydrate Polymers,* 87, 676– 686.

- Yeun, J-H., Bang, G-S., Oark, B. J., Ham, S. K., & Chang, J-H. (2005). Poly(vinyl alcohol) nanocomposite films: thermooptical properties, morphology, and gas permeability. Journal of *Applied Polymer Science*, 101, 591–596.

Part B: Effect of nano-reinforcement (CNCs).

Amalia I. Cano, Elena Fortunati, Maite Cháfer, Chelo González-Martínez, Amparo Chiralt, José M. Kenny. **Effect of cellulose nanocrystals on the properties of pea starch- poly(vinyl alcohol) blend films.** *Journal of Materials and Science, **2015**,* 50(21), 6979-6992.

Abstract

Incorporation of cellulose nanocrystals (CNCs) to pea starch-poly(vinyl alcohol) (PVA) (1:2 ratio) blend films was carried out in order to improve their mechanical and barrier properties and film stability throughout storage, thus overcoming some drawbacks of starch based films. Different ratios (1, 3 and 5 %) of CNCs were used and structural, thermal and physical (barrier, mechanical and optical) properties were analysed in comparison to the control film without CNCs. Incorporation of CNCs enhanced phase separation of polymers in two layers. The upper PVA rich phase contained lumps of starch which emerged from the film surface, thus reducing the film gloss. CNCs were dispersed in both polymeric phases as aggregates, whose size increased with the CNCs ratio rise. CNCs addition did not implied changes in water vapour barrier of the films, but they became slightly stiffer and more stretchable, while crystallization of PVA was partially inhibited.

Keywords: microstructure, mechanical properties, nanocomposites, optical properties, phase transitions, water vapour permeability.

1. INTRODUCTION

The growing interest in environmentally-friendly materials has promoted research into the development of biodegradable polymers as an alternative to non-biodegradable synthetic petroleum-derived polymers (Armentano *et al*., 2010; Fortunati *et al*., 2013a). In response to the consumer requirements for safer and environmentally friendly packaging materials, the combination of biodegradable polymers with bio-based additives has also been analysed to improve the properties of these materials (Siracusa *et al*., 2008). In this sense, bio-resources obtained from agricultural-related industries have received special attention. Crops fibre components provide a wide range of opportunities for developing new applications in different industrial sectors such as packaging, building, automotive and aerospace industries, electronics, etc. (Anandjiwala, 2006).

In the development of packaging materials for food applications, polysaccharides, such as starch, cellulose and their derivatives have commonly been used as film-forming compounds (Chen *et al*., 2009). Cellulose is the most abundant renewable natural polymer resource available in the biosphere (Habibi *et al*., 2010; Zhang *et al*., 2011). It is well known that when cellulose fibres are subjected to acid hydrolysis, the fibres yield defect-free, rod-like crystalline residues (Habibi *et al*., 2010). The use of cellulose nanocrystals (CNCs) as fillers in packaging materials has been studied not only because of their interesting physical and chemical properties but also due to their inherent renewability, sustainability and abundance. The most common sources of these nanocrystals include cellulose fibres from cotton, hemp, flax, microcrystalline cellulose, bacterial cellulose (Habibi *et al*., 2010; Lee *et al*., 2009; Fortunati *et al*., 2012a; Fortunati *et al*., 2013b). The production of cellulose nanocrystals consists of subjecting pure cellulose material to strong acid hydrolysis under controlled conditions such as

temperature, agitation and time, which determine the structure and characteristics of the crystals. Cellulose nanocrystals are used as a reinforcement material due to their large specific surface area (150 $m^2 g^{-1}$) (Cavaille *et al*., 2000), surface energy (Khoshkava & Kamal, 2014) and very high elastic modulus (about 150 GPa) (Sturcová *et al*., 2005). Moreover, their low density, about 1.566 g cm^{-3} (Fortunati *et al*., 2013b), biocompatibility, biodegradability, low energy consumption in manufacturing, and low cost represent remarkable advantages of cellulose nanocrystals (Fortunati *et al*., 2013b; Khoshkava & Kamal, 2014; Fortunati *et al*., 2012b; Rescignano *et al*., 2014) in comparison to others nanomaterials such as nanoclays, SiO_2 and Au nanoparticles for elaboration of low cost nanocomposites. All of this makes cellulose nanostructures to be advantageous bio-based edible additives, which are able to enhance the bio-polymer performance, in terms of the mechanical, thermal and barrier properties (Fortunati *et al*., 2013b; Zhang *et al*., 2011). However, cellulose nanocrystals have some drawbacks, such as the difficulty to disperse homogenously in the polymer matrix (Fortunati *et al*., 2012b), as a result of their agglomeration into flakes during film formation. Due to the hydrophilic character of cellulose nanocrystals, the main technique employed to transfer them from an aqueous dispersion into an organic polymer has been the casting-evaporation process (Habibi *et al*., 2010).

Biopolymer nanocomposites are the result of the combination of biopolymers and nanoparticles of inorganic/organic fillers (Rescignano *et al*., 2014). Cellulose nanocrystals have been incorporated into a wide variety of biopolymer matrices including (poly)caprolactone (Siquiera *et al*., 2013), carboxymethyl cellulose (Choi *et al*., 2006), (poly)vinyl alcohol (Lee *et al*., 20029; Zhang *et al*., 2011; Fortunati *et al*., 2013b; Rescignano et al., 2014), (poly)lactic acid (Fortunati *et al*., 2012b; Fortunati *et al*., 2012b), chitosan (Pereda *et al*., 2014), starch (Chen *et al*., 2009; Ma *et al*., 2008) and biopolymer blends, like poly(lactic acid)-poly(hydroxybutyrate) (Arrieta *et al*., 2014a-b). In general,

the hydrophilic nature of both biopolymer and nanocrystals leads to excellent interfacial compatibility, resulting in enhanced mechanical and thermal properties of the composite material (Chen *et al*., 2009; Rescignano *et al*., 2014).

The use of starch as a biopolymer matrix in combination with other polymers to reduce the starch film drawbacks (poor mechanical and water vapour barrier properties) has been explored by different authors (Jiménez *et al*., 2012a; Bonilla *et al*., 2013). The incorporation of PVA into gelatinized pea starch matrices implied the formation of interpenetrated polymer networks. In fact, the blend films showed beneficial effects on the mechanical properties of the films, these becoming much more extensible and stable during storage, and on water barrier properties (Cano *et al*., 2015). Different studies into starch-PVA blends have been carried out, focusing on their biodegradability (Siddaramaiah & Somashekar, 2004; Priya *et al*., 2014) and the effect of the incorporation of different additives to the blends. The effect of adding citric acid (Shi *et al*., 2008), glutaraldehyde (Luo *et al*., 2012), calcium chloride (Jiang *et al*., 2012), or nanoparticles like nano-sized poly(methyl methacrylate-co-acrylamide) particles (Yoo *et al*., 2012) on PVA-starch blend properties has been analysed for different aims (compatibility enhancement or development of biomedical and packaging materials). Nevertheless, no studies have been found into the effect of cellulose nanocrystals on the properties of pea starch-PVA blend films.

The aim of the present work was to study the effect of incorporating cellulose nanocrystals into pea starch-PVA blend films in terms of their nano- and micro-structure, thermal behaviour and physical properties at different ageing times.

2. MATERIALS AND METHODS

2.1. Materials

Pea starch (S) was purchased from Roquette Laisa España S.A. (Benifaó, Valencia, Spain), poly(vinyl alcohol) (PVA) (M_w: 89.000-98.000, hydrolysed, +99%, viscosity: 11.6-15.4 cP, 4% in H_2O at 20 ºC), microcrystalline cellulose (MCC) (powder,15 - 20 µm) were from Sigma Aldrich Química S.L. (Madrid, Spain).Glycerol and magnesium nitrate-6-hydrate ($Mn(NO_3)_2$) were supplied by Panreac Química S.A. (Castellar de Vallès, Barcelona, Spain). Sulphuric acid, ion resin (Dowex Marathon MR-3 hydrogen and hydroxide), Whatman 541 filter paper and NaOH were also purchased from Sigma Aldrich Química S.L. (Milan, Italy).

2.2. Extraction of Cellulose nanocrystals (CNCs)

A suspension of cellulose nanocrystals (CNCs) was prepared from microcrystalline cellulose (MCC) by hydrolysis using sulphuric acid, 64 % (wt/wt) at 45 ºC for 30 min, as previously reported by Cranston & Gray (2006) and Fortunati *et al*. (2012a). Immediately following the acid hydrolysis, the suspension was diluted 20 fold with deionized water and maintained at rest overnight. Afterwards, the dispersion was centrifuged at 4,500 rpm for 20 min to separate the cellulose crystals. The precipitate was dialyzed against deionized water for 5 days and then neutralized with mixed bed ion resin for 48 h. Afterwards, the suspension was filtered through filter paper. The CNC filtrate was neutralized by adding 1.0 % (v/v) of 0.25 M NaOH. Finally, the CNC dispersion was homogenized by ultrasonic treatment, using a tip sonicator (Vibracell, 750 Sonics & Materials, Inc., Newton, USA) for 10 min in an ice bath. The dry matter content of the CNC dispersion was determined by the drying oven method (UNE-EN ISO, 2008), giving 11.1 ± 0.2 %. This value was a little low compared with that reported by other authors (Arrieta *et al*., 2014b). CNC obtained nano-crystals showed dimensions ranging from

100 to 200 nm in length and 5 to 10 nm in width, according to FESEM observations (Fortunati *et al*., 2013b).

2.3. Preparation of films

Films were obtained by casting from film forming dispersions (FFDs). Starch (1 %w/w) was dispersed in an aqueous solution at 90 ºC for 30 min with continuous stirring to induce starch gelatinization. Thereafter, the dispersion was homogenized using a rotor-stator homogenizer (Ultraturrax D125, Janke and Kunkel, Germany) at 13,500 rpm for 1 min and 20,500 rpm for 3 min. Immediately following the starch gelatinization, PVA was dispersed in the aqueous solution in a S-PVA ratio of 1:2 (w/w), and maintained at 90 ºC for 30 min until complete dissolution. When the dispersion was cooled, 0.25 g of glycerol per g of starch was added on the basis of previous studies (Jiménez *et al*., 2012b). This FFD was used to obtain the control films. Cellulose nanocrystal dispersion was homogenized with the polymer FFDs by means of a tip sonicator for 4 min in ice bath. Different CNC mass ratios were considered: 0, 1, 3 and 5 g of CNC per 100 g of total polymers (sample codes: C, 1 %, 3 % and 5 %, respectively), considering the dry weight of CNC and polymers.

To obtain the films, the FFDs were poured into Petri dishes, in a proper amount to provide a surface density of solids of 145 g m^{-2}. Films were dried at 40 ºC in a convection oven for 48 h and afterwards, peeled off the casting surface and conditioned at 53 % RH, using magnesium nitrate-6-hydrate ($Mn(NO_3)_2$) saturated solution at room temperature (≈ 25 ºC) until further analysis. The film thickness was measured at six random positions with a calliper (MicrometerStarrett) to the nearest 0.001 mm.

2.4. Characterization of films

2.4.1. Microstructure

Microstructural analysis of films was carried out using both a field emission scanning electron microscope (FESEM) (Supra™ 25-Zeiss, Germany) and an atomic force microscope (AFM) (Multimode 8, Bruker AXS, Inc. Santa Barbara, California, USA), with a NanoScope® V controller electronics. To this end, two replicates per formulation were observed. FESEM observations were carried out on the film surface and on their cross section. To prepare the cross section samples, films were frozen in liquid nitrogen and cryofractured. Afterwards, samples were gold coated, and observed using an accelerating voltage of 2 and 5 kV, for the surface and cross-section observations, respectively.

The surface morphology was also analysed using AFM. The resulting data were transformed into a 2D image. Measurements were taken from 50 x 50 μm and 3 x 3 μm areas of the film surface, using the phase imaging mode.

AFM with the peak force QNM (Quantitative NanoMechanics) mode was also used to analyse the film surface nanostructure. Measurements were taken from 20 x 20 μm areas of the film surface and the resulting data were transformed into a 2D image (DMT modulus map).

2.4.2. Fourier Transform Infrared (FT-IR) spectroscopy

FT-IR spectra of the films were obtained by a Jasco FT-IR 615 spectrometer, (Easton MD, USA) in transmission mode, in the range of 400-4000 cm^{-1}. A few drops of different film forming dispersions were cast on silicon plates, after which they were dried and measured. Each sample was characterized in duplicate.

2.4.3. Thermogravimetric analysis

Thermal weight loss (TG) and its derivate (DTG) of film samples vs. temperature were obtained using a thermogravimetric analyzer (Seiko Exstar 6300, Italy). In the test, samples were heated from 30 ºC to 600 ºC at 10 ºC min^{-1}, using a nitrogen flow. Prior to the analyses, samples were conditioned for 1 week. Thermal degradation temperatures (the maximum of the DTG curves (T_{mp}) and secondary degradation temperature peak (T_p) were obtained. Measurements were taken in triplicate.

2.4.4. Differential scanning calorimetry

Differential scanning calorimeter (DSC) (TA Instrument, Q200, USA) was used to analyse phase transitions in the films as a function of the temperature. Measurements were carried out in triplicate under nitrogen flow in the temperature range −25 to 230 ºC, at 10 ºC min^{-1}, by performing three scans: First, samples were heated from room temperature to 230 ºC and maintained for 5 min at 230 ºC. Then, samples were cooled down to – 25 ºC and heated again until 230 ºC. Data were recorded both during the cooling and second heating steps. From thermograms of the cooling step, the crystallization temperatures (Tc) and enthalpy (∆Hc) values were obtained. From the second heating step, glass transition temperature (Tg), melting temperature (Tm) and melting enthalpy (∆Hm) values were obtained. Prior to the analyses, samples were conditioned for 1 week.

The crystallinity degree of PVA was calculated as shown in equation 1:

$$X = \frac{1}{X_{PVA}}\left[\frac{\Delta H}{\Delta H_0}\right]100 \quad (1)$$

where ΔH, is the melting enthalpy of the sample (expressed in J g^{-1} PVA), ΔH_0, the melting enthalpy of a 100% crystalline PVA sample (161.6 J.g^{-1}, Roohani *et al*., 2008) and X_{PVA}, the mass fraction of PVA in the film.

2.4.5. Moisture content

Film moisture content (MC) was analysed by drying the film samples in a vacuum oven at 60 ºC for 24 h. Later on, the pre-dried samples were placed in desiccators containing P_2O_5 until reaching a constant weight. Five replicates per film formulation for one and five weeks were analysed.

2.4.6. Water vapour permeability (WVP)

Water vapour permeability (WVP) was evaluated in films equilibrated for 1 and 5 weeks, following the gravimetric method ASTM E96-95 (ASTM, 1995) by using Payne permeability cups (Payne, elcometer SPRL, Hermelle/sd Argenteau, Belgium) of 3.5 cm diameter. Deionised water was used inside the testing cup to achieve 100 % RH on one side of the film, while an oversaturated magnesium nitrate solution was used to control the RH on the other side of the film. A fan placed on the top of the cup was used to reduce resistance to water vapour transport. Water vapour transmission rate measurements (WVTR) were performed at 25 ºC. To calculate WVTR, the slopes in the steady state period of the weight loss *vs.* time curves were determined by linear regression. WVP was calculated according to Cano *et al*., (2014). For each type of film, WVP measurements were taken in quadruplicate.

2.4.7. Mechanical properties

Mechanical properties were measured using a Universal Test Machine (Digital Lloyd instrument, West Sussex, UK), following the UNI ISO 527-1 (2012), by using 5 $mmmin^{-1}$ and a load cell of 1.5 N. Equilibrated film samples (1 x 5 cm) for 1 and 5 weeks were mounted in the film-extension grips (A/TG model), which were set 20 mm apart. Stress-Hencky strain curves were obtained and the tensile strength at break (TS), percentage

of elongation at break (E) and elastic modulus (EM) were calculated. Measurements were taken at room temperature with eight replicates per formulation.

2.4.8. Ultraviolet-visible spectrophotometry

Film samples equilibrated (1 x 1 cm) for 1 and 5 weeks were analysed by means of a UV–VIS spectrophotometer (Perkin Elmer Instruments, Lambda 35, Waltham, USA), by using a wavelength range between 250 and 1000 nm.

2.4.9. Internal transmittance

Internal transmittance (Ti) as a measure of the transparency of the films was determined through the surface reflectance spectra in a spectrocolorimeter CM-3600d (Minolta Co, Tokyo, Japan) with a 30 mm illuminated sample area by applying the Kubelka–Munk theory for multiple scattering to the reflection spectra, following the methodology described by Cano, *et al*. (2014). Measurements were taken in triplicate in films equilibrated for 1 and 5 weeks.

2.4.10. Gloss

Gloss was measured using a flat surface gloss meter (Multi- Gloss 268, Minolta, Langenhagen, Germany) at an incidence angle of 60º, according to the ASTM standard D523 (1999). Prior to gloss measurements, films were conditioned for 1 and 5 weeks. Gloss measurements were performed in triplicate. Results were expressed as gloss units, relative to a highly polished surface of standard black glass with a value close to 100.

2.4.11. Overall migration

Overall migration tests in films conditioned for 1 week were carried out by following current legislation (EN 1986-1:2002; EU No 10/2011). Rectangular film strips of 20 cm^2

total area were immersed in a glass tube with 20 ml of food simulants (ethanol 10 % (v/v) -simulant A- (Sigma Aldrich Química S.L., Milan, Italy) and isooctane - simulant to D2- (Sigma Aldrich Química S.L., Milan, Italy)), keeping the established relation of 6 dm^2 kg^{-1}. Samples in simulant A were kept in a controlled chamber at 40 ºC for 10 days, while samples in isooctane were kept at 20 ºC for 2 days. After the incubation period, the films were removed and simulants were evaporated to dryness. Afterwards, the residue was weighed with ± 0.001 mg precision in order to determine the overall migration value in mg kg^{-1} of simulant. For each sample, three determinations were carried out.

2.5. Statistical analysis

Results were analysed by analysis of variance (ANOVA), using the Statgraphics Plus 5.1. Program (Manugistics Corp., Rockville, MD). To differentiate samples, Fisher's least significant difference (LSD) was used at the 95 % confidence level.

3. RESULTS AND DISCUSSION

3.1. Nano- and micro-structure of the films

Figures 1 and 2 show the FESEM micrographs of the surfaces and cross sections of the different films, respectively. Control films showed phase separation of starch and PVA due to the lack of polymer compatibility, according to what was previously observed by other authors (Cano *et al*., 2015; Sreekumar *et al*., 2012). Surface of control films shows the formation of globular structures which can be attributed to domains of one of the polymeric phases dispersed in the continuous phase of the other. When CNC nanocrystals were incorporated into the film formulation, the surface concentration of dispersed domains increased, this being more marked for the highest CNC content (5 %).

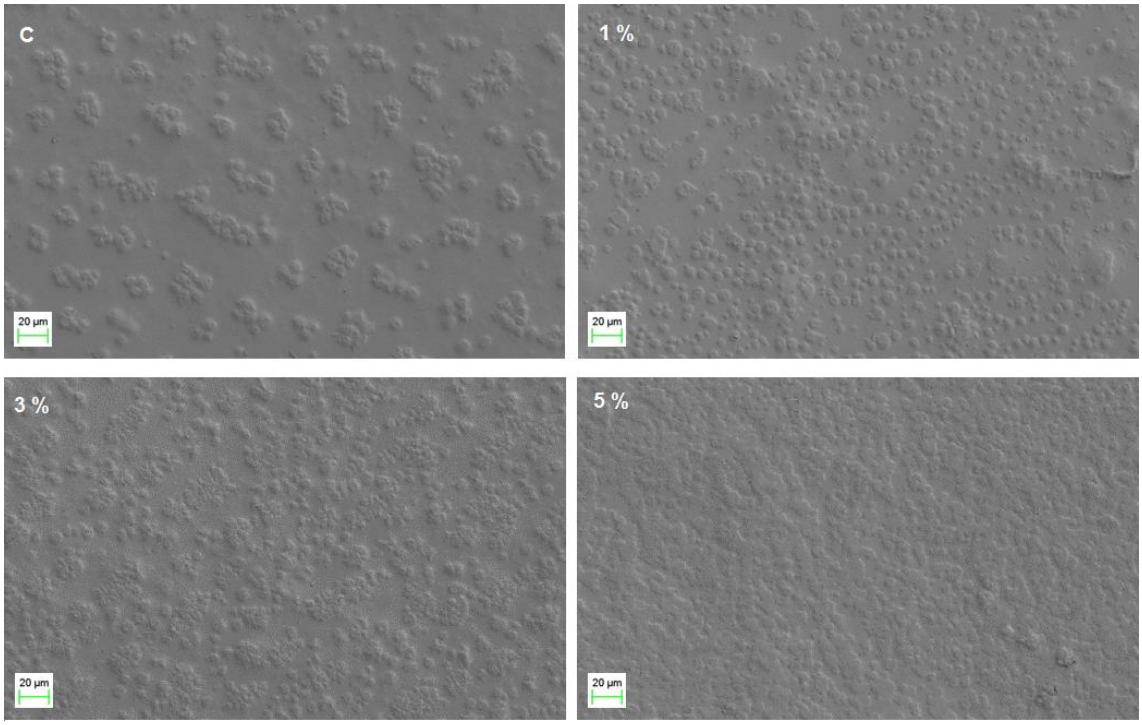

Figure 1. FESEM micrographs of the surface of control blend and composite films with different contents of CNC (samples 1 %, 3 % and 5 %).

The cross section micrographs of control films (Figure 2) showed two interpenetrated networks of both polymers where the crystalline zones of PVA can also be appreciated. In films containing CNCs the formed two layers in the films are more clearly differentiated. The top phase corresponds to about one third of the film thickness, according to the ratio of starch to PVA, which suggest that starch rich phase mostly separated at the top of the films whereas PVA predominate in the down layer. The top layer generally shows a less smooth appearance, showing the coexistence of PVA dispersed domains in a more continuous starch matrix. Some of them emerged to the film surface, as shown in the surface micrographs (Figure 1). The PVA rich phase also shows lumps of starch phase. Distribution of nanoparticles in the different phase cannot be clearly appreciated at the magnification level of micrographs, although the PVA phase shows a more granular aspect which could indicate that nanoparticles could be present in this phase to a greater extent. Micrographs at higher magnification allow us to

appreciate this effect. For the highest ratio of CNCs (5 %), these appear distributed in both phases, thus modifying their general appearance. The aggregation of CNCs in some film areas could be observed, which is due to their strong hydrogen bonding capacity. Khoshkava & Kamal (2014) also reported that at higher CNC concentration CNC aggregation occurs to a great extent.

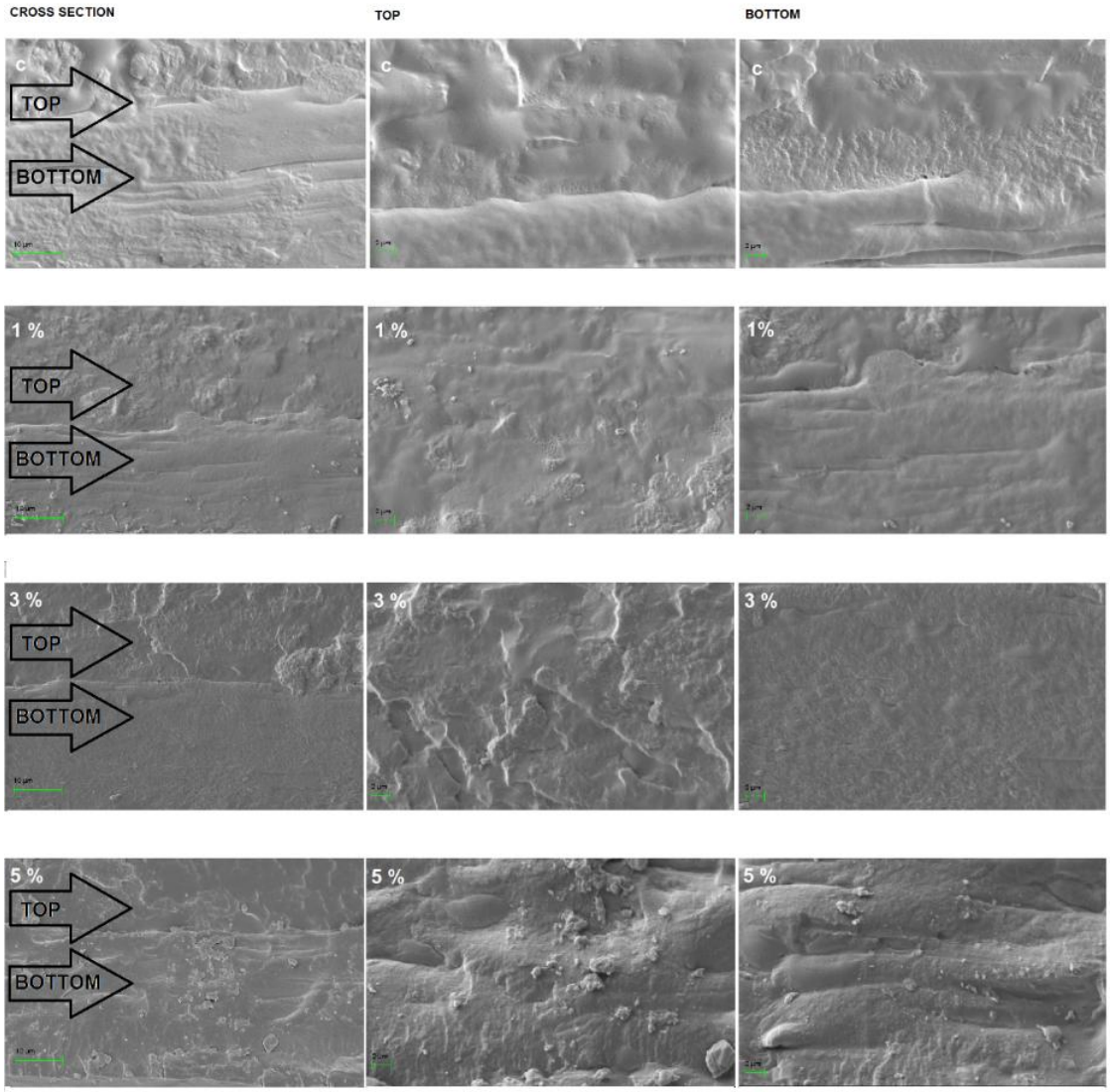

Figure 2. FESEM micrographs of the cross section of control blend and composite films with CNC contents (samples 1 %, 3 % and 5 %). Higher magnification images from top and bottom of the films are included to observe the different separated phases.

Figure 3 shows AFM images of control film and those containing CNCs, obtained by using Phase Imaging mode derived from Tapping Mode. Raw data were converted into 2D images and their scale is expressed as degrees. Phase Imaging allows to detect variations in composition, adhesion, friction, viscoelasticity and other properties in the material surface at nano-scale level, providing material property contrast. Surface of 50 μm^2 of control films shows two different phases in agreement with that observed in the surface FESEM images. The dispersed phase in the control film corresponds to emerging PVA lumps in the starch continuous phase of the upper layer of the films. Nevertheless, the dispersed phase concentration at the film surface increased when CNC ratio rose in the formulation. Observations a higher magnification (areas of 9 μm^2) were carried out on the continuous and dispersed surface phases to observe possible location of CNCs at the film surface. These images are shown in Figure 3. For 1 % of CNCs, no evidences of the nanocrystals in any phase are detected, probably due to their low ratio in film formulation. Nevertheless, at 3 % and 5 %, CNCs were observed in both, dispersed and continuous polymer phases. At 3 % of CNCs, great aggregates of particles are present in the continuous phase (mean size 200 nm) whereas particles are better dispersed in the PVA dispersed phase. At 5 % CNCs, particle aggregation is more accused appearing as enlarged formations whose perimeter is completely covered by flocculated nanocrystals. This formations appeared in both PVA and starch phases at the surface. As reported by Arrieta *et al*. (2014b) the greater the CNC concentration, the higher the aggregation level in the system.

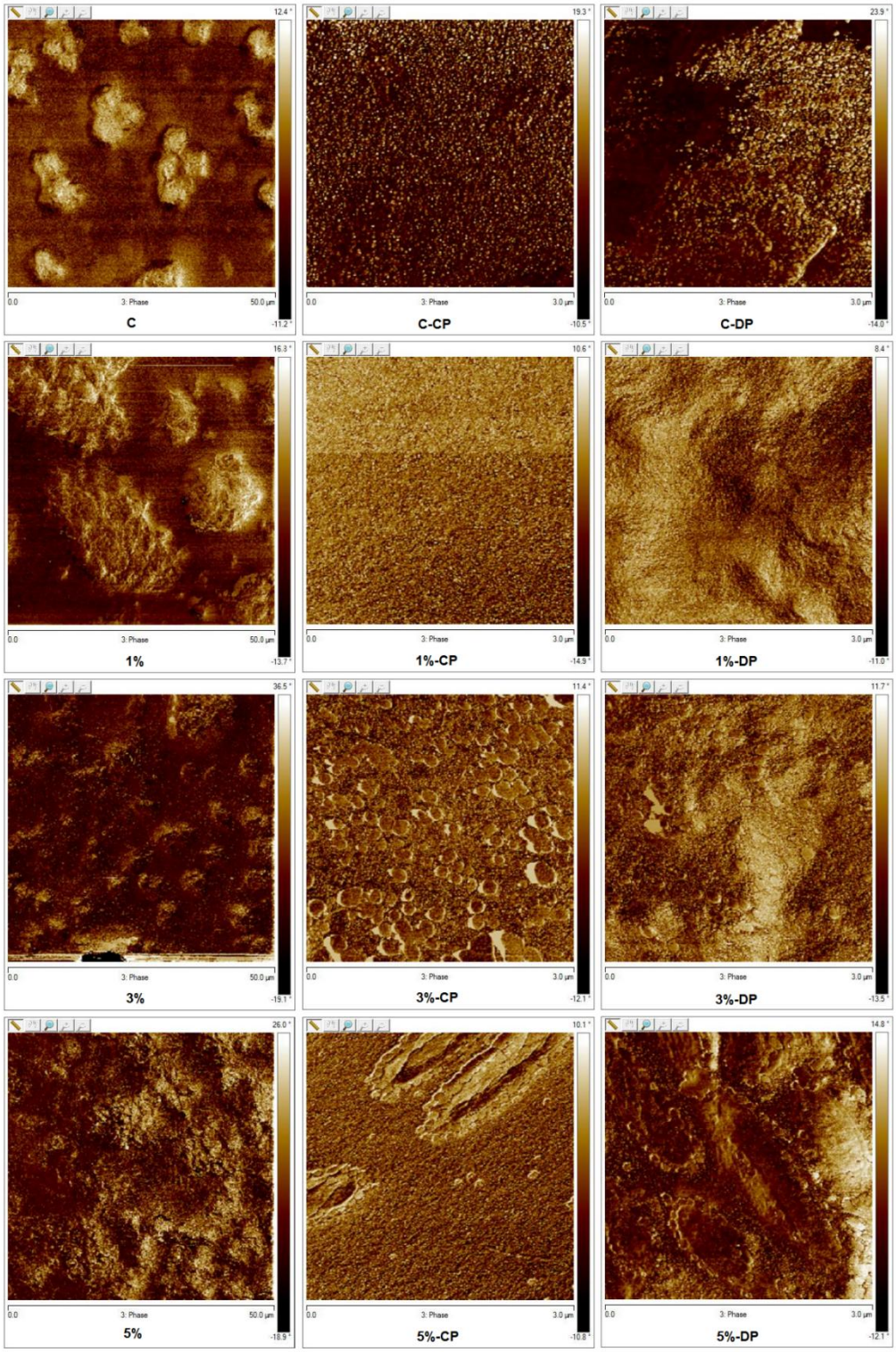

Figure 3. Phase imaging AFM maps of surface of control blend and composite films with different CNC contents (1 %, 3 % and 5 %). Higher magnification for continous (CP) and dispersed (DP) phases at the film surface.

Differences in the surface mechanical resistance were observed by means of AFM in Peak Force QNM mode (Figure 4).

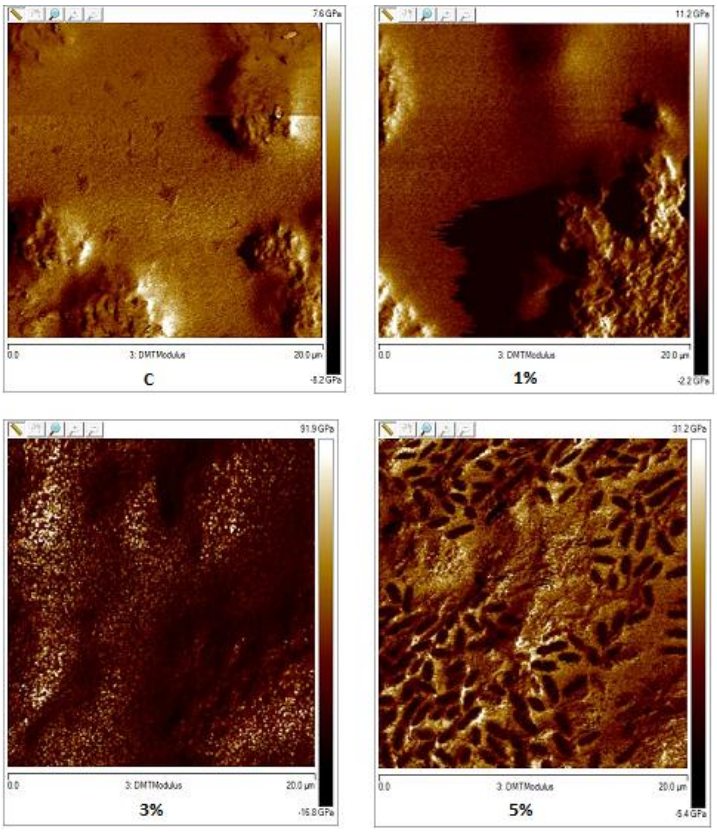

Figure 4. Maps of Log DTM modulus obtained from AFM in surface of control blend and composite films with different contents of CNCs.

The maps of Log DMT modulus for control films revealed the two phases previously mentioned at surface level, but no great differences in mechanical resistance between both could be detected. In 1 % CNC film formulation, similar values of log DMT modulus to those of control films were observed, probably due to low concentration of CNCs in the observed area, as deduced in phase imaging. The incorporation of 3 % and 5 % of CNCs gave rise to much higher differences in the values of DMT modulus of a given surface, especially for 3 %. In this case, the hardest areas are particulate in shape, which agrees with the greater hardness of crystalline structure of dispersed CNCs. At 5 %, a high proportion of very soft small areas can be observed, which can be attributed to voids

left by the aggregates of CNCs which probably are separated from the surface by the cantilever during the test, in part due to their big size, despite the images reveals good interfacial adhesion of CNCs to the pea starch-PVA matrix.

Figure 5 shows FT-IR spectra for control and nanocomposite films, showing the wavenumber values corresponding to the main peaks in each sample. The spectrum of the control film showed several characteristic peaks of stretching and bending vibrations of groups of starch and PVA chains. The broad band located between 3200-3600 cm^{-1} corresponds to the stretching vibration mode of hydroxyl groups from the absorbed water and from the polymers themselves (Fortunati *et al*., 2013b; Chen *et al*., 2008; Jiménez *et al*., 2013). The relative intensity of this band decreased when the ratio of CNCs increased in the films. The peak at around 2940 cm^{-1} is related with alkyl groups, C-H stretching (Fortunati *et al*., 2013b; Jiménez *et al*., 2013; Jagadish & Raj, 2011) and it increased in intensity as the CNC ratio increased, which can be explained by the contribution of C-H vibration in the crystalline structures. The peak at 1645 cm^{-1} corresponds to the H-O-H group deformation (Fortunati *et al*., 2013b) and it appears better resolved in films with CNCs. The peaks associated with the bending vibration mode of hydroxyl group appear at around 1420 cm^{-1} and they show a slight displacement of 20 units with respect to the control film when CNCs are present in the matrix, while an increase in intensity and resolution of this peak was observed when CNC ratio increased up to 3 %. The stretching vibration of C-O in the C-C-O group and in the starch glucose ring corresponds to the peaks at 1032 and 854 cm^{-1}, respectively (Fortunati *et al*., 2013b). These bands also suffered changes due to the presence of CNCs in the films.

The addition of CNCs, especially at 3 and 5 %, resulted in a slight reduction of the intensity of the -OH stretching band, a widening of band at 2940 cm^{-1} due to C-H stretching, the appearance of an additional peak at 1733 cm^{-1}, assigned to the C-C-O stretching, and changes in the peaks resolved between 850 and 1670 cm^{-1}. In this sense,

it is remarkable that the C-OH bending vibrations of alcohol groups present in cellulose appear at 1100 cm^{-1} (Fortunati *et al*., 2013b). The slight changes introduced by CNC in the FT-IR spectra of PVA-starch films suggest the interactions between hydroxyl groups (-OH) on the CNC surface and the –OH of the polymer blend chains, as proposed by other authors (Fortunati *et al*., 2013c).

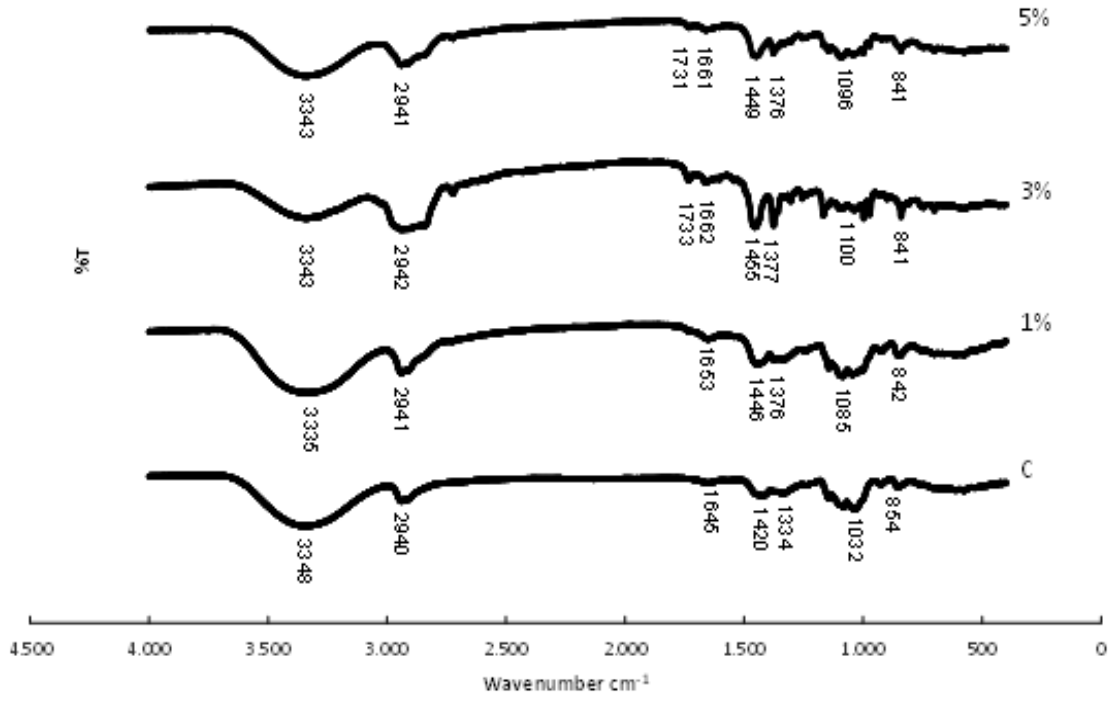

Figure 5. FT-IR spectra of control blend and composite films with different amounts of CNCs (1 %, 3 % and 5 %).

3.2. Thermal properties of the films

DSC and TGA measurements were used to study the thermal behaviour of the films, in order to know phase transitions and the thermal stability of the materials (Abdelrazek *et al*., 2010) as affected by the addition of CNCs at different contents.

Table 1 shows the results obtained from the DSC analysis. The PVA crystallization pattern showed one secondary peak at about 144 °C and a main peak located around

201 ºC. Secondary peak appeared at lower temperatures (supercooling) due to kinetic hindrances attributable to the low mobility of the polymer chain segments at the end of the crystallization process. The melting temperature (Tm) of control films was 227 ºC, without the split observed in crystallization. No significant effect of the CNC incorporation was observed in the Tm values, as previously found by Habbi *et al*. (2010).

Crystallization enthalpy (Table 1), expressed as J g^{-1} of PVA, showed a certain degree of variability and there were no significant differences among samples. The average value was 70 J g^{-1} of PVA, slightly lower than the melting enthalpy value, which indicates that supercooling occurred during the cooling step. Values of melting enthalpy, expressed in J g^{-1} of PVA, reveal that PVA crystallization was partially inhibited by the presence of CNCs, since the ΔHm value decreased as the CNC ratio in the films rose. In fact, the degree in crystallinity of PVA (X in Table 1) was reduced by about 50 %, with respect to the control film, when 5 % of CNC was added. However, Rescignano *et al*. (2014) observed that the crystallinity increases slightly with the addition of cellulose nanocrystals in PVA films, although their reported values are much smaller (15 %) as compared with the obtained values in this study (close to 70 % in control film). The CNC inhibition effect in PVA crystallization is also deduced from the greater supercooling observed in the cooling scan for samples containing CNCs.

Glass transition observed in the films must be assigned to the PVA phase bearing in mind the temperature range where it occurs, while this transition was not detected for the starch phase, due to its lower ratio in the film. Our previous studies (Cano *et al*., 2015) on PVA-starch blend films found the Tg values at 124±2 ºC and at 76±4 ºC, respectively for the starch and PVA phases. Tg values were taken from the heating step when crystallization of PVA is completed and the amorphous phase contains the non-crystallized fraction. In all cases, the values obtained in the cooling step were slightly lower, which indicates that the mean molecular weight of the amorphous fraction is lower

when crystallization was not completed. Therefore, this would point to the fact that the longer chains crystallize prior to the shorter ones. The obtained Tg value of PVA in the control films was 79 ºC, which was similar to that reported by other authors for PVA films (Fortunati *et al*., 2013b; Rescignano *et al*., 2014). The incorporation of CNCs to the films provoked a decrease of about 2 ºC, which can be related with the partial inhibition of the PVA crystallization (especially the shorter chains, as commented on above) and the subsequent decrease of the mean molecular weight of the amorphous PVA fraction. Other authors (Habibi *et al*., 2012; Fortunati *et al*., 2012a; Rescignano *et al*., 2014) did not found changes in the glass transition temperature of the polymer (PLA and PVA) when cellulose nanocrystals were incorporated to the matrix.

DSC analysis reveals that PVA crystallization was partially inhibited when CNCs are present as filler in the blend films, this effect being more marked when they contain 5 % of nanocrystals. The lack of crystallization gave rise to a decrease in the Tg of the amorphous phase which suggests that the shorter PVA chains remain in the amorphous phase.

Figure 6 shows the weight loss (TG curve) and its derivate (DTG curve) as a function of the temperature for control films and formulations containing cellulose nanocrystals. The temperatures for the main degradation steps of the films are summarized in Table 1. For control films, three weight loss steps were observed. Similar multi-step weight loss behaviour was described for PVA films (Lee *et al*., 2009; Rescignano *et al*., 2014) and for corn starch-PVA blend films obtained by casting (EU 10/2011). The initial weight loss, up to about 90 ºC, can be attributed to the loss of bonded water in the film (Lee *et al*., 2009; Zhang *et al*., 2011; Luo *et al*., 2012) with total weight loss in this range of about 10 %. The second step, between 150-380 ºC, is related to the main degradation process (peak temperature 347 ºC), in which dehydration reactions, followed by polymer scission and decomposition, take place. Total weight loss in this range is about 70 %. Moreover,

in this step the acetyl groups of PVA were transformed into acetic acid molecules and successive catalytic degradation of the main chain by in situ stripping at higher temperatures occurs (Rescignano *et al*., 2014; Peresin *et al*., 2010). The third step takes place at between 380 – 500 ºC and it can be attributed to the degradation of the by-products generated by PVA during the thermal process (Lee *et al*., 2009; Bonilla *et al*., 2013). In previous studies, it was observed that in pea starch films only two weight loss steps occur: the loss of bonded water up to 100 ºC and the main degradation at 315 ºC.

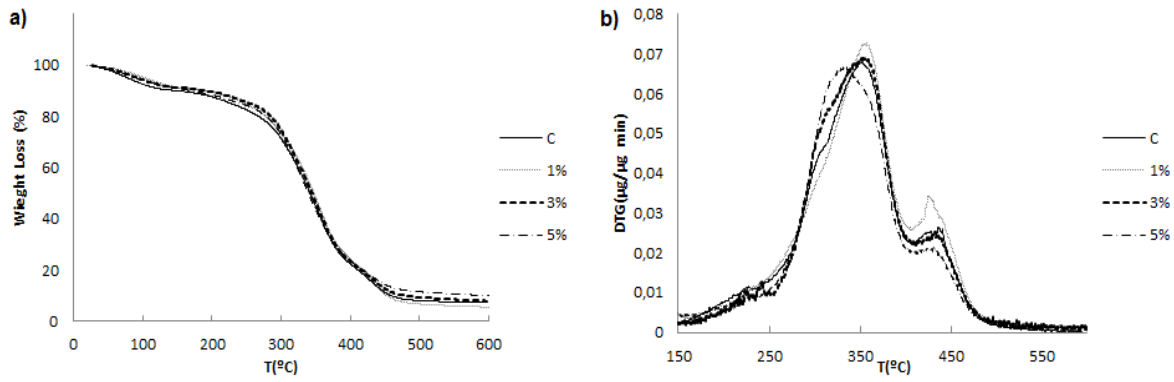

Figure 6. TG (a) and DTG (b) curves obtained from TGA of control blend and composite films with CNCs (1 %, 3 % and 5 %).

The addition of cellulose nanocrystals into the films led to a similar weight loss pattern to the control films, showing the three weight loss steps commented on above (Figure 6). There were no notable changes in the pattern of thermal degradation of nanocomposites or in the temperature of the main peaks (Table 1), except for films with 5 % CNCs, where a slight decrease in T_{mp} was observed. Likewise, the temperature of the secondary peak was slightly higher due to the influence of cellulose thermal behaviour (Rescignano *et al*., 2014).

3.3. Physical properties of the films

The analysis of the physical properties of studied films was carried out to know their barrier, optical and mechanical behaviour. Film thickness was 98 ± 8 μm for all formulations. Table 2 shows the water vapour permeability values (WVP) of the films at 25 ºC and at a 53-100 % RH gradient, together with their equilibrium moisture content and optical properties after 1 and 5 storage weeks. After 1 week, the moisture content was slightly lower for samples containing 3 % and 5 % CNCs, but their value increased throughout 5 storage weeks, reaching a similar value in all cases in the range 6-7 %. This suggests that CNCs limit the moisturising rate till sample equilibration, despite the hydrophilic character of these nanoparticles (Habibi *et al*., 2010; Fortunati *et al*., 2013), probably due to the structural changes induced in the films and the increase in the tortuosity factor in the matrix associated with the presence of the dispersed nanoparticles.

The WVP values of the films must be as low as possible to efficiently limit the water vapour transfer when it is in contact with food systems (Ma *et al*., 2008). Mean values of studied films ranged between 3.1-3.6 $g.mm.kPa^{-1}.h^{-1}.m^{-2}$ and no notable differences are found among formulations or due to the storage time. Nevertheless, as deduced from the moisture equilibration time, CNCs seem to slightly reduce WVP values (increase in the tortuosity factor for mass transfer), but to a very limited extent, probably due to their high water affinity which contributes to the hydrophilic character of the matrix and to solubility of water molecules, thus enhancing water transport.

Optical properties, UV-VIS spectra, transparency (Ti) and gloss of the films are directly related with their nano- and micro-structure. The UV-VIS spectra of control and cellulose nanocrystals based films in the UV range are shown in Figure 7, where the greatest differences were observed. The films exhibit higher values of transmittance (T)

in the visible light range (400-800 nm) than in the UV range (200-400 nm), according to Chen *et al*. (2008) for PVA films.

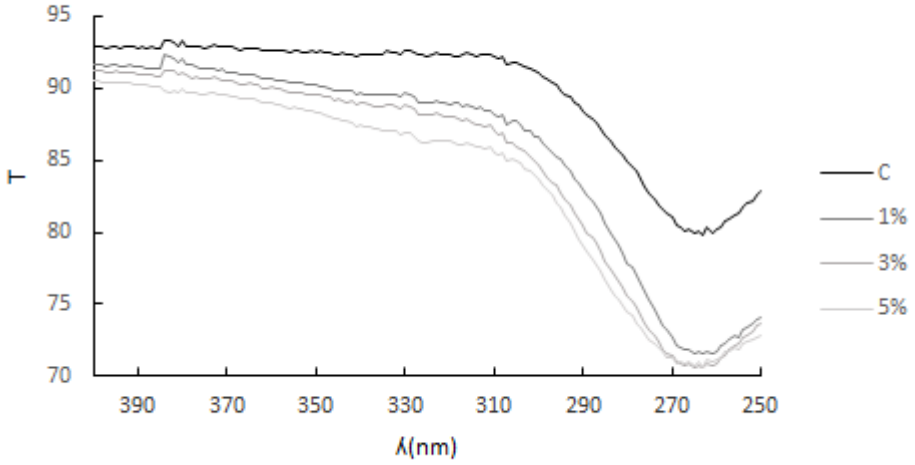

Figure 7. Spectral distribution in the UV range of the UV-VIS spectra of control blend (C) and composite films with CNCs (1 %, 3 % and 5 %).

The control films exhibited values of transmittance above 90 % in the visible light range, whereas the values were much lower in the UV range. The addition of cellulose nanocrystals provoked a decrease in film transmittance over the whole UV-VIS range, but this is more marked in the UV range, where T values decreased by about 60 % for the films with the highest ratio of nanocrystals. These results confirm the greater opacity to UV radiation of nanocomposites observed by other authors (Fortunati *et al*., 2013b; Arrieta *et al*., 2014a), which represents an advantage in terms of the food protection against oxidative processes or other UV induced reactions. In terms of transparency to visible light, the internal transmittance (Ti) at 450 nm (Table 2) reveals a small progressive increase in opacity as the CNC ratio rose in the films, regardless of the storage time, in agreement with the rise in the concentration of the nanocrystal dispersed phase. As concerns the film' gloss, they showed very low values at 60º incidence angle, as compared with the gloss values of pure pea starch or PVA films (27 and 150 units,

respectively, data not reported). This can be attributed to the surface roughness of the films where lumps of the starch-rich phase are dispersed in the continuous PVA-rich phase, as discussed above. This provoked irregularities at the film surface which contributes to light dispersion, giving a matt appearance. The incorporation of CNCs did not significantly affect the gloss of the films.

The mechanical behaviour of the films is shown in Figure 8 where the typical stress-strain curves of control blend (C) and CNC composite films 1 %, 3 % and 5 % , after 5 weeks of storage time are shown. The different tensile behaviour of control films and composites can be clearly observed. The presence of CNCs affected the film extensibility; the higher the CNC ratio, the more stretchable the material. Similar behaviour has been reported by several authors (Zhang *et al*., 2011; Arrieta *et al*., 2014a) for other films containing CNCs. It is highlighted that the extensible response of films is closely related to the different concentrations of nanocrystals in the matrix, determining the volume fraction of the reinforcement, the dispersion degree in the matrix, and the interactions between the nanocrystals and the polymers (Rescignano *et al*., 2014).

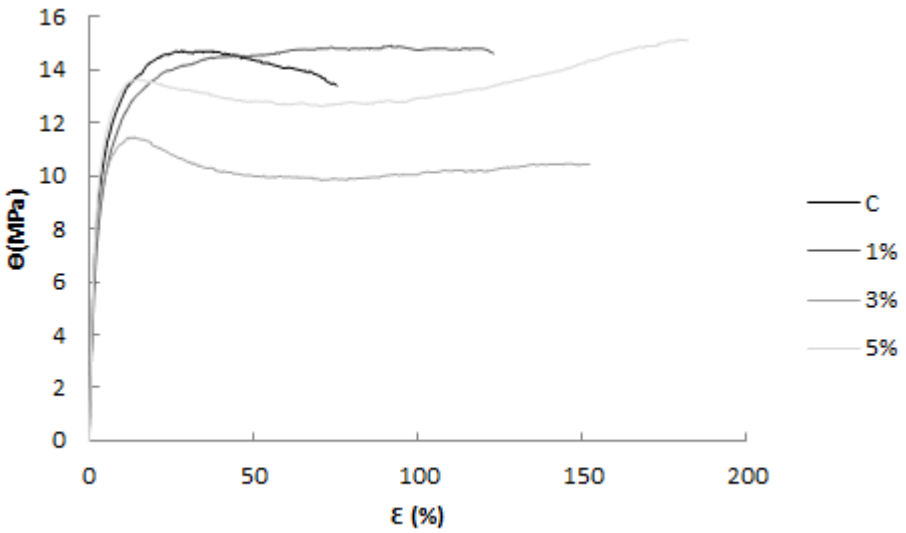

Figure 8. Typical strain-stress curves of control blend (C) and compsosite films with CNCs (1 %, 3 % and 5 %) after 5 weeks of storage.

Table 1: Thermal properties of control blend films and those containing 1, 3 and 5 % of CNCs obtained by DSC and TGA analysis. Mean values and standard deviation.

	Cooling				Heating				TGA analysis
Films	T_{c1} (ºC)	T_{c2} (ºC)	ΔH_c (J.g$^{-1}_{pva}$)	T_g (ºC)	T_m (ºC)	ΔH_m (J.g$^{-1}_{pva}$)	X (%)	T_{mp} (ºC)	T_p(ºC)
C	143.8±0.9^{a}	200.7±0.1^{a}	65±6^{a}	78.6±0.2^{a}	227.04±1.12^{a}	108±6^{a}	67±4^{a}	347.3±0.4^{a}	419±2^{a}
1 %	135±4^{a}	201.1±1.2^{a}	74±8^{a}	76.4±0.2^{ab}	226.8±0.9^{a}	85±2^{b}	53±1^{b}	356±6^{a}	429±3^{b}
3 %	141±3^{b}	201.2±1.2^{a}	71±6^{a}	73.9±1.4^{b}	225.8±1.8^{a}	85±3^{b}	53±2^{b}	355±2^{a}	431.9±1.3^{b}
5 %	145.9±0.1^{ab}	202.3±0.2^{a}	60.7±0.2^{a}	76.3±1.8^{ab}	225.6±0.7^{a}	61±6^{c}	38±4^{c}	323±5^{b}	427±2^{b}

T_c: crystallization temperature; T_m: melting temperature; T_g: glass; transition temperature; ΔH_c: enthalpies of crystallization ; ΔH_m: enthalpies of melting, X:; percentage of crystallinity; T_{mp}: main peak temperature and T_p: temperature of second degradation peak.

$^{a, b,c}$ different letters in the same column indicate significant differences among formulations ($p<0.05$).

Table 2: Moisture content (MC), water vapour permeability (WVP), internal transmittance (Ti) at 450 nm and gloss values at 60º of control films and those containing 1 %, 3 % and 5 % of CNCs, after 1 (1W) and 5 (5W) storage weeks. Mean values and standard deviation.

	MC (%d.b.)		WVP (g.mm.kPa^{-1}h^{-1}m-^{2})		Ti (450nm)		Gloss 60º	
Films	1W	5W	1W	5W	1W	5W	1W	5W
C	6.6±0.8^{a1}	6.7±0.3^{ab1}	3.5±0.3^{a1}	3.41±0.15^{a1}	18±3^{ab1}	20±3^{a1}	3.5±0.3^{a1}	3.41±0.15^{a1}
1 %	6.4±0.5^{b1}	6.9±0.2^{a1}	3.4±0.3^{a1}	3.6±0.3^{a1}	21±3^{a1}	24±3^{b1}	3.4±0.3^{a1}	3.6±0.3^{a1}
3 %	4.73±0.07^{c1}	6.5±0.3^{b2}	3.43±0.15^{a1}	3.25±0.14^{a1}	15±4^{bc1}	21±3^{a2}	3.43±0.1 ^{a1}	3.25±0.14^{a1}
5 %	4.5±0.2^{c1}	5.8±0.2^{c2}	3.2±0.3^{a1}	3.07±0.66^{a1}	13±4^{c1}	16±3^{c1}	3.2±0.3^{a1}	3.1±0.6^{a1}

Elastic modulus (EM), tensile strength at break (TS) and percentage of elongation at break (E, %) are used to describe the mechanical behaviour of films. Table 3 shows the mean values of these parameters for control films and composites. The obtained values are coherent with those reported by other authors for pea or corn starch-PVA films (Cano *et al*., 2015; Shi *et al*., 2008; Yoon *et al*., 2012). Cellulose nanocrystals improved the mechanical behaviour of films in terms of their stretchability, without decreasing their resistance to break ($p<0.05$), while the elastic modulus tends to increase slightly. After 5 weeks' storage time, a similar behaviour was observed for both blend and composite films: the resistance to break is reduced, as well as the elastic modulus, which can be attributed to the moisture gain of the films during storage, which makes the network cohesion forces weaker. Nevertheless, at this time, the reinforcement effect of CNCs was more evident since the elastic modulus of composites containing 3 or 5 % CNCs was higher.

Table 3: Values of elastic modulus (EM), tensile strength at break (TS) and percentage of elongation at break (E, %) of control blend films and those containing 1 %, 3 % and 5 % of CNCs, after 1 (1W) and 5 (5W) storage weeks. Mean values and standard deviation.

	EM (MPa)		TS (MPa)		E (%)	
Films	1W	5W	1W	5W	1W	5W
C	420 ± 90^{a1}	330 ± 130^{a1}	19 ± 5^{a1}	13 ± 5^{a2}	90 ± 30^{ab1}	120 ± 90^{ab1}
1 %	590 ± 110^{b1}	380 ± 90^{ab2}	23 ± 4^{a1}	13 ± 3^{a2}	60 ± 30^{a1}	90 ± 50^{a1}
3 %	400 ± 100^{a1}	450 ± 100^{bc1}	19 ± 6^{a1}	13 ± 3^{a2}	130 ± 70^{b1}	160 ± 80^{b1}
5 %	440 ± 170^{a1}	460 ± 70^{c1}	19 ± 5^{a1}	12 ± 3^{a2}	140 ± 60^{b1}	170 ± 40^{b1}

^{a,b,c} different letter in the same column indicate significant differences among formulations ($p<0.05$).

^{1,2} different number in the same file indicate significant differences among storage time ($p<0.05$).

The mechanical impact of CNCs on blend films can be, in part, explained by the limitation of crystallization of PVA, but also by the formation of a percolating network within the polymer matrix, as reported by other authors (Habibi *et al*., 2010). In this network, the stress is assumed to be transferred through crystal-crystal interactions and crystal-polymer matrix interactions (Fortunati *et al*., 2013b). According to Favier *et al*. (1997), the critical percolation volume fraction (percolation threshold: *Xc*) can estimated from statistical percolation theory for cylindrically shaped particles taking into account their aspect ratio (A) by the relation: (Xc = 0.7/A). For composite films with CNCs, A can be estimated as 20 and Xc is 0.035. So, percolation threshold was reached for all composites and percolation network formation can explain the enhancement of mechanical behaviour of the films.

PVA-starch films containing cellulose nanocrystals were more stretchable and stiffer with comparable resistance to break than pea starch-PVA films and so, they can be considered more adequate for food packaging applications.

Overall migration tests with simulants were carried out to determine the total amount of non-volatile substances that might migrate into foodstuffs from film matrices (Schimdt *et al*., 2011) for the purposes of checking whether they meet the migration limit (60 mg kg^{-1} simulant) established by current legislation (EN 1186-1:2002). Table 4 shows the obtained values of overall migration for control and nanocomposite films in both food simulants. After 20 days in ethanol 10 % (v/v) simulant, no significant differences in overall migration ($p \leq 0.05$) between control and composite films were found, except for films with 5 % of CNCs which showed higher values, although well below the established limit. However, after 2 days at 20 ºC in isooctane, the maximum migration level was reached for the control films, although migrated amounts are in the order of 1000 times lower than that obtained in the polar simulants. The different migration behaviour of control and nanocomposites in the two food simulants reveals the greater hydrophilic

nature of films containing CNCs, as reported by Fortunati, *et al*. (2012c). The CNC addition significantly decreased ($p<0.05$) the amount of material that migrates to non-polar food simulants, while increasing the migrated amounts in polar simulants. Therefore, CNCs make the films more adequate for applications in high fat content foods.

Table 4: The overall migration of control blend films and those containing 1 %, 3 % and 5 % of CNCs, in 10% (v/v) ethanol and isooctane food simulants. Mean values and standard deviation.

Films	Ethanol 10% (v/v) (mg/kg simulant)	Isoctane (µg/kg simulant)
C	4.6 ± 0.7^{a}	34 ± 3^{a}
1%	4.5 ± 0.2^{ab}	22 ± 2^{b}
3%	4.8 ± 0.2^{ab}	12 ± 3^{c}
5%	5.8 ± 1.5^{b}	15 ± 2^{c}

[a, b] different letter in the same column indicate significant differences among formulations ($p<0.05$).

4. CONCLUSIONS

The pea starch-PVA blend films showed phase separation and CNCs are distributed in both, starch rich phase and PVA rich phase. They are present as aggregates of different sizes depending on their ratio in the film; the higher the ratio, the greater the aggregates, as deduced from the AFM analysis at surface level. No changes in water vapour permeability occurred due to the presence of CNCs, despite the increase in the hydrophilic nature of the films revealed by the overall migration values in polar and non-polar food simulants. Films with CNCs became slightly stiffer and more stretchable than control films, while crystallization of PVA was partially inhibited by CNC addition. The improvements conferred by CNCs in mechanical properties of pea starch-PVA blend films make them more adequate for food applications, especially for high fat foods, where overall migration values were very low.

Acknowledgments

The authors acknowledge the financial support from the Spanish Ministerio de Economía y Competitividad throughout the projects AGL2010-20694 and AGL2013-42989-R. Amalia Cano also thanks the Spanish Ministerio de Educación, Cultura y Deporte for the FPU grant and COST-STSM-FA1001-14253 for the financial support for the collaboration.

References

- Abdelrazek, E. M., Elashmawi, I. S., & Labeeb, S. (2010). Chitosan filler effects on the experimental characterization, spectroscopic investigation and thermal studies of PVA/PVP blend films. *Physica B*, 405, 2021-2027.
- Anandjiwala, R. D. (2006). The role of research and development in the global competitiveness of natural fibre products. Natural Fibres Vision 2020 New Delhi, 8-9 December 2006: 1-15.
- Armentano, I., Dottori, M., Fortunati, E., Mattioli, S., & Kenny, J. M. (2010). Biodegradable polymer matrix nanocomposites for tissue engineering: A review. *Polymer Degradation and Stability*, 95, 2126-2146.
- Arrieta, M., Fortunati, E., Dominici, F., Rayón, E., Lopez, J., & Kenny, J. M. (2014a). PLA-PHB/cellulose based films: mechanical, barrier and disintegration properties. *Carbohydrate Polymers,* 107, 139-149.
- Arrieta, M., Fortunati, E., Dominici, F., Rayón, E., Lopez, J., & Kenny, J. M. (2014b). Multifunctional PLA-PHB/cellulose nanocrystals films: processing, structural and thermal behaviour. *Carbohydrate Polymers,* 107, 16-24.
- ASTM (1995) Standard test methods for water vapour transmission of materials. Standard designations: E96-95 Annual book of ASTM standards, Philadelphia PA: American Society for Testing and Materials, 406 - 413.
- ASTM (1999) Standard test methods for specular gloss. Designation (D523). In Annual book of ASTM standards, Vol. 06.01. Philadelphia, PA: American Society for Testing and Materials.

- Bonilla, J., Atarés, L., Vargas, M., & Chiralt, A. (2013). Properties of wheat starch film-forming dispersions and films as affected by chitosan addition. *Journal of Food Engineering*, 114 (3), 303-312.

- Cano, A., Fortunati, E., Cháfer, M., Kenny, J. M., Chiralt, A., & González, C. (2015). Properties and ageing behaviour of pea starch films as affected by blend with poly(vinyl alcohol), *Food Hydrocolloids*, 48, 84-93.

- Cano, A., Jiménez, A., Cháfer, M., González, C., & Chiralt, A. (2014). Effect of amylose:amylopectin ratio and rice bran addition on starch films properties. *Carbohydrate Polymers,* 111, 543-555.

- Cavaille, J. Y., Ruiz, M. M., Dufrense, A., Gerard, J. F., & Graillat, C. (2000). Processing and characterization of new thermoset nanocomposites based in cellulose whiskers. *Composite Interfaces*, 7(2), 117-131.

- Chen, J., Liu, Ch., Chen, Y., Chen, Y., & Chang, P. R. (2008). Comparative study on the films of poly(vinyl alcohol)/pea starch nanocrystals and poly(vinyl alcohol)/native pea starch. *Carbohydrate Polymers,* 73, 8-17.

- Chen, Y., Liu, Ch., Chang, P. R., Cao, X., & Anderson, D. P. (2009). Bionanocomposites based on pea starch and cellulose nanowhiskers hydrolyzed from pea hull fibre: Effect of hydrolysis time. *Carbohydrate Polymers*, 76, 607-615.

- Choi, Y., & Simonsen, J. (2006). Cellulose nanocrystals-filled carboxymethyl cellulose nanocomposites. *Journal of Nanoscience and Nanocomposites*, 6(3), 633-639.

- Commission Regulation (EU) No 10/2011 of 14 January 2011 on plastic materials and articles intended to come into contact with food.

- Cranston, E. D. & Gray, D. G. (2006). Morphological and optical characterization of polyelectrolyte multilayers incorporating nanocrystalline cellulose. *Biomacromolecules*, 7, 2522–2530.

- European Standard EN 1186-1:2002 Materials and articles in contact with foodstuffs. Plastics. Guide to the selection of conditions and test methods for overall migration.

- Favier, V., Cavaillé, J. Y., Canova, G. R., & Shrivastavas, S. C. (1997). Mechanical percolation in cellulose whisker nanocomposites. *Polymer Engineering & Science,* 37(10), 1732-1739.

- Fortunati, E., Armentano, I., Zhou, Q., Iannoni, A., Saino, E., Visai, L., Berglund, L. A., & Kenny, J. M. (2012a). Multifunctional bionanocomposite films of poly(lactic acid), cellulose nanocrystals and silver nanoparticles. *Carbohydrate Polymers,* 87, 1596-1605.

- Fortunati, E., Armentano, I., Zhou, Q., Puglia, D., Terenzi, A., Berglund, L. A., & Kenny, J. M. (2012b). Microstructure and nanoisothermal cold crystallization of PLA composites based on silver nanoparticles and nanocrystalline cellulose. *Polymer Degradation and Stability*, 97, 2027-2036.

- Fortunati, E., Peltzer, M., Armentano, I., Jiménez, A., & Kenny, J. M. (2013a). Combined effects of cellulose nanocrystals and silver nanoparticles on the barrier and migration properties of PLA nano-biocomposites. *Journal of Food Engineering,* 118, 117-124.

- Fortunati, E., Peltzer, M., Armentano, I., Torre, L., Jiménez, A., & Kenny, J. M. (2012c). Effects of modified cellulose nanocrystals on the barrier and migration properties of PLA nano-biocomposites, *Carbohydrate Polymers,* 90, 948-956.

- Fortunati, E., Plugia, D., Luzi, F., Santulli, C., Kenny, J. M., & Torre, L. (2013b). Binary PVA bio-nanocomposites containing cellulose nanocrystals extracted from different natural sources: Part I. *Carbohydrate Polymers,* 97, 825-836.

- Fortunati, E., Puglia, D., Monti, M., Santulli, C., Maniruzzaman, M., & Kenny, J. M. (2013c). Cellulose nanocrystals extracted from Okra Fibers in PVA nanocomposites. *Journal of Applied Polymer Science*, 3220-3230, DOI: 10.1002/APP.38524.

- Habibi, Y., Lucia, L. A., & Rojas, O. J. (2010). Cellulose Nanocrystals: Chemistry, self-assembly, and applications. *Chemical Reviews*, 110(6), 3479-3500.

- Jagadish, R. S. & Raj, B. (2011). Properties and sorption studies of polyethylene oxide-starch blended films. *Food Hydrocolloids*, 25, 1572-1580.

- Jiang, X., Jiang, T., Gan, L., Zhang, X., Dai, H., & Zhang, X. (2012). The plasticizing mechanism and effect of calcium chloride on starch/poly (vinyl alcohol) films. *Carbohydrate Polymers,* 90, 1677-1684.

- Jiménez, A., Fabra, M. J., Talens, P., & Chiralt, A. (2012a). Influence of hydroxypropylmethylcellulose addition and homogenization conditions on properties and ageing of corn starch based films. *Carbohydrate Polymers,* 89(2), 676-686.

- Jiménez, A., Fabra, M. J., Talens, P., & Chiralt, A. (2012b). Effect of re-crystallization on tensile, optical and water vapour barrier properties of corn starch films containing fatty acids. *Food Hydrocolloids*, 26, 302-310.

- Jiménez, A., Sánchez-González, L., Desorby, S., Chiralt, A., & Tehrany, E. A. (2013). Influence of nanoliposomes incorporation on properties of film forming dispersions and films based on corn starch and sodium caseinate. *Food Hydrocolloids,* 35, 159-169.

- Khoshkava, V., & Kamal, M. R. (2014). Effect of drying conditions on cellulose nanocrystals (CNC) agglomerate porosity and dispersibility in polymer nanocomposites. *Powder Technology*, 261, 288-298.

- Lee, S. Y., Mohan, D. J., Kang, I. E., Doh, G-H., Lee, S., & Han, S. O. (2009). Nanocellulose reinforced PVA composite films: effects of acid treatment and filler loading. *Fibers and Polymers*, 10, 77-82.

- Luo, X., Li, J., & Lin, X., (2012). Effect of gelatinization and additives on morphology and thermal behaviour of cornstarch/PVA blend films. *Carbohydrate Polymers,* 90, 1595-1600.

- Ma, X., Chang, P. R., & Yu, J. (2008). Properties of biodegradable thermoplastic pea starch/carboxymethyl cellulose and pea starch/microcrystalline cellulose composites. *Carbohydrate Polymers,* 72, 369-375.

- Pereda, M., Dufresne, A., Aranguren, M. I., & Marcovich, E. (2014). Polyelectrolyte films based on chitosan/olive oil and reinforced with cellulose nanocrystals. *Carbohydrate Polymers,* 101, 1013-1026.

- Peresin, M. S., Habibi, Y., Zoppe, J. O., Pawlak, J. J., & Rojas, O. J. (2010). Nanofiber composites of polyvinyl alcohol and cellulose nanocrystals: manufacture and characterization. *Biomacromolecules,* 11(3), 674-681.

- Priya, B., Gupta, V. K., Pathania, D., & Singh, A. S. (2014). Synthesis, characterization and antibacterial activity of biodegradable starch/PVA composite films reinforced with cellulosic fibre. *Carbohydrate Polymers,* 109, 171-179.

- Rescignano, N., Fortunati, E., Montesano, S., Emilianini, C., Kenny, J. M., Martino, S., & Armentano, I. (2014). PVA bio-nanocomposites: A new take-off using cellulose nanocrystals and PLGA nanoparticles. *Carbohydrate Polymers,* 99, 47-58.

- Roohani, M., Habibi, Y., Belgacem, N. M., Ebrahim, G., NaghiKarimi, A., & Dufresne, A. (2008). Cellulose whiskers reinforced polyvinyl alcohol copolymers Nanocomposites. *European Polymer Journal*, 44, 2489–2498.

- Schmidt, B., Katiyar, V., Plackett, D., Larsen, E. H., Gerds, N., & Bender Koch, C. (2011). Migration of nanosized layered double hydroxide platelets from polylactide nanocomposite films. *Food Additives and Contaminants*, 28, 956–966.

- Shi, R., Bi, J., Zhang, Z., Zhu, A., Chen, D., Zhou, X., Zhang, L., & Tian, W. (2008). The effect of citric acid on the structural properties and cytotoxicity of the polyvinylalcohol/starch films when molding at high temperature. *Carbohydrate Polymers*, 74, 763–770.

- Siddaramaiah, Raj. B., & Somashekar, R. (2004). Structure–property relation in polyvinyl alcohol/starch composites. *Journal of Applied Polymer Science*, 9, 630–635.

- Siqueira, G., Brasa, J., Follain, N., Belbekhouche, S., Marais, S., & Dufresne, A. (2013). Thermal and mechanical properties of bio-nanocomposites reinforced by Luffa cylindrical cellulose nanocrystals. *Carbohydrate Polymers,* 91(2), 711-717.

- Siracusa, V., Rocculi, P., Romani, S., & Rosa, M. D. (2008). Biodegradable polymers for food packaging: A review. *Trends in Food Science & Technology*, 19, 634-643.

- Sreekumar, P. A., Al-Harthi, M. A., & De, S. K. (2012). Studies on compatibility of biodegradable starch/polyvinyl alcohol blends. *Polymer Engineering & Science*, 52(10), 2167-2172.

- Sturcová, A., Davies, G. R., & Eichhorn, S. J. (2005). Elastic modulus and strees-transfer properties f tunicate cellulose whiskers. *Biomacromolecules*, 6, 1055-1061.

- UNE-EN ISO (2008) Paper, board and pulps - Determination of dry matter content -Oven-drying method, Vol 638.

- UNE-ISO 527-1 (2012) Plastics e determination of tensile properties e Part 1: General principles.

- Yoon, S., Park, M., & Byun, H. (2012). Mechanical and water barrier properties of starch/PVA composite films by adding nano-sized poly (methylmethacrylate-co-acrylamide) particles. *Carbohydrate Polymers,* 87, 676– 686.

- Zhang, W., Yang, X., Li, C., Liang, M., Lu, C., & Deng, Y. (2011). Mechanical activation of cellulose and its thermoplastic polyvinyl alcohol composites with enhanced physicochemical properties. *Carbohydrate Polymers,* 83, 257-263.

Chapter III: Development of starch-PVA active films, containing $AgNO_3$ or essential oils. Effect of antimicrobials on film biodegradability.

Amalia I. Cano, Maite Cháfer, Amparo Chiralt, Chelo González-Martínez. **Physical and antimicrobial properties of starch-PVA blend films as affected by the incorporation of natural antimicrobial agents.** *Foods from MDPI* (pending for approval).

Abstract

Incorporation of natural antimicrobial substances into coatings or packaging films to improve food preservation is being widely studied in line with the current consumer demand for safer and healthier foods and environmentally friendly production systems. In this work, active films based on a starch and PVA blend were developed by incorporating natural antimicrobials (neem oil: N and oregano essential oil: O). First, a screening about the antifungal effectiveness of different natural extracts (echinacea, horsetail extract, liquid smoke and neem seed oil) against two fungus (*Penicillium expansum* and *Aspergillus niger)* was carried out. The effect of N and O incorporation on the films' physical and antimicrobial properties was analysed. Composite films containing potentially antimicrobial oils, only exhibited antibacterial and antifungal activity when they contain O. Antibacterial activity occurred at low O concentration (6.7 % O in the dried matrix), while antifungal effect required higher doses of O in the films. Incorporation of oils did not notably affect the water sorption capacity and water vapour barrier properties of S-PVA films, but reduced their transparency and gloss, especially at the highest concentrations. Mechanical performance of the S-PVA films was also modified by oil incorporation but this was only relevant at the highest oil ratio (22 % in the dried matrix). S-PVA films with 6.7 % of O exhibited the best physical properties, without significant differences with respect to the S-PVA matrix, while exhibit antibacterial activity, thus representing a good alternative for food packaging applications.

Key words: Oregano essential oil, Neem oil, water vapour permeability, mechanical properties, *E. coli*, *L. innocua*, *A. niger*, *P. expansum*

1. INTRODUCTION

In the last few years, the consumer's demand for natural ingredients and foods without synthetic preservatives has promoted the popularity of natural antimicrobial agents. So far, many studies have been carry out in order to take advantage of the antibacterial and/or antioxidant activities of natural substances from different sources such as microorganisms, animals and plants (Farjana *et al*., 2014).

Extracts from natural sources have been used against food spoilage since ancient times to extend the food shelf-live and to prevent foodborne diseases. Substances from different nature, such as alkaloids, tannins, flavonoids and phenolic compounds becoming from the plant extracts, are responsible for bioactivity (Shihabudeen *et al*., 2010; Utama *et al*., 2002). These substances have been widely used as food flavoring agents and most of them are generally recognized as safe (GRAS) by the Food and Drug Administration, FDA. In Europe, extracts from natural resources are regulated under Regulation EU 872/2012 that contains the list of flavouring substances authorized for food uses.

Among bioactive plant extracts, it is well known that those from Echinacea (*Echinacea purpurea*), field horsetail (*Equisetum*), neem (*Azadirachta indica*) or essential oils have shown antimicrobial activity against foodborne pathogens or inhibited the food spoilage. Significant antimicrobial activity has been attributed to Echinacea extracts, in a series of in vitro tests, against *Saccharomyces cerevisiae,* various *Candida* species, *Listeria monocytogenes and Staphylococcus (*Barrert, 2003; Stanisavljević *et al*., 2009*).* Field horsetail has been also described as an herb with antioxidant and antimicrobial properties (Garcia *et al*., 2013). Some studies revealed its inhibitory effect on the *Aspergillus spp.* and *Fusarium spp.* growth and toxin production (Mahoney & Molyneux, 2004; Radulovic *et al*., 2006; Samapundo *et al*., 2007). Garcia *et al*. (2012) confirmed that a hydro-alcoholic extract of *Equistum arvense* inhibited the growth of

Aspergillus flavus and *Fusarium verticillioides* in maize seeds, especially at high water activity levels (simulating pre-harvest conditions).

Neem is also a non-toxic plant which possesses excellent antimicrobial properties (Sanuja *et al*., 2015; Pu *et al*., 2010; Xu *et al*., 2010). In fact, Baswa *et al*. (2001) revealed that the neem oil has bactericidal activity against 14 strains of pathogenic bacteria such as *Staphylococcus aureus* (Rao *et al*., 1986), *Staphylococcus typhus* (Patel &Trivedi, 1962), and *Escherichia coli*, *Streptococcus mutans* and *lactobacilli* (Vanka *et al*., 2001). On the other hand, Mahfuzul Hoque *et al*. (2007) determined the antibacterial activity of neem extracts against 21 strains of foodborne pathogens: *Listeria monocytogenes*, *Staphylococcus aureus*, *Escherichia coli* O157:H7, *Salmonella Enteritidis*, *Vibrio parahaemolyticus*, and *Bacillus cereus*, and five food spoilage bacteria: *Pseudomonas aeroginosa*, *Psuedomas putida*, *Alcaligenes faecalis*, and *Aeromonas hydrophila*. They concluded that neem extracts generally showed higher antimicrobial activity against Gram-positive bacteria than against Gram-negative, and none of the extracts showed antimicrobial activity against *E. coli* O157:H7 and *Salmonella Enteritidis*. The action mechanism of the neem extracts is mainly attributed to the inhibition of cell-membrane synthesis in the bacteria (Baswa *et al*., 2001).

Nevertheless, the most widely used extracts from natural sources are essential oils which have exhibited antimicrobial activity against a wide spectrum of bacteria and fungi. They are constituted by hydrophobic, volatile compounds with low molecular weight (Sánchez-González *et al*., 2011). Among them, the oregano essential oil is one of the most effective antimicrobial oil and its active properties have been demonstrated in numerous studies (Aguirre *et al*., 2013; Emiroğlu *et al*., 2010; Zivanovic *et al*., 2005). These have been mainly attributed to carvacrol, thymol, γ-therpinene and p-cymene (Burt, 2004; Jouki *et al*., 2014; Sadaka *et al*., 2014). The action mode of the major components, carvacrol and thymol, as explained by Burt (2004), consists of the

disintegrations of the outer cell membranes of bacteria, releasing lipopolysaccharides and increasing the permeability of the cytoplasmic membrane to ATP. Some authors reported that gram-positives bacteria are slightly more sensitive to the essential oil action than gram-negatives, according to the described mechanism (Burt, 2004; Corrales *et al*., 2014; Martucci *et al*., 2015).

Other natural antimicrobial agent is the traditional wood smoke that has been used for centuries to preserve food quality on the basis of its antioxidant and antimicrobial properties (Lingbeck *et al*., 2014; Saloko *et al*., 2014). The antimicrobial properties of the pyrolysis condensate or "liquid smoke" from different woods, with different levels of phenols, carbonyl compounds and organic acids, against *Staphylococcus aureus*, *Aeromonas hydrophila, Salmonella*, *Listeria monocytogenes* and *Escherichia coli* have been recently studied (Lingbeck *et al*., 2014).

As concerns the way of incorporation of antimicrobial agents into the food systems, a new concept has gained increasing acceptance in the recent years, which is the incorporation of bioactive natural extracts in the food package, thus obtaining active packaging materials (Sadaka *et al*., 2014). In this sense, active coating applications in postharvest or minimally processed fruits and vegetables, cheeses, meats, etc. or the development of bioactive films for food packaging, are some of the reasons for the recent gain in importance of the natural bioactive substances.

Incorporation of bioactive substances in food coatings or packaging films shows some advantages, such us the compounds are not directly exposed to external conditions (Cho *et al*., 2009), they can act only at the surface level and can be applied at any stage of the food supply chain (Rodrigues & Han, 2000; Rodrigues *et al*., 2002). Thus, natural agents have been incorporated into a wide spectrum of natural and synthetic polymer matrices to obtain active materials (Lanciotti *et al*., 2004), although no previous studies about the incorporation of bioactive substances into starch-PVA blends

has been found, despite that recent studies reported different benefits of this blend films in terms of water vapour barrier and mechanical properties. Starch-PVA films were much more extensible and stable throughout storage and exhibit lower water sorption capacity than pure starch films (Cano *et al*., 2015). However, the incorporation of antimicrobial substances can affect the film properties which are relevant for a specific target application, such barrier capacity to water vapour, oxygen, CO_2 or aroma compounds and mechanical and optical properties (Sánchez-González *et al*., 2010).

The aim of this work was to obtain bioactive S-PVA films for extending the food shelf life by controlling the microbial spoilage. To this end, the antifungal activity of different natural compounds (Echinacea and horsetail extracts, liquid smoke and neem seed oil) against two fungus (*Penicillium expansum* and *Aspergillus niger*) was tested at different concentrations. Afterwards, on the basis of the obtained, and previously reported, results, neem oil and oregano essential were incorporated in S-PVA films to analyse their effect on the barrier, optical and mechanical properties of the films as well as the film antimicrobial activity against two fungus, *P. expansum* and *A. niger* and two bacteria, *Listeria innocua* and *Escherichia coli*.

2. MATERIALS AND METHODS

2.1. Materials

Pea starch (S) was purchased from Roquette Laisa España S.A. (Benifaió, Valencia, Spain), poly(vinyl alcohol) (PVA)(M_w: 89,000-98,000, degree of hydrolysis > 99 %, and viscosity at 4 % H_2O, 20 ºC is 11.6-15.4 cP) was obtained from Sigma Aldrich Química S.L. (Madrid, Spain) and glycerol and magnesium nitrate-6-hydrate were provided by Panreac Química S.A. (Castellar de Vallès, Barcelona, Spain).

Different natural antimicrobial substances used were: echinacea (E) and horsetail extract (HS) extract from Soria Natural S.A. (Lérida, Spain), liquid smoke (LS), provided by G. Mariani & C. S.p.a. (Cellatica, Italy), neem oil (N) purchased from Magnolia Holland Ibérica S.A. (Vilassar de Mar, Barcelona, Spain) and oregano essential oil (O) from Herbes del Molí (Benimarfull, Alicante, Spain).

Stock culture of *Escherichia coli* (CECT 515), *Listeria innocua* (CECT 910), and *Asperguillus niger* (CECT 20156) supplied by Colección Española de Cultivos Tipos (CECT, Burjassot, Spain) were kept frozen (- 25 ºC) respectively in Tryptone Soy Broth (TSB, Scharlab, Barcelona, Spain) for bacteria and Potato Dextrose Broth (Scharlab, Barcelona, Spain) for fungus, supplemented with 30% glycerol. *Penicillium expansum* was provided from the culture collection of Department of Biotechnology (Universitat Politècnica de València, Valencia, Spain).

2.2. Preparation of film forming dispersion and films

Films were obtained by solvent casting procedure after the preparation of the corresponding film forming dispersions (FFDs). First, starch (2 % w/w) was dispersed and heated in an aqueous solution at 95 ºC for 30 min to induce starch gelatinization. Thereafter, the dispersion was homogenized using a rotor-stator homogenizer (Ultraturrax D125, Janke and Kunkel, Germany) at 13,500 rpm for 1min and 20,500 rpm for 3 min. Afterwards, PVA was incorporated to the pregelatinized starch dispersion in a S:PVA ratio of 2:1, and heated, while stirred, at 95 ºC for 30 min until complete dissolution. Finally, glycerol was added at a starch:glycerol ratio of 1:0.25, on the basis of previous studies (Cano *et al*., 2015). This FFD is used to obtain the control films (S-PVA) and was also used to incorporate the different antimicrobial substances: oregano essential oil (O) or neem oil (N). These were incorporated into the films at two different ratios with respect to the starch, 1:0.125 (S-PVA-1O and S-PVA-1N) and 1:0.5 (S-PVA-

2O, S-PVA-2N), which corresponds to 6.7 and 22 g/100 g total solids in the film, respectively. Afterwards, The FFD was homogenized at 12,500 rpm for 4 min to disperse the lipids.

Controlled volumes of film-forming dispersions (equivalent to 1.5 g of total solids) were cast into levelled Teflon casting plates (15 cm diameter) and dried at 25 ºC and 45 %RH for 48 h. Then, they were peeled intact from the plates and were conditioned at 53 % RH using magnesium nitrate-6-hydrate saturated solution at 25 ºC until further analysis.

2.3. Physical properties of films

2.3.1. Film thickness

Thickness of the films was measured at six random positions with a Palmer digital micrometre to the nearest 0.0025 mm.

2.3.2. Moisture content

The moisture content of the films (MC), equilibrated at 53 % RH and 25 ºC for one and five weeks, was analysed by drying the samples in a vacuum oven at 60 ºC for 24 h. Later on, the pre-dried samples were placed in desiccators containing P_2O_5 until reaching constant weight. Five replicates per film formulation were considered.

2.3.3. Water vapour permeability

Water vapour permeability (WVP) was evaluated in the films equilibrated at 25 ºC and 53 % RH after one and five storage weeks, following the ASTM E96-95 gravimetric method by using Payne permeability cups (Payne, elcometer SPRL, Hermelle/sd Argenteau, Belgium) 3.5 cm in diameter. The temperature was 25 ºC and the relative humidity gradient was 53-100 %, which was obtained using magnesium nitrate-6-hydrate

and pure water, respectively. Cups were introduced into desiccators and these into a temperature-controlled chamber at 25 ºC. Weight control of the cups was performed every 2 h using an analytical balance (±0.00001 g). The water vapour transmission (WVTR) was determined from the slope obtained from the regression analysis of weight loss data versus time, once the steady state had been reached, divided by the film area. Five replications were carried out for each type of film.

2.3.4. Internal transmittance

The transparency was determined by applying the Kubelka–Munk theory for multiple scattering to the reflection spectra obtained in a spectrocolorimeter CM-3600d (Minolta Co., Tokyo, Japan) with a 30 mm illuminated sample area. This theory assumes that each light flux which passes through the film is partially absorbed and scattered, which is quantified by the absorption (K) and the scattering (S) coefficients. Transparency (K/S) was calculated, as indicated by Hutchings (1999), from the reflectance of the sample layer on a white background of known reflectance and on an ideal black background. Measurements were taken triplicate in samples equilibrated at 25 ºC and 53 % RH for one and five weeks, using both a white and a black background.

2.3.5. Gloss

Gloss was measured using a flat surface gloss metre (Multi-Gloss 268, Minolta, Langenhagen, Germany) at an angle of 60º with respect to the normal to the film surface, according to the ASTM standard D523 (ASTM, 1999). Prior to gloss measurements, films were conditioned at 25 ºC and 53 % RH for one and five weeks. Gloss measurements were carried out over a black matte standard plate and were taken in triplicate. Results were expressed as gloss units, relative to a highly polished surface of standard black glass with a value close to 100.

2.3.6. Mechanical properties

Mechanical properties were measured with a Universal Test Machine (TA.XT plus, Stable Micro Systems, Haslemere, England) following the ASTM standard method D882 (ASTM, 2001). Equilibrated film (25 ºC for 1 and 5 weeks at 53 %RH) specimens (2.5 cm wide and 10 cm long) were mounted in the film-extension grips (A/TG model) which were set 50 mm apart. The speed of the testing machine during stretching was 50 mm min^{-1} until breaking. Force-distance curves were obtained and transformed into Stress-Hencky curves which allowed tensile strength at break (TS, MPa), percentage of elongation at break (E, %) and elastic modulus (EM, MPa) to be obtained. Eight samples per formulation were measured.

2.4. Microbiological analysis

2.4.1. Screening test of the antifungal natural substances

For the screening test, samples of the potentially bioactive substances were introduced in tubes with Potato Dextrose Broth-PDB (Scharlab S.L., Barcelona, Spain) at two concentrations, 1 and 10 % (ml substance/100 ml PDB). Immediately after, each tube were inoculated with the inoculum at 10^5 spores per ml for both *Aspergillus niger* and *Penicillium expansum*, previously sporulated on Potato Dextrose Agar –PDA- at 25 ºC. The inoculums' concentration was adjusted by means of a haemocytometer. As control samples, tubes without antimicrobial substance were considered. After 24 h of incubation, a count of colonies was performed in triplicate. To this end, the tube content was extended on petri dishes (Sterilin Limited, UK) with PDA (Scharlab S.L., Barcelona, Spain) and incubated for 5 days at 25 ºC.

2.4.2. Antimicrobial effectiveness of the films

In vitro analysis of the antimicrobial effectiveness of films was carried out by a method adapted from Kristo *et al*. (2008) and Sánchez-González *et al*. (2010) by using two fungus, *Aspergillus niger* and *Penicillium expansum*, and two bacterias, *Listeria innocua* as Gram+ bacteria and *Escherichia coli* as Gram-.

Bacteria were regenerated by transferring a loopful of bacteria into 10 ml of TSB and incubating at 37 ºC overnight. A 10 µL aliquot from the overnight culture was again transferred to 10 ml of TSB and grown at 37 ºC to the end of the exponential phase of growth. This culture, appropriately diluted, was then used for inoculation of the agar plates in order to obtain a target inoculums of 10^2 UFC/cm^2. Tryptone soy agar with 3% NaCl (Panreac química, S.A., Castellar del Vallés, Barcelona, Spain) was used as a model solid food system (TSA-NaCl). Aliquots of TSA-NaCl (20 g) were poured into Petri dishes. After the culture medium solidified, properly diluted overnight culture of each bacteria was inoculated on the surface.

On the other hand, fungi were inoculated on potato dextrose agar (PDA) and incubated at 25 ºC until sporulation. The cells were counted in a haemocytometer and diluted to a concentration of 10^5 spores per ml. Aliquots of PDA (20 g) were poured into Petri dishes. After the culture medium solidified, diluted spore solution of each fungus was inoculated on the surface.

The different tested films of the same diameter as the Petri dishes (containing or not antimicrobial substance) were placed on the inoculated surface. Inoculated and uncoated Petri dishes were used as control in the respective culture medium, for bacteria or fungi. Plates were then covered with parafilm to avoid dehydration and stored for 12 days at 25 ºC for fungi and 10 ºC for bacteria strains. Selected temperatures tried to simulate practical conditions of application. Microbial counts on plates were carried out

immediately after the inoculation and periodically during the storage period (0, 3, 5, 7, 10 and 12 days).

To this end, the agar was removed aseptically from Petri dishes and placed in a sterile fitter stomacher bag (Seward, West Sussex, United Kingdom) with 100 ml of tryptone phosphate water (Sharlab S.A., Barcelona, Spain). The bag was homogenized for 2 min in a Stomacher blender (Bag Mixer 400, Interscience,). Afterward serial dilutions were prepared and poured onto plates with selective microbial medium. PDA plates were used to obtain the fungus counts while a selective microbial medium was used for bacteria to obtain high selectivity and good colonies. *E. coli* was counted in Violet Red Bilis agar (Sharlab S.A., Barcelona, Spain) plates and in the case of *L. innocua* in Palcam Agar Base (Sharlab S.A., Barcelona, Spain) supplemented with Palcam Selective Supplement (Sharlab S.A., Barcelona, Spain). Then an incubation of 5 days at 25 ºC for fungi and 24 or 48 h at 37 ºC for *Listeria* or *E. coli*, respectively, was carried out. All microbial counts were performed in triplicate.

2.5. Statistical analysis

Statgraphics Centurion XV.I (Manugistics Corp., Rockville, MD) was used for carry out the statistical analysis of results through analysis of variance (ANOVA). To differentiate samples, Fisher's least significant difference (LSD) was used at the 95 % confidence level.

3. RESULTS AND DISCUSSION

3.1. Screening test: selection of antimicrobials

Table 1 shows the viable cell counts obtained for *Aspergillus niger* and *Penicillium expansum* after 24 hours in contact with the different extracts at the two different

concentrations (1 % v/v and 10 % v/v) in PDB liquid culture. Only neem oil at 10 % showed a significant antifungal effect compared with the control sample.

Table 1. Viable counts of *Aspergillus niger* and *Penicillium expansum* after 24 hours in contact with the different plant extracts (E) in PDB at 25 ºC.

E	Concentration (v/v)	*A. niger* Log(CFU/ml)	*P. expansum* Log(CFU/ml)
Control	-	4.36±0.10^{a}	4.56 ±0.09^{ab}
Echinacea extract	1%	4.35±0.16^{a}	4.7±0.4^{b}
	10%	4.44±0.12^{a}	4.60±0.10^{ab}
Horsetail extract	1%	4.64±0.07^{b}	4.64±0.02^{ab}
	10%	4.72±0.02^{b}	4.9±0.2^{c}
Liquid smoke	1%	4.53±0.05^{ab}	4.56±0.02^{a}
	10%	5.04±0.22^{c}	5.252±0.002^{d}
Neem oil	1%	4.35±0.10^{a}	4.34±0.06^{e}
	10%	0^{d}	0^{f}

$^{a, b, c, d, e,.}$different letters in the same column indicate significant differences among formulations ($p<0.05$).

The assay tubes were also subjected to a qualitative analysis after the incubation for 1 week at 25 ºC. As can be observed in Figure 1, for tubes containing different extracts, the sporulation of both fungi occurred at surface level due to the vital necessity of the oxygen for fungi growth. Only samples containing 10 % concentration of liquid smoke or neem oil at 1 and 10 % showed no fungi sporulation, regardless the fungi genera. These results partially agree with data of the viable cell counts commented on above, where only neem oil at 10 % inhibited the growth of both fungi, *A. Niger* and *P. expansum,* showing fungicidal activity after 24 h of contact. This result and those previously reported (Upadhyay *et al*., 2010; Mahfuzul Hoque *et al*., 2007; Jahan *et al*., 2007) justify the interest of neem oil extracts as active additive for obtaining of bioactive films. According to the lack of notable antifungal activity of the rest of tested extracts, active films were formulated with neem oil and with oregano essential oil with proved antimicrobial activity (Aguirre *et al*., 2013; Burt *et al*., 2004).

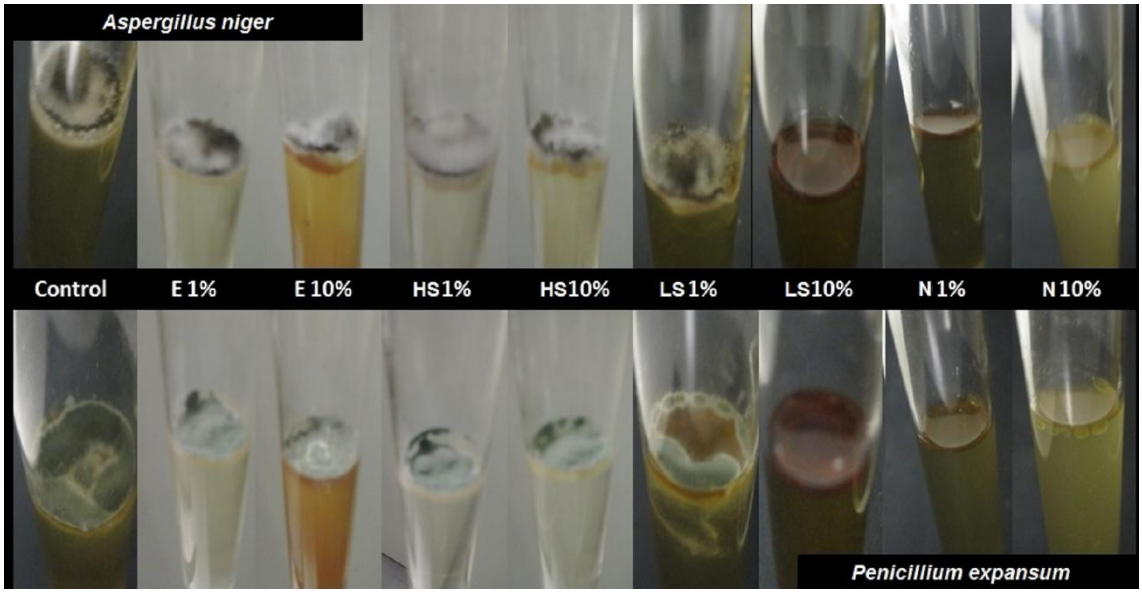

Figure 1. Photographs of natural extracts (1 and 10 %wt) in PDB broth, inoculated with both fungi, *A. niger* and *P. expansum*, incubated for one week at 25 ºC.

E: echinacea extract; HS: horsetail; LS: liquid smoke; N: neem oil.

3.2. Physical characterization of bioactive films

Uncontrolled migration of water is generally recognized as one of the biggest problems during food storage (Pavlath & Orts, 2009). Food coating or packaging can control or slow down this process if the water sensitivity and barrier capacity of packaging or coating materials are adequate. So, these properties are relevant in defining the functionality of the materials. Moisture content and water vapour permeability of the obtained films were characterized in films conditioned at 53 % RH for 1 and 5 weeks at 25 ºC and are shown in Table 2.

The moisture content of the S-PVA blend films was 6.3 and 7.9 % after 1 and 5 weeks of storage respectively, which indicates that equilibrium was not reached after 1 week. These values agree with those previously reported by Cano *et al*. (2015) for the same type of films. Films containing bioactive substances showed lower moisture contents after 1 storage week, but no notable differences were observed among water sorption capacity of the films after 5 storage weeks. This indicates that the more

hydrophobic nature of actives slow down the water sorption kinetics but did not notably modify the equilibrium values. Films with the highest content of neem oil (S-PVA-2N) reached the equilibrium value after 1 storage week. The different behaviour of the films could be related with the specific interactions between the oil components and the matrix depending on the concentration (Aguirre *et al*., 2013; Jouki *et al*., 2014). Oil components could be linked to hydroxyl groups available in starch and PVA limiting polymer–water interactions, by hydrogen bonding, thus resulting in a decrease of the film moisturizing rate (Park & Zhao, 2004).

Table 2: Moisture content (MC) and water vapour permeability (WVP) of blend control and oil composite films.

	MC (% d.b.)		WVP ($gmms^{-1}m^{-2}kPa^{-1}$)	
Films	1W	5W	1W	5W
S-PVA	6.3 ± 0.5^{a1}	7.9 ± 0.3^{a2}	4.39 ± 0.14^{ab1}	5.1 ± 0.8^{a1}
S-PVA-1O	4.4 ± 0.2^{b1}	8.3 ± 0.2^{b2}	4.6 ± 0.6^{bc1}	5.2 ± 0.5^{a1}
S-PVA-2O	4.33 ± 0.13^{b1}	7.66 ± 0.11^{a2}	4.9 ± 0.5^{c1}	4.7 ± 0.3^{ab1}
S-PVA-1N	4.5 ± 0.3^{b1}	7.0 ± 0.3^{c2}	3.7 ± 0.3^{a1}	3.6 ± 0.8^{bc1}
S-PVA-2N	6.70 ± 0.13^{a1}	6.69 ± 0.14^{d1}	4.1 ± 0.4^{ab1}	3.9 ± 0.8^{c1}

$^{a, b, c, d}$ different letter in the same column indicate significant differences among formulations ($p<0.05$).

$^{1, 2}$ different number in the same file indicate significant differences among storage time ($p<0.05$).

WVP value for S-PVA films was similar to that previously reported by Cano *et al*. (2015) for the same type of films and no significant changes occurred in this value due to the storage time. Incorporation of oils to the films did not provoke notable changes in the WVP values which were also constant during storage. So, the structural changes introduced in the polymer matrices by oils did not suppose significant changes in their water vapour barrier capacity.

The film thickness values ranged between 64 and 88 μm and were slightly influenced by the oil incorporation; no significant effect was observed for neem oil, but incorporation of oregano essential oil gave rise to slightly thicker films (83 ± 13 μm against 70 ± 14 μm for the rest of the films) despite the constant value of the solid surface concentration used (Han & Krochta, 1999). This increase in thickness can be attributed to a less compact polymer matrix due to the weakening of the interchain forces provoked by the interactions of the essential oil compounds with the polymer chains. Similar behaviour was described by Zivanovic *et al*., 2005 and Benavides *et al*., 2012 for oregano essential oil incorporated to chitosan and alginate matrices.

The gloss and transparency of the films are relevant properties of coatings, since they have a direct impact on the appearance of the coated product (Sánchez-González *et al*., 2010). Figure 2 shows the internal transmittance spectra in the visible light range (400-700 nm) of the films where the highest transparency was observed for S-PVA blend films. Films containing oils exhibited lower transparency due to the presence of a lipid dispersed phase into the polymer matrix, which promote light dispersion, as has been previously observed by several authors (Villalobos *et al*., 2005; Fabra *et al*., 2009). This behaviour has also been reported for films containing both neem and oregano oils (Sanuja *et al*., 2015; Wu *et al*., 2014; Hosseini *et al*., 2015). Table 3 shows the values of Ti at 450 nm, where the highest difference among the films was found. S-PVA films were the most transparent with Ti values around 86 % according to previous studies (Cano *et al*., 2015). Ti values decreased in line with the ratio of dispersed lipid; the higher the oil ratio the lower the film transparency, due to the promotion of light dispersion by the dispersed phase.

In general, Ti slightly decreased throughout storage time, which could be attributed to an increase in the film compactness of the polymer matrices in line with the progressive chain aggregation during storage (Cano *et al*., 2015). It is noticeable that

neem oil gave rise to more opaque films, especially in the low wave length range, which is due to contribution of the selective light absorption of neem oil components. In this sense, the addition of oils to the films improved their light barrier property.

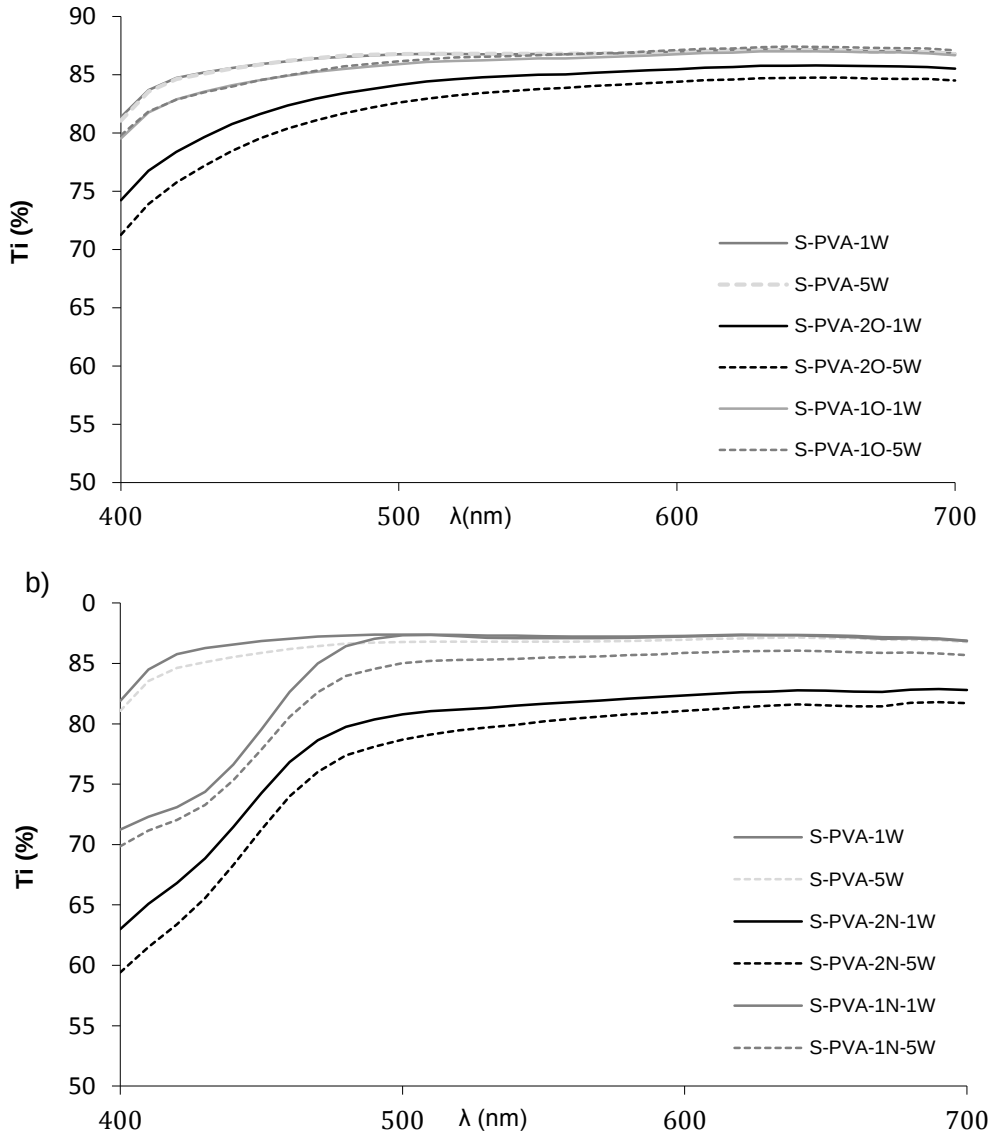

Figure 2. Internal transmittance of control and composite films: a) films containing oregano essential oil (O) and b) films containing neem oil (N) after one (1W) and five (5W) weeks of storage.

Table 3: Internal transmittance (Ti) at 450nm and gloss at 60º incidence angle of blend control and oil composite films.

	Ti - λ=450 nm (%)		Gloss (60º)	
Films	1W	5W	1W	5W
S-PVA	86.2±0.6^{a1}	85.9±0.6^{a1}	13.2±1.6^{ab1}	12.9±1.2^{a1}
S-PVA-1O	84.5±0.7^{c1}	84.5±0.7^{c1}	14.2±1.6^{a1}	13.5±0.3^{a1}
S-PVA-2O	81.6±0.2^{b1}	79.5±0.2^{b1}	12.3±1.2^{b1}	10.7±0.8^{b1}
S-PVA-1N	79.5±0.8^{e1}	77.9±0.6^{e1}	12±3^{b1}	11±3^{b1}
S-PVA-2N	74.3±0.8^{d1}	71.2±1.4^{d1}	8.5±0.9^{c1}	7. 9±0.3^{c1}

$^{a, b, c, d}$ different letter in the same column indicate significant differences among formulations ($p<0.05$).

$^{1, 2}$ different number in the same file indicate significant differences among storage time ($p<0.05$).

As concerns film gloss, Table 3 shows the values at 60º incidence angle. In general, gloss of films was significantly affected by the amount of the oil content in the matrix; the higher the content, the lower the gloss values. No significant changes ($p>0.05$) in gloss occurred during storage although a decreasing tendency was observed. Gloss is related to the surface roughness of the films (Ward & Nussinovitch, 1996; Villalobos *et al*., 2005) and, in this sense, oil incorporation usually enhance the presence of surface irregularities due to the flocculation and creaming of oil droplets during the film drying step and their accumulation on the film surface. Likewise, an excessive creaming could imply coalescence at surface level and the formation of a lipid layer at the top of the film. Exceptionally, S-PVA-1O films were glossier than other films containing oils, with values similar to the control film (S-PVA). This suggest that the oil droplets at this oil concentration are well stabilized in the film forming emulsion and no notable flocculation and creaming occurred during the film drying step.

Table 4 shows the mechanical parameters usually used to describe the film mechanical behaviour: elastic modulus (EM), tensile strength (TS) and percentage of

elongation (E) at break. This behaviour is strongly dependent on the microstructural features of the films. TS is the maximum tensile stress that the film can sustain without break, E % is the maximum change in length before breaking, and the elastic modulus (EM) quantify the film stiffness. Values of mechanical properties obtained for S-PVA films agreed with those previously found by Cano *et al*. (2015) for similar S-PVA blend films. The mechanical properties of composite films were strongly affected by the oil concentration and storage time.

Table 4: Elastic modulus (EM), tensile strength (TS) and percentage of elongation (E, %) of blend control film and oil composite films.

	EM (MPa)		TS (MPa)		E (%)	
Films	1W	5W	1W	5W	1W	5W
S-PVA	506 ± 63^{a1}	690 ± 44^{a2}	26.8 ± 1.4^{a1}	32.3 ± 1.6^{a2}	40 ± 4^{a1}	41 ± 3^{a1}
S-PVA-1O	502 ± 50^{a1}	329 ± 53^{bc2}	26 ± 2^{a1}	20.6 ± 1.5^{b2}	42 ± 11^{a1}	61 ± 9^{b2}
S-PVA-2O	271 ± 49^{b1}	355 ± 37^{b1}	4.33 ± 0.13^{b1}	7.66 ± 0.11^{c1}	4.9 ± 0.5^{b1}	4.7 ± 0.3^{c1}
S-PVA-1N	413 ± 32^{c1}	296 ± 11^{c2}	21.5 ± 1.0^{c1}	19 ± 2^{d1}	44 ± 7^{a1}	60 ± 17^{b2}
S-PVA-2N	174 ± 14^{d1}	124 ± 20^{d1}	7.2 ± 0.6^{d1}	6.8 ± 0.7^{e1}	11 ± 2^{b1}	21 ± 6^{d2}

$^{a, b, c, d}$ different letter in the same column indicate significant differences among formulations ($p<0.05$).

$^{1, 2}$ different number in the same file indicate significant differences among storage time ($p<0.05$).

In general, films containing oil showed poorer mechanical performance than control films, especially when the highest oil concentration was added: lower values of EM and mechanical resistance (TS) and, for the highest oil contents, lower extensibility. This is a typical behaviour when heterogeneities (oil droplets) are introduced in the matrix structure due to the lack of miscibility of components, thus reducing the overall cohesion forces of the polymer networks (Aguirre *et al*., 2013; Hosseini *et al*., 2015). In some cases, lipid incorporation to the polymer matrices led to an increase in the film

extensibility, when specific lipid-polymer interactions occurred with the subsequent plasticization effect which enhanced the film's stretchability (Fabra *et al*., 2010).

For films with the highest oil contents, tensile strength decreased with respect to S-PVA films in more than 75 % and the percentage of elongation at break was also dramatically reduced from 40 % to 20 or 5 %, for films containing neem oil and oregano essential oil, respectively. On the contrary, Hosseini *et al*. (2015) report an increase in the plastic deformation for fish gelatin-chitosan films when increased the content of oregano essential oil in the films.

After five storage weeks S-PVA films showed an increase the resistance to break and rigidity whilst no significant changes in their elongation capacity were observed. These changes can be attributed to the progressive increase in the matrix compactness in line with the progress of chain aggregation (Cano *et al*., 2015). On the contrary, films containing oil (except that containing the highest ratio of O) became less stiff and resistant and more stretchable. This behaviour suggests that oil components interactions with the polymer chains were progressively established, this contributing to an effective plasticization effect in the matrix and inhibiting the polymer chain aggregation. The different behaviour of films with the highest ratio of the O could be explained by an excessive oil content to be effectively entrapped in the polymer network, giving rise to a predominant effect of network weakening.

Oregano essential oil at the highest ratio imparted the poor mechanical response to the films and, in general, the better results were obtained for films containing the lowest levels of both oils (good values of rigidity and resistance and the greatest stretchability). These films exhibit similar mechanical parameters to some commercial plastics very flexible and resistant, such as those found by Cano *et al*. (2015) for low density polyethylene (LDPE) bags with similar thickness (EM = 370 MPa, TS = 27 MPa and %E = 40 %).

3.3. Antibacterial activity of composite films

Population viability of *Listeria innocua* and *Escherichia coli* in control plates and in plates coated with the different films are shown in Figure 3 and 4, respectively. For both bacteria, population increased from 2.5 to 8 logs UFC/cm^2 at the end of the storage period. No significant antimicrobial activity (about 1 log reduction) was observed for S-PVA films without oil throughout the incubation time at 10 ºC, where the bacterial growth was very similar to that of control plates (without film).

The incorporation of neem oil at both ratios, (Fig.3.b and 4.b), did not improved the antimicrobial properties of S-PVA films, even more, neem oil seems to promote the early growth of bacteria at the first storage time, showing higher population than S-PVA films. On the other hand, the incorporation of oregano essential oil at the two proportions, (Fig.3.a and 4.a), promoted antimicrobial properties in S-PVA films, showing a significant antibacterial activity since the first storage time. This effect depended on the essential oil concentration. At the highest oil concentration (S-PVA-2O) films showed bactericidal effect even just two hours after the plate coating. Meanwhile, the lowest concentration of this oil in the films (sample S-PVA-1O) only slowed down the bacterial growth throughout incubation time.

Different authors reported that films containing essential oils are more effective against Gram-positive than against Gram-negative bacteria (Aguirre *et al*., 2013; Hosseini *et al*., 2015; Martucci *et al*., 2015; Sánchez-González *et al*., 2010). However, oregano essential oil gave rise to S-PVA active films, with antibacterial and bactericidal effect specially stronger against Gram-negative bacteria, as can be observed in Figures 3.a and 4.a. Similar results were also reported by Muriel-Galet *et al*., 2015 for the oregano essential oil embedded in ethylene–vinyl alcohol copolymer (EVOH) films. This behaviour has been previously described as a specific action of the oregano essential oil compounds (Burt, 2004; Helander *et al*., 1998; Lambert *et al*., 2001). In this sense, O

main components (carvacrol and thymol) are able to disintegrate the outer membrane of Gram-negative bacteria, releasing lipopolysaccharides and increasing the permeability of the cytoplasmic membrane to ATP.

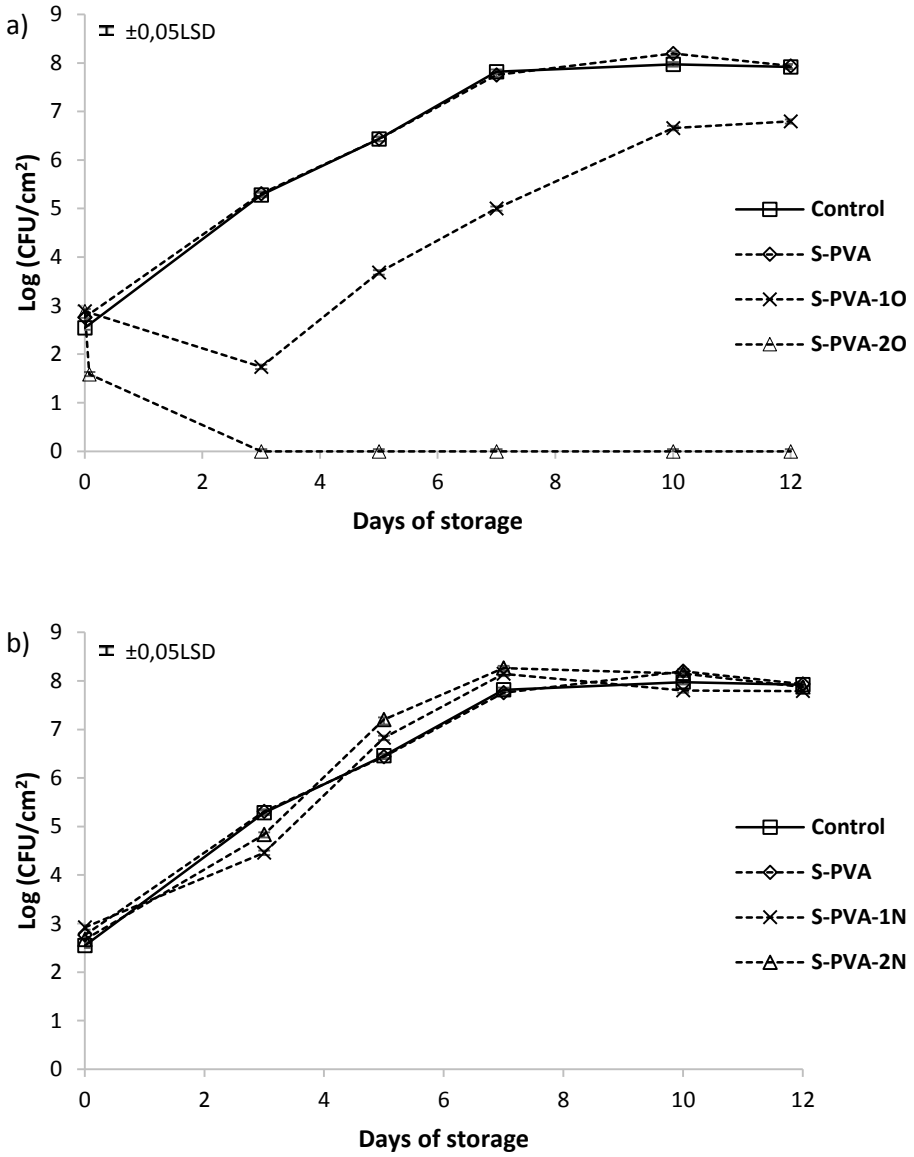

Figure 3. Population viability of *Listeria innocua* in TSA-NaCl medium at 10 ºC a) films with and without oregano essential oil (O) and b) films with and without neem oil (N). Mean values for each incubation time and 95 % LSD interval is included in the plot.

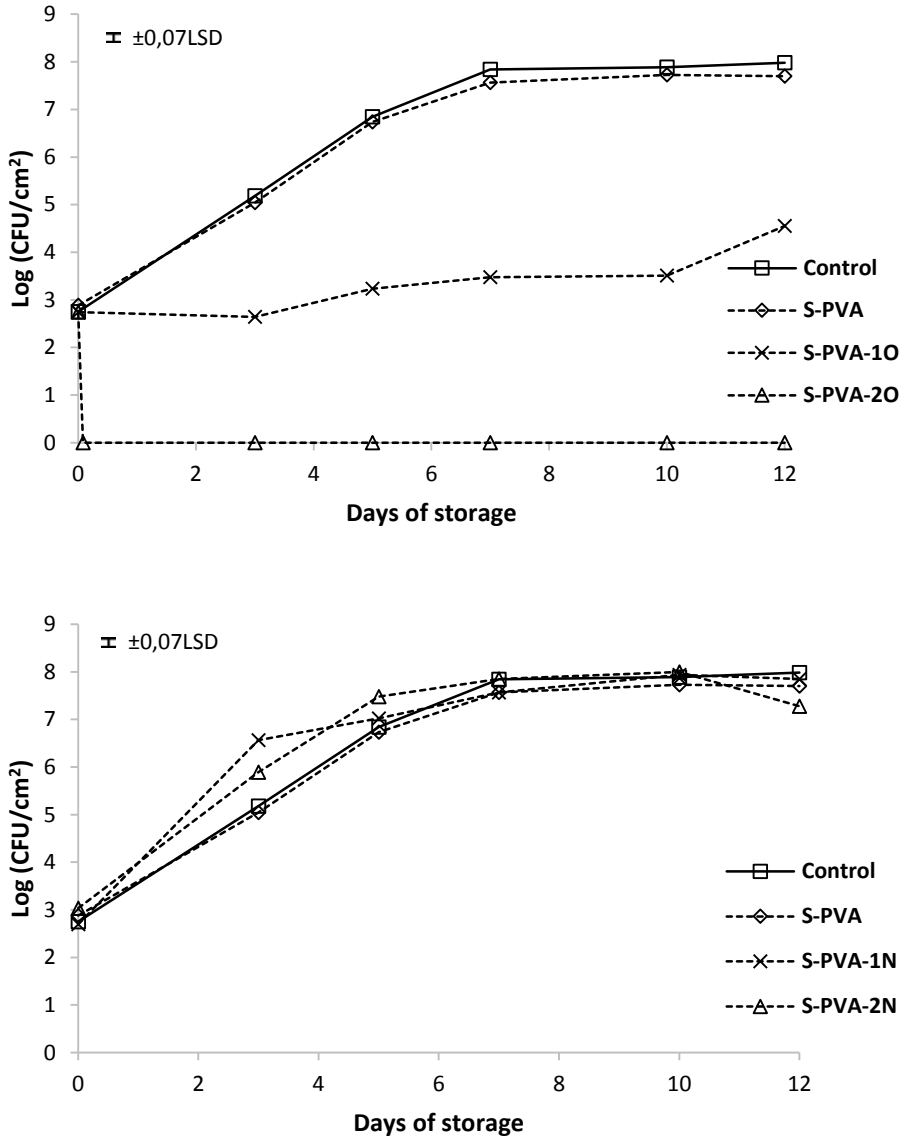

Figure 4. Population viability of *Escherichia coli* in TSA-NaCl medium at 10 ºC a) films with and without oregano essential oil (O) and b) films with and without neem oil (N). Mean values for each incubation time and 95 % LSD interval is included in the plot.

3.4. Antifungal activity of composite films

The possible antifungal effect of developed S-PVA films against *Penicillium expansum* and *Aspergillus niger* was analysed at 25 ºC. Figures 5 and 6 show the cell viability level, for 10^5 spores/ml initial population, of *P. expansum* and *A. niger*,

respectively. For both fungi, population increased from 2.5 to 6.5 log UFC/cm^2 at the end of the incubation period in all cases, except for the films containing the highest amount of oregano essential oil. Control plates (without film) and those coated with S-PVA films (without oil) showed a similar trend without antifungal activity.

The presence of oregano essential oil in the films affected the fungal growth of both fungi genera, depending on its concentration in the matrix, as previously observed by Sánchez-González *et al*., 2010 for tea tree essential oil embedded in chitosan films. At the lowest O level (S-PVA-1O), no antifungal effect was observed against *A. niger* whilst the growth of *P. expansum* was inhibited throughout the first seven incubation days (2 log reduction with respect to the control film). Nevertheless, after seven storage days no significance difference in the fungus growth with respect to the control film was observed. This behaviour could be due to the losses of active compounds throughout time, maintaining adequate concentration of actives on the agar medium surface till seven days. After this time, the low availability of the active compounds on the surface led to the growth of fungi due to the prevalent contamination (Kristo *et al*., 2008; Sánchez *et al*., 2010).

At the highest oregano oil concentration (S-PVA-2O), fungicide effect was observed just after two hours of plate coating. No growth of fungi throughout storage time was observed, thus indicating the lethal fungicidal effect of the oil components (carvacrol and thymol) in agreement with those reported by other authors (Muriel-Galet *et al*., 2015).

From the obtained results, it can be deduced that oregano essential oil is highly effective to limit the growth of gram positive and gram negative bacteria embedded in the S-PVA films, even at very low concentrations and was effective to control fungus at moderate ratios. The higher effect on the bacteria growth can be attributed to the more simply cellular wall of this microorganism as compared to the fungal cell walls.

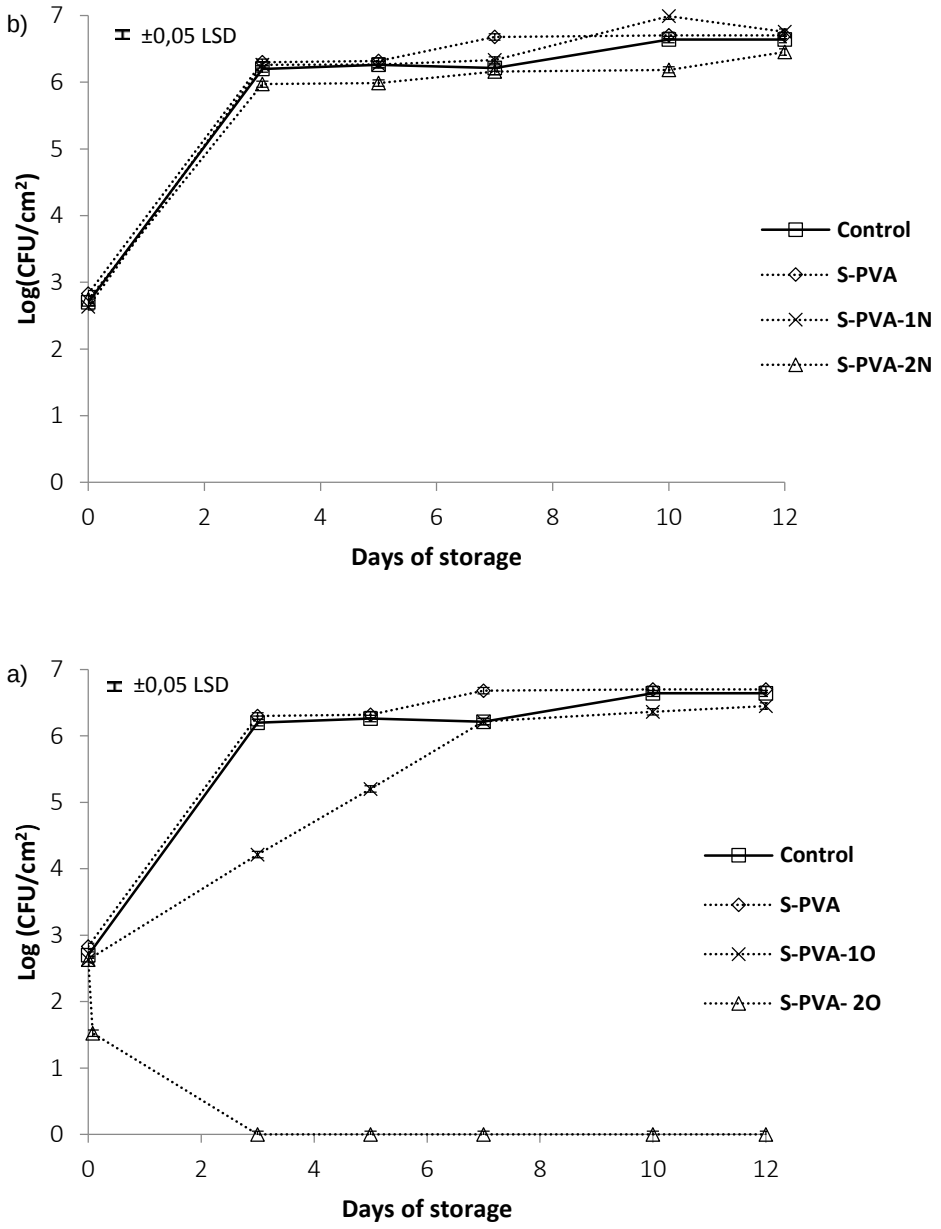

Figure 5. Population viability of *Penicillium expansum* on PDA medium incubated at 25 ºC. a) films with and without oregano essential oil (O) and b) films with and without neem oil (N). Mean values for each incubation time and 95 % LSD interval is included in the plot.

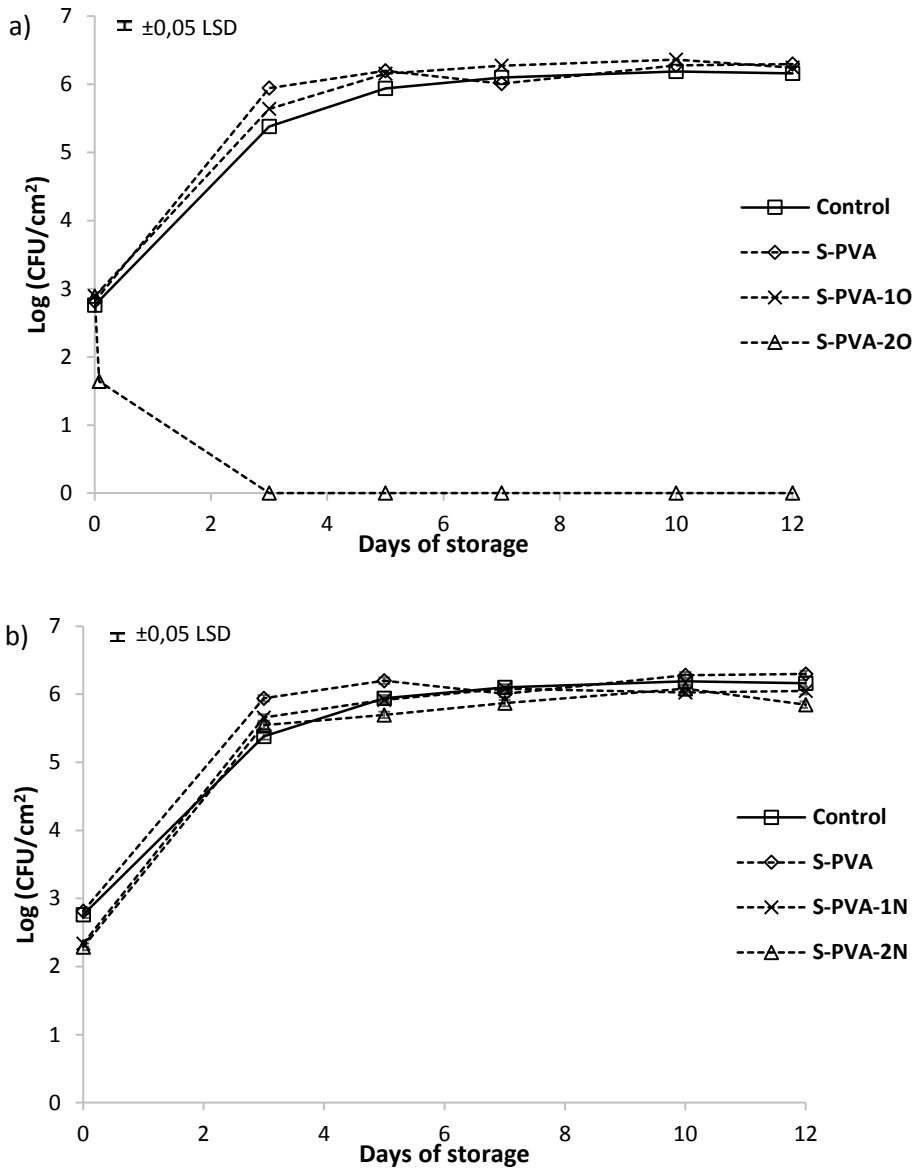

Figure 6. Population viability of *Aspergillus Niger* on PDA medium incubated at 25 ºC. a) films with and without oregano essential oil (O) and b) films with and without neem oil (N). Mean values for each incubation time and 95 % LSD interval is included in the plot.

4. CONCLUSIONS

Composite films based on starch-PVA blends, containing potentially antimicrobial oils, exhibit antibacterial (*L. innocua* and *E. coli*) and antifungal (*A. niger* and *P. expansum*) properties when they contain oregano essential oil (O), whereas active neem oil did not impart these properties to the matrix. Antibacterial activity occurred at low O

concentration (6.7 % in the dried matrix), while antifungal effect required higher doses of oil in the films. Incorporation of oils did not notably affect the water sorption capacity and water vapour barrier properties of S-PVA films, but reduced their transparency and gloss, especially at the highest concentration (22 % in the dried matrix). Mechanical performance of the S-PVA films was also modified by incorporation of oils but this was only relevant at the highest oil ratios. For the lowest oil concentration, mechanical properties of the S-PVA composites were in the range of those of some commercially available bags, becoming slightly more plasticized after 5 storage weeks. Among developed composite films, those containing 6.7 % of O exhibited the best physical properties, without significant differences with respect to the S-PVA matrix, while exhibit antibacterial activity. So, this represents a good alternative for food packaging applications.

Acknowledgements

The authors acknowledge the financial support from the Spanish Ministerio de Economía y Competitividad throughout the projects AGL2013-42989-R. Amalia Cano also thanks the Spanish Ministerio de Educación, Cultura y Deporte for the FPU grant.

References

- Aguirre, A., Borneo, R., & León, A. E. (2010). Antimicrobial, mechanical and barrier properties of triticale protein films incorporated with oregano essential oil. *Food bioscience*, *1*, 2-9.
- ASTM (1995). Standard test methods for water vapour transmission of materials. Standard Designations: E96-95 Annual Book of ASTM Standards. American Society for Testing and Materials, Philadelphia, PA, 1995, pp. 406–413.
- ASTM (1999). Standard test methods for specular gloss. Designation (D523). In Annual book of ASTM standards, 1999, vol. 06.01. American Society for Testing and Materials, Philadelphia, PA.

- ASTM (2001). Standard test method for tensile properties of thin plastic sheeting. Standard D882 Annual Book of American Standard Testing Methods. American Society for Testing and Materials, Philadelphia, PA, 2001, pp. 162–170.
- Barret, B. (2003). Medicinal properties of Echinacea: A critical review. *Phytomedicine*, 10, 66–86.
- Baswa, M., Rath, C. C., Dash, S. K., & Mishra, R. K. (2001). Antibacterial activity of Karanj (*Pongamia pinnata*) and Neem (*Azadirachta indica*) seed oil: a preliminary report. *Microbiology*, 105, 183-189.
- Benavides, S., Villalobos-Carvajal, R., & Reyes, J. E. (2012). Physical, mechanical and antibacterial properties of alginate films: Effect of the crosslinking degree and oregano essential oil concentration. *Journal of food engineering*, *110*, 232-239.
- Burt, S. (2004). Essential oils: their antimicrobial properties and potential applications in foods-a review. *International Journal of Food Microbiology*, *94*, 223-253.
- Cano, A. I., Cháfer, M., Chiralt, A., & González-Martínez, C. (2015). Physical and microstructural properties of biodegradable films based on pea starch and PVA. *Journal of Food Engineering*, 167, 59-64.
- Cho, S.Y., Lee, D.S., & Han, J.H. (2009). Antimicrobial packaging. In: Yam, K. (Ed.), Encyclopedia of Packaging Technology. Wiley Blackwell Publishing, Ames, IA, pp. 50-58.
- Corrales, M., Fernández, A., & Han, J. H. (2014). Chapter 7, Antimicrobial packaging systems. In J. H. Han (Ed.), Innovations in food packaging (second edition) (pp. 133-170). *Academia Press: San Diego*, 2014, CA, USA.
- Emiroğlu, Z. K., Yemiş, G. P., Coşkun, B. K., & Candoğan, K. (2010). Antimicrobial activity of soy edible films incorporated with thyme and oregano essential oils on fresh ground beef patties. *Meat Science*, 86, 283–288.
- EU 872/2010. Regulations commission implementing regulation EU 872/2010, adopting the list of flavouring substances, 2010.
  http://ec.europa.eu/food/food/fAEF/flavouring/flavouringsubstance_en.htm

- Fabra, M.J., Talens, P., & Chiralt, A. (2010). Water sorption isotherms and phase transitions of sodium caseinate-lipid films as affected by lipid interactions. *Food Hydrocolloids*, 24(4), 384-391.

- Fabra, M.J., Talens, P., & Chiralt, A. (2009). Microstructure and optical properties of sodium caseinate films containing oleic acid - beeswax mixtures. *Food hydrocolloids*, 23(3), 676-683.

- Farjana, A., Zerin, N., Kabir, & Md. S. (2014). Antimicrobial activity of medicinal plant leaf extracts against pathogenic bacteria. *Asian Pacific Journal of Tropical Disease*, 4(2), S920-S923.

- FDA. Title 21. Food and Drugs. Chapter I. Food and Drug Administration, department of health and human services. Subchapter B, Food for human consumption. Part 182, Substances generally recognized as safe. http://www.accessdata.fda.gov/

- García, D., Ramos, A. J., Sanchis, V., & Marín, S. (2012). Effect of *Equisetum arvense* and *Stevia rebaudiana* extracts on growth and mycotoxin production by *Aspergillus flavus* and *Fusarium verticillioides* in maize seeds as affected by water activity. *International Journal of Food Microbiology*, 153, 21–27.

- García, D., Ramos, A. J., Sanchis, V., & Marín, S. (2013). *Equisetum arvense* hydro-alcoholic extract: phenolic composition and antifungal and antimycotoxigenic effect against *Aspergillus flavus* and *Fusarium verticillioides* in stored maize. *Journal of the Science of Food and Agriculture*, 93, 2248–2253.

- Han, J. H., & Krochta, J. M. (1999). Wetting properties and water vapor permeability of whey–protein-coated paper. *Transactions of the ASAE*, *42*, 1375–1382.

- Hosseini, S.F., Rezaei, M., Zandi, M., & Farahmandghavi, F. (2015). Bio-based composite edible films containing *Origanum vulgare* L. essential oil. *Industrial Crops and Products*, *67,* 403–413.

- Helander, I.M., Alakomi, H.-L., Latva-Kala, K., Mattila-Sandholm, T., Pol, I., Smid, E.J., Orris, L.G.M., & Von Wright, A. (1998). Characterization of the action of selected essential oil

components on Gram-negative bacteria. *Journal of Agricultural and Food Chemistry*, *46*, 3590–3595.

- Hutchings, J.B. (1999). Food and Colour Appearance, second ed. Chapman and Hall Food Science Book, Aspen Publication, Gaithersburg, Maryland.

- Jahan, T., Begum, Z.A., & Sultana, S. (2007). Effect of neem oil on some pathogenic bacteria. *Bangladesh J. Pharmacol*, *2*, 71-72.

- Jouki, M., Yazdi, F.T., Mortazavi, S.A., & Koocheki, A. (2014). Quince seed mucilage films incorporated with oregano essential oil: physical, thermal, barrier, antioxidant and antibacterial properties. *Food Hydrocolloids*, *36*, 9-19.

- Kristo, E., Koutsoumanis, K.P., & Biliaderis, C.G. (2008). Thermal, mechanical and water vapor barrier properties of sodium caseinate films containing antimicrobials and their inhibitory action on Listeria monocytogenes. *Journal of Food Hydrocolloids*, *22*, 373–386.

- Lambert, R.J.W., Skandamis, P.N., Coote, P.J., & Nychas, G.-J.E. (2001). A study of the minimum inhibitory concentration and mode of action of oregano essential oil, thymol and carvacrol, *Journal of Applied Microbiology*, *91*, 453-462.

- Lanciotti, R., Gianotti, A., Patrignani, F., Belletti, N., Guerzoni, M.E., & Gardini, F. (2004). Use of natural aroma compounds to improve shelflife and safety of minimally processed fruits. *Trends in Food Science & Technology*, 15, 201–208.

- Lingbeck, J. M., Cordero, P., O'Bryan, C. A., Johnson, M. G., Ricke, S. C., & Crandall, P. G. (2014). Functionality of liquid smoke as an all-natural antimicrobial in food preservation. *Meat Science*, 97, 197-206.

- Mahfuzul Hoque, M.D., Bari, M.L., Inatsu, Y., Juneja, V.K., & Kawamoto, S. (2007). Antimbacterial activity of Guava (*Psidium guajava* L.) and Neem (*Azadirachta indica* A. Juss.). Extracts against foodborne pathogens and spoilage bacteria. *Foodborne Pathogens and Disease*, *4(4),* 481-488. doi:10.1089/fpd.2007.0040.

- Mahoney, N. & Molyneux, R. J. (2004). Phytochemical inhibition of aflatoxigenicity in *Aspergillus flavus* by constituents of walnut (*Juglans regia*). *Journal of Agriculture and Food Chemestry*, 52, 1882-1889.

- Martucci, J.F., Gende, L.B., Neira, L.M., & Ruseckaite, R.A. (2015). Oregano and lavender essential oils as antioxidant and antimicrobial additives of biogenic gelatin films. *Industrial Crops and Products*, *71*, 205–213.

- Muriel-Galet, V., Cran, M. J., Bigger, S. W., Hernández-Muñoz, P., & Gavara, R. (2015). Antioxidant and antimicrobial properties of ethylene vinyl alcohol copolymer films based on the release of oregano essential oil and green tea extract components. *Journal of Food Engineering*, 149, 9-16.

- Park, S., & Zhao, Y. (2004). Incorporation of a high concentration of mineral or vitamin into chitosan-based films. *Journal of Agricultural and Food Chemistry*, 52, 1933-1939.

- Patel, R. P., & Trivedi, B. M. (1962). The *in vitro* antibacterial activity of some medicinal oils. *Indian Journal of Medical Research*, 8, 218-222.

- Pavlath, A.E., & Orts, W. (2009). Edible films and coatings: Why, What and How?. In book Edible films and coatings for food applications. Embuscado, M.E., Huber, K.C. *Springer*, 1-23. doi:10.1007/978-0-387-92824-1.

- Pu, Z-h., Zhang, Y-q., Yin, Z-q., Xu, J., Jia, R-y., Lu, Y., & Yang, F. (2010). Antibacterial Activity of 9-Octadecanoic Acid-Hexadecanoic Acid- Tetrahydrofuran-3,4-Diyl Ester from Neem Oil. *Agricultural Sciences in China*, 9(8), 1236-1240.

- Radulovic, N., Stojanovic, G., & Palic, R. (2006). Composition and antimicrobial activity of *Equisetum arvense L*, essential oil. *Phytotherapy Research,* 20, 85-88.

- Rao, D. V. K., Singh, I., & Chopra, P. (1986). *In vitro* antibacterial activity of neem oil. *Indian Journal of Medical Research*, 6, 314-316.

- Rodrigues, E.T., & Han, J.H. (2000). Antimicrobial whey protein films against spoilage and pathogenic bacteria. IFT Annual Meeting: Book of Abstracts. Institute of Food Technologists, Chicago, IL, 191.

- Rodrigues, E.T., Han, J.H., & Holley, R.A. (2002). Optimized antimicrobial edible whey protein films against spoilage and pathogenic bacteria. IFT Annual Meeting: Book of Abstracts. Institute of Food Technologists, Chicago, IL, 252.

- Sadaka, F., Nguimjeu, C., Brachais, C-H., Vroman, I., Tighzert, L., & Couvercelle, J-P. (2014). Review on antimicrobial packaging containing essential oils and their active biomolecules. *Innovative Food Science and Emerging Technologies*, http://dx.doi.org/10.1016/j.ifset.2014.03.002.

- Saloko, S., Darmadji, P., Setiajic, B., & Pranoto, Y. (2014). Antioxidative and antimicrobial activities of liquid smoke nanocapsules using chitosan and maltodextrin and its application on tuna fish preservation. *Food Bioscience*, 7, 71-79.

- Samapundo, S., De Meulenaer, B., Osei-Nimoh, D., Lamboni, Y., Debevere, J. & Devlieghere, F. (2007). Can phenolic compounds be used for the protection of corn from fungal invasion and mycotoxin contamination during storage? *Food Microbiology*, 24, 465-473.

- Sánchez- González, L., González-Martínez, C., Chiralt, A., & Cháfer, M. (2010). Physical and antimicrobial properties of chitosan-tea tree essential oil composite films. *Journal of Food Engineering, 98*, 443–452

- Sánchez-González, L., González-Martínez, C., Chiralt, A., & Cháfer, M. (2011). Use of Essential Oils in Bioactive Edible Coatings. *Food Engineering Review*, 3, 1–16.

- Sanuja, S., Agalya, A., & Umapathy, M. J. (2015). Synthesis and characterization of zinc oxide-neem oil-chitosan bionanocomposite for food packaging application. *International Journal of Biological Macromolecules*, 74, 76–84

- Shihabudeen, M. H., Priscilla, D. H., & Thirumurugan, K. (2010). Antimicrobial activity and phytochemical analysis of selected Indian folk medicinal plants. *International Journal Pharmaceutical Science and Research*, 1, 430-434.

- Stanisavljević, I., Stojičević, S., Veličković, V., & Lazić, M. (2009). Antioxidant and Antimicrobial Activities of Echinacea (*Echinacea purpurea L.*) Extracts Obtained by Classical and Ultrasound Extraction. *Chinese Journal of Chemical Engineering*, 17(3), 478-483.

- Upadhyay, R.K., Dwivedi, P., & Ahmad, S. (2010). Screening of antibacterial activity of six plant essential oils against pathogenic bacterial strains. *Asian J. Med. Sci., 2(3),* 152-158. ISSN: 2040-8773.

- Utama, I. M. S., Willis, R. B. H., Ben-Yehoshua, S., & Kuek, C. (2002). In vitro efficacy of plant volatiles for inhibiting the growth of fruit and vegetable decay microorganisms. *Journal of Agricultural and Food Chemistry*, 50, 6371–6377.

- Vanka, A., Tandon, S., Rao, S. R., Udupa, N., & Ramkumar, P. (2001). The effect of indigenous Neem (*Adirachtaindica*) mouth wash on *Streptococcus mutans* and *lactobacilli* growth. *Indian Journal of Dental Research*, 12, 133-144.

- Villalobos, R., Chanona, J., Hernández, P., Gutiérrez, G., & Chiralt, A. (2005). Gloss and transparency of hydroxypropyl methylcellulose films containing surfactants as affected by their microstructure. *Food Hydrocolloids*, *19*, 53–61

- Ward, G., & Nussinovitch, A. (1996). Gloss properties and surface morphology relationships of fruits. *Journal of Food Science*, 61 (5), 973-977.

- Wu, J., Ge, S., Liu, H., Wang, S., Chen, S., Wang, J., Li, J., & Zhang, Q. (2014). Properties and antimicrobial activity of silver carp (Hypophthalmichthys molitrix) skin gelatin-chitosan films incorporated with oregano essential oil for fish preservation. *Food packaging and shelf life*, 2, 7-16.

- Xu, J., Du, Y. H., Yin, Z. Q., Li, X. T., Jia, R. Y., Wang, K. Y., Lv, C., Fan, Q. J., Ye, G., & Geng, Y., *et al*. (2010). The preparation of neem oil microemulsion (*Azadirachta indica*) and the comparison of acaricidal time between neem oil microemulsion and other formulations *in vitro*. *Veterinary Parasitology*, 164 (3-4), 399-403.

- Zinanovic, S., Chi, S., & Draughon, A.F. (2005). Antimicrobial activity of Chitosan films enriched with essential oils. *Journal of Food Science*, *70 (1)*, M45–M51.

Amalia I. Cano, Maite Cháfer, Amparo Chiralt, Chelo González-Martínez. **Development and characterization of active films based on starch-PVA, containing silver nanoparticles.**

Abstract

In order to obtain antimicrobial packaging films, starch-PVA-based films with silver nanoparticles (AgNPs) have been developed and characterized as to their physical and antimicrobial properties and silver release kinetics to polar (A, B, C and D1) and non-polar (D2) food simulants. Antimicrobial activity against two bacteria, *Listeria innocua* and *Escherichia coli,* and two fungi, *Aspergillus niger* and *Penicillium expansum,* was studied. Silver-loaded starch-PVA films exhibited antimicrobial activity against the tested microorganisms, which depended heavily on the concentration of AgNPs. Their addition only led to notable physical changes in the colour and transparency of the films, which underwent significant changes and turned brownish-yellow and opaque, this being more notable when the silver concentration rose. Silver was released into aqueous simulants in its entirety within the first 60 minutes of contact. In the non-polar simulant (oleic acid), the release capacity of the films drastically decreased, being the only case where the established limit (60 mg/Kg simulant) was met. As a consequence, the use of the developed films as food packaging materials should be restricted to fat-rich foodstuffs.

Key words: antimicrobial activity, release kinetics, mechanical properties, optical properties.

1. INTRODUCTION

About one third of the food produced for human consumption is lost or wasted worldwide, this being approximately 1,300 million tonnes per year (FAO, 2011). These losses take place along the food supply chain due to physical, chemical and biological factors. For example, as a result of microbial growth, off-odors and changes in the aroma, color, and texture can be accelerated. Additionally, some microorganisms and their toxins may cause food recalls and serious foodborne outbreaks (Corrales *et al*., 2014).

The considerable pressure placed on achieving a reduction in these losses has increased the interest in developing new packaging materials which lead to the retardation of deterioration, the extension of the shelf-life, and the quality maintenance of the foodstuff. The incorporation of natural active substances in film matrices is a current alternative means of preventing food spoilage (Lanciotti *et al*., 2004).

Heavy metals from mineral sources have been used in the form of salts, oxides, and colloids for thousands of years because of their antimicrobial properties. . These metals can be incorporated into food-contact polymers to enhance the mechanical and barrier properties and to extend food shelf life (Pal *et al*., 2007). Of the metals, silver exhibits a higher degree of toxicity to microorganisms while being less toxic to mammalian cells in minute concentrations (Rai *et al*., 2009). Silver has strong inhibitory or bactericidal effects for a broad spectrum of bacteria, fungi, and viruses (Ghosh *et al*., 2010; Mohanty *et al*., 2012; Li *et al*., 2010). Moreover, its high thermal stability, low volatility and cost of production are remarkable (Duran *et al*., 2007, Martínez-Abad, 2014b).

Silver in its metallic state is an inert material, but it can react with the environmental moisture to provide silver ions. The catalytic oxidation of metallic silver and the reaction with dissolved monovalent silver ion probably contribute to the bactericidal effect. (Martínez-Abad, 2014a; Pal *et al*., 2007; Rai *et al*., 2009). In spite of that, the exact mechanism of the action of silver species is not well known. Some studies describe it as

based on the morphological and structural changes found in the bacterial cells (Rai *et al*., 2009). The mechanism of action of metallic silver, silver ions and silver nanoparticles (AgNPs) is linked with its interaction with the thiol group (-SH) compounds found in the respiratory enzymes of bacterial cells. For example, the interactions of silver with L-Cysteine residues cause the denaturation and loss of enzymatic functions (Feng *et al*., 2000; Martínez-Abad, 2014b; Liau *et al*., 1997). The mode of antibacterial action of AgNPs is probably similar to that of silver ions (Mohanty *et al*., 2010) and different authors report that the antimicrobial effect of silver nanoparticles depends on their size and shape (Ghosh *et al*., 2010; Rai *et al*., 2009; Raimondi *et al*., 2005).

Wet chemical reduction is the most frequently applied method for the synthesis of AgNPs. For the chemical synthesis, the use of different radiation sources and/or a combination of different strong reducing agents have been applied in the presence of stabilizers in order to prevent the unwanted agglomeration of the colloidal forms (Mohanty *et al*., 2012; Neto *et al*., 2008). Most of these methods, which make use of strong reducers, lead to environmental toxicity risks. As an alternative, the green synthesis of AgNPs has been developed, which involves the selection of a solvent medium and environmentally-friendly reducing agents and stabilizers (Raveendran *et al*., 2003; Sharma *et al*., 2009). Some authors followed these steps by using sunlight or UV radiation (Pourjavadi & Soleyman, 2011; Vimala *et al*., 2011), reducing biopolymers such as poly(vinyl alcohol) (Bryaskova *et al*., 2010), poly(vynil pyrrolidone) (Morales *et al*., 2009), gelatin (Durroudi *et al*., 2011; Pourjavadi & Soleyman, 2011), starch (Torres-Castro *et al*.,2011), poly(ethylene glycol) (Vimala *et al*., 2010), or even plant extracts (Mohapatra *et al*., 2015; Roy *et al*., 2015). The preparation of nanoparticles within biopolymers provides several advantages due to the fact that macromolecular chains possess a large number of hydroxyl groups that can complex the metal ion, thus enabling a good control of the size, shape and dispersion of nanoparticles, increasing

biocompatibility and biodegradability, and giving rise to species that are less toxic to mammalian cells (Mohanty *et al*., 2010).

The Food and Drug Administration/Centre for Food Safety and Applied Nutrition (FDA/ CFSAN – USA) accepted the use of silver nitrate as a food additive in bottled water and silver zeolites for use in all types of food-contact polymers (FDA, 2007), while in the European Regulation silver is accepted under 94/36/EC Directive as a colouring agent (E-174) with no restrictions. Silver is one of the most widely used antimicrobial additives in polymer films for food packaging applications (Martínez-Abad *et al*., 2012). This approach has been tested on a wide variety of biopolymer matrices including hydroxyl propyl methyl cellulose (de Moura *et al*., 2012), agar (Ghos *et al*., 2010; Rhim *et al*., 2013), (poly)vinyl alcohol (Bryskova *et al*., 2010; Sedlarik, *et al*., 2009), gelatin (Kanmani *et al*., 2014) or blends such as chitosan-cellulose (Lin *et al*., 2015), starch-clay (Abreu *et al*., 2015) or chitosan-PVA-Glutaraldehide (Vimala *et al*., 2011).

Previous studies revealed that blend films based on starch-PVA presented several advantages over pure starch films. The incorporation of PVA into gelatinized starch matrices implied the formation of interpenetrated polymer networks with beneficial effects on the mechanical and water barrier properties of the films, these becoming much more extensible and stable during storage (Cano *et al*., 2015). These results suggest that starch-PVA-based films could be a proper alternative for the development of active films containing silver nanoparticles. These silver particles might be able to improve the physical properties of films and to control the food spoilage.

In the development of silver-loaded films, knowledge of the release kinetics of the active compound is needed in order to ensure that it complies with the current legislation for food packaging materials (EU n. 10/2011 commission 14 January 2011), while assuring antimicrobial effectiveness.

The aim of the work was to develop active starch-PVA-based films which are able to deliver silver species. In this sense, the release kinetics of silver from starch-PVA films to different food simulants as well as their physical properties and antimicrobial activity against two bacteria *Listeria innocua* and *Escherichia coli* and two fungi, *Aspergillus niger* and *Penicillium expansum* were studied.

2. MATERIALS AND METHODS

2.1. Materials

Pea starch (S) was purchased from Roquette Laisa España S.A. (Benifaió, Valencia, Spain), poly(vinyl alcohol) (PVA)(M_w: 89,000-98,000, degree of hydrolysis > 99 %, and viscosity: 11.6-15.4cP) and silver nitrate ($AgNO_3$) were obtained from Sigma Aldrich Química S.L. (Madrid, Spain) and glycerol, magnesium nitrate-6-hydrate ($Mg(NO_3)_2$), ethanol, 98% glacial acetic acid and oleic acid were provided by Panreac Química S.A. (Castellar de Vallès, Barcelona, Spain).

2.2. Preparation of film forming dispersions

Films were obtained by means of the solvent casting procedure after the preparation of film forming dispersions (FFDs) following the methodology described by Cano et al. (2015). Starch (2% w/w) was dispersed in an aqueous solution at 95 ºC for 30 min, while being stirred, to induce starch gelatinization. Thereafter, the dispersion was homogenized using a rotor-stator homogenizer (Ultraturrax D125, Janke and Kunkel, Germany) at 13,500 rpm for 1 min and 20,500 rpm for 3 min. Afterwards, PVA was incorporated into the previously gelatinized starch dispersion in a S:PVA ratio of 2:1 and the dispersion was maintained at 90 ºC for 30 min under stirring. Finally, glycerol was added at a starch:glycerol ratio of 1:0.25, on the basis of previous studies (Jiménez et al., 2012).

Starch-PVA film forming dispersions containing silver nanoparticles were obtained by the reduction of silver nitrate salts using UV light (Monge, 2009) in the starch-PVA dispersion itself, taking advantage of the stabilizing properties of the polymers (Torres-Castro et al., 2011). The synthesis can be summarized as follows: different amounts of 40 mM $AgNO_3$ were added to the previously described starch-PVA dispersions so as to obtain different S:$AgNO_3$ ratios: 1:0.006, 1:0.06, 1: 0.16 and 1:0.32. Each mixture was maintained at 90 ºC for 30 min under stirring and UV radiation till the dispersion turned brown due to the formation of AgNPs. Finally, glycerol was also added in the same ratio as in the control film. The reduction of silver nitrate into an AgNPs formation was monitored by using a DU 730 spectrophotometer (Thermo Scientific, England) at 420 nm.

2.3. Films formation

From the above described silver starch-PVA dispersions, dried films were obtained by means of the casting method. Newly obtained dispersions were poured into a Teflon plate at a surface density of solids of 85 g m^{-2}. For antimicrobial tests, films were casted into Petri dishes, by using the same amount of the film-forming dispersion. Films were dried at 22 ºC and 45 % HR for 48 h and afterwards, peeled off the casting surface. They were conditioned at 25 ºC and 53 %RH in a chamber using a $Mg(NO_3)_2$ saturated solution until further analysis. The film thickness was measured at six random positions with a Palmer digital micrometer to the nearest 0.0025 mm, reaching values of between 0.058 and 0.067 mm. The control film (S-PVA) and four silver-loaded films were obtained with the increasing amounts of $AgNO_3$ (S-PVA1, S-PVA2, S-PVA3, S-PVA4). All the films were analyzed after one or five storage weeks, according to previous studies (Cano et al., 2014). For antimicrobial analysis and release studies, the films were only conditioned for one week.

2.4. Characterization of composite films

2.4.1. Moisture content

Moisture content (MC) was evaluated by drying. Firstly, the film samples were dried in a vacuum oven at 60 ºC for 24 h. Later on, the pre-dried samples were placed in desiccators containing P_2O_5 until reaching a constant weight. Five replicates per film formulation were analysed.

2.4.2. Water vapour permeability

Water vapour permeability (WVP) was evaluated in films equilibrated by following the gravimetric method, ASTM E96-95 (ASTM, 1995), using Payne permeability cups (Payne, elcometer SPRL, Hermelle/sd Argenteau, Belgium) of 3.5 cm diameter. Deionised water was used inside the testing cup to achieve 100 % RH on one side of the film, while an oversaturated magnesium nitrate solution was used to control the RH on the other side of the film. A fan placed on the top of the cup was used to reduce resistance to water vapour transport. Four replicates of each type of films were analysed at 25 ºC. The water vapour transmission (WVTR) was determined from the slope obtained from the regression analysis of weight loss data *vs* time, once the steady state had been reached, divided by the film areas.

2.4.3. Mechanical properties

Mechanical properties were measured using a Universal Test Machine (TA.XT plus, Stable Micro Systems, Haslemere, England) following the ASTM standard method D882 (ASTM, 2001). Equilibrated film specimens (2.5 cm wide and 10 cm long) were mounted in the film-extension grips (A/TG model) which were set 50 mm apart. The speed of the testing machine during stretching was 50 mm min^{-1} until breaking. Force-distance curves were obtained and transformed into Stress-Hencky curves which allowed tensile strength

at break (TS, MPa), percentage of elongation at break (E, %) and elastic modulus (EM, MPa) to be obtained. Eight replicates were carried out per formulation.

2.4.4. Optical properties

The CIE-L*a*b* coordinates and internal transmittance (Ti) of the films was quantified by means of the reflection spectrum on the white and black background from 400 to 700 nm with a MINOLTA spectrocolorimeter CM.36000d (Minolta Co. Tokyo, Japan) with a 30 mm illuminated sample area, using D65 illuminant/ 10 º observer. Measurements were taken on the side of film which was in contact with air during drying and each formulation was analyzed in triplicate. Ti was calculated applying the Kubelka–Munk theory for multiple scattering to the reflection spectra, following the methodology described by Cano, et al. (2014).

2.4.5. Thermogravimetric analysis (TGA)

A thermogravimetric analyzer (Mettler Toledo, Switzerland) was used to obtain the thermal weight loss (TG) curve, and its derivative (DTG), of the samples. To this end, approximately 10 g of sample were poured into an alumina crucible and heated from 25 ºC to 600 ºC at 10 ºC/min, using nitrogen flow. The onset, peak and end temperatures (T0, Tp and Te, respectively) were obtained for each degradation step in the films. The measurements were taken in duplicate for each film.

2.4.6. Kinetics of silver release

The kinetic studies of silver release were carried out by following current legislation (Commission Regulation EU 10/2011). Rectangular film strips of 12 cm^2 total area were immersed in a glass tube with 20 mL of food simulants: simulant A (ethanol 10 % (v/v)), simulant B (acetic acid (3 % (w/v)), simulant C (ethanol 20 % (v/v)), simulant D1 (ethanol 50 % (v/v)) and simulant D2 (oleic acid as a vegetal oil), following the established

relationship of 6 dm^2 kg^{-1}. Samples were kept at 20 ºC for 7 days. Simulant samples were removed at different times and the released silver was quantified by atomic absorption spectroscopy, Analyst 100 (Perkin Elmer, Madrid, Spain). Before the injection, 5 ml of simulant were properly diluted in distilled water in the case of simulants A, B, C and D1 and in ethanol in the case of simulant D2. The Ag concentrations, expressed as mg kg^{-1} of simulant, were determined from the absorbance values by using a standard curve for $AgNO_3$ solutions. Two replicates per film formulation were performed. Finally, release kinetics were modelled using the Peleg equation (Eq. 1) (Peleg, 1988), determining the k_1, k_2 and V_{eq} values for each experimental series.

$$\frac{t}{(M_t - M_0)} = k_1 + k_2 t \quad (1)$$

where M_0 and M_t (mg Kg^{-1}) are the concentrations of Ag in the simulant at initial and t (h) times, respectively, k_1 is the Peleg constant rate and k_2 is the Peleg constant capacity. k_2 is also related to the release at $t \rightarrow \infty$ (Eq. 2):

$$V_{eq} = M_0 + \frac{1}{k_2} \quad (2)$$

2.4.7. Microbial analysis

The antimicrobial effectiveness of films was analysed by a method adapted from Kristo *et al.* (2008) and Sánchez-González *et al.* (2010). Stock cultures of *Escherichia Coli* (CECT 515), *Listeria. Innocua* (CECT 910) and *Asperguillus Niger* (CECT 20156), supplied by Colección Española de Cultivos Tipos (CECT, Burjassot, Spain), were kept frozen (-25ºC) in Tryptone Soy Broth (TSB, Scharlab, Barcelona, Spain), for bacteria, and Potato Dextrose Broth (Scharlab, Barcelona, Spain), for fungi, supplemented with 30% glycerol.The Department of Biotechnology (Universitat Politècnica de València, Valencia, Spain) provided *Penicillium expansum* from their culture collection.

Bacteria were regenerated by transferring a loopful of bacteria into 10 ml of TSB and incubating them at 37 ºC overnight. A 10 µl aliquot from the overnight culture was again transferred to 10 ml of TSB and grown at 37 ºC to the end of the exponential phase of growth. This culture, appropriately diluted, was then used for the inoculation of the agar plates in order to obtain a target inoculum of 10^2 UFC/cm^2. Tryptone soy agar with 3 % NaCl (Panreac química, S.A., Castellar del Vallés, Barcelona, Spain) was used as a model solid food system (TSA-NaCl). Aliquots of TSA-NaCl (20 g) were poured into Petri dishes. After the culture medium solidified, a properly diluted overnight culture was inoculated on the surface.

On the other hand, fungi were inoculated on potato dextrose agar (PDA) and incubated at 25 ºC until sporulation. The cells were counted in a hemocytometer and diluted to a concentration of 10^5 spores/ml. Aliquots of PDA (20 g) were poured into Petri dishes. After the culture medium solidified, a diluted spore solution was inoculated on the surface.

Films of the same diameter as the Petri dishes (containing or not an antimicrobial substance) were placed on the inoculated surfaces. Non-coated inoculated TSA-NaCl and PDA Petri dishes were used as controls. Plates were then covered with para-film to avoid dehydration and stored for 12 days at 25 ºC and 10 ºC, for fungi and bacteria strains, respectively. The microbial counts on the TSA-NaCl and PDA plates were examined immediately after the inoculation and periodically throughout the storage period (0-3-5-7-10-12 days). To this end, the agar was removed aseptically from Petri dishes and placed in a sterile fitter stomacher bag (Seward, West Sussex, United Kingdom) with 100 ml of tryptone phosphate water (Sharlab S.A., Barcelona, Spain). The bag was homogenized for 2 min in a Stomacher blender (Bag Mixer 400, Seward, UK). Afterwards, serial dilutions were made and then poured onto plates for incubation, for 5 days at 25 ºC and for 24 - 48 h at 37 ºC, for fungus and bacteria respectively, before

colonies were counted. PDA plates were used to obtain the fungus counts while a selective microbial medium was used for bacteria to obtain a high degree of selectivity and good colonies. *E. coli* was counted in Violet Red Bilis agar (Sharlab S.A., Barcelona, Spain) plates and *L. Innocua* in Palcam Agar Base (Sharlab S.A., Barcelona, Spain) supplemented with Palcam Selective Supplement (Sharlab S.A., Barcelona, Spain). All the tests were performed in triplicate.

2.5. Statistical analysis

Statgraphics Centurion XV.I (Manugistics Corp., Rockville, MD) was used to carry out the statistical analysis of the results through an analysis of variance (ANOVA). To differentiate the samples, Fisher's least significant difference (LSD) was used at the 95 % confidence level.

3. RESULTS AND DISCUSSION

3.1. Physical properties of films

Table1 shows the elasticity modulus (EM), tensile strength and elongation values at the break point of the films after the two different storage times (one and five weeks) under controlled conditions. Control films (S-PVA) exhibited mechanical behaviour that was halfway between what was observed in the pure pea starch and pure PVA films (Cano *et al.,* 2015).

As can be observed, EM and tensile strength values were enhanced at low concentrations of silver (S-PVA-1 and S-PVA-2), afterwards decreasing as the silver concentration rose while the films became significantly more stretchable at the highest silver concentration. Several authors also obtained similar results, which were attributed to the adsorption of silver to the polymer chains, in line with the van der Waals interactions between the hydroxyl groups of PLA/starch and the partial positive charge

on the surface of the silver nanoparticles (Rhim *et al*., 2013; Shameli *et al*., 2010). The contrasting behaviour of EM and TS induced by AgNPs from a determined concentration level upwards could be attributed to an oversaturation effect of the polymer network active points for silver adsorption, which leads to a plasticizing effect of silver species in the matrix. In this sense, it is remarkable that the increase in the ionic strength in the aqueous media when the concentration of silver nitrate increases, implies a reduction of the free-volume of macromolecules before the film formation which will affect the chain extension and aggregation level during the film formation step. This effect will reduce the intermolecular forces among polymeric chains, giving rise to weaker films.

Table 1: Elastic modulus (EM), tensile strength at break (TS) and percentage of elongation at break (E, %) of S-PVA and silver composite films after 1 (1W) and 5 (5W) storage weeks. Mean values and standard deviation.

	EM (MPa)		TS (MPa)		E (%)	
Film	1W	5W	1W	5W	1W	5W
S-PVA	506 ± 63^{a1}	690 ± 44^{a2}	26.8 ± 1.4^{ab1}	32.3 ± 1.6^{a2}	40 ± 4^{ab1}	41 ± 3^{a1}
S-PVA-1	638 ± 38^{b1}	552 ± 58^{b2}	29 ± 3^{bc1}	32 ± 3^{a1}	37 ± 8^{ab1}	$47\pm9a^{b2}$
S-PVA-2	771 ± 42^{b1}	652 ± 34^{a2}	30.7 ± 1.6^{c1}	30.2 ± 1.6^{a1}	33 ± 4^{a1}	42 ± 7^{a2}
S-PVA-3	518 ± 65^{a1}	542 ± 56^{b1}	25.3 ± 1.3^{a1}	30 ± 3^{a2}	41 ± 6^{b1}	50 ± 7^{b2}
S-PVA-4	229 ± 34^{c1}	262 ± 45^{c1}	18.3 ± 1.4^{d1}	22 ± 3^{b2}	53 ± 5^{c1}	54 ± 5^{b1}

$^{a, b, c, d}$ different letters in the same column indicate significant differences among formulations ($p<0.05$).

$^{1, 2}$ different numbers in the same row indicate significant differences between storage times ($p<0.05$).

Thermogravimetric analysis also revealed a decrease in polymer attraction forces when the silver concentration increased. Table 2 shows the onset, peak and end temperatures of the different degradation steps observed for the S-PVA films deduced from the DGTA curves (Figure 1). Previous studies reported the polymer separation in PVA-S blend films (Cano *et al*., 2015) and, coherently, each polymer degraded

independently. The first step was attributed to the starch degradation according to previously reported data (Cano *et al*., 2015), and the second and third steps to the PVA thermodegradation, as deduced from other authors: a main degradation stage followed by a final decomposition of the previously formed compounds (Bonilla *et al*., 2014). The addition of the silver compound significantly reduced the thermal stability of the starch and PVA fractions in the film. Nevertheless, whereas the degradation temperature of the starch phase decreased as the silver concentration rose, the same temperature values were observed for PVA degradation regardless of the silver content. The disappearance of the second PVA degradation step was observed from the lowest concentration level of silver. This suggests that Ag interacted to a different extent with the starch and PVA fractions in the film, but in both cases, the chain extension and bonds in the film network were notably affected by the presence of silver (and other ions: NO_3^-) in the system.

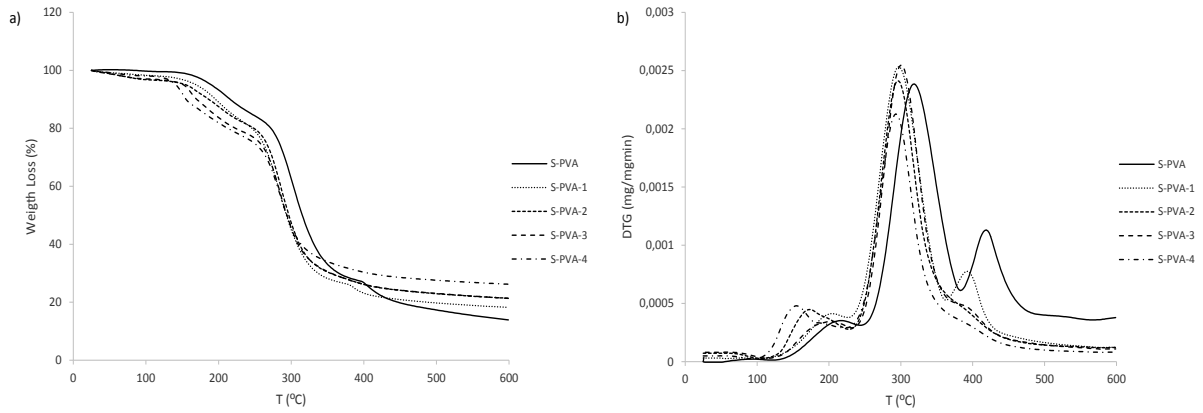

Figure 1. TG (a) and DTG (b) curves obtained from TGA of S-PVA and silver-loaded composite films.

Table 2. Onset, peak, end temperatures (T_o, T_p, T_e respectively) and residual mass (RM) obtained from TGA analysis. Mean values and standard deviation.

	First degradation (S)			Second degradation (PVA)			Third degradation (PVA)			RM 600 ºC (%)
Films	T_0	T_p	T_e	T_0	T_p	T_e	T_0	T_p	T_e	
S-PVA	163±12^{a}	210±7^{ab}	244±3^{a}	262.3±1.6^{a1}	305.3±0.7^{a1}	357.4±1,7^{a1}	387,8±1,7^{a1}	417±2^{a1}	447±3^{a1}	13.7±0.3^{a1}
S-PVA-1	153.36±1.14^{ab}	193.5±0.7^{c}	225.7±0.9^{ab}	243.8±0.4^{b1}	286.8±0.8^{b1}	338.7±1.3^{b1}	369±5^{b1}	396±5^{c1}	421±5^{b1}	17.0±1.7^{ab1}
S-PVA-2	135±3^{bcd}	181.9±0.8^{d}	227,8±1.5^{ab}	246.9±0.9^{b1}	287±2^{b1}	333±5^{b1}				21.21±0.09^{ab1}
S-PVA-3	133.4±0.9^{cd}	169.6±0.4^{e}	216.83±1.15^{ab}	246.1±0.2^{b1}	287.3±0.4^{b1}	332±3^{b1}				21.25±0.14^{ab1}
S-PVA-4	119.5±1.9^{d}	154±5^{b}	196±8^{b}	245.0±0.2^{b1}	286.5±0.9^{b1}	330.1±1.4^{b1}				25±1^{b1}

$^{a, b, c,}$ different letters in the same column indicate significant differences among formulations at the same time of the analysis (0 or 73 says) ($p<0.05$).

The moisture content of the films (Table 3) was not significantly affected either by the incorporation of $AgNO_3$ or by the storage time, which indicates that the equilibrium moisture content was reached after 1 storage week. Likewise, there were no remarkable differences between the WVP values (Table 3) as a consequence of silver addition. However, these values tended to decrease when low amounts of silver were added, afterwards rising when the concentration increased. This could be related with the structural differences in the polymer matrix, commented on above, referring to the different chain arrangement as a function of the initial ionic strength in the aqueous media and molecular interactions with the silver species. At a low silver concentration, macromolecular chains would be more extended with linked silver species, which will lead to an increase in the tortuosity factor for the diffusion of the water molecules (Cussler *et al*., 1998; Rhim *et al*., 2013). On the contrary, higher amounts of silver will inhibit the extension of macromolecules in the aqueous media, giving rise to a less compact film structure, where water molecules can be transferred more quickly.

Table 3: Mositure content (MC) and water vapour permeability (WVP) of S-PVA and silver composite films after 1 (1W) and 5 (5W) storage weeks. Mean values and standard deviation.

	MC (% d.b.)		WVP(g-mmh^{-1}m^{-2}kPa^{-1})	
Film	5W	5W	1W	5W
S-PVA	8.2±0.3^{a1}	7.1±1.7^{ab1}	5.09±1.17^{a1}	5.1±0.4^{bc1}
S-PVA-1	6.8±1.5^{a1}	6.4±1.9^{ab1}	4.6±0.4^{ab1}	4.6±0.5^{ab1}
S-PVA-2	6.5±1.1^{a1}	5.1±0.5^{a1}	3.8±0.2^{b1}	4.04±0.27^{a1}
S-PVA-3	7.2±1.2^{a1}	8±0.9^{b1}	5.2±0.5^{ac1}	5.4±0.7^{c1}
S-PVA-4	7.6±1.3^{a1}	7.1±1.3^{ab1}	6.1±0.4^{c1}	6.4±0.4^{d1}

$^{a, b, c, d}$ different letters in the same column indicate significant differences among formulations ($p<0.05$).

$^{1, 2}$ different numbers in the same row indicate significant differences between storage times ($p<0.05$).

The optical properties of the films were analysed in terms of internal transmittance at 450 nm (Ti) , as a measure of the transparency of the films, and by means of clarity (L*), hue (h*) and chrome (C*) , which are shown in Table 4. While the control starch-PVA films were colourless and transparent, the films loaded with silver particles turned from pale brown to dark brown, depending on the $AgNO_3$ concentration. In Table 4, a significant ($p<0.05$) reduction in the values of transparency (Ti), luminosity (L*) and hue (h*) of silver-loaded films can be observed, while the colour saturation (C*) increased. This is due to the silver reduction forming the silver nanoparticles (AgNPs), which generates a yellow to brownish colour, attributed to the characteristic surface plasmon resonance of AgNPs (Puiso *et al.*, 2008; Zeng *et al*., 2001). A colour analysis of the films can consequently be an efficient and easy tool with which to monitor the reduction process.

The extent of the changes in the optical parameters during film storage was dependent on the concentration of AgNPs. Thus, films loaded with higher amounts of $AgNO_3$ exhibited greater changes (decrease in L*, h* and C*), which indicates that the silver reducing process progressed throughout storage, and confirms that free Ag+ remains in the films after 1 week of storage. Silver ions are known to readily reduce to elemental particles in slightly reducing environments (Martinez Abad, 2014a).

3.2. Silver release

Silver release was studied as a function of time in five different food simulating liquids (aqueous solutions with 10, 20 and 50 % of ethanol, 3% of acetic acid and a non-polar medium, oleic acid). Figure 2 shows the total accumulated silver released into the different simulants from the films throughout time. Simulants A, C and D1 exhibited a very similar release profile, so the release profile for the D1 simulant (with 50% ethanol)

is not shown. Simulants B (with low pH) and D2 (non-polar medium) behaved differently, as can be observed in Figure 2.

In aqueous systems, the water uptake in the film enhanced the release of silver into the simulants, as can be deduced from Figure 2. Once the film was immersed in the aqueous simulants, most of the release took place within the 60 first minutes, depending on the type of aqueous simulant used. Samples released 100% of their silver content after 1 h of immersion in the acidic medium (simulant B) and after 4 to 10 h in those media containing 10 to 50 % of ethanol, respectively, which represent 16, 157, 393 and 787 mg of silver / kg of simulant, for S-PVA-1, S-PVA-2, S-PVA-3 and S-PVA-4 films, respectively. This agrees with the hydrophilic nature of the films, which became completely hydrated, swollen and plasticized after very short times of immersion. During the hydration process, the polymer network becomes more open, favouring the migration of silver to the aqueous media.

Martinez-Abad *et al*. (2013) showed that the release kinetics was greatly affected by the silver speciation in the matrix (silver ions or solid nanoparticles).Thus, a 100 % burn release of silver within the first 30 minutes was obtained from hydrophilic ethylene-vinyl alcohol copolymer (EVOH) films loaded with free silver ions; nevertheless, the release kinetics dramatically slowed down when using silver nanoparticles, as they were retained in the polymer network. The behaviour shown by the silver-loaded S-PVA composite films suggests the presence of both kinds of silver specimens, silver nanoparticles and silver ions. The release of silver into a liquid system depends on different factors, such as the liquid migration to the polymer matrix and its swelling, the polymer solubility in the liquid phase and the diffusion of the active compound through the polymer matrix to the liquid.

Table 3: Colour parameters (Clarity: L*, chrome: C_{ab}* and hue: h_{ab}*) and internal transmittance (Ti) of S-PVA and silver composite films after 1 (1W) and 5 (5W) storage weeks. Mean values and standard deviation.

	L*		C_{ab}*		h_{ab}*		Ti (450nm)	
Films	1W	5W	1W	5W	1W	5W	1W	5W
S-PVA	84.3 ± 1.1^{a1}	82.1 ± 1.6^{a}	3.6 ± 0.4^{a1}	4.4 ± 1.4^{a1}	110 ± 9^{a1}	112 ± 7^{a1}	86.2 ± 0.5^{a1}	85.9 ± 0.2^{a1}
S-PVA-1	49.0 ± 1.4^{b1}	39.4 ± 1.3^{b2}	12.9 ± 0.6^{b1}	17.5 ± 0.4^{b2}	56 ± 1^{b1}	55.7 ± 0.6^{c1}	58 ± 2^{b1}	29 ± 3^{b2}
S-PVA-2	39.4 ± 0.7^{c1}	34.2 ± 0.4^{c2}	19.0 ± 0.3^{c1}	14.5 ± 0.2^{c2}	64.3 ± 0.6^{c1}	56 ± 3^{c2}	24 ± 2^{c1}	12 ± 2^{c2}
S-PVA-3	38.2 ± 1.0^{cd1}	33.0 ± 0.3^{cd2}	17.6 ± 0.4^{c1}	12.3 ± 0.6^{d2}	60.3 ± 1.1^{bc1}	49 ± 2^{c2}	20 ± 3^{c1}	10.5 ± 0.5^{cd2}
S-PVA-4	36.8 ± 1.3^{d1}	31.8 ± 0.4^{d2}	13.9 ± 1.7^{b1}	6.3 ± 0.9^{e2}	57 ± 3^{b1}	37 ± 8^{b2}	20 ± 3^{c1}	5 ± 3^{d2}

$^{a, b, c, d, e}$ different letters in the same column indicate significant differences among formulations ($p<0.05$).

$^{1, 2}$ different numbers in the same row indicate significant differences between storage times ($p<0.05$).

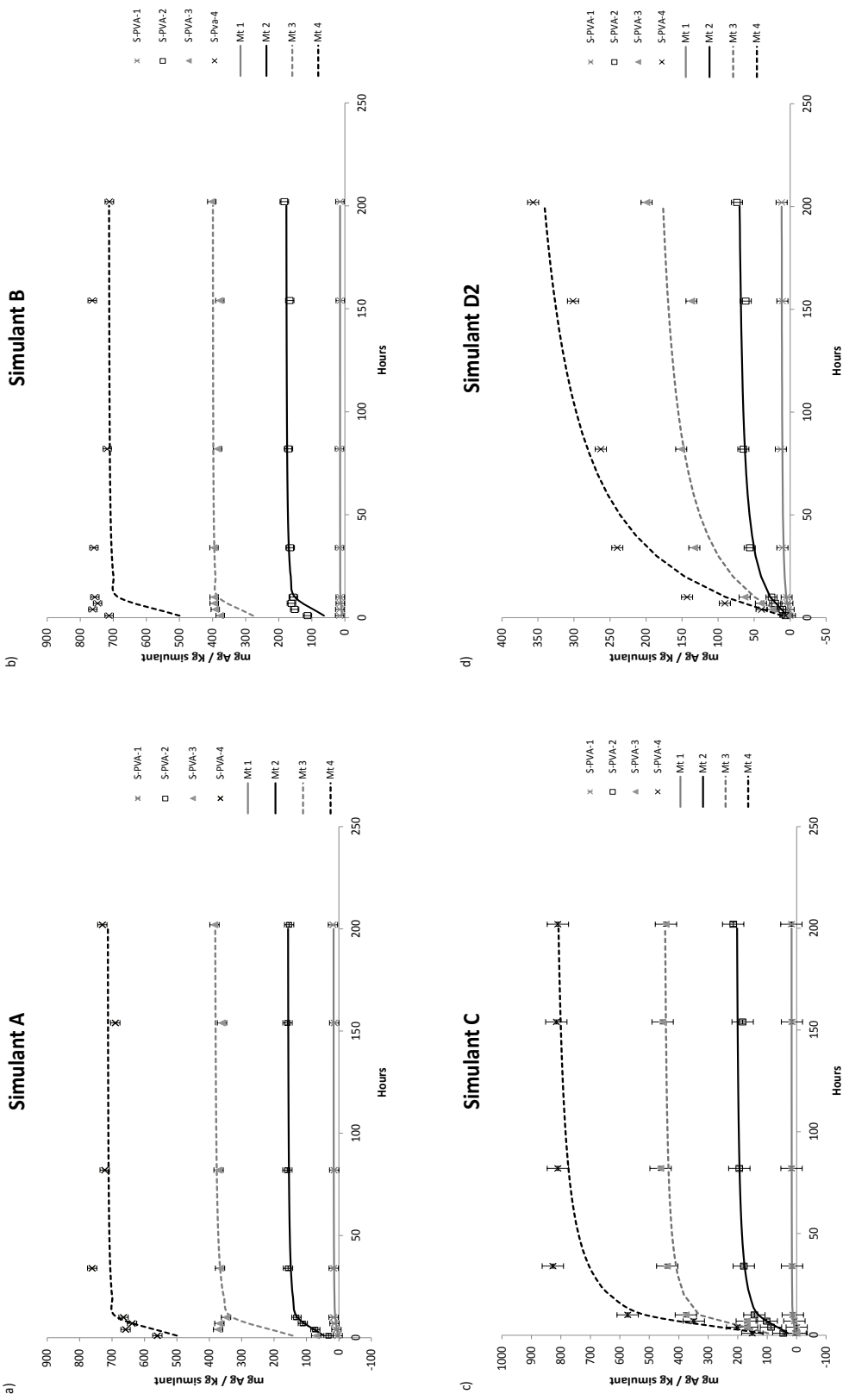

Figure 2. The experimental points and predicted curves (M_t) of silver release profiles from the films into the A, B, C and D2 food simulants throughout time.

The different release behaviour in non-polar simulant D2 can be explained by the limited diffusion of oleic acid in the highly polar polymer matrix, thus maintaining a closed network structure, which hinders the diffusion and release of silver into the simulant. As can be deduced from Figure 2-d, in contact with low-polar systems, i.e. fat-rich foods, the S-PVA polymeric matrix will exhibit a limited silver release, up to 50-78 %, depending on the initial silver concentration.

An empirical model (Peleg model, Eq. 1) was applied to fit the release kinetics of silver to food simulants from the films. Parameter k_1 is inversely related to the mass transfer rate at the very beginning of the process and k_2 is inversely related to the maximum attainable value of the function (equilibrium value $-V_{eq}$, Eq. 2) (Abu-Ghannam & McKenna, 1997; Turhan *et al*., 2002, Atarés *et al*., 2008). Figure 2 shows the experimental points and predicted curve, where the close fit of the model can be observed in every case.

Table 5 shows the values of kinetic constant k_1 for the different films and simulants (A, B, C and D1). The equilibrium value deduced from k_2 (not shown) did not significantly differ from the values commented on above for each film, deduced from the total silver concentrations in the respective formulation. For simulant D2, the values of k_1 and k_2 for each film are shown in Table 6. The estimated equilibrium value and the corresponding percentage of release, with respect to the total amount of silver in the film, are also shown.

The release rate (inverse of k1) of silver decreased as the amount of ethanol in the aqueous solution rose (Table 5). The increase in the ethanol concentration in the simulant reduced the polarity of the medium and limited the hydration process of the polymer network and the weakening effect on the matrix, leading to a slower diffusion of silver through the film. Likewise, the release rates were affected by the initial silver concentration in the films according to the different values of the driving force for the

mass transfer process; thus, the films loaded with the greatest silver concentration released silver into the different simulants faster. This is especially true in the case of samples S-PVA-3 and S-PVA-4, where a greater amount of silver ions, with higher mobility, could remain.

Table 5: Values of the kinetic constant k_1 (h mg_{Ag} $kg_{simulant}^{-1}$) for the silver release of the different films into the simulants (A, B, C and D1).

	Simulant			
Film	A	C	D1	B
SPVA-1	0.037	0.173	0.292	0.0493
SPVA-2	0.015	0.029	0.038	0.0102
SPVA-3	0.002	0.003	0.003	0.0011
SPVA-4	0.001	0.003	0.003	0.0001

Table 6: Values of the Peleg's parameters of the different films in D2 simulant: k_1 (h mg_{Ag} $kg_{simulant}^{-1}$), k_2 (mg_{Ag} $kg_{simulant}^{-1}$), V_{eq} ($kg_{simulant}$ mg_{Ag}^{-1}) and percentage released with respect to the total silver amount in the films.

Film	k_1	k_2	V_{eq}	% Released
SPVA-1	1.033	0.08	13	78
SPVA-2	0.189	0.015	66	42
SPVA-3	0.154	0.005	204	52
SPVA-4	0.087	0.003	400	51

The degree and rate of film hydration, which greatly facilitates molecular mobility and silver diffusion, will be dependent on the water content and pH of the simulant. In the case of simulant B (3 % acetic acid), the release of silver was favoured (lower k1) because of the greater solubility of the film at low pH. This is due to the partial hydrolysis of the polymer caused by acetic acid, which led to smaller and thus, more soluble

fragments. This effect has also been reported by several authors working with starch and starch-PVA films under acidic environments (Yoon *et al.*, 2006, Olivato *et al*., 2011; Carvalho *et al*., 2005; Ortega-Toro *et al*., 2015).

Taking into account the total release into the different simulants, and the established overall migration limit (OML) for food contact packaging materials: 60 mg of substances/kg of food simulant or foodstuff (EN1186-1, 2002, Commission Regulation Nº 10/2011), the only films that fulfilled this requirement are S-PVA-1 (for all types of foodstuffs) and S-PVA-2 for fat-rich foodstuffs. Nevertheless, more research has to be carried out on real foodstuffs in order to check the viability of its application.

3.3. Antimicrobial activity

The antimicrobial activity of silver-loaded films was analysed against two fungi, *A. niger* and *P. expansum*, and two bacteria, *L. innocua* and *E. coli*. The antimicrobial efficacy was evaluated through the analysis of the growth (or survival) of a determined infection level of the microorganism (10^5 spores/ml and 10^2 UFC/cm^2), for fungi and bacteria, respectively) following the above-described methodology.

Silver-loaded films exhibited antimicrobial activity, which depended on the concentration used. As expected, the highest antibacterial activity was observed for the formulation with the greatest silver concentration (S-PVA-4), showing a bactericidal effect (defined as a decrease of 3 magnitudes in the bacterial load, in comparison with the control) for both bacteria. Several authors (Rhim *et al*., 2013; Bryaskova *et al*., 2010; Martinez-Abad *et al*., 2014a) also found that the antibacterial activity of films with embedded AgNPs increased as the concentration of silverrose.

S-PVA-3 and S-PVA-2 also exhibited a bactericidal effect but only throughout the first 5 or 7 days for *L. innocua* and *E. coli*, respectively. After this period, the inhibition level of these silver-loaded films decreased throughout the storage period. On the other

hand, the antibacterial activity was greater in *E. coli* than in *L. innocua* (Figure 3) due to the difference cell wall structures of both types of bacteria. The presence of the negatively charge lipopolysaccharide in Gram negative bacteria attracts the positively charged silver ions or silver nanoparticles, thus dramatically increasing the permeability of the membrane. Moreover, the cell wall of gram positive cells (*Listeria*) presents a thicker cell wall of peptidoglycans, which makes the penetration of silver nanoparticles difficult (Bryaskova *et al*., 2010). In fact, formulations S-PVA-2 and S-PVA-3 exhibited reductions in the *E. coli* population of around 5 logs during the first 7 days of storage, while for *L. innocua*, the maximum reduction reached was 3 logs up to the 5^{th} day.

As regards the fungus, control films without silver were able to grow to a maximum of about 10^8 CFU/cm^2 for both fungi under the stated conditions (Figure 4). At low silver concentrations in the films (S-PVA-1 and S-PVA-2), almost no antifungal effect was observed: S-PVA1 reduced the initial microbial load by about 1 log and S-PVA-2 reduced the plate counts of *P. expansum* by about 4 logs during the first 3 days of incubation. When using moderate concentrations of silver (S-PVA-3), the growth of both fungi was inhibited up to the first five or seven days of storage, for *Aspergillus* and *Penicillium*, respectively. The level of reduction in the fungal population during this time period was remarkable; around 4-5 logs with respect to the control film. After this period, the inhibition level also decreased throughout storage, as commented on above, reaching a maximum value of 3 logs after 12 days of incubation.

Only when using the highest silver concentration (S-PVA4), was a completely fungistatic activity detected during storage, as no sign of cultivable counts were observed during the whole period. To the best of our knowledge, very little information related with the antifungal activity of AgNPs-loaded films has been found. Only Abreu *et al*. (2015) reported antifungal tests against Candida albicans for agar films loaded with silver nanoparticles, but they observed no antifungal effect.

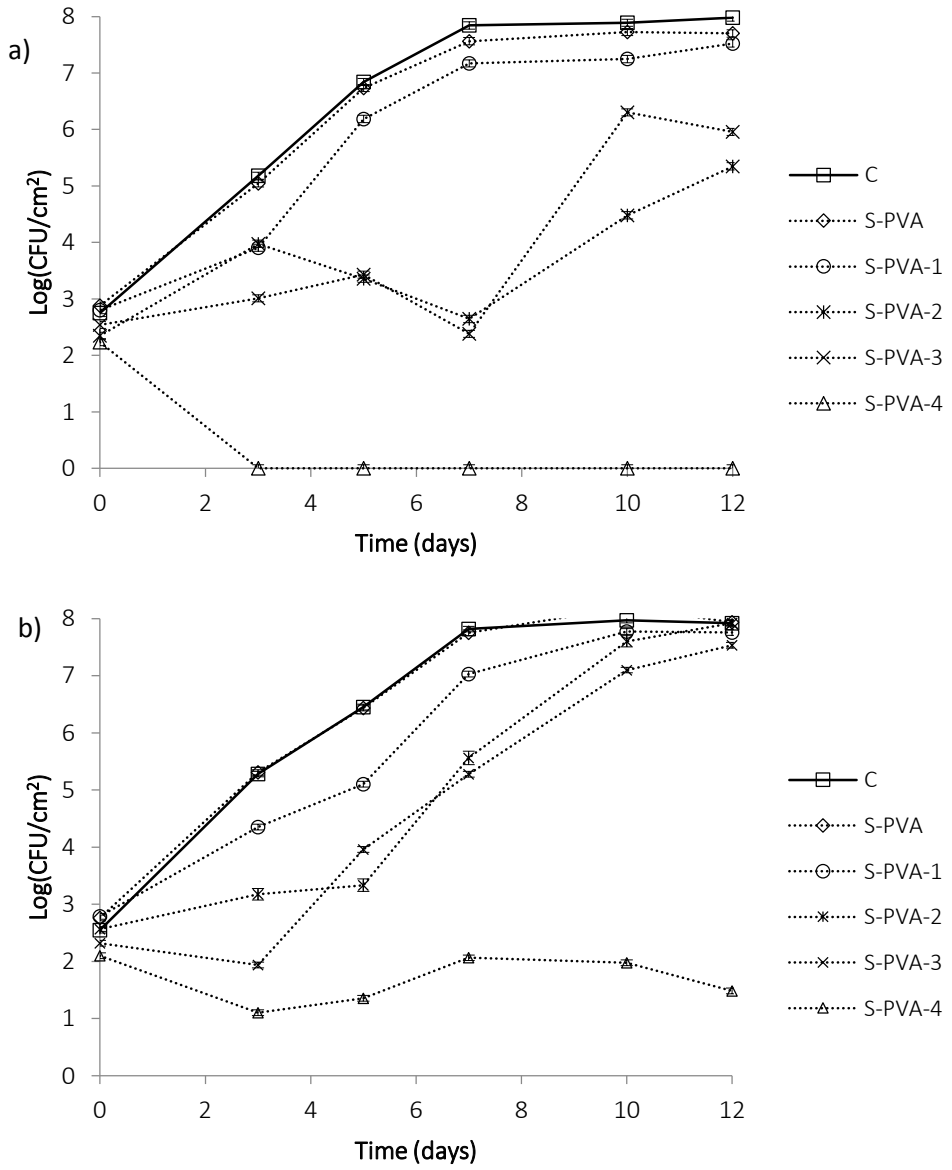

Figure 3. Effect of control and silver loaded composite films on the growth and survival of *Escherichia coli* (a) and *Listeria innocua* (b) in TSA-NaCl medium at 10 ºC. Mean values and 95 % LSD intervals.

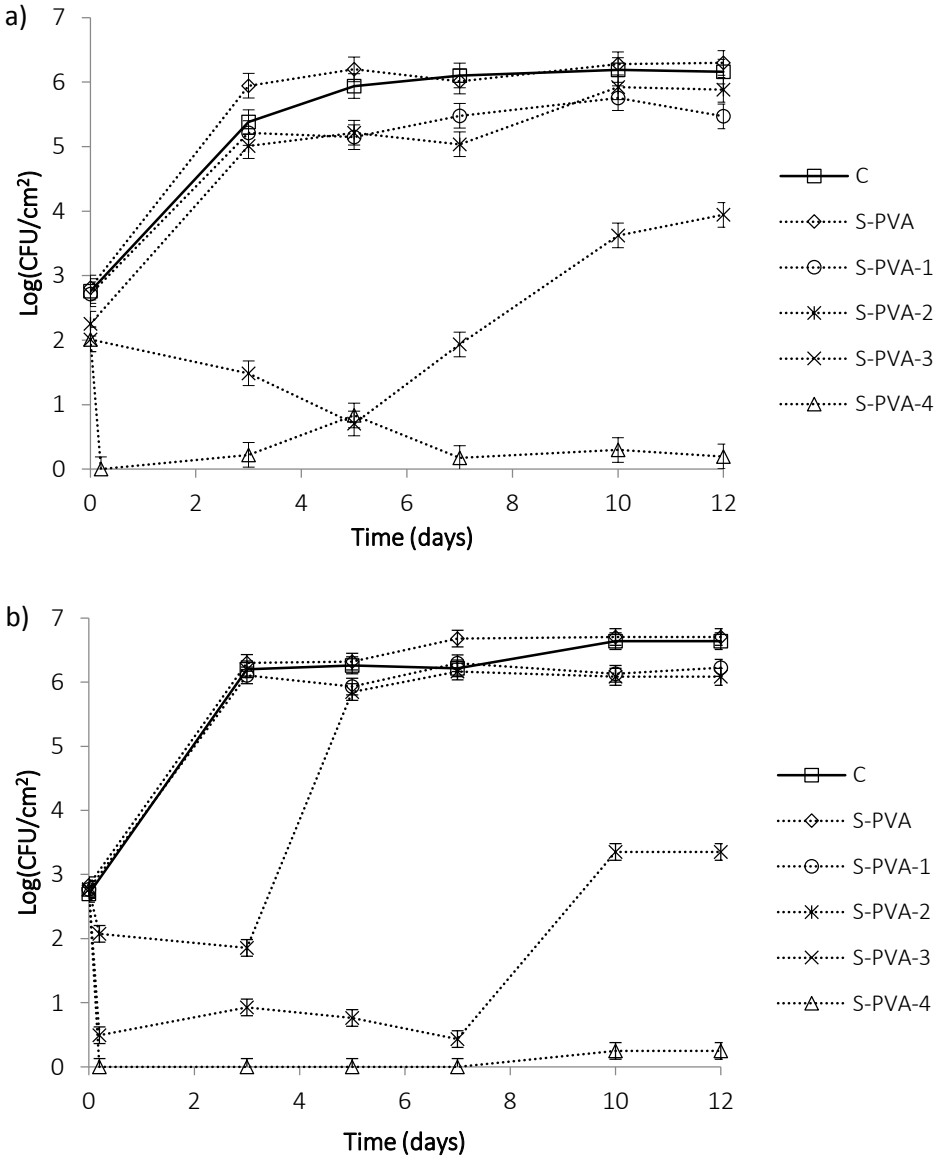

Figure 4. Effect of control and silver loaded composite films on the growth and survival of *Aspergillus niger* (a) *Penicillium expansum* (b) on PDA medium stored at 25 ºC. Mean values and 95 % LSD intervals.

At this point, some considerations have to be taken into account. From the reported data, silver concentrations of around 10-500 ppm are needed to exert bactericidal activity in a rich medium, such as TSB supplemented with NaCl (Halminton & Shan, 1996; Nomiya *et al*., 2004; Ruparelia *et al*., 2008; Sondi *et al.*, 2004; Martinez-Abad *et al*., 2012). If water or salt buffers are used, the bactericidal concentrations are proven to be much lower, in the range of 0.01-1ppm (Bjarnsholt *et al*., 2007; Hwang *et al*., 2007; Kim

et al., 1998). Taking into account the release studies, 100 % of silver is delivered into the aqueous simulants by the films, giving rise to a minimum concentration of silver of 16 ppm (S-PVA-1) in the liquid simulants. This suggests that the release of silver into the TSB/PDA medium in the Petri dishes was not completed (as occurred in liquid aqueous simulants), being retained in the polymer matrix and, so, not able to act as an antimicrobial. As commented on above, the release kinetics was closely related with the hydration of the polymer network and, therefore, the hydration level of the film in contact with the agar medium could be constrained as the water molecules entrapped in the agar gel are not able to diffuse so effectively, which will affect the silver release and antimicrobial activity of the films.

4. CONCLUSIONS

Starch-PVA based films embedding silver nanoparticles exhibited remarkable antibacterial activity against *Listeria innocua* and *Escherichia coli* and antifungal activity against *Aspergillus niger* and *Penicillium expansum,* which depended heavily on the concentration of AgNPs in the film. This incorporation did not imply relevant changes in the physical properties of the films, except for their colour and transparency; these both underwent significant changes, becoming brownish-yellow and opaque, especially when the silver concentration in the films increased.

The antimicrobial effectiveness of silver-loaded films was limited by the release behaviour of silver from the films in contact with the agar plate, seemingly reduced as compared to food simulants. The silver was delivered to aqueous simulants (including the acidic one) in its entirety within the first 60 minutes of contact. Nevertheless, when using a non-polar simulant, the release capacity of the films drastically decreased. The silver released into the food simulants widely exceeds the maximum amount permitted (60 mg/Kg simulant) in all cases, except when using the non-polar simulant (oleic acid).

So, the use of the developed films as food packaging materials should be restricted to fat-rich foodstuffs. For the purposes of optimizing the release capacity of the films with moderate silver concentrations, additional studies should be carried out in order both to reduce the burst release in contact with highly aqueous environments and also to comply with the current legislation.

Acknowledgements

The authors acknowledge the financial support from the Spanish Ministerio de Economía y Competitividad through the project AGL2013-42989-R. Amalia Cano also thanks the Spanish Ministerio de Educación, Cultura y Deporte for the FPU grant.

References

- Abreu, A. S., Olivera, M., Rodeigues, M., Cerqueira, A., Vicente, A. A., & Machado, A.V. (2015). Antimicrobial nanostructured starch based films for packaging. *Carbohydrate Polymers*, accepted date: 8-4-2015 http://dx.doi.org/10.1016/j.carbpol.2015.04.021.
- Abu-Ghannam, N., & McKenna, B. (1997). The application of Peleg's equation to model water absorption during the soaking of red kidney beans (Phaseolus vulgaris L). *Journal of Food Engineering*, 32, 391-401.
- ASTM. (2001). Standard test method for tensile properties of thin plastic sheeting. In Standard D882 annual book of American Standard Testing Methods. Philadelphia, PA: American Society for Testing and Materials. ASTM.
- ASTM. (1995). Standard test methods for water vapour transmission of materials. Standard designations: E96-95 Annual book of ASTM standards. Philadelphia, PA: American Society for Testing and Materials. (pp. 406 e 413).
- Atarés, L., Chiralt, A., & González- Martínez, C. (2008). Effect of solute on osmotic dehydration and rehydration of vacuum impregnated Apple cylinders (cv. Granny Smith). *Journal of Food Engineering*, 89, 46-56.

- Bjarnsholt, T., Kirketerp-Møller, K., Kristiansen, S., Phipps, R., Nielsen, A. K., Jensen, P. Ø., Høiby, N., & Givskov, M. (2007). Silver against *Pseudomonas aeuruginosa* biofilms. APMIS 115, 921-928.

- Bryaskova, R., Pencheva, D., Kale, G. M., Lad, U., & Kantardjiev, T. (2010) Synthesis, characterisation and antibacterial activity of PVA/TEOS/Ag-Np hybrid thin films. *Journal of Colloid and Interface Science*, 349, 77–85.

- Cano, A., Jiménez, A., Cháfer, M., González, C., & Chirialt, A. (2014). Effect of amylose:amylopectin ratio and rice bran addition on starch films properties. *Carbohydrate Polymers,* 111, 543-555.

- Cano, A., Fortunati, E., Cháfer, M., Kenny, J. M., Chiralt, A., & González, C. (2015). Properties and ageing behaviour of pea starch films as affected by blend with poly(vinyl alcohol), *Food Hydrocolloids*, 48: 84-93.

- Carvalho, A. J. F., Zambon, M. D., da Silva Curvelo, A. A., & Gandini, A. (2005). Thermoplastic starch modification during melt processing hydrolysis catalyzed by carboxylic acids. *Carbohydrate Polymers,* 62 (4), 387-390.

- Commission Regulation (EU) No 10/2011 of 14 January 2011 on plastic materials and articles intended to come into contact with food.

- Corrales, M., Fernández, A., & Han, J.H. (2014). Chapter 7, Antimicrobial packaging systems. In J. H. Han (Ed.), Innovations in food packaging (second edition) (pp. 133-170). *Academia Press: San Diego*, CA, USA.

- Cussler, E. I., Highes, S. E., Ward, W. J. & Aris, R. (1998). Barrier membranes. *Journal of Membrane Science*, 38, 161-174.

- Darroudi, M., Ahmad, M. B., Zamiri, R., Zak, A. K., Abdullah, A. H., & Ibrahim, N. A. (2011). Time-dependent effect in green synthesis of silver nanoparticles. *International Journal of Nanomedicine*, 6, 677-681.

- De Moura, M. R., Mattoso, L. H. C., & Zucolotto, V. (2012). Development of cellulose-based bactericidal nanocomposites containing silver nanoparticles and their use as active food packaging. *Journal of Food Engineering*, 109, 520-524.
- Duran, N., Marcarto, P. D., De Souza, G. I. H., Alves, O. L., & Esposito, E. (2007). Antibacterial effect of silver nanoparticles produced by fungal process on textile fabrics and their effluent treatment. *Journal of Biomedical Nanotechnology*, 3, 203-208.
- European Commission. (1994). European parliament and council directive 94/36/EC of 30th June 1994 on colours for use in foodstuffs.
- European Standard EN 1186-1:2002. Materials and articles in contact with foodstuffs. Plastics. Guide to the selection of conditions and test methods for overall migration.
- FAO. (2011). Global food losses and food waste – Extent, causes and prevention. Rome.
- FDA/CFSAN (2010). Listing of food additive status: Silver nitrate-172.167, U. FDA/CFSAN, Editor.
- Feng, Q. L., Wu, J., Chen, G. Q., Cui, F. Z., Kim, T. N., & Kim, J. O. (2000). A mechanistic study of the antibacterial effect of silver ions on Escherichia coli and *Staphylococcus aureus*. *Journal of Biomedical Materials Research*, 52(4), 662-668.
- Ghosh, S., Kaushik, R., Nagalakshmi, K., Hoti, S. L., Menezes, G.A., Harish, B.N. & Vasan, H. N. (2010). Antimicrobial activity of highly stable silver nanoparticles embedded in agar–agar matrix as a thin film. *Carbohydrate Research*, 345, 2220-2227.
- Halminton-Miller, J. M. T., & Shah, S. (1996). A microbiological assessment of silver fusidate, a novel topical antimicrobial agent. *International Journal of Antimicrobial Agents*, 7, 97-99.
- Hutchings, J.B. (1999). Food and Colour Appearance, Second Edition. Gaithersburg, Maryland: Chapman and Hall Food Science Book, Aspen Publication.
- Hwang, M. G., Katayama, H., & Ohgaki, S. (2007). Inactivation of *Legionella pneumophilia* and *Pseudomonas aeruginosa*: evaluation of the bactericidal ability of silver cations. *Water Research*, 41, 4097-4104.

- Jiménez, A., Fabra, M.J., Talens, P., & Chiralt, A. (2012). Effect of re-crystallization on tensile, optical and water vapour barrier properties of corn starch films containing fatty acids. *Food Hydrocolloids*, 26, 302-310.

- Judd, D. B. & Wyszecki, G. (1975). Colour in Business, Science and Industry. New York: John Wiley and Sons, Inc. ISBN. 0471452122.

- Kanmani, P., & Rhim, J-W. (2014). Physicochemical properties of gelatin/silver nanoparticle antimicrobial composite films. *Food Chemistry*, 148, 162-169.

- Kim, T. N., Feng, Q. L., Kim, J. O., Wu, J., Wang, H., Chen, G. C., & Cui, F. Z. (1998). Antimicrobial effects of metal ions (Ag+, Cu2+, Zn2+) in hydroxyapatite. *Journal of Materials Science: Materials in Medicine*, 9, 129-134.

- Kristo, E., Koutsoumanis, K.P., & Biliaderis, C.G. (2008). Thermal, mechanical and water vapor barrier properties of sodium caseinate films containing antimicrobials and their inhibitory action on Listeria monocytogenes. *Journal of Food Hydrocolloids,* 22, 373–386.

- Lanciotti, R., Gianotti, A., Patrignani, F., Belletti, N., Guerzoni, M.E., & Gardini, F. (2004). Use of natural aroma compounds to improve shelflife and safety of minimally processed fruits. *Trends in Food Science & Technology*, 15, 201–208.

- Li, W-R., Xie, X-B., Shi, Q-S., Zeng, H-Y., OU-Yang, Y-S., & Chen, Y-B. (2010). Antibacterial activity and mechanism of silver nanoparticles on Escherichia coli. *Applied Microbiology and Biotechnology*, 85, 1115-1122.

- Liau, S. Y., Read, D. C., Pugh, W. J., Furr, J. R., & Russell, A. D. (1997). Interaction of silver nitrate with readily identifiable groups: Relationship to the antibacterial action of silver ions. *Letters in Applied Microbiology*, 25(4), 279-283.

- Lin, S., Chen, L., Huang, L., Cao, S., Luo, X., & Liu, K. (2015). Novel antimicrobial chitosan–cellulose composite filmsbioconjugated with silver nanoparticles. *College Industrial Crops and Products*, 70, 395-403.

- Martínez- Abed, A., (2014a). Thesis: Development of silver based antimicrobial films for coating and food packaging applications. Supervised by: Ocio, M. J., & Lagarón, J. M. Universitat Politècnica de València, Valencia, Spain, Febrero, 2014.

- Martínez-Abad, A., Lagarón, J. M., & Ocio, M.J. (2014b). Antimicrobial beeswax coated polylactide films with silver control release capacity. *International Journal of Food Microbiology*, 174, 39–46.

- Martínez-Abad, Sánchez, G., A., Lagarón, J. M., & Ocio, M.J. (2013). Influence of speciation in the release profiles and antimicrobial performance of electrospun ethylene vinyl alcohol copolymer (EVOH) fibers containing ionic silver ions and silver nanoparticles. *Colloid and Polymer Science*, 291, 1381-1392.

- Martínez-Abad, Sánchez, G., A., Lagarón, J. M., & Ocio, M.J. (2012). On the different growth conditions affecting silver antimicrobial efficacy on *Listeria monocytogenes* and *Salmonella enterica*. *Internaticonal Journal of Food Microbiology*, 158 (2), 147-154.

- Morales, J., Morán, J., Quintana, M., & Estrada, W. (2009). Synthesis and characterization of silver nanoparticles by Sol-Gel route from silver nitrate. *Rev Soc Quim Peru*, 75 (2), 177-184.

- Mohanty, S., Mishra, S., Jena, P., Jacob, B., Sarkar, B., & Sonawane, A. (2012). An investigation on the antibacterial, cytotoxic, and antibiofilm efficacy of starch-stabilized silver nanoparticles. *Nanomedicine: Nanotechnology, Biology, and Medicine*, 8, 916–924.

- Mohapatra, B., Kuriakose, S., & Mohapatra, S. (2015). Rapid green synthesis of silver nanoparticles and nanorods using *Piper nigrum* extract. *Journal of Alloys and Compounds*, 637, 119-126.

- Monge, M. (2009). Nanopartículas de plata: métodos de síntesis en disolución y propiedades bactericidas. Real Sociedad Española de Química*. Anales de Química*, 105(1), 33−41.

- Neto, E. A. B., Ribeiro, C., & Zucolotto, V. (2008). Síntese de Nanopartículas de Prata para Aplicação na Sanitização de Embalagens. Comunicadp técnico, 99. Sao Pablo, SP. ISSN 1517-4786.

- Nomiya, K., Yoshizawa, A., Tsukagoshi, K., Kasuga, N. C., Hirakawa, S., & Watanabe, J. (2004). Synthesis and structural characterization of silver (I), aluminium (III) and cobalt (II) complexes with 4-isopropyltropolone (hinokitol) showing noteworthy biological activities. Action of silver (I)-oxygen bonding complexes on the antimicrobial properties. *Journal of Inorganic Biochemestry*, 98, 46-60.

- Olivato, J. B., Grossmann, M. V. E., Yamashita, F., Eiras, D., & Pessan, L. A. (2011). Citric acid and maleic anhydride as compatibilizers in starch/poly(butylene adipate-co-terephthalate) blends by one-step reactive extrusion. *Carbohydrate Polymer*, 87, 2614-2618.

- Ortega-Toro, R., Collazo-Bigliardi, S., Talens, P., & Chiralt, A. (2015). Influence of citric acid on the properties and stability of starch-polycaprolactone based films. *Journal of Applied Polymer Science*, DOI: 10.1002/APP.42220.

- Pal, S., Tak, Y. K., & Song, J. M. (2007). Does the antibacterial activity of silver nanoparticles depend on the shape of the nanoparticle? A study of the Gram-negative bacterium Escherichia coli. *Applied and Environmetal Microbiology*, 73, 1712-1720.

- Peleg, M. (1988). An empirical model for the description of moisture sorption curves. *Journal of Food Science*, 53, 1216-1219.

- Pourjavadi, A., & Soleyman, R. (2011). Silver nanoparticles with gelatin nanoshells: photochemical facile green synthesis and their antimicrobial activity. *Journal of Nanoparticles Research*, 13, 4647-4658.

- Puišo, J., Prosyšenvas, I., Guobienė, A., & Tamulevišius, S. (2008). Plasmonic properties of silver in polymer. *Materials Science and Engineering: B*, 149, 230-236.

- Rai, M., Yadav, A., & Gade, A. (2009). Silver nanoparticles as a new generation of antimicrobials. *Biotechnology Advances*, 27, 76–83.

- Raimondi, F., Scherer, G. G., Kotz, R., & Wokaun, A. (2005). Nanoparticles in energy technology: examples from electochemistry and catalysis. *Angewandte Chemmie International Edition*, 44, 2190-209.

- Raveendran, P., Fu, J., & Wallen, S.L. (2003). Completely “green” synthesis and stabilization of metal nanoparticles. *Journal of the American Chemical Society*, 125 (46), 13940-13941.

- Rhim, J. W., Wang, L. F., & Hong, S. I. (2013). Preparation and characterization of agar/silver nanoparticles composite films with antimicrobial activity. *Food Hydrocolloids*, 327-335.

- Roy, K., Sarkar, C. K., & Ghosh, C. K. (2015). Photocatalytic activity of biogenic silver nanoparticles synthesized using potato (*Solanum tuberosum*) infusion. *Spectrochimica Acta*, Part A: Molecular and Biomolecular Spectroscopy, 146, 286-291.

- Ruparelia, J. P., Chatterjee, A. K., Duttagupta, S. P., & Mukhereji, S. (2008). Strain specificity in antimicrobial activity of silver and copper nanoparticles. *Acta Biomaterialia*, 4, 707-716.

- Sánchez-González, L., González-Martínez, C., Chiralt, A., & Cháfer, M. (2010). Physical and antimicrobial properties of chitosan-tea tree essential oil composite films. *Journal of Food Engineering*, 98, 443-452.

- Sedlarik, V., Galya, T., Sedlarikova, J., Valasek, P., & Saha, P. (2010). The effect of preparation temperature on the mechanical and antibacterial properties of poly(vinyl alcohol)/silver nitrate films. *Polymer Degradation and Stability*, 95, 399-404.

- Shameli, K., Ahmad, M. B., Yunus, W. Z. W., Ibrahim, N. A., Rahman, R. A., & Joakar, M., *et al*. (2010). Silver/poly (lactic acid) nanocomposites: preparation, characterization, and antibacterial activity. *International Journal of Nano-medicine*, 5, 573-579.

- Sharma, V.K., Yngard, R.A., & Lin, Y. (2009). Silver nanoparticles: Green synthesis and their antimicrobial activities. *Advances in Colloid and Interface Science*, 145, 83–96.

- Sondi, I., & Salopek-Sondi, B. (2004). Silver nanoparticles as antimicrobial agent: A case study on E. coli as a moder for Gram-negative bacteria. *Journal of Colloid and Interface Science*, 275, 177-182.

- Torres-Castro, A., González-González, V. A., Garza-Navarro, M., & Guana-González, E. (2011). Sintesís de nanocómpositos de plata con almidón. *Ingenierías* XIV (50), 34-41.

- Turhan, M., Sayar, S., & Gunasekaran, S. (2002). Application of Peleg model to study water absorption in chickpea during soaking. *Journal of Food Engineering,* 53 (2), 153-159.

- Vimala, K., Murali, Y., Varaprasad, K., Narayana, N., Ravindra, S., Sudhakar, N., & Mohona, K. (2011). Fabrication of Curcumin Encapsulated Chitosan-PVA Silver Nanocomposite Films for Improved Antimicrobial Activity. *Journal of Biomaterials and Nanobiotechnology*, 2, 55-64.
- Vimala, K., Mohan, M., Sivudu, S., Varaprasad, K, Ravinadra, S., Narayana Reddya, N., Padmab, Y., Sreedharc, B., & MohanaRajua, K. (2010). Fabrication of porous chitosan films impregnated with silver nanoparticles: A facile approach for superior antibacterial application. *Colloids and Surfaces B: Biointerfaces*, 76, 248-258.
- Yoon, S., Park, M., & Byun, H. (2012). Mechanical and water barrier properties of starch/PVA composite films by adding nano-sized poly(methylmethacrylate-co-acrylamide) particles. *Carbohydrate Polymer*, 87, 676-686.
- Zheng, R., Rong, M. Z., Zhang, M. Q., Lianm, H. C. & Zeng, H. M. (2001). Interfacial interaction in Ag/polymer nanocomposite films. *Journal of Materials Science Letters*, 20, 1473-1476.

Amalia I. Cano, Maite Cháfer, Amparo Chiralt, Chelo González-Martínez. **Biodegradability behaviour of starch-PVA films as affected by the incorporation of different antimicrobials.**

Abstract

The effect of the incorporation of different antimicrobial substances into S-PVA films on their disintegration and biodegradation process was analysed. To this aim, starch, PVA and S-PVA films containing different concentrations of neem oil, oregano essential oil and silver nanoparticles were submitted to composting conditions to determine the disintegration and biodegradability percentages during 73 and 45 days, respectively. Additionally, thermogravimetric and structural analysis throughout the composting period were also carried out. The incorporation of starch into pure PVA films significantly improved its biodegradation and disintegration behaviour. The addition of neem and oregano essential oils slightly affected the biodegradation and disintegration profile of starch-PVA films, enhancing both disintegration and biodegradation levels. So, the presence of these antimicrobials did not compromise the compostable and biodegradable character of the starch-PVA blend films. Nevertheless, films containing silver species at 9.8 % in the dried film were seriously affected in their biodegradation capacity, reaching values of only 58 % after 45 days of composting, despite their high disintegration capacity. Thus, lower silver concentrations are recommended to avoid possible alterations in compost microbial activity.

Key words: Neem oil, oregano essential oil, silver nanoparticles, composting process, disintegration.

1. INTRODUCTION

Most of the conventional plastics are non-biodegradable and remain for 100-450 years in the environment (Alvira, 2007). The current activities to handle the plastic wastes include incineration and recycling, but they are not enough to solve the environmental problems. As alternative, biodegradable plastics have attracted growing attention because of their potential use in the replacement of traditional non-degradable plastic items deriving from fossil fuel feed stocks to ensure a significant contribution to sustainable development in view of the wider range of disposal option at lower environmental impact (Avérous & Pollet, 2012).

Composting is the aerobic process designed to produce stabilized organic residues from the biodegradable parts of packaging waste under controlled conditions and using microorganisms (94/62/EC). Nowadays, in food packaging area, current studies are focused on the disintegrability, biodegradability and ecotoxicity properties of films under compostable controlled conditions in order to evaluate their compostable behaviour. In this sense, new ISO standards test methodologies, where specific disposal pathways, specific time frames and passing criteria are indicated in order to unify a proper composting analysis of plastics.

On the other hand, the considerable pressure for attending the current consumer food habits, healthier, free of synthetic chemical substances and sustainably manufactured, has boosted investigations in order to develop new food packaging which should provide protection against chemical, physical and biological agents (Corrales *et al*., 2014). The incorporation of natural active substances into biodegradable film matrices is a current alternative to prevent food spoilage (Lanciotti *et al*., 2004) for retardation of deterioration, extension of shelf-life, and maintenance of quality of foodstuff.

It is well known, that starch biopolymer such as starch and PVA are suitable biodegradable materials which are able to form blend films with proper physical properties (Cano *et al*., 2015a). In addition, their blends form interpenetrated polymer networks with beneficial effects on the film properties, mainly enhancing the water vapour barrier and mechanical properties, the films becoming much more stretchable and stable during storage (Cano *et al*., 2015a). Both, pure and blend films, could act as carriers of bioactive substance such as antimicrobials. These films could contribute to decrease the food spoilage whereas extending the shelf life of food. Among natural antimicrobial substances, essential oils and silver nanoparticles have shown an interesting activity against a wide variety of microorganisms (Aguirre *et al.* 2013; Martínez-Abad *et al*., 2014; Sánchez-González *et al*., 2011).

However, the incorporation of films containing active substances in the compost could affect the biodegradation behaviour. Few studies have been found about the degradation processes of films containing antimicrobial substances. It is likely that the different additives incorporated into the film will affect the degradation processes. In addition, although the biodegradation of both polymers has been reported by different authors (Avella *et al*., 2005; Du *et al*., 2008, Julinová *et al*., 2010; Azahari *et al*., 2011; Chen *et al*., 1997; Jayasekara *et al*., 2003), scarce information has been found.

The aim of the present work was to analyse the effect of antimicrobial substances into S-PVA blend films on their disintegration and biodegradation under controlled composting process. Thermogravimetrical, structural and visual analysis throughout the composting period were also analysed.

2. MATERIALS AND METHODS

2.1. Materials

Pea starch (S) was provided from Roquette Laisa España S.A. (Benifaió, Valencia, Spain), poly(vinyl alcohol) (PVA) (M_w: 89,000-98,000, degree of hydrolysis > 99 %, and viscosity at 4 % H_2O, 20 ºC is 11.6-15.4 cP) was purchased from Sigma Aldrich Química S.L. (Madrid, Spain) and glycerol and phosphorus pentoxide (P_2O_5) were provided by Panreac Química S.A. (Castellar de Vallès, Barcelona, Spain).

Different bioactive substances used for the work were: neem oil (N) purchased from Magnolia Holland Ibérica S.A. (Vilassar de Mar, Barcelona, Spain), oregano essential oil (O) from Herbes del Molí (Benimarfull, Alicante, Spain) and silver nitrate ($AgNO_3$) from Sigma Aldrich Química S.L. (Madrid, Spain) to obtain the silver nanoparticles (AgNPs).

2.2. Preparation of film forming dispersions and films

Films were obtained by solvent casting procedure after the preparation of film forming dispersions (FFDs). Starch (2% w/w) was dispersed in an aqueous solution at 95 ºC for 30 min to induce starch gelatinization. Thereafter, the dispersion was homogenized using a rotor-stator homogenizer (Ultraturrax D125, Janke and Kunkel, Germany) at 13,500 rpm for 1 min and 20,500 rpm for 3 min. Afterwards, PVA was incorporated into the previously starch dispersion in S:PVA ratio of 2:1 and the dispersion was maintained at 90 ºC for 30 min with stirring until complete dissolution. Finally, glycerol was added at a starch:glycerol ratio of 1:0.25, on the basis of previous studies (Cano *et al*., 2014). This FFD is used to obtain the control films (S-PVA) and to incorporate the antimicrobial substances. Moreover, starch-glycerol and PVA FFDs were also obtained by the same procedure in order to obtain pure films for comparative analyses.

S-PVA film forming dispersion containing AgNPs were obtained by a green synthesis method. The reduction of $AgNO_3$ was induced by means of UV light as reducing agent (Mongue, 2009) and starch and PVA present in the FFD acted as polymeric stabilizers (Torres-Casto *et al*., 2011). $AgNO_3$ was added to the S-PVA FFD at different weight ratio with respect to starch (1:0.006, 1:0.06, 1:0.16 and 1:0.32) and the mixtures were maintained at 90 ºC for 30 min under stirring and UV radiation till the dispersion was turned brown due the formation of AgNPs. The reduction of silver nitrate into AgNPs formation was monitored by using DU 730 spectrophotometer (Thermo scientific, Helios UV-VIS, England).

In the case of neem oil and oregano essential oil, two S:oil ratios were considered (1:0.5 and 1:0.125). After oil addition to the FFD, homogenization at 12,500 rpm for 4 min was carried out in order to emulsify the lipid. FFDs containing or not antimicrobials were poured into Teflon casting plates (15 cm diameter) in the amount which provide a surface solid density of 84.8 $g.m^{-2}$. Films were dried at 25 ºC and a 45 % HR for 48 h and afterwards, peeled off the casting surface. Afterwards, film thickness was measured at six random positions with a Palmer digital micrometre to the nearest 0.0025 mm. Table 1 shows the different formulations of active films and their sample code.

Table 1. Different S-PVA active films (and sample code) showing the ratio of antimicrobial agents (N, O or Ag) with respect to starch and their wt. percentage with respect to the total film solids.

Antimicrobial (AA)	S:AA ratio	wt.% (d.b.)	Sample code
Neem oil (N)	1:0.125	6.7	S-PVA-1N
	1:0.5	22.2	S-PVA-2N
Oregano essential oil (O)	1:0.125	6.7	S-PVA-1O
	1:0.5	22.2	S-PVA-2O
Silver nitrate (Ag)	1:0.006	0.2*	S-PVA-1Ag
	1:0.06	2.1*	S-PVA-2Ag
	1:0.16	5.3*	S-PVA-3Ag
	1:0.32	9.8*	S-PVA-4Ag

*wt of silver respect to the total solid of the films.

2.3. Compost conditioning and characterization

For both, disintegration and biodegradation test, the ripe compost was supplied by a plant composting the organic fraction of solid municipal waste in order to ensure sufficient diversity of microorganisms.

For the disintegration test, a solid synthetic waste was formulated on the basis of the ISO 20200 International Standard, (ISO, 2004). In this sense, a blend of the ripe compost (10 %) with sawdust (40 %), rabbit-feed (30 %), corn starch (10 %), sucrose (5 %), corn seed oil (4 %) and urea (1 %) was prepared.

For the biodegradation test, ripe compost was mixed with vermiculite to prevent the compost compaction, thus ensuring a good oxygen access was used. Afterwards, the water content was adjusted to 50 - 55 % in total, for both test medium. Aerobic conditions in the medium were guaranteed by mixing softly. The matter compost appearance was sticky and without free water. These conditions were maintained throughout the assay by adding de-ionized water to ensure a proper composting process.

Dry mass (DM) and burned-out solid (BS) content of the control sample synthetic waste before and after composting process were determined by triplicate. DM was obtained by drying the sample in a convection oven at 105 ºC until constant weight (Eq. (1)) whilst BS was evaluated by treating the dried samples in a muffle to obtain ash (Selecta, Barcelona, Spain) at 550 ºC until constant weight (Eq. (2)). The C/N ratio was also determined according to the ISO 20200:2004.

$$\mathrm{DM}\ (\%) = \frac{\mathrm{W_d^{105}}}{\mathrm{W_w^i}}\ 100 \quad (1)$$

$$\mathrm{BS}\ (\%) = \frac{\mathrm{W_d^{105}} - \mathrm{W_d^{550}}}{\mathrm{W_d^{105}}}\ 100 \quad (2)$$

where $\mathrm{W_w^i}$ is the initial weight of the sample, $\mathrm{W_d^{105}}$ is its weight after drying at 105 ºC and $\mathrm{W_d^{550}}$ is the weight of the ashes after the treatment at 550 ºC.

2.4. Disintegration test

Laboratory-scale disintegration test for S, PVA, S-PVA and composite films under thermophilic incubation period in composting conditions were carried out following an adapted method based on the current ISO 20200: 2004 International Standard. Polypropylene plastic boxes (20 x 30 x 12 cm) with a hole of 5 mm diameter to 6.5 cm height were used as reactors in order to provide gas exchange between the inner atmosphere and the outside environment. Approximately 5 g of films samples (25 x 25 mm) were weighted using an analytical balance (±0.00001 g) and then introduced in the reactors containing 1 kg of the produced synthetic waste. Reactors were also weighted (Sartorius, Goettingen, Germany) and introduced in an oven (Selecta, J.P. Selecta S.A., Barcelona, Spain) at 58 ± 2 ºC for 73 days. Throughout the test, the reactors were also weighted and, if needed, the initial mass was restored total or partially by adding de-ionized water. For each sample, 4 reactors were tested: 3 for the calculation of the percentage of disintegration (D), Eq. (3)) after the composting period, and 1 for the monitoring of the studied films during the process by thermogravimetric, structural and appearance analysis (t = 0 and 73 days).

$$D\ (\%) = \frac{m_i - m_r}{m_i}\ 100 \quad (3)$$

where m_i is the initial dry mass of the samples and m_r is the dry mass of the residual tested material.

2.5. Film characterization techniques

2.5.1. Moisture content

Moisture content (MC) was evaluated by film drying following the method described by Cano *et al*., (2015a). Firstly samples were dried in a vacuum oven at 60 ºC for 24 h. Later on, the pre-dried samples were transferred to desiccators containing P_2O_5 until

reaching a constant weight. Five replicates per film formulation were analysed before the composting process.

2.5.2. Structure and visual appearance

The microstructural analysis of the films was carried out by using optical microscopy (Leica, model DM LM, Química y Medio Ambiente S.L., Spain). To this end, films were dried in a vacuum oven at 60 ºC for 1 week, before the observations. Two replicates per formulation/time were observed at a magnification of 63X at time 0 and 73 days of composting period. Microscopy images were captured and digitised by a video module Leica ICC A (Integrated Camera Compound-Analogue) using the software Leica IM50 v. 1.2.

In order to analysed changes in the film's appearance and surface area photographs of films samples were taken by using a digital camera (Stylus XZ-2, Olympus, Indonesia) and image analysis were done by using the Photoshop CS4 (Adobe Systems Software Ireland) to determine the total area reduction of the films during composting.

2.5.3. Thermogravimetric analysis (TGA)

A thermogravimetric analyzer (Mettler Toledo, Switzerland) was used to obtain the thermal weight loss (TG) curve, and its derivative (DTG), of the samples. To this end, approximately 10 g of sample were poured in alumina crucible and heated from 25 ºC to 600 ºC at 10 ºC/min, using nitrogen flow. The onset, peak and end temperatures (T_0, T_p and T_e, respectively) were obtained for each degradation step in the films.

Prior to the analyses, the samples were dried in a convention oven at 60 ºC for one week and then were transferred to a desiccator with P_2O_5 until constant weight to ensure complete drying. The measurements were taken in duplicate for each film, before and after 73 days of the composting process.

2.6. Biodegradation test

The ultimate aerobic biodegradation level of films were tested under composting controlled conditions following the adapted method from the UNE-EN ISO 14855-1: 2012 European Standard. The test is based on the measure of the CO_2 generated in the process, which is considered proportional to the percentage of biodegradation.

Prior to the test, the C, N and H content of the different samples was determined by elemental analysis (Elemtan, microanalyzer, Eager 200, Micro TruSpec de LECO instrumentos S.L., Madrid, Spain) in duplicate.

For the biodegradation test, bioreactor consisted of a hermetic 2 litres glass jar, modified for air withdrawal with a rubber septum, containing two 60 ml polypropylene flasks. One of them contained 3 g of dry compost mixed with 50 mg of equivalent carbon ground dry samples and 1g of vermiculite. The other flask contained de-ionized water in order to ensure a 100 % RH. The bioreactors were closed and incubated at 58 ± 2 ºC for 45 days. S, PVA, S-PVA and composite films with the highest concentration of each antimicrobial compound (S-PVA-2O, S-PVA-2N and S-PVA-4Ag) were tested. The blank samples contained only compost and CMC (cellulose microcrystalline from Sigma Aldrich Química S.L., Madrid, Spain) mixed with compost as a reference sample was also analysed. All samples were measured in triplicate.

The change in the gas composition inside each bioreactor was monitored during the biodegradation process by means of an O_2 and CO_2 gas analyser (Dansensor, Checkmate 9900, Spain) in order to calculate the CO_2 produced. Oxygen concentration was maintained above 6% throughout the experiment to ensure aerobic conditions. To this end, flasks were periodically open (24 hours after ach determination).

The theoretical amount of CO_2 (Eq. 5) corresponding to the total sample degradation and the percentage of biodegradation (Eq. 6) were calculate according to Balaguer *et al*., 2015, assuming that for degraded sample, all carbon was converted in CO_2.

$$CO_2^{Th} = Ws\,.\,Cs.\frac{MWco_2}{MWc} \quad (5)$$

$$B\,(\%) = \frac{\sum CO_{2S} - \sum CO_{2B}}{CO_2^{Th}}\ 100 \quad (6)$$

where Ws is the dry weight of the samples, Cs is the proportion of organic carbon in the dry samples and, $MWco_2$ and MWc are the molecular weights of carbon dioxide and carbon, respectively. $\sum CO_{2s}$ and $\sum CO_{2B}$ are the CO_2 accumulative amount produced in the sample and blank bioreactor, respectively.

Hills equation (Eq. 7) was used to fit kinetics of sample biodegradation:

$$\%B = \%Bmax\ \frac{t^n}{k^n + t^n} \quad (7)$$

where $= \%Bmax$ is the percentage of biodegradation at infinite time, t is the time, k is the time at which the 50 % of the maximum biodegradation occurred (0.5 % $Bmax$) and n is the curve radius of the sigmoid function.

2.7. Statistical analysis

Statgraphics Centurion XV.I (Manugistics Corp., Rockville, MD) was used in order to carry out the statistical analysis of results through analysis of variance (ANOVA). To differentiate samples, Fisher's least significant difference (LSD) was used at the 95 % confidence level.

3. RESULTS AND DISCUSSION

3.1. Compost properties

Table 2 shows the dry matter (DM) and burned-out solids (BS), as a measure of the organic matter content, and the ratio N/C of the used synthetic compost before and at the end of the composting process. The three parameters significantly decreased ($p<0.05$) after 73 days of the composting period, due to the aerobic activity of the microorganisms involved in the fermentation at 58 ºC. The fermentation also provoked some colour changes in the compost, which turned darker, in agreement with that observed by other authors (Arrieta *et al*, 2014).

Table 2. Dry mass (DM) and burned-out solids (BS) of the synthetic compost at the beginning (0 day) and at the end (73 days) of the composting process.

Composting time	DM (%)	BS (%)	C/N ratio
0 day	143±6[a]	96±2[a]	48±2[a]
73 days	93±5[b]	88±3[b]	42±2[b]

[a, b] different letters in the same column indicate significant differences among formulations ($p<0.05$).

3.2. Moisture content and thickness of films

The moisture content (MC) of pure starch and PVA films was 4.6 % and 6.85 %, respectively. The MC values for blend S-PVA films, with and without antimicrobials, are shown in Table 3, which ranged between 4.6 - 6.4 %. In general, MC values were not significantly affected by the incorporation of the different antimicrobial agents. Likewise, blend film thickness values ranged between 58-74 μm (Table 3) and for neat polymer matrices, these were between 60-80 μm. Some differences were found among films, in spite of using the same solid surface density in the casting process for all the samples. In general, films containing oils were thicker than the blend S-PVA, whereas AgNPs

composite films were the thinnest. Zivanovic *et al*. (2005) and Benavides *et al*. (2012) also described an increase in the film thickness due to the oil incorporation. On the contrary, AgNPs seems to provoke a greater chain aggregation due to the more intense interaction forces, leading to an increment in the film compactness.

Table 3. Film´s moisture content (MC) and thickness (mm) before the composting process and percentage of disintegration ($\%D_{73}$) and surface reduction (ΔS_{73}) of the films after 73 days under aerobic composting conditions.

Films	MC (% d.b.)	Thickness (mm)	$\%D_{73}$	ΔS_{73} (%)
S-PVA	5.4 ± 0.9^{ab}	0.067 ± 0.013^{a1}	60 ± 4^{a}	35 ± 7^{ab}
S-PVA -1O	5.13 ± 0.09^{d}	0.073 ± 0.006^{b1}	59 ± 3^{ab}	31 ± 2^{a}
S-PVA -2O	5.6 ± 0.7^{c}	0.074 ± 0.011^{b1}	68 ± 3^{c}	60 ± 19^{b}
S-PVA-1N	6.4 ± 0.2^{b}	0.064 ± 0.003^{a1}	63 ± 2^{abc}	57 ± 6^{b}
S-PVA-2N	4.64 ± 0.12^{e}	0.074 ± 0.014^{b1}	64 ± 2^{bc}	55.6 ± 1.4^{b}
S-PVA-1Ag	6.06 ± 0.13^{ab}	0.063 ± 0.004^{a1}	60.24 ± 1.1^{ab}	50.434 ± 1.1^{b}
S-PVA-2Ag	6.33 ± 0.14^{ab}	0.058 ± 0.004^{c1}	63.83 ± 1.0^{bc}	45 ± 20^{ab}
S-PVA-3Ag	6.0 ± 0.2^{a}	0.059 ± 0.004^{c1}	63.7 ± 0.5^{bc}	68 ± 20^{b}
S-PVA-4Ag	5.11 ± 0.13^{ad}	0.062 ± 0.007^{a1}	66.5 ± 1.5^{c}	60 ± 11^{b}

$^{a, b, c, d, e}$ different letters in the same column indicate significant differences among formulations ($p<0.05$).

3.3. Disintegration test

The degree of disintegration (D) of films when exposed to a laboratory-scale composting environmental conditions (58 ± 2 ºC for 73 days) informed about the physical breakdown of the material into smaller fractions. The test was validated according to the standard method, which established a BS reduction (R) in the control sample of the compost greater than 30 %, with standard deviation for % D values lower than 10 units.

In the performance tests, R ranged between 55 ± 4 and 62 ± 2 % and the standard deviations for % D values were lower than 10, as shown in Table 3.

The disintegration values (D) of pure starch and PVA films were 97 ± 3 % and 3 ± 2 %, respectively. The values found for blend films with and without antimicrobials, shown in Table 3, revealed that S-PVA films exhibited intermediate D values (60 ± 4) between those obtained for both, pure S and PVA films. Azhari *et al*., 2011 also observed that the presence of starch into PVA films favoured the film disintegration, while pure PVA films exhibited a strong resistance. Hashimoto *et al*., (1980) reported that the bacteria capable of degrading PVA are commonly distributed in various environments, but a long period is necessary to observe an apparent PVA-degrading activity.

The incorporation of active substances significantly increased the D values (Table 3), this effect only being significant when using the highest concentration of the essential oils and more than 2.1 wt.% of silver species in the total film solids (samples S-PVA-3Ag, S-PVA-4Ag). Several authors have attributed this effect to the lower mechanical resistance of these samples (Rhim *et al*., 2013), in line with the continuity interruption of the polymer network by the presence of oil droplets/solid particles and the weaker interactions between polymer chains, which enhance the matrix erosion. This behaviour was more noticeable in films containing the highest content of oregano essential oil, surely because of its greater content of volatile compounds, in comparison with Neem oil. Neem oil is mainly constituted by long fatty acids (oleic, stearic, and palmitic acids), which became around the 87 % of the total (Vijayan *et al*., 2013) and 97 % of oregano essential oil are constituted by volatile compounds (Milos *et al*., 2000). The volatilization of the oil compounds led to presence of empty voids in the polymer network, thus contributing to the mechanical instability. Similar effect was described for PLA-PHB films containing limonene as antimicrobial agent (Arrieta *et al*., 2014).

Visual appearance of the recovered films at different disintegration days of exposure to composting conditions are shown in Figure 1, where the different degradable character of the samples can be observed. At the beginning of the process, all films exhibited a continuous structure with no visible holes. It is also possible to observe that the PVA films were more transparent than S films, in agreement with that previously reported (Cano *et al*., 2015a). The incorporation of antimicrobial oils conferred opacity and yellowness colour to the films, meanwhile the AgNPs, led to brownish films as a consequence of the silver reduction to form silver nanoparticles. This generated a yellow to brownish colour attributed to their characteristic surface plasmon resonance (Torres-Castro *et al*., 2011). These effects were more marked when the concentration of the antimicrobial agents rose in the films.

After the composting process, S films were completely disintegrated while PVA films were almost no degraded. Blend films with and without antimicrobial agents exhibited an intermediate behaviour, as commented on above. In the case of silver loaded films, some metallic silver spots appeared throughout the time, surely due to the agglomeration of silver particles.

Figure 2 shows the development of the film surface area (mm^2) for S, PVA and S-PVA films with and without antimicrobials at different times under composting conditions. Two different behaviours were observed. On the one hand, the surface of some films (S, blend films with O and silver loaded films) continuously decreased throughout the composting period, or even completely disappeared after 14 days (as in the case of S film). This fast disintegration of the pure starch films could be related to the high diffusion of water into the matrix, due to its high hydrophilic nature.

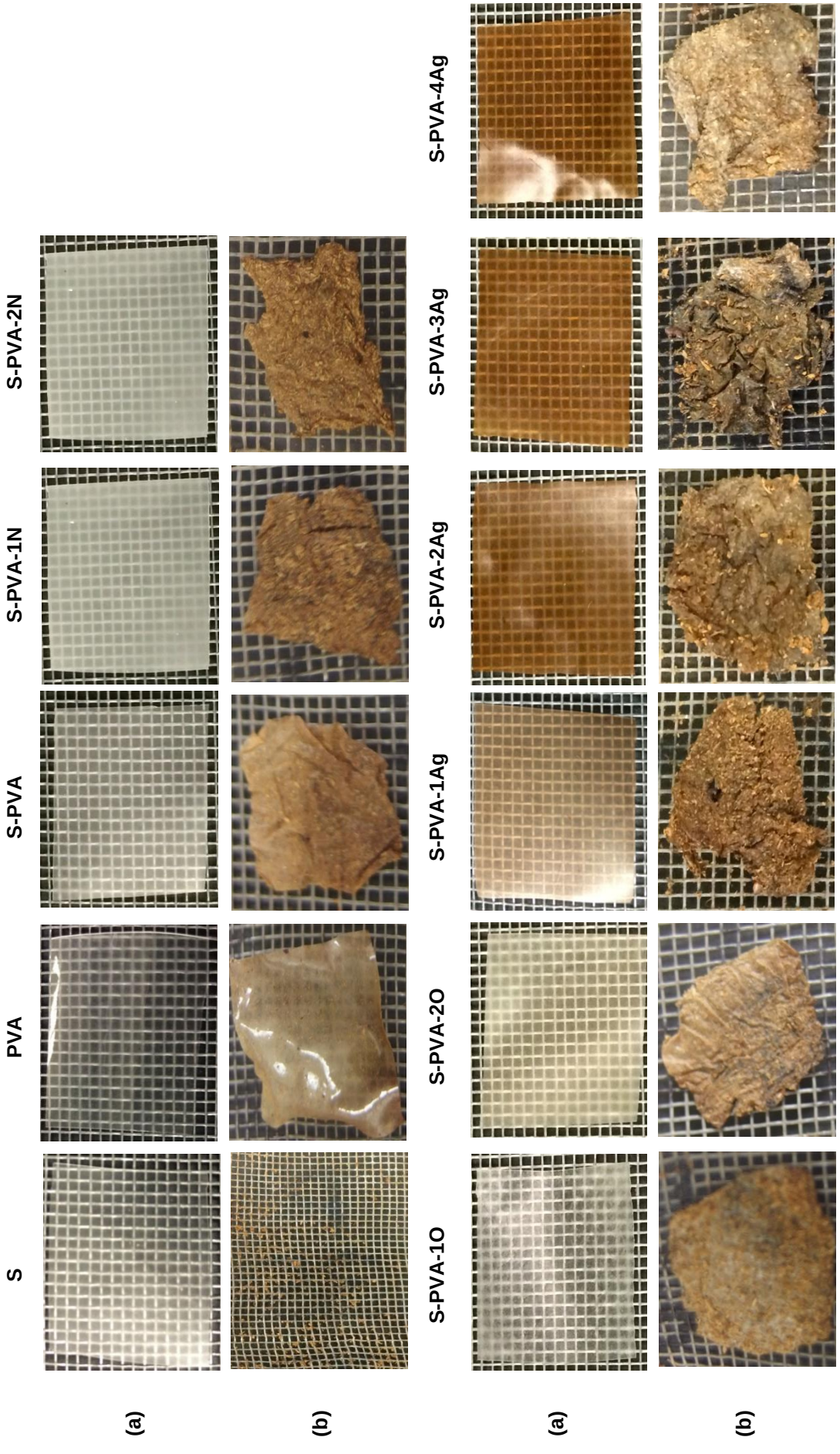

Figure 1. Visual appearance of S. PVA and S-PVA films with and without antimicrobials before (a) and after (b) 73 days of the composting process.

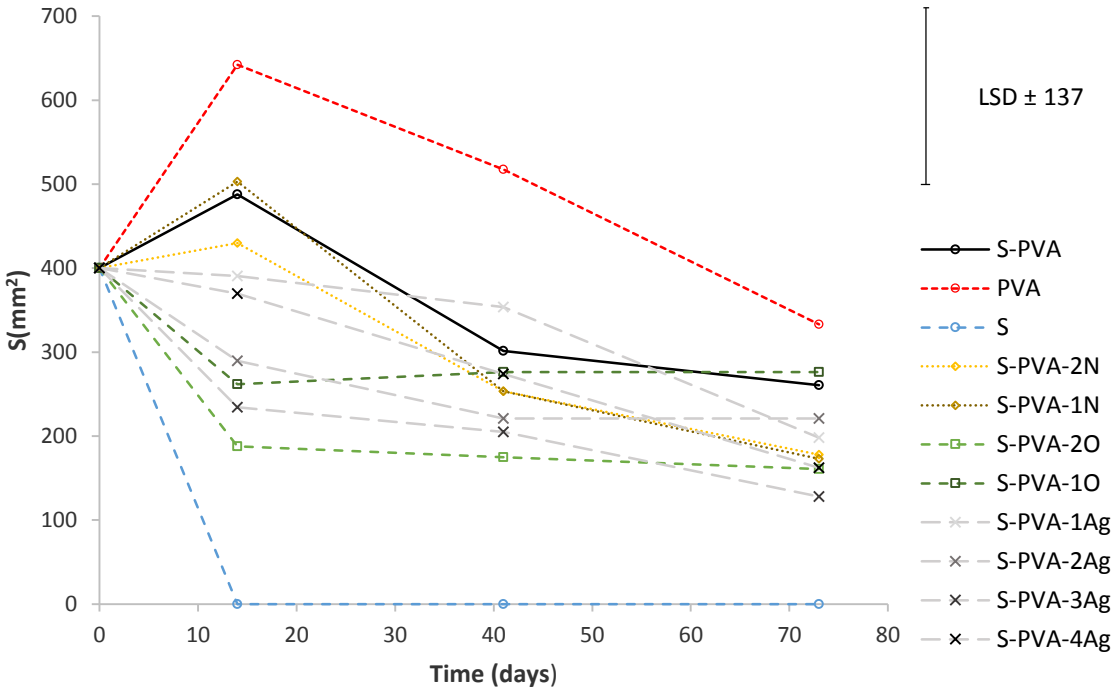

Figure 2. Development of the film surface area reduction (mm^2) throughout composting process for the different films.

On the other hand, neat PVA films and blends with neem underwent a surface expansion during the first 14 days, attributed to the water absorption and the subsequent swelling of the polymer network. Afterwards, a gradual reduction in their surface area was observed.

Observed differences between both film groups can be explained taking into account the rate at which the different phenomena involved in the degradation process occur: in the first group (where no swelling is detected), the degradation rate of the polymer backbone seems to be faster than the diffusion of water penetrating through the polymer. In this case, surface erosion quickly occurred, without enough time for water diffusion through the material and film swelling. In the second film group, the water diffusion process was faster than the degradation process; then, the polymer swelled and bulk erosion occurred more delayed (Burkersroda *et al.*, 2002).

In Table 3, the total surface reduction reached by the films after the composting period is shown. The surface of S-PVA films were reduced around 35 ± 7 % and, in general, the incorporation of antimicrobials agents led to significantly greater values (around 60 %, regardless of the type of antimicrobial), in agreement with the disintegration (D) values.

3.4. Structure of films throughout the composting period

Figure 3 (a) shows the optical microscopy images of S, PVA and blend films before the composting process. S films exhibited a homogenous microstructure much more disordered than the smooth surface showed by PVA, in which the alignment of the polymer chains can be deduced. Blend films were more heterogeneous, due to the lack of polymer miscibility and the co-existence of two phases, as previously reported (Cano *et al*., 2015a-b). At the end of the composting process (Figure 3b), PVA and blend films exhibited more disordered and fragile structures. Images of pure S films at the end of the composting period are not shown because they completely disintegrated after 7 days.

The incorporation of the different active compounds led to different structure and appearance of the film, with respect to the S-PVA films, especially before the composting period (Figures 4 and 5). The incorporation of oregano essential oil provoked films with coarser structure in comparison with those containing neem oil (Figure 4). The different nature of the lipids and the interactions established with the polymer network will define the final structure, appearance and mechanical resistance of the composite films (Fabra *et al*., 2009).

Films incorporating different contents of AgNPs showed similar structures than S-PVA films at the magnification level of the microscopic observations. Thus, in Figure 5 only the silver loaded films with the lowest (S-PVA-1Ag) and the highest (S-PVA-4Ag) silver concentrations are shown. Composting time affected in all cases the observed film

structure, giving rise to more porous systems, where holes could be observed in some cases.

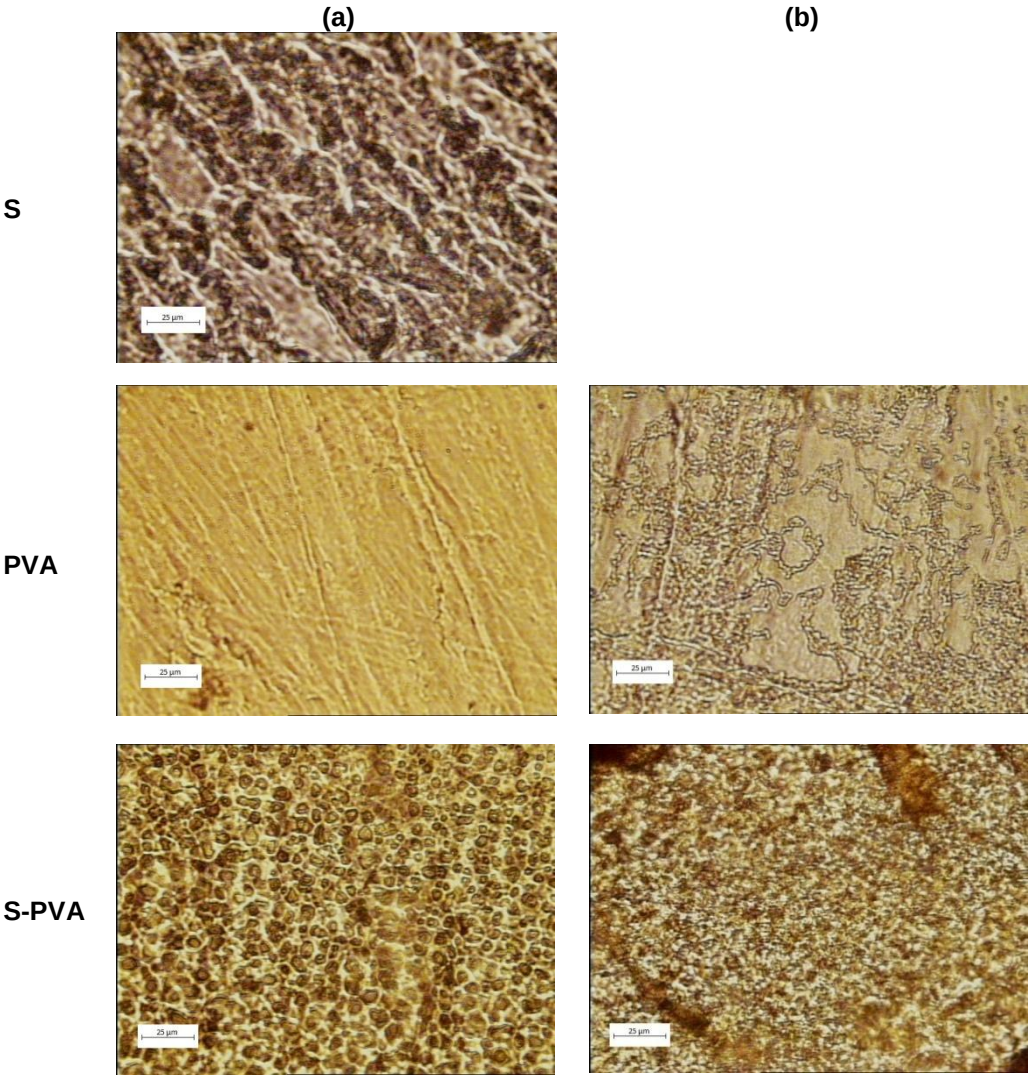

Figure 3. Optical microscopy images (x63) of S, PVA and S-PVA films before (a) and after (b) 73 days of the composting process.

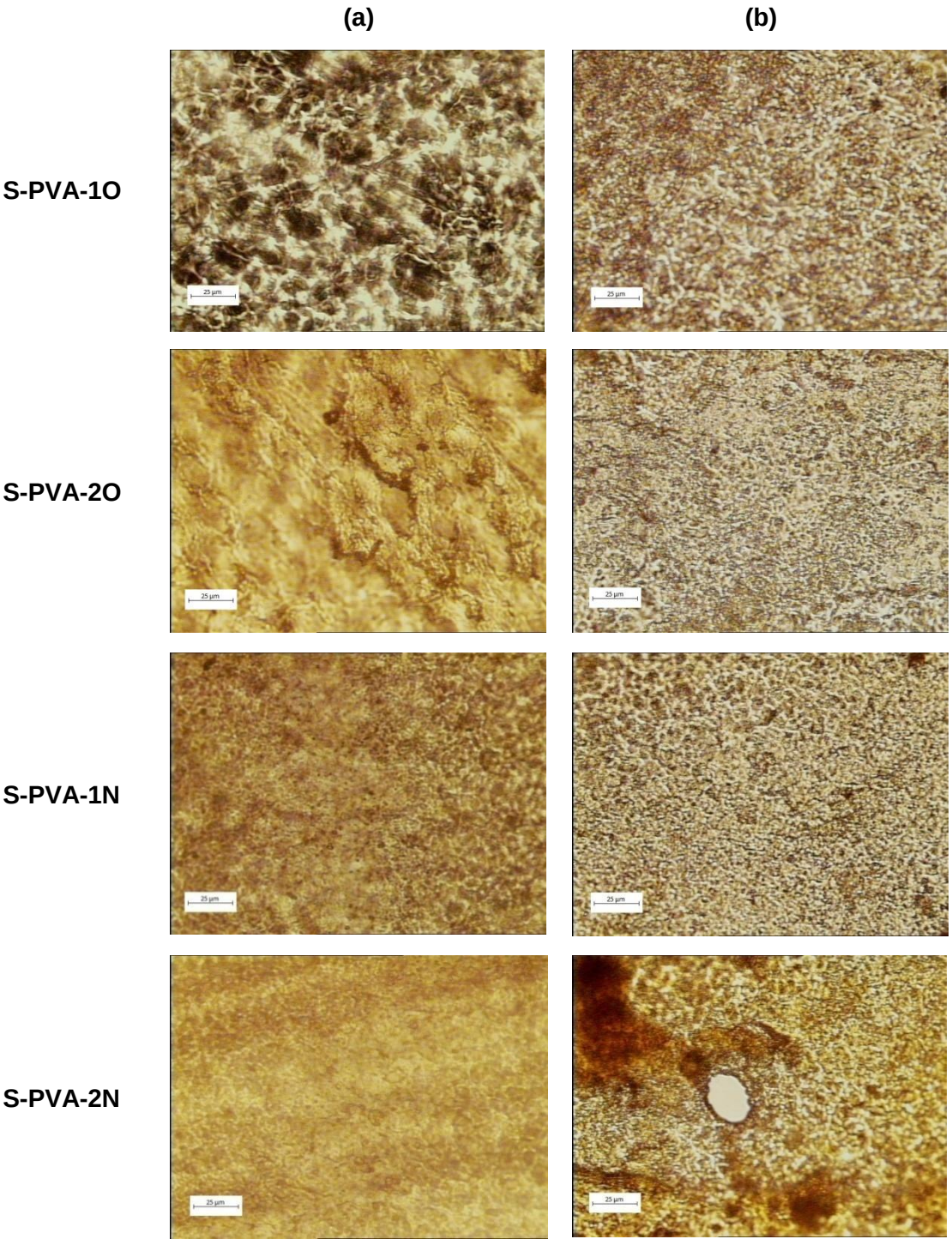

Figure 4. Optical microscopy images (x63) of oil composite films before (a) and after (b) 73 days of the composting process.

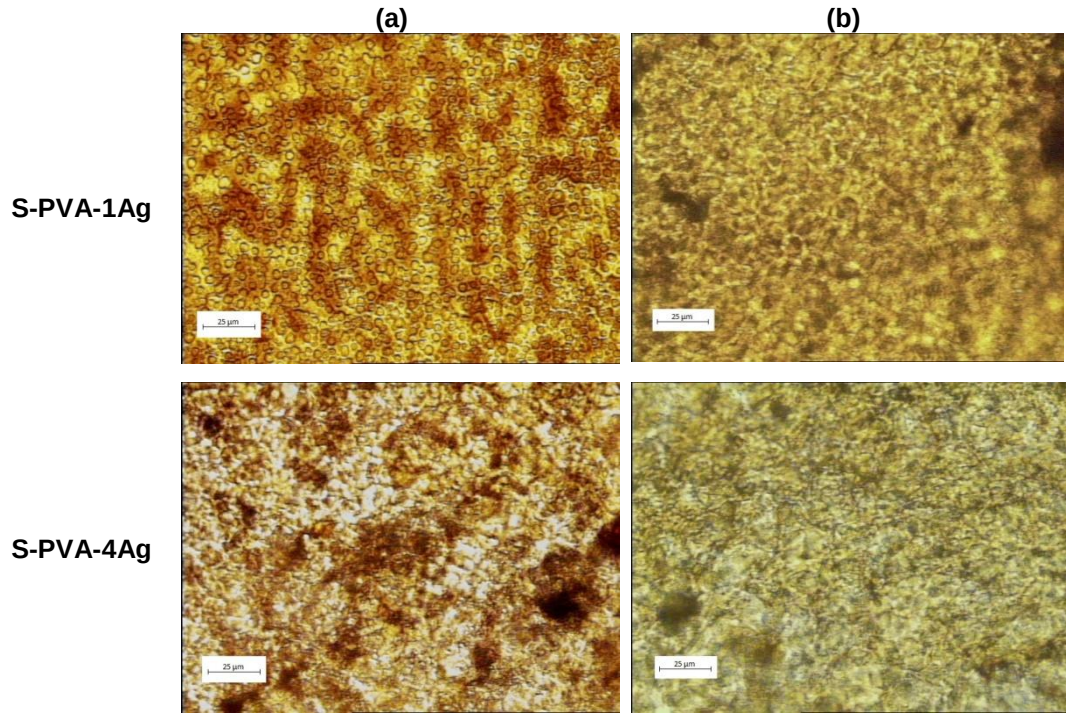

Figure 5. Optical microscopy images (x63) of silver loaded films (a) before and (b) after 73 days of the composting process.

3.5. Thermogravimetric behaviour

Changes in the thermal decomposition of S, PVA and S-PVA films during composting process was studied trough TGA (a) and DTG (b) curves (Figure 6). S-PVA films with antimicrobial substances (data non-shown) exhibited similar behaviour than S-PVA blend.

Starch showed a typical single decomposition step with a maximum degradation rate focused at 315 ºC. On the contrary, pure PVA films exhibited two process steps: the first one occurred between 260 and 357 ºC (sample weight loss about 80 %), in which the dehydration of the PVA takes place, followed by chain scission and decomposition (Frone *et al*., 2011). The second step, around 387 and 450 ºC, was attributed to the degradation of the by-products generated by PVA during the thermal process (Bonilla *et al*., 2014). In the case of S-PVA blend films incorporating or not antimicrobials, three process steps were observed. Their onset (T_0), peak (T_p) and end (T_e) temperatures for

these degradation steps before and after the composting process are shown in Table 4. In these S-PVA films, the first step shows a maximum degradation rate (T_p) at relatively low temperature, around 200 ºC, attributed to thermo-degradation of the starch fraction. The second and third steps were similar to those observed for pure PVA films, showing peak temperatures at 305 and 417 ºC, respectively. These results agree with those previously reported by Sreekumar *et al*. (2012) and Cano *et al*., 2015b for starch:PVA films with different polymer ratios.

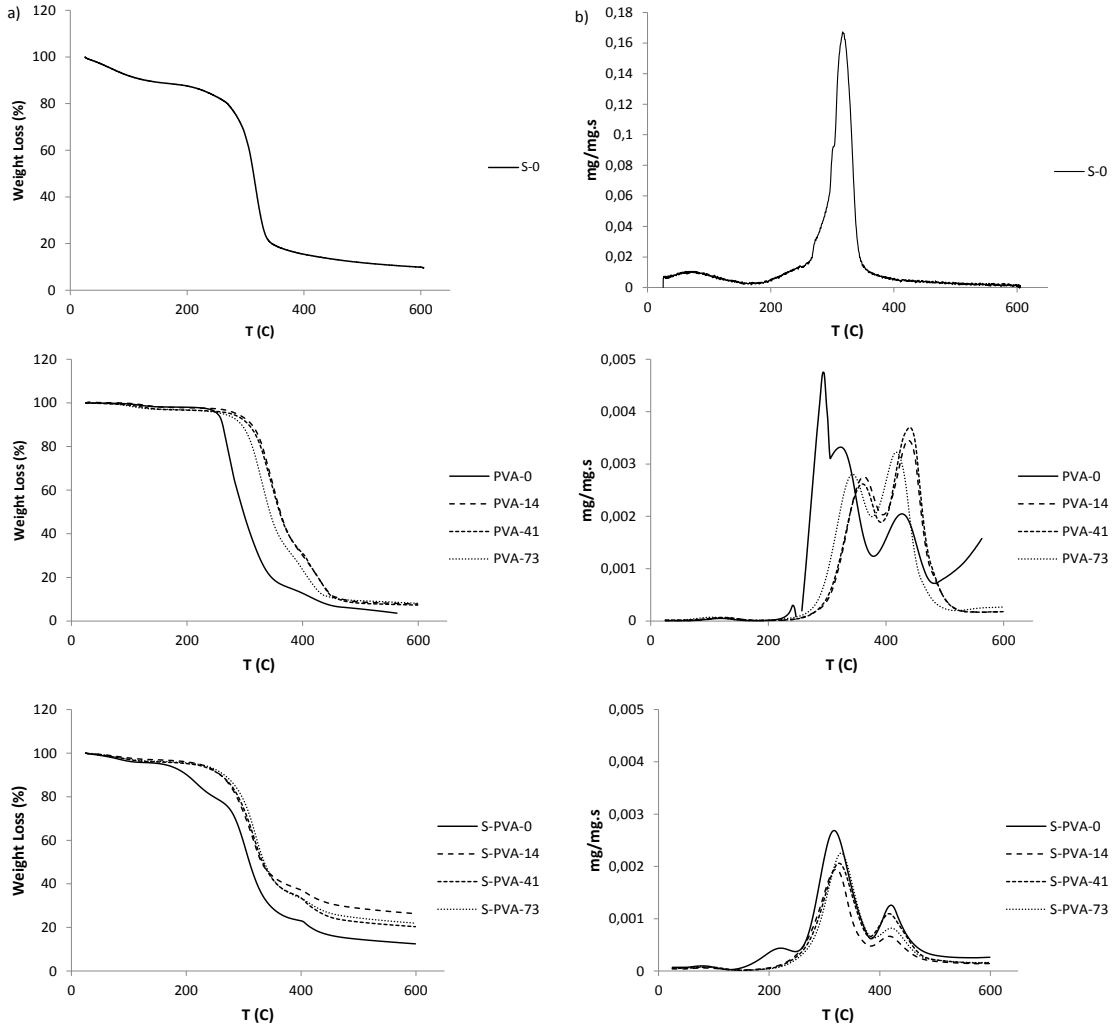

Figure 6. a) TG and b) DTG curves of S, PVA and S:PVA films at different times under composting process.

The addition of antimicrobial oils (Oregano and Neem) did not significantly affect ($p>0.05$) the onset, peak and end temperatures of the three degradation processes. Nevertheless, silver loaded films were less thermostable ($p<0.05$), as they exhibited lower T_o and T_p values especially when the silver content of the films rose. The presence of ions (NO_3^-) and silver species could reduce the extent of the polymer chain interactions, in line with the effect of the ionic strength on the chain folding degree in the film forming dispersion, thus reducing the film thermal stability.

The influence of the composting time was noticeable for the first and second thermal degradation steps of S-PVA films. The first step disappeared in all samples, coherently with the degradation of starch, which is not notably present in the degraded films. In general, the temperatures of the second step increased for samples biodegraded for 73 days, which suggests that the residual components in the films were also the more thermostable. This behaviour has been also observed in pure PVA films by Tudorachi *et al*. (2000) for different S-PVA ratios. Therefore, a faster degradation of the species less thermo resistant occurred during the composting process.

The percentage of residual mass at 600 ºC is also shown in Table 4. All formulations showed low pyrolysis residuals wastes, which increased ($p<0.05$) in some cases at the end of the composting period.

Table 4. Onset, peak and end temperatures (T_o, T_p, T_e respectively) and residual mass obtained from TGA analysis of S-PVA blend films before and after 73 days of the composting process.

Films	Time (days)	First degradation step (starch fraction)			Second degradation step (PVA fraction)			Third degradation step (PVA fraction)			Residual mass
		T_0	T_p	T_e	T_0	T_p	T_e	T_0	T_p	T_e	
S-PVA	0	163±12^{a}	210±7^{ab}	244±3^{a}	262.3±1.6^{a1}	305.3±0.7^{a1}	357.4±1,7^{a1}	387,8±1,7^{a1}	417±2^{a1}	447±3^{a1}	13.7±0.3^{a1}
	73				264±6^{a1}	316±6^{a2}	362±8^{a1}	390±3^{a1}	421.3±1.4^{a}	457±2^{a1}	24±3^{a2}
S-PVA-1O	0	150±21^{abc}	202±5^{ac}	238.6±0.3^{ab}	258.2±0.7^{a1}	307.09±0.12^{a1}	305±69^{b1}	393±3^{a1}	431±10^{b1}	458±12^{a1}	15.24±0.0
	73				267±2^{a2}	320.4±1.5^{ab2}	369±6^{a2}	390±3^{a1}	420±3^{a2}	458±2^{a1}	22±2^{a1}
S-PVA-2O	0	169±5^{a}	210.5±0.5^{a}	243.9±0.2^{abc}	261.59±1.06^{a1}	311.0±1.2^{a1}	361±7^{a1}	389±8^{a1}	423±2^{ab1}	457±7^{a1}	11.6±1.2^{a1}
	73				269±10^{a1}	325±9^{b2}	372±10^{a1}	390±6^{a1}	419±4^{a1}	452±2^{a1}	25±10^{a2}
S-PVA-1N	0	168±3^{a}	213.4±1.8^{b}	247.1±0.9^{ac}	265.2±0.2^{a1}	307.3±0.2^{a1}	362.4±1.8^{a1}	394±3^{a1}	421±2^{a1}	448±1^{a1}	12.9±0.9^{a1}
	73				266.6±1.7^{a1}	320.4±0.6^{ab2}	373±2^{a1}	392±2^{a1}	420.3±1.3^{a}	457.4±0.4^{a1}	23.42±1.0
S-PVA-2N	0	157±3^{a}	206±2^{ab}	292±69^{c}	263.2±1.3^{a1}	308.42±0.12^{a1}	397±23^{a1}				9.5±0.3^{a1}
	73				266.4±0.2^{a1}	323±2^{b2}	375±8^{a1}	391±7^{a1}	419±6^{a}	453.7±1.2^{a}	24±2^{a2}
S-PVA-1Ag	0	153.36±1.14^{ab}	193.5±0.7^{c}	225.7±0.9^{ab}	243.8±0.4^{b1}	286.8±0.8^{b1}	338.7±1.3^{b1}	369±5^{b1}	396±5^{c1}	421±5^{b1}	17.0±1.7^{ab}
	73				238±7^{b1}	295±5^{b2}	340±7^{b1}	354±8^{b1}	385±9^{b1}	439.6±0.3^{b1}	19.75±1.0
S-PVA-2Ag	0	135±3^{bcd}	181.9±0.8^{d}	227,8±1.5^{ab}	246.9±0.9^{b1}	287±2^{b1}	333±5^{b1}				21.21±0.0
	73				216±4^{c2}	282±8^{c1}	331±8^{b1}				30±12^{a1}
S-PVA-3Ag	0	133.4±0.9^{cd}	169.6±0.4^{e}	216.83±1.15^{a}	246.1±0.2^{b1}	287.3±0.4^{b1}	332±3^{b1}				21.25±0.1
	73				224±15^{bc2}	287.6±1.8^{bc1}	336±5^{b1}				27±6^{a1}
S-PVA-4Ag	0	119.5±1.9^{d}	154±5^{b}	196±8^{b}	245.0±0.2^{b1}	286.5±0.9^{b1}	330.1±1.4^{b1}				25±1^{b1}
	73				226.3±2.3^{bc2}	289.4±0.2^{bc1}	335.1±0.2^{b1}				31.6±0.6^{a1}

$^{a, b, c,}$ different letters in the same column indicate significant differences among formulations at the same time of the analysis (0 or 73 says) ($p<0.05$).

^{1,2,} different numbers in the same column indicate significant differences between times for the same formulation ($p<0.05$).

3.6. Biodegradation behaviour

Biodegradability of films was evaluated submitting the samples under laboratory-scale composting environmental conditions (58 ± 2 ºC for 45 days). Prior to the test, the theoretical maximum quantity of carbon dioxide that can be produced by the biodegradation of the samples was calculated from their carbon content, which was determined by elemental analysis (Table 5). Cellulose microcrystalline (CMC) was also evaluated and used as positive reference.

Table 5. Elemental composition (Nitrogen-N, Carbon-C, Hydrogen-H) of cellulose microcrystalline (CMC) and S-PVA blend films with and without antimicrobial agents.

Sample	N (%)	C (%)	H (%)
CMC	0.145±0.02	42.2±0.2	5.9±1.3
S-PVA	0.12±0.02	44.41±0.04	4.91±0.7
S-PVA-2O	0.11±0.02	47.5±0.2	6.0±0.6
S-PVA-2N	0.11±0.02	50.745±0.106	6.8±1.5
S-PVA-4Ag	0.100±0.014	36.60±0.03	4.2±0.6

Figure 7 shows the biodegradation kinetics in terms of percentage of biodegradation (Eq. 6) as a function of time for CMC, S, PVA and S-PVA films (Figure 7a) and for S-PVA films containing the highest concentration of antimicrobials (S-PVA-2O, S-PVA-2N and S-PVA-4Ag) (Figure 7b).

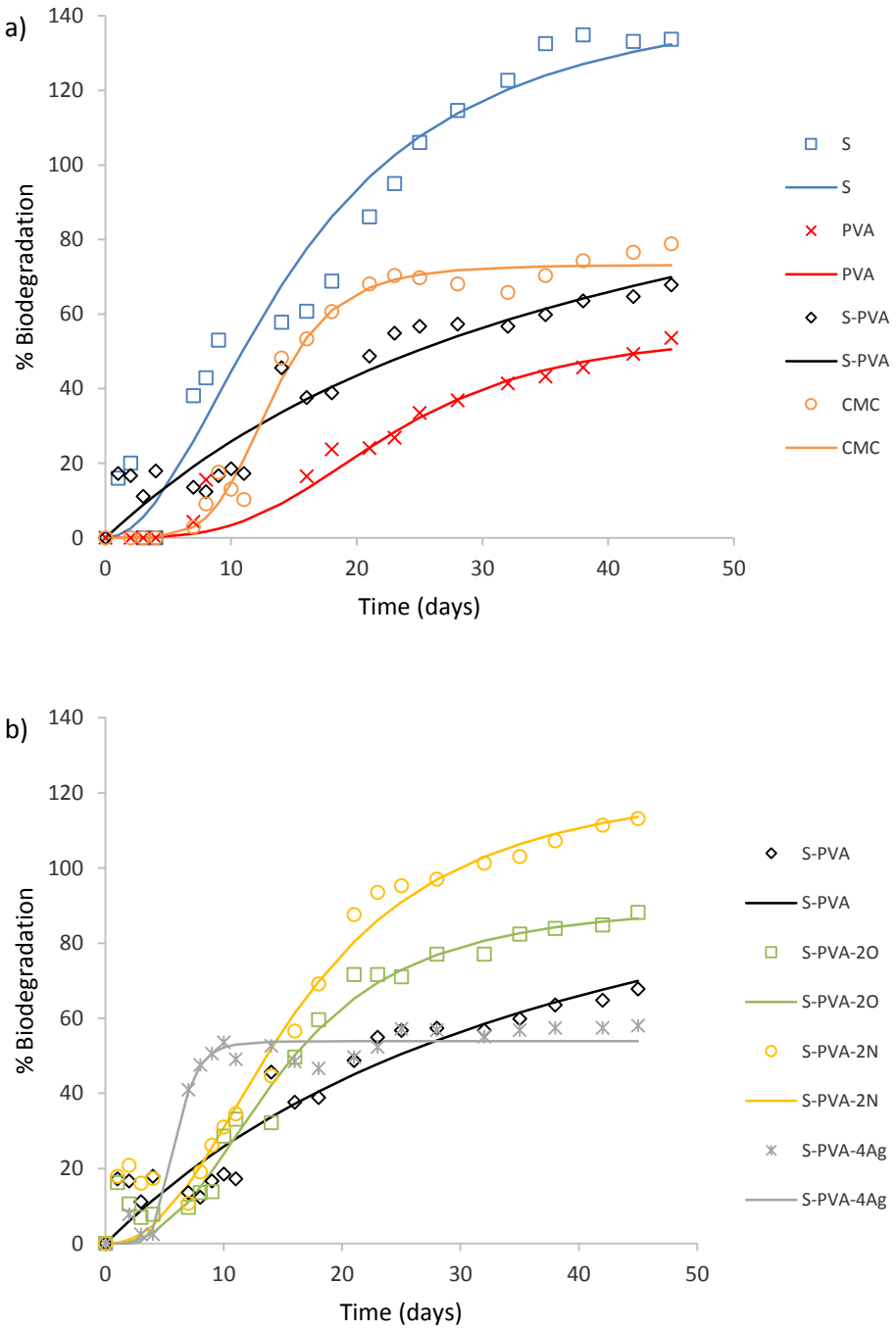

Figure 7. Biodegradation kinetics of a) CMC, starch, PVA and S-PVA films and b) S-PVA films with and without antimicrobials throughout the composting time. Experimental data (symbols) and fitted Hill's equation (lines).

Starch and CMC exhibited the characteristic sigmoid profiles of respirometric test with three different phases (an initial lag period lasting 2-8 days, a biodegradation phase

and a plateau), in agreement with that reported by Balaguer *et al*., 2015. For both polysaccharides, glycosidases are responsible of the cleavage of glycosidic bonds, amylases act on starch hydrolysing the α-1,4 and/or α-1,6 glucoside linkages and cellulases act on cellulose β-1,4 glucoside linkages (Whitaker *et al*., 1994). The link of water-induced hydrolysis in the polymer's films and enzymatic degradation caused by microorganisms increased their susceptibility to biodegradation.

On the other hand, pure PVA films exhibited a flatter biodegradation profile, similar to that reported by Chiellini *et al*., 2003. In the initial biodegradation step, the specific oxidation of 1,3-hydroxil groups, mediated by oxidase and dehydrogenase type enzymes, is carried out to give β-hydroxilketones as well as 1,3-diketone moieties. The latter entities are susceptible to carbon-carbon bond cleavage promoted by specific β-diketone hydrolase, giving rise to the formation of carboxyl and methyl ketone end groups (Chiellini *et al*., 2003).

Starch films completely biodegraded (B = 100 %) after 32 days. After 45 days, they reached percentages of biodegradation greater than 100 % (134 %) which was also observed for S-PVA-2N. This effect is attributed to the priming effect, which occurs when the compost inoculum in the test reactor containing the samples is producing more CO_2 than the compost inoculum in the blank reactors, due to the stimulation of organic matter mineralization that occur after the addition of easily-decomposable organic matter (Kuzyakov *et al*., 2000). However, the mechanism by which priming effects are produced remain unknown (Fontaine *et al*., 2003), but it is believed that it is a natural process consequence of the interaction of microorganisms and organic matter (Balaguer *et al*., 2015).

S-PVA films showed an intermediate degradation profile between that showed by the pure polymeric films, thus suggesting that the vinyl polymer did not affect the microbial assimilation of the blend film under composting exposure. Thus, PVA

degradation was improved by the starch incorporation in the matrix, surely due to easier permeation of the enzyme into the film matrix (Azhari *et al*., 2011; Chiellini *et al*., 2003; Julinová *et al*., 2010; Jayasekara *et al*., 2003).

The incorporation of antimicrobial oils followed the same biodegradation profile trend as S-PVA films, whereas the silver films behaved completely different, exhibiting an active composting initial stage followed by a plateau period (Figure 7b). This difference is surely due to the higher antimicrobial activity of silver and its greater persistence throughout time in the environment, in comparison to oregano and neem oil.

Table 6 shows the percentage of biodegradation of films after 45 days (B_{45}) under controlled composting conditions. CMC reached 79 % of biodegradation after 45 days, in agreement to the level established by the ISO 14855 standard. The same percentage was obtained by Du *et al*., 2008 for this material. PVA films reached a 54 % of biodegradation after 45 days. Different authors has reported the important role played by the composting temperature and the type of active sludge on the biodegradation behaviour of PVA (Chiellini *et al*., 1999; Julinová *et al*., 2010).

The incorporation of antimicrobial substances tended to provide poorer biodegradation percentages (B_{45}), especially in samples containing silver (Table 6). Similar behaviour was found by Balaguer *et al*., (2015), for cinmaldehyde containing gliadin films. Nevertheless, no significant differences in the B_{45} values were found for the different film formulations if data variability is considered. (Mean variation coefficients 39%).

Biodegradation curves were fitted to Hill's equation (Eq. 7) and the fitting parameters are reported in Table 6. As expected, the maximum biodegradation percentage corresponded to the S films (148 %, due to the priming effect) while the minimum was observed for PVA films (56 %). The S-PVA blend films reached values of 102 %, which was closer to that found for pure S film. The presence of active antimicrobial compounds

does not inhibit the biodegradation process of film matrices, but they tend to reduce the percentage of final biodegradation level, depending on the antimicrobial effectiveness of the film. The most active antimicrobial films (silver loaded) exhibited the lower B_{45} values.

Table 6. Hill's parameters ($\%B_{max}$, k and n) percentage of biodegradation after 45 days of composting exposure ($\%B_{45}$), maximum biodegradation rate (τ_{max}) and time at this maximum ($t\tau_{max}$), for the different films and cellulose microcrystalline (CMC, reference).

	Hill's parameters						
Samples	$\%B_{max}$	k (days)	n	R^2	$\%B_{45}$	τ_{max} (%B/day)	$t\tau_{max}$ (days)
CMC	73	13.1	5.1	0.98	79	7.4	12
S	148	15.2	2.0	0.94	134	6.3	9
PVA	56	22.8	3.3	0.85	54	2.2	19
S-PVA	102	25	1.2	0.92	68	2.8	3
S-PVA-2O	91	14.8	2.6	0.97	88	4.7	11
S-PVA-2N	125	16.2	2.3	0.97	114	5.4	11
S-PVA-4Ag	54	5.9	6.6	0.98	58	14.7	6

$\%B_{max}$: Percentage of biodegradation at infinite time.

k: time required to reach 50 % of the maximum biodegradation.

n: curve radius if the sigmoid function.

$\%B_{45}$: Percentage of biodegradation at 45 days.

R^2: correlation coefficient for model fitting.

In general, about 15 days were required to reach 50 % of biodegradation (k values) in the films, except for pure PVA, S-PVA blend and silver containing films. 23-25 days, were needed for pure PVA, S-PVA blend, whilst films with silver only needed 6 days, coherently with the differences in the biodegradation pattern of these samples.

Figure 8 shows the biodegradation rates obtained from the first derivative of Hill's equation as a function of time, for each film. Table 6 shows the maximum biodegradation rate (τ_{max}) and the time needed to reach the maximum biodegradation rate ($t\tau_{max}$). PVA films and the blend S-PVA films without antimicrobials exhibited the most constant and low biodegradation rate, reaching a maximum of 2 %/day after 19 and 5 days, respectively. CMC, starch and S-PVA containing antimicrobial oils exhibited similar biodegradation rates, of about 5 to 7 %/ day, after 9-12 days, respectively. Silver loaded films showed the maximum biodegradation rate (about 15 %/day) after 6 days under composting exposure. Afterwards, a sharp decrease in the biodegradation rate was observed until the 15th day of composting. This behaviour could be associated with changes in the culture medium, where the release of the antimicrobial compounds could affect the compost microbial activity (Domenek *et al*., 2004, Balaguer *et al*., 2014).

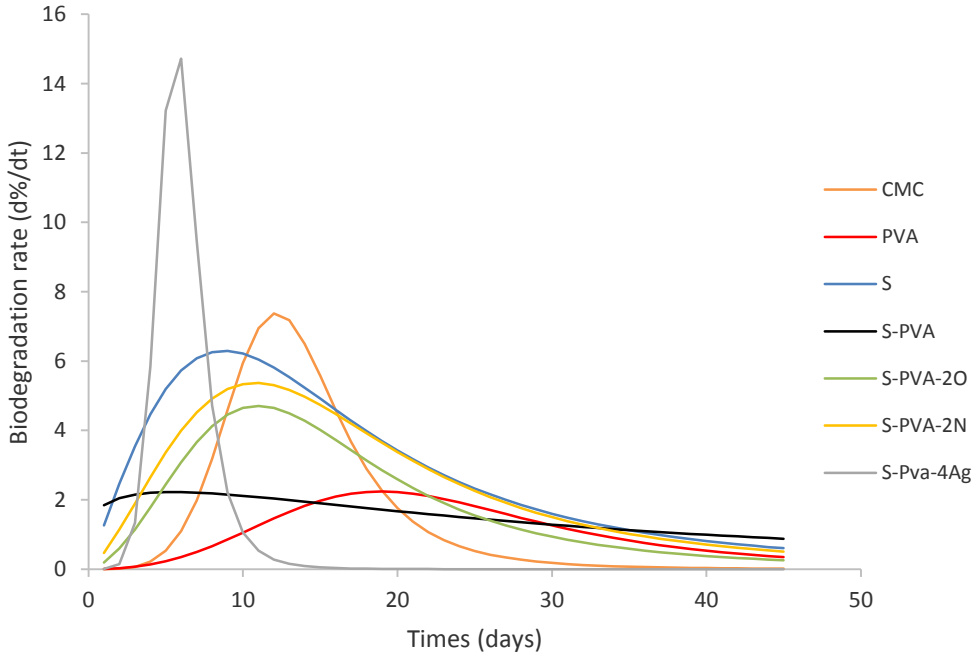

Figure 8. Biodegradation rates of CMC starch, PVA, S-PVA films with and without antimicrobials throughout the composting time.

4. CONCLUSIONS

The incorporation of starch into PVA films improved significantly its disintegration and biodegradation behaviour in comparison with those with pure PVA. The addition of antimicrobial substances enhanced film disintegration, due to the introduction of structural discontinuities in the polymer network; the greater the antimicrobial content the more intense the effect. Likewise, antimicrobials affected the biodegradation profile of starch-PVA films, depending on the type of and concentration of the compounds. Neem and oregano essential oils slightly decreased the maximum percentage of biodegradation without effect on the time needed to reach this maximum. However, silver species completely change the biodegradation profile of the films, slowing degradation rate and reducing the degradation extent, this suggesting a partial alteration of the compost inoculum.

On the basis of the obtained results, it is possible to conclude that the used concentrations of antimicrobial oils did not apparently compromise degradation of active S-PVA film. Thus, these active compounds provided additional functional properties to the films at the same time that satisfy the new consumer demand for friendly environmental technologies. In the case of silver loaded films, silver concentrations low in the dried film are recommended to avoid serious alterations in the biodegradation process. In the future, in vivo eco-toxicity studies will be carried out in order to evaluate the possible negative biological effect exerted by the metabolites from the biodegradation of these antimicrobial films.

Acknowledgements

The authors acknowledge the financial support from the Spanish Ministerio de Economía y Competitividad throughout the projects AGL2013-42989-R. Amalia Cano also thanks the Spanish Ministerio de Educación, Cultura y Deporte for the FPU grant.

References

- Aguirre, A., Borneo, R., & León, A. E. (2013). Antimicrobial, mechanical and barrier properties of triticale protein in films incorporated with oregano essential oil. *Food Bioscience*, 1, 2-9.
- Alvira, M.I. (2007). Los plásticos como residuos Antecedentes y Problemática Ambiental. Boletin Ambiental IDEA, Universidad Nacional de Colombia.
- Arrieta, M. P., Fortunati, E., Dominici, F., Rayón, E., López, J., & Kenny, J. M. (2014). PLA-PHB/ cellulose based films: Mechanical, barrier and disintegration properties. *Polymer Degradation and Stability*, 107, 139-149.
- Avella, M., De Vlieger, J. J., Errico, M. E., Fischer, S., Vacca, P., & Volpe, M.G. (2005). Biodegradation starch/clay nanocomposite films for food packaging applications. *Food Chemistry*, 93, 467-474.
- Avérous, L., & Pollet, E. (2012). Biodegradable polymers. In L. Avérous & E. Pollet (Eds), Environmental Silicate Nano-Biocomposites (pp. 13-39). *Springer-Verlag*, London. ISBN: 978-1-4471-4101-3. DOI: 10.1007/978-1-4471-4108-2_2.
- Azahari, N. A., Othman, N., & Ismail, H. (2011). Biodegradation studies of polyninyl alcohol/corn starch blend films in solid and solution media. *Journal of Physical Science*, 22(2), 15–31.
- Balaguer, M. P., Villanova, J., Cesar, G., Gavara, R., & Hernández-Muñoz, P. (2015). Compostable properties of antimicrobial bioplastics base don cinnamaldehyde cross-linked gliadins. *Chemical Engineering Journal*, 262, 447-455.
- Benavides, S., Villalobos-Carvajal, R., & Reyes, J.E. (2012). Physical, mechanical and antibacterial properties of alginate films: Effect of the crosslinking degree and oregano essential oil concentration. *Journal of food engineering*, 110, 232-239.
- Bonilla, J., Fortunati, E., Atarés, L., Chiral, A., & Kenny, J. M. (2014). Physical, structural and antimicrobial properties of poly vinyl alcohol-chitosan biodegradable films. *Food Hydrocolloids*, 35, 463-470.

- Burkersroda, F. V., Schedl, L., & Gopferich, A. (2002). Why degradable polymers undergo surface erosion or bulk erosion. *Biomaterials*, 23, 4221-4231.

- Cano, A. I., Cháfer, M., Chiralt, A., & González-Martínez, C. (2015a). Physical and microstructural properties of biodegradable films based on pea starch and PVA. Journal of Food Engineering, 167, 59-64.

- Cano, A., Fortunati, E., Cháfer, M., Kenny, J.M., Chiralt, A., & González-Martínez, C. (2015b). Properties and ageing behaviour of pea starch films as affected by blend with poly(vinyl alcohol). *Food Hydrocolloids*, 48, 84-93.

- Cano, A., Jiménez, A., Cháfer, M., González, C., & Chiralt, A. (2014). Effect of amylose:amylopectin ratio and rice bran addition on starch films properties. *Carbohydrate Polymers*, 111, 543-555.

- Chaléat, C.M., Halley, P.J.H., & Trussb, R.W. (2012). Study on the phase separation of plasticised starch/poly(vinylalcohol) blends. *Polymer Degradsdation and Stability*, 97, 1930-1939.

- Chen, L., Iman, S. H., Gordon, S. H., & Greène, R. V. (1997). Starch-polyvinyl alcohol crosslinked films-performance and biodegradation. *Journal of Environmental Polymer Degradation*, 5 (2), 111-117.

- Chiellini, E., Corti, A., D'Antone, S., & Solaro, R. (2003). Biodegradation of poly (vinyl alcohol) based materials. *Progress in Polymer Science*, 28, 963-1014.

- Chiellini, E., Corti, A., & Solaro, R. (1999). Biodegradation of poly(vinyl alcohol) based blown films under different environmental conditions. *Polymer Degradation and Stability*, 64, 305-12.

- Corrales, M., Fernández, A., & Han, J.H. (2014). Chapter 7, Antimicrobial packaging systems. In J. H. Han (Ed.), Innovations in food packaging (second edition) (pp. 133-170). *Academia Press: San Diego*, CA, USA.

- European Parliament and Council directive 94/62/EC of 20 December 1994 on packaging and packaging waste.

- Domenek, S., Feuilloley, P., Gratraud, J., Morel, M. –H., & Guilbert, S. (2004). Biodegradability of wheat gluten based bioplastics. *Chemosphere*, 54, 551-559.

- Du, Y. L., Cao, Y., Fang, L., Li, F., Cao, Y., Wang, X-L., & Wang, Y-Z. (2008), Biodegradation behaviours of thermoplastic starch (TPS) and thermoplastic dialdehyde starch (TPDAS) under controlled composting conditions. *Polymer Testing*, 27, 924-930.

- Fabra, M. J., Jiménez, A., Atarés, L., Talens, P., & Chiralt, A. (2009). Effect of fatty acids and beeswax addition on properties of sodium caseinate dispersions and films. *Biomacromolecules*, 10, 1500-1507.

- Fontaine, S., Mariotti, A., & Abbadie, L. (2003). The priming effect of organic matter: a question of microbial competition. *Soil Biology & Biochemistry*, 35, 837-843.

- Frone, A. N., Panaitescu, D. M., Donescu, D., Spataru, C. I., Radovici, C., & Trusca, R. (2011). Preparation and characterization of PVA composites with cellulose nanofibers obtained by ultrasonication. *BioResources*, 6, 487-512.

- Hashimoto, S., & Ozaki, Y. (1980). Study on treatment of recalcitrant substances by activated sludge. *J Jpn Sew Works Assoc*, 17, 17-26.

- ISO 20200. 2004. Plastics- Determination of the deree of disintegration of plastic materials under simulated composting in a laboratory-scale test.

- Jayasekara, R., Harding, I., Bowater, I., & Christie, G. B. Y. (2003). Biodegradation by composting of surface modified starch and PVA blended films. *Journal of Polymers and the Environment*, 11 (2), 49-56.

- Julinová, M., Kupec, J., Alexy, P., Hoffmann, J., Sedlařik, V., Vojtek, T., Chromčáková, J., & Bugaj, P. (2010). Lignin and starch as potential inductors for biodegradation of films based on poly(vinyl alcohol) and protein hydrolysate. *Polymer Degradation and Stability*, 95, 225-233.

- Kuzyakov, Y., Friedel, J.K., & Stahr, K. (2000). Review of mechanisms and quantification of priming effects. *Soil Biology and Biochemestry*, 32, 1485-1498.

- Lanciotti, R., Gianotti, A., Patrignani, F., Belletti, N., Guerzoni, M.E., & Gardini, F. (2004). Use of natural aroma compounds to improve shelflife and safety of minimally processed fruits. *Trends in Food Science & Technology*, 15, 201–208.

- Martínez-Abad, A., Lagarón, J. M., & Ocio, M.J. (2014). Antimicrobial beeswax coated polylactide films with silver control release capacity. *International Journal of Food Microbiology*, 174, 39–46.

- Milos, M., Mastelilc, J., & Jerkovic, I. (2000), Chemical composition and antioxidant effect of glycosidically bound volatile compounds from oregano. *Food Chemistry*, 71 (1), 79-83.

- Monge, M. (2009). Silver nanoparticles: methods of synthesis by dissolution and bactericidal properties. Anales de la Real Sociedad Española de Química, ISSN 1575-3417, 1, 33-41.

- Petersen, K., Nielsen, P. V., Bertelsen, G., Lawther, M., & Olsen, M. B., & Mortensen, G. (1999). Potential of biobased materials for food packaging. *Trends in Food Science & Technology*, 10, 52-68.

- Rhim, J. W., Wang, L. F., & Hong, S. I. (2013). Preparation and characterization of agar/silver nanoparticles composite films with antimicrobial activity. *Food Hydrocolloids*, 327-335.

- Sánchez-González, L., González-Martínez, C., Chiralt, A., & Cháfer, M. (2011b). Use of Essential Oils in Bioactive Edible Coatings. *Food Engineering Review*, 3, 1–16.

- Sreekumar, P. A., Al-Harthi, M. A., & De, S. K. (2012). Studies on compatibility of biodegradable starch/polyvinyl alcohol blends. *Polymer Engineering and Science*, 52(10), 2167-2172.

- Torres-Castro, A., González, V. A., Garza, M., & Gauna, E. (2011). Síntesis de nanocompósitos de plata con almidón. *Ingenierías*, 50 (14), 34-41.

- Tudorachi, N., Cascaval, C. N., Rusu, M., & Pruteanu, M. (2000). Testing of polyvinyl alcohol and starch mixtures as biodegradable polymeric materials. *Polymer Testing*, 19, 785-799.

- UNE-EN ISO 14855-1: 2012. Determinación de la biodegradabilidad aeróbica final de materiales plásticos en condiciones de compostaje controladas. Método según el análisis de dióxido de carbono generado. Parte 1: Método general.

- Vijayan, V., Aafreen, S., Sakthivel, S., & Ravindra, K. (2013). Formulation and characterization of solid lipid nanoparticles loaded Neem oil for topical treatment of acne V. *Journal of Acute Disease*, 282-286. doi: 10.1016/S2221-6189(13)60144-4.

- Whitaker, J.R. (1994). Principles of Enzymology for the Food Sciences, Marcel Dekker, *Inc., New York*.

- Zinanovic, S., Chi, S., & Draughon, A.F. (2005). Antimicrobial activity of Chitosan films enriched with essential oils. *Journal of Food Science*, 70 (1), M45–M51.

Chapter IV: Active films for fresh cheese preservation.

Amalia I. Cano, Maite Cháfer, Amparo Chiralt, Pilar Molina, Milagros Borrás, Mª Carmen Beltran, Chelo González-Martínez. **Quality of goat´s milk cheese as affected by coating with edible chitosan-essential oil films.** *International Journal of Dairy Technology* (pending for approval).

Abstract

The effectiveness of applying chitosan coatings containing rosemary and oregano essential oils to cheeses was analysed. Cheeses were coated by immersing the samples two or three successive times in the different formulations. The ripening indexes, water loss, fungal growth and sensory properties of the coated and non-coated cheeses throughout ripening were evaluated. The coatings both prevented weight loss and improved the microbial safety. The lipolytic and proteolytic activities were reduced in coated cheese in line with the antimicrobial effect of active coatings. Sensory evaluation revealed that the cheeses double coated with chitosan-oregano oil were the best evaluated in terms of aroma and flavour.

Keywords*:* oregano; rosemary; chitosan; antifungal effect; weight loss; sensory analysis

1. INTRODUCTION

Semi-hard cheeses, usually ripened for around 15-30 days, have a smooth, creamy interior with little or no rind. These cheeses have a high moisture content and short shelf life, of about 21 days, under chilling. The most common causes of spoilage are the appearance of discolorations due to excessive surface dehydration or the growth of spoilage microorganisms on the cheese surface, mainly gram negative psycrotrophes, moulds and yeasts, which lead to undesirable flavours and taste, a clinging surface and important visual alterations (Chen & Hotchkiss, 1993; Mannhein & Soffer, 1996). Moulds usually develop on the cheese surfaces during ripening and could penetrate the inner part of the pieces, especially when defects or cracks appear after pressing. This supposes important losses in cheese manufacturing and a drop in profits. Some preservatives, such as sorbic acid or its salts, have been employed to lengthen the shelf life of these cheeses (Var *et al*., 2006). Nevertheless, these preservatives could impart an unpleasant taste, which represents a drawback (Liewen & Marth, 1985).

The application of antibiotics, such as piramicin or natamicyn (E235), to the cheese surface, is a common practice in cheese manufacturing as a means of preventing surface spoilage, thus extending the shelf life. These compounds are usually applied by spraying or by dipping the cheese in 500 ppm piramicin aqueous solutions containing polyvinyl acetate, which also help to control the excessive water losses and fungal growth throughout storage. The incorporation of antibiotics on the rind surface makes it inedible while the extent of their penetration into the interior of the cheese, depending on the cheese type, could cause safety problems (Var *et al*., 2006).

Packaging under vacuum or modified atmospheres with N_2 or CO_2 to reduce the O_2 availability has also been used, in combination or not with preservatives, to lengthen the shelf life of semi-hard cheeses. These techniques do not represent a total solution to the problem

as the microbial spoilage by yeast and bacteria is not avoided even at low oxygen concentrations and high carbon dioxide concentrations (Cerqueira *et al*., 2009). In fact, an excess of CO_2 is not desirable as this gas dissolves in the fat fraction, leading to alterations in the taste and flavour of the cheese (Chen & Hotchkiss, 1993). Moreover, once the packaging is opened, the protective environment completely disappears during the consumption period. Additionally, migration from the plastic packaging constituents to the cheese matrix could be an added problem (Var *et al*., 2006).

The application of edible coatings to prolong the shelf life and quality of semi-hard cheeses could become a viable alternative means of solving some of the above-mentioned problems. These coatings are usually based on biopolymers (polysaccharides, proteins, etc.), which create a modified atmosphere surrounding the commodity, similar to that achieved by controlled or modified atmosphere packaging (Conte *et al*., 2009; Mastromatteo *et al*., 2013). Additionally, they can be carriers for antimicrobial agents, embedded in the polymer matrix. Chitosan, in particular, has a great film-forming capacity while exhibiting antibacterial and antifungal activity, which makes it an interesting compound with which to develop active coatings for food application, in response to the growing demand for safe and healthy foods.

In this sense, Cerqueira *et al*., (2009) applied chitosan and galactomannana-based coatings to semi-hard cheeses to evaluate how the coating affects the surface spoilage of these cheeses. They found a decrease in the mould growth and the respiration rates of the cheeses when coating was applied. Duan *et al*., (2007) showed that chitosan–lysozyme films and coatings can be applied in Mozzarella packaging to control the post-processing microbial contamination, improving the microbial safety of the cheese products.

Previous in vitro and in vivo studies reported promising results when using chitosan-essential oil- blend films/coatings. The incorporation of essential oil into chitosan films

offers the possibility not only of imparting greater antimicrobial activity, but also of improving the film's water vapour permeability (Sánchez-González *et al*., 2010). This improvement could contribute to the decrease in water loss throughout the product storage.

The antifungal properties of oregano and rosemary essential oils have been extensively studied by several authors (Aguirre *et al*., 2013). Both essential oils have been reported to be active against a wide spectrum of microorganisms, derived from their high polyphenol content, the most abundant of which are carvacrol, eugenol and thymol (Lambert *et al*., 2001).

The aim of this work is to analyse the antifungal effect of chitosan coatings containing rosemary and oregano essential oils in semi-hard goat's milk cheeses and their water vapour barrier effect during ripening. Their effect on the main cheese quality parameters was also analysed. To this end, the water loss and fungal growth of coated and non-coated cheeses throughout 15 days' ripening were analysed, as well as the respiration rates. Likewise, the lipolytic and proteolytic activities and the cheese sensory properties were evaluated.

2. MATERIALS AND METHODS

2.1. Raw materials

Milk from Murciano-Granadina goats supplied by the University dairy farm (Universitat Politècnica de València, Spain) was used to produce the cheeses. A total of 150 L (3 bathes of 50 L) was used to conduct all the experiments.

The chemical composition analysis of milks was carried out at LICOVAL (Laboratorio interprofesional lechero de la Comunidad Valenciana, UPV, Valencia, Spain). The

analyses were performed by a CombiFoss 6000 (Foss, Hillerød, Denmark) to obtain fat, protein and lactose contents and somatic cell counts.

High molecular weight chitosan (CH), with a deacetylation degree of 75.6 % (CAS Number 9012-76-4, Batch 8530V, Sigma–Aldrich, USA), 98 % glacial acetic acid (Panreac Química S.L.U. Barcelona, Spain) and oregano and rosemary essential oils (EO) (Herbes del Molí, Alicante, Spain) were used to prepare the film-forming dispersion.

The film-forming dispersions were prepared by dispersing 1.5 % (w/w) chitosan (CH) in an aqueous solution of glacial acetic acid (0.5 %, v/w) at room temperature. After an overnight agitation, oregano (O) and rosemary (R) essential oils were added in a CH:EO ratio of 1:0.5. The mixture was emulsified using a rotor–stator homogenizer (Ultraturrax T25, Jankel & Kunkel, Germany) at 13,500 rpm for 4 min.

2.2. Cheese-making process and treatments

Cheeses were manufactured from pasteurised milk (30 min at 65 ± 5 ºC) following a standard protocol (Consellería de Agricultura, Pesca y Alimentación, December 23, 2008) at the pilot plant of the Animal Science Department at the Universitat Politècnica de València. Milk (50 L / batch) was heated up to 33 ºC and 0.17 % (w/v) lactic starter (Choozit® , Danisco, France), 0.25 (ml/l) of $CaCl_2$ and 0.65 (v/v) of commercial liquid animal rennet (Laboratorios Arroyo, Santander, Spain) were added. After 30 min, the milk coagulum was cut into 8–10 mm cubes with a wire knife. The curds were heated at 36 ºC and kept at this temperature for 10 min prior to adding NaCl at 8 % w/v. When the curds' grain size was adequate, the whey was removed and the curd was moulded into cylindrical pieces of about 250 g and pressed in two steps: first, it was pressed for 1 h at 2 bars; afterwards, the cheeses were turned upside down, and pressed again for 1h at 3 bars. After 24 h pressing, the coating treatments were applied.

Cheeses were coated by immersing the pieces in the different coating formulations (CH-O and CH-R) for 30 seconds followed by surface drying in the ripening chamber. Two or three successive coatings were applied once the cheese surface was completely dried (treatments CH-O2, CH-R2, CH-O3 and CH-R3). Preliminary tests showed that the application of only one coating was not effective enough at reducing the cheese weight loss or fungal growth during ripening and so, only weight loss data for CH-R1 treatments are reported. Uncoated cheeses were also ripened and analysed as control samples (C), as well as cheeses treated with the commercial antibiotic (A) for comparisons. To this end, the pieces were immersed in an aqueous solution of 1.5 g/L piramicin (Proquiga, S.A., La Coruña, Spain) for 30 seconds to simulate the conventional process. For each treatment (C, A, CH-O2, CH-O3, CH-R2, CH-R3), ten replicates were carried out.

Finally, the cheeses were placed in a ripening chamber under controlled conditions (10 ± 5 ºC, 80 ± 5 %RH) for 15 days (t_1). Afterwards, the cheeses were vacuum packaged (Tecnotrip Guerrero Coves, S.L., Valencia, Spain) and stored under chilling at 10 ºC for 15 more days (t_2).

2.3. Cheese characterization

2.3.1. Chemical composition of cheeses

The fat, protein, NaCl and moisture content of the cheeses were analysed by using a NIRS FoodScan (Foss, Hillerød, Denmark). The analyses were carried out in triplicate by grinding the cheeses in a homogenizer (Moulinex, Spain) and, afterwards, the proper amount of the sample was taken.

2.3.2. pH and water activity

The pH of the cheese samples was measured in triplicate by means of a pH-Meter, GLP 21+ (Barcelona, Spain), in two zones of the cheeses (the centre and near the rind).

Measurements were taken immediately after manufacture (t_0), after 15 days' ripening (t_1) and after 15 more days under chilling, vacuum packaged (t_2).

The water activity (a_w) was measured in duplicate by using Decagon Devices Inc. Aqua LaB (Lab-Ferrer, Lleida, Spain). Measurements were also taken in two different zones (the centre and near the rind) at the three times (t_0, t_1 and t_2).

2.3.3. Determination of Free fatty acids (FFA)

The FFA were determined following the method described by González-Martínez *et al.*, 1999. For free fatty acid extraction, 10 g of cheese and 6 g of Na_2SO_4 (Sigma-Aldrich, USA) were homogenized in a mortar, and the mix was stirred for 2 hours with 60 ml of diethyl-eter (Panreac, Barcelona, Spain). The final extract was titrated with an ethanolic solution of KOH 0.1 N, using phenolphthalein as indicator (Nuñez *et al*., 1986). Finally the solvent was evaporated and the solids dried in a desiccator. Total fat content was determined from the weight of the solids. The FFA concentration was expressed as meq/100 g of fat. Three replicates were carried out per sample at the different ripening times (t_1 and t_2).

2.3.4. Determination of free aminoacids (FAA)

The FAA were measured by using the Cd-ninhydrin reagent, as reported by Folkertsma & Fox (1992). 30 g of sample was added to distilled water (70 ml) and homogenized for 5 min at 5,000 rpm using a rotor–stator-homogenizer (Ultraturrax D125, Janke and Kunkel, Germany). Afterwards, the samples were placed in a water bath at 40 ^oC for 1 hour prior to centrifuging them at 7,000 rpm and 10 ^oC for 30 min. Finally, the supernatants were carefully removed and the FAA fractions were filtered. For the analysis, aliquots were taken and made up to 1 ml with distilled water. Then, 2 ml of previously prepared Cd-ninhydrin reagent were added. This new solution was placed in

a water bath at 84 ºC for 5 min and afterwards, cooled down to room temperature. The FAA content was determined spectrophotometrically (Evolution 201, Thermo Scientific, Sanghai, China) at 507nm. The FAA concentration was measured in triplicate at the different ripening times (t_1 and t_2), and expressed as mg of leucine/g of cheese by using a standard curve of leucine (Sigma–Aldrich, Madrid, Spain).

2.3.5. Weight loss and fungal growth evaluation

The weight of eight cheese pieces per treatment was monitored throughout the ripening period (till t_1) and expressed as the relative weight loss with respect to the initial weight.

The fungal growth was evaluated at surface level by a visual inspection of the cheese surface, by counting the number of fungus colonies developed at every control time. These counts were performed in eight cheeses for each treatment. To identify the genera of fungi, each fungus was isolated from the cheese surface, incubated in agar at 25 ºC for 4-6 days in an incubation oven and identified by optical microscopy (Optika SRL, Ponteranica, Italy).

2.3.6. Respiration rate

The closed system method was used to measure the gas exchange rate of the cheeses (Cerqueira *et al*., 2010) at the beginning (t_0) and the end of the first ripening period (t_1). Glass, air-tight, cylindrical containers (1945 ml) were used, whose top lid was fitted with a septum for gas sampling. A whole, intact cheese sample was placed in each container.

The change in gas composition (O_2 and CO_2 concentrations) inside each container was monitored by means of a gas analyser (Dansensor, Checkmate 9900, Spain) for 24

hours. The O_2 consumption and CO_2 generation rates were determined by applying Eqs. (1) and (2) (Cerqueira *et al*., 2010).

$$R_{O_2} = -\left(\frac{dy_{O_2}}{dt}\right) \cdot \left(\frac{V_f}{W}\right) \quad (1)$$

$$R_{CO_2} = -\left(\frac{dy_{CO_2}}{dt}\right) \cdot \left(\frac{V_f}{W}\right) \quad (2)$$

Where, R_{O2} is the O_2 consumption rate, ml[O_2] kg^{-1} h^{-1}, R_{CO2} is the CO_2 generation rate, ml[CO2] kg^{-1} h^{-1}, w (kg) is the weight of the cheese and V_f (ml) is the head space volume of the container, calculated by Eq. (3).

$$V_f = V_p - \frac{W}{\rho_{ch}} \quad (3)$$

Where, V_p (ml) is the total volume of the container, w (kg) is the weight of the cheese and ρ_{ch} is the true density of the cheese (1.08 kg l^{-1}), obtained experimentally by the water displacement method according to Owolarafe *et al.* (2007). From the slope of the relationships between O_2 or CO_2 concentration (volume fractions) vs. time, the values of the derivatives dy_{O2} /dt or dy_{CO2} /dt, were obtained. The respiration rate measurements were carried out in triplicate.

2.3.7. Sensory analysis

All the sensory evaluations were conducted in individual booths under white illumination at room temperature in an EU homologated sensory room at the Institute of Food Engineering for Development at Universitat Politècnica de València (Valencia, Spain), which follows the UNE 87-004-79 (AENOR, 1979). Mineral water was used as a palate cleanser between samples (AENOR, 1979).

After the t_2 ripening period, samples were coded by a random three-digit code and analysed by a non-trained panel consisting of 100 judges, 21-57 year-old volunteers. The rind of the samples was eliminated before the test.

The judges were asked to taste six kinds of samples (C, A, CH-O2, CH-O3, CH-R2, CH-R3) and to indicate the pleasantness of each sample in terms of appearance, aroma, flavour, texture and overall preference by using a 9-point Likert-type scale (1, not pleasant at all; 9, extremely pleasant).

2.4. Statistical analysis

The results were analysed by means of analysis of variance (ANOVA), using the Statgraphics Plus 5.1. Program (Munugistics Corp., Rockville, MD). Fisher's least significant difference (LSD) was used at the 95 % confidence level to distinguish the samples.

3. RESULTS AND DISCUSSION

3.1. Physicochemical and ripening parameters of the cheeses

Milk composition ranged from 4.4-5.1 g fat/100 g, 3.2-3.8 g protein/100 g and 4.4-4.5 g lactose/100 g and the somatic cell counts from 852-2115 10^{-3} cell/ml. No significant differences in composition were found for the different batches used. The initial water content of the cheeses was 49.4 ± 0.8 g water/100 g cheese, while the percentages (g/100 g cheese) of fat, protein and NaCl were 26.82 ± 0.07, 19.71 ± 0.07 and 1.43 ±0.03, respectively. Taking their water and fat contents into account, these cheeses can be classified as "full fat semi-hard cheeses" according to CODEX STANDARD (2013).

The treatments did not significantly affect the initial pH of the cheeses, this being around 5.2 ± 0.2. As expected, the pH decreased ($p<0.05$) throughout the first ripening period to 4.85 ± 0.04 (at t_1) and during the second period, packaged under vacuum, to 4.75 ± 0.12 (t_2), in agreement with the progress of the enzymatic activity. No significant differences between the pH of the external and internal zones in the cheeses were observed. In no case were the water activity values significantly affected by the coating

treatments. At the beginning of the ripening time (t_0), the water activity values of all the cheeses (untreated and treated) were 0.989 ± 0.001, for both the inner and the external parts of the cheese. This value became 0.987 ± 0.002 and 0.981 ± 0.001 for the inner and external parts of the cheese, respectively, after 15 days' ripening (t_1). No significant changes were observed during the second storage period (t_2). The obtained water activity values are in the normal range for these kinds of cheeses (Ramos *et al*., 2012).

Figures 1 and 2 show the mean values of the Free Fatty Acids (FFA) and Free Aminoacids (FAA) of the different cheeses at the end of the first ripening period (t_1) and after 15 days under chilling and vacuum packaging conditions (t_2). These parameters are good indicators of the advance of the cheese ripening, mainly due to the lipase and peptidase activities carried out by the microflora. The degree of lipolysis (FFA) in cheese varies widely from variety to variety, from about 6 meq free fatty acids per 100 g of fat in Gouda to 45 meq in Danish Blue (Gripon, 1993; El-Hofi *et al*., 2011).

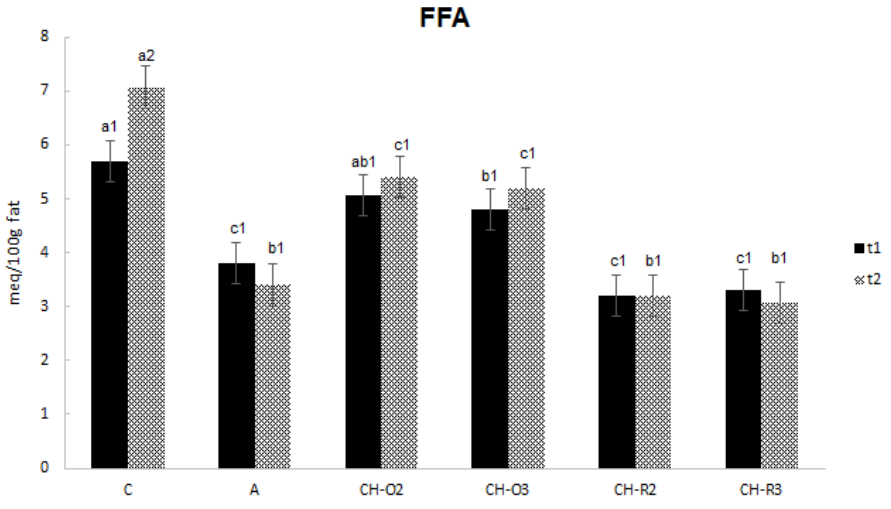

Figure 1. Concentration of Free Fatty Acids (FFA) in the non-treated cheeses (C), cheeses treated with antibiotic (A) and double (2) and triple (3) coated cheeses with chitosan-oregano oil (CH-O) and chitosan-rosemary oil (CH-R) after the first ripening period (t1) and after 15 days under vacuum packaging and chilling conditions (t2). Mean values and LSD intervals.

[a, b, c] letters indicate significant differences among formulations ($p<0.05$).

[1, 2] numbers indicate significant differences among times ($p<0.05$).

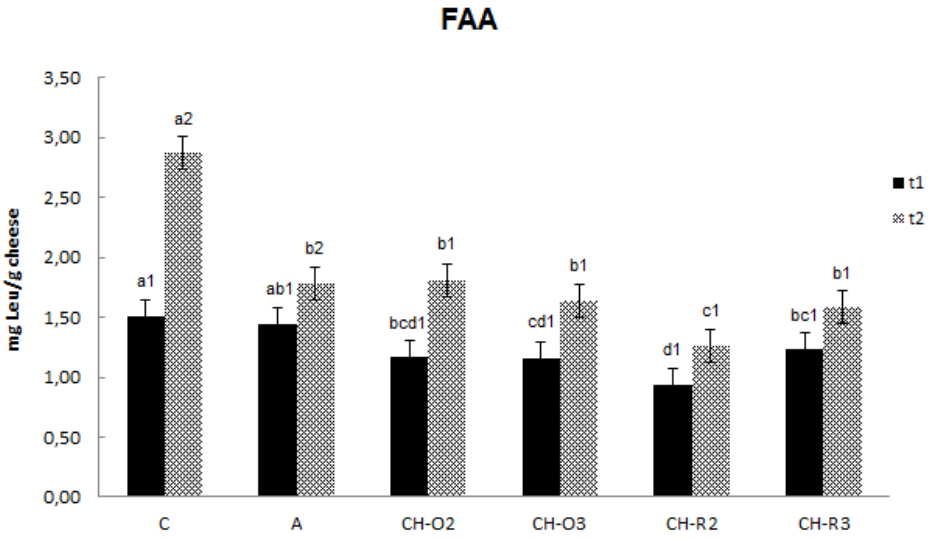

Figure 2. Concentration of Free Amino Acids (FAA) in the non-treated cheeses (C), cheeses treated with the antibiotic (A) and double (2) and triple (3) coated cheeses with chitosan-oregano oil (CH-O) and chitosan-rosemary oil (CH-R) after the first ripening period (t1) and after 15 days under vacuum packaging and chilling conditions (t2). Mean values and LSD intervals.

[a, b, c] letters indicate significant differences among formulations ($p<0.05$).

[1, 2] numbers indicate significant differences among times ($p<0.05$).

The FFA and FAA values obtained for the control samples were 5.7 meq/100 g fat and 1.5 mg leucine/g sample, respectively at t_1. These values were in the order of those shown by other authors for one-month ripened non-blue cheeses (Nuñez *et al*., 1986; González-Martínez *et al*., 1999). As can be observed in Figures 1 and 2, every treated cheese (those treated with the antibiotic and those coated) exhibited lower FFA and FAA values than the non-treated control, thus indicating that the lipolytic and proteolytic activities were limited due to the antimicrobial action of antibiotic or coatings. After 15 days' chilling (t_2), no notable change in the ripening indexes was observed, except in the case of the control sample where they significantly rose. These results indicate that, in samples treated/coated with antimicrobials, these compounds mainly controlled the microbial growth on the surface they were applied to, thus affecting ripening indexes. The concentration of antimicrobials inside the cheese will be limited by the slow diffusion

processes (Fajardo *et al*., 2010). Thus, whereas the ripening process in treated cheeses mainly takes place due to the lipolytic and proteolytic activity of the starters added during the manufacturing process, in the control samples, surface moulds also seem to contribute to the lipolysis and proteolysis responsible for ripening. Nevertheless, the increase in FFA during the chilling period is relatively gentle due to the fact that the lipase activity mainly occurs during the first fifteen days of ripening and, after that, the level of lipolysis stabilizes due to the simultaneous generation and degradation of FFA through the chemical and biochemical pathways that are a consequence of the esterification and oxidative processes (Eck, 1990).

3.2. Weight loss of cheeses during ripening

Figure 3 shows the mean values of the weight losses throughout the ripening time of both uncoated cheeses and those coated with different successive chitosan coatings containing rosemary essential oil. Cheeses coated with oregano essential oil behaved similarly.

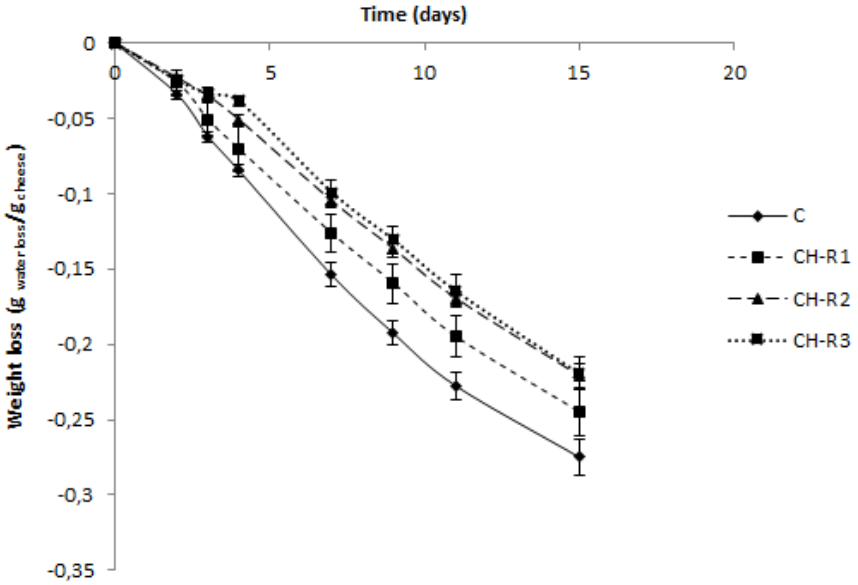

Figure 3. Weight loss development of non-treated cheeses (C) and double (CH-R2) and triple (CH-R3) coated cheeses with chitosan containing rosemary essential oils during ripening. Mean values and standard deviation.

As can be observed, the weight loss undergone by uncoated cheeses (C) was significantly greater ($p<0.05$) than that observed for coated samples throughout the entire ripening time due to the water vapour barrier produced by the coatings. The application of two or three successive coatings reduced the weight losses incurred by the cheeses in comparison with those samples coated only once, in agreement with the increase in both the total solid content of the coatings and their thickness. Nevertheless, no significant differences ($p>0.05$) were found between the weight loss of double and triple-coated cheeses.

The water vapour permeability of chitosan films was reduced when they contained essential oils, coherent with the hydrophobic nature of these lipid components and the discontinuities introduced in the polymer matrix by oil droplets, which increases the tortuosity factor for the transfer of water molecules (Sánchez-González *et al*. 2010). Similar trends were found by other authors for cheeses coated with galactomannan films (Cerquiera *et al*., 2009), whey protein (Ramos *et al*., 2012) and blend films based on carrageenan, alginate and gellan (Kampf & Nussinovitch, 2000). The differences in the rate of water loss increased as the ripening time lengthened due to the fact that the film became progressively drier, implying a less plasticized structure with a greater resistance to mass transfer.

After 15 days' ripening, the final weight loss in the case of uncoated samples, those coated with one layer and those coated with two or three layers was 0.275 ± 0.012, 0.25±0.02, and 0.220 ± 0.008 g weight loss/100 g cheese, respectively, regardless of the essential oil used.

3.3. Effect of coatings on fungal growth and respiration rates

The fungi developed in the cheeses throughout ripening were identified to belong to the genera *Mucor* and *Penicilium* two of the fungi species most frequently occurring on cheeses (Hocking, 2014).

The level of fungal incidence in cheeses treated using the different methods, as a function of the ripening time, is shown in Figure 4 where the percentage of cheeses infected by the natural fungal incidence of both genera is shown. As can be observed, cheeses treated with the antibiotic (A) showed no fungal growth during ripening, while the uncoated ones (C) exhibited an intense mould growth of both genera, especially from the 9th day of ripening onwards. The application of coatings delayed or inhibited the fungal growth, depending on the type of essential oil and the number of coatings applied.

Oregano essential oil exhibited a great antimicrobial activity against both fungi, *Penicillium* and *Mucor*. This is probably related to its high content in carvacrol (Aguirre *et al*., 2013), a potent antimicrobial compound with a wide spectrum activity against food spoilage or pathogenic fungi, yeast and bacteria.

The application of three successive coatings was more effective than two, especially when using oregano essential oil. This result suggests that successive applications of coatings help to retain the active compounds on the cheese surface, making their antifungal action more effective. The CH-O3 treatment exhibited the greatest antifungal power, similar to that of the antibiotic (A).

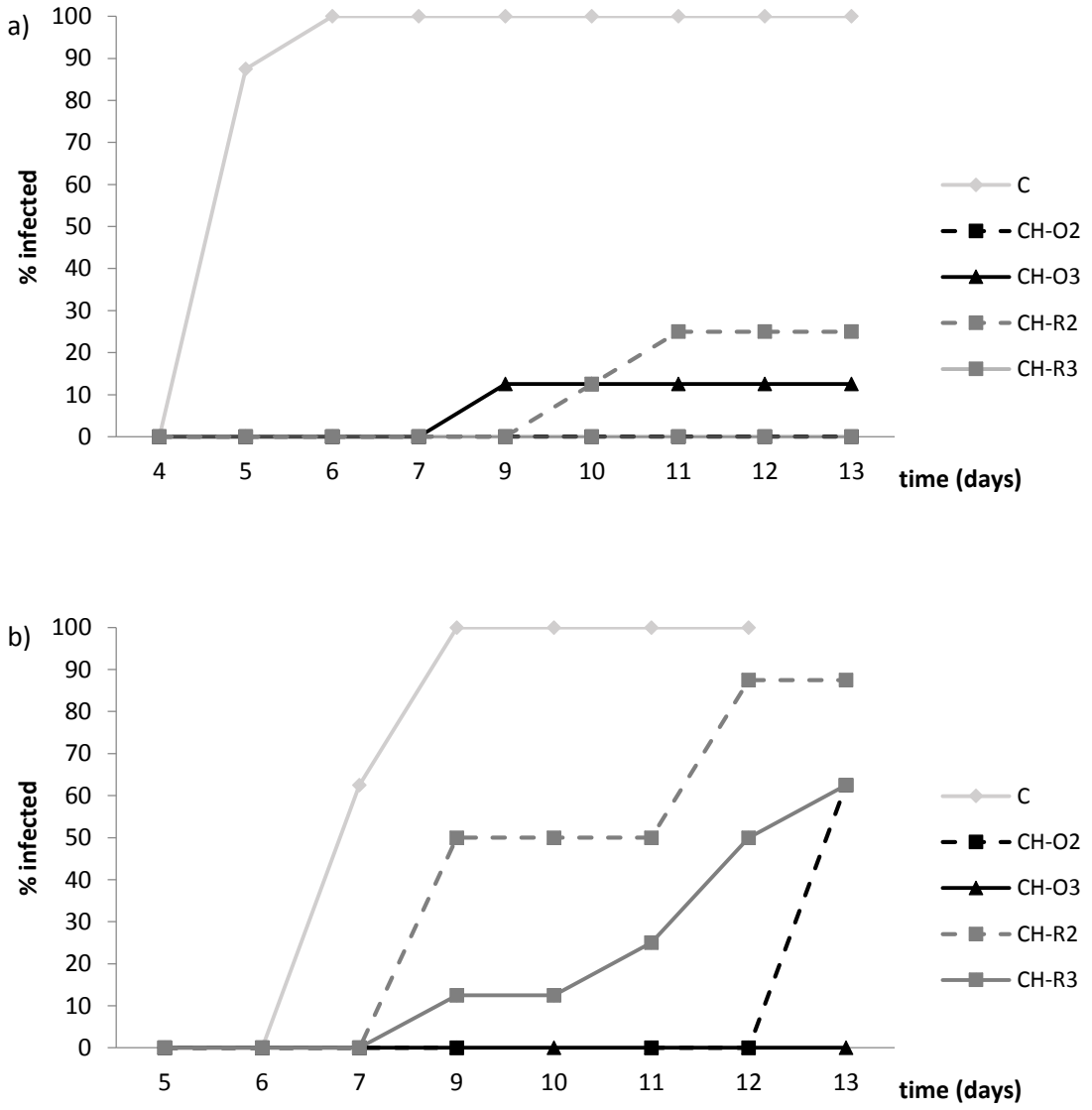

Figure 4. Percentage of cheeses infected by natural fungal incidence of a) *Mucor* and b) *Penicillium*, during the ripening time under controlled conditions (10±5 ºC, 80±5 %RH). The average number of CFU per cheese for each treatment is shown below.

Table 1 shows the mean values of the respiration rates of samples analysed at both the initial (t_0) and final time of the first ripening period (t_1), in terms of O_2 consumption and CO_2 generation.

Table 1. Respiration rate (RR) of cheeses submitted to different treatments at initial time (t_0) and after the first 15 days of ripening at 10 ºC and 80 % RH (t_1), in terms of O_2 consumption and CO_2 generation. Mean values and standard deviation.

	RR (ml[O_2] $kg^{-1}h^{-1}$)		RR (ml[CO_2] $kg^{-1}h^{-1}$)	
	Storage time (days)			
Treatment	t_0	t_1	t_0	t_1
C	8 ± 2^{a1}	5.3 ± 0.5^{a2}	5.09 ± 0.08^{a1}	5.6 ± 0.7^{a1}
A	$1.9\pm1,4^{b1}$	1.8 ± 0.5^{b1}	5.2 ± 1.3^{b1}	0.42 ± 0.17^{b2}
CH-O2	0.8 ± 0.2^{b1}	0.37 ± 0.09^{c1}	2.994 ± 0.008^{c1}	1.1 ± 0.8^{bc2}
CH-O3	1.058 ± 0.005^{b1}	0.206^{c1}	2.6 ± 0.2^{c1}	1.2 ± 0.2^{c2}
CH-R2	1.3 ± 0.4^{b1}	0.52 ± 0.13^{c1}	2.6 ± 0.2^{c1}	1.35 ± 0.14^{c2}
CH-R3	1.4 ± 0.4^{b1}	0.4^{c1}	2.4 ± 0.2^{c1}	1.4 ± 0.2^{c2}

$^{a, b, c}$ letters indicate significant differences among formulations ($p<0.05$).

$^{1, 2}$ indicate significant differences among times ($p<0.05$).

The initial values for the O_2 consumption rate ranged from 8 to 1.3 ml kg^{-1} h^{-1} for untreated and treated cheeses, respectively. The obtained values were low when compared with those reported for *Regional Saloio* semi-h*ard* cheese by Cerqueira *et al*. (2009), but higher than those found by Fedio *et al*. (1994) working on Swiss cheese. The composition of the cheese, the manufacturing process, the degree of cheese maturation and the microbial load all affect the respiration rates; the higher the microbial load, the greater both the O_2 consumption and the CO_2 generation (Robertson, 2006). This can be observed in the cheeses treated with antibiotics and coatings, which exhibited a great reduction in the oxygen consumption with respect to the control (about 76 % in treatment A) due to the lower microbial load. The value of the CO_2 production rate at initial time (t_0) in treatment A was similar to that of the control cheese, whereas the oxygen consumption was lower. This indicates that the antibiotic affected the microbial activity near the cheese surface, where oxygen diffusion allows aerobic respiration, but did not at this time affect the anaerobic microorganisms located in the internal part of the cheese. A similar effect

was observed for coated cheeses but with a greater reduction in CO_2 generation. The coating effect on gas exchanges cannot only be attributed to antimicrobial activity but also to the gas barrier effect. The oxygen permeability of chitosan films is very low and, in some cases, the use of essential oils leads to a decrease in their values in line with their antioxidant activity (oxygen scavenger) (Bonilla *et al*., 2013).

At the end of the ripening time, the exchange of gases considerably decreased in all of the treated samples. Vivier *et al.* 1996 attributed the reduction in respiration rates throughout ripening to several reasons: the lower microbial survival rate, the exhaustion of available lactose and the changes in the metabolic pathway of the microorganisms from aerobic to anaerobic. Untreated cheeses had respiration quotients close to 1 at both control times. However, both coated cheeses and those treated with antibiotics exhibited much higher values (2-6), due to their antimicrobial effect on aerobics at surface level. The internal diffusion of antimicrobials could also affect the survival of the starter microorganism, thus modifying the long-time ripening behaviour.

3.4. Sensory analyses

The results of the sensory analyses are summarized in Figure 5 and Table 2, where the different evaluated attributes are shown. As can be observed in Table 2, no significant differences ($p>0.05$) were detected in the appearance of the different cheeses. On the other hand, significant differences ($p<0.05$) were found between the aroma and flavour appreciation of the uncoated and coated samples, due to the impact of the essential oils on the overall flavour and aroma of the cheeses. Nevertheless, CH-O2 treated samples received the highest flavour and aroma scores ($p<0.05$), very likely due to the pleasant attributes imparted by oregano oil to the cheese matrix. On the contrary, both cheeses treated with the antibiotic and those triple-coated had the lowest scores in aroma and taste attributes, regardless of the essential oil used in the coating.

This suggests the existence of a threshold for the perception of the essential oils in cheese matrices, from which point on a negative effect on sensory appreciation occurs.

The judges found no significant differences between the texture of uncoated and coated cheeses, except for those treated with the antibiotic and those double-coated with CH containing rosemary oil, which were more negatively appreciated (the lowest score) ($p<0.05$). In general, the panellists did not find a marked overall preference among the cheeses, as can be observed in Figure 5. Nevertheless, those cheeses double-coated with CH containing oregano oil were considered to be the ones which were the most similar to the control, but with enhanced cheese flavour; this can be considered positive in terms of product quality for the studied cheeses, although this could objectionable for other cheeses varieties.

Table 2. Score obtained for sensorial attributes of cheeses submitted to different treatments after the first ripening period plus 15 days chilling under vacuum (t_2). Mean values and standard deviation.

Treatment	Appearance	Aroma	Texture	Flavour	Overall preference
C	6.8 ± 1.3^{a}	6.6 ± 1.4^{a}	6.7 ± 1.4^{a}	6.2 ± 1.8^{a}	6.5 ± 1.5^{ab}
A	6.7 ± 1.3^{a}	6.2 ± 1.3^{b}	6.2 ± 1.7^{bc}	6.2 ± 1.7^{a}	6.2 ± 1.5^{bc}
CH-O2	6.75 ± 1.14^{a}	6.8 ± 0.9^{a}	6.6 ± 1.3^{ab}	6.7 ± 1.2^{b}	6.6 ± 1.3^{ab}
CH-O3	6.80 ± 1.17^{a}	6.2 ± 1.5^{b}	6.7 ± 1.3^{a}	5.9 ± 1.9^{a}	5.9 ± 1.7^{c}
CH-R2	6.6 ± 1.3^{a}	6.8 ± 0.9^{a}	5.9 ± 1.6^{c}	6.0 ± 1.7^{a}	6.2 ± 1.4^{bc}
CH-R3	6.7 ± 1.3^{a}	5.9 ± 1.5^{b}	6.7 ± 1.3^{a}	6.2 ± 1.7^{a}	6.9 ± 0.9^{a}

$^{a, b, c}$ letters indicate significant differences among formulations ($p<0.05$).

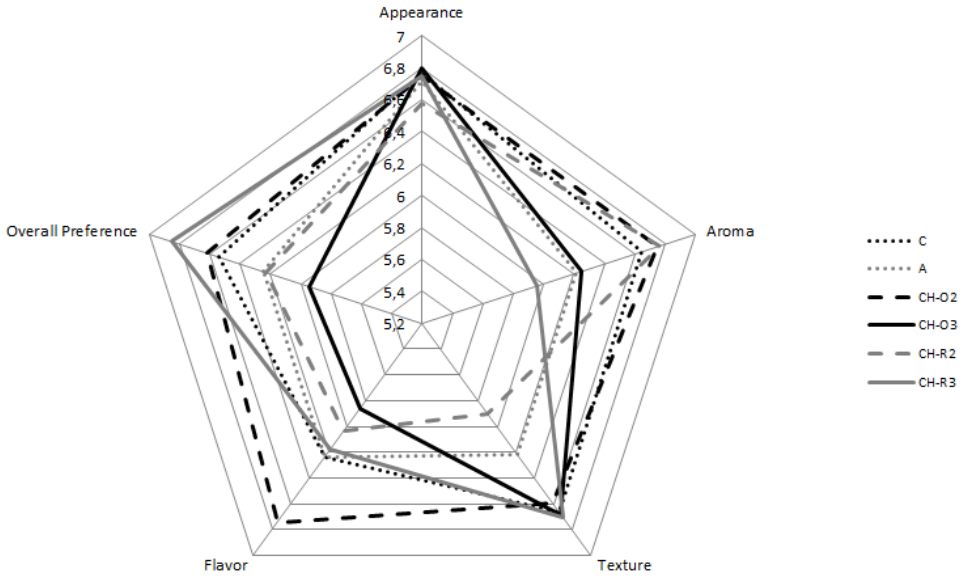

Figure 5. Sensory profile of the cheeses submitted to different treatments.

4. CONCLUSIONS

Chitosan-essential oil coatings prevent weight loss in semi-hard cheeses during ripening, while improving their microbial safety. As occurred in the samples treated with the antibiotic, lipolytic and proteolytic activity was reduced in coated cheeses, in line with the antimicrobial effect of essential oils and/or chitosan which, in turn, affected the enzymatic activity during ripening. An analysis of the impact of the essential oils on the cheese sensory attributes reveals that when three successive coating treatments were applied, the threshold for undesirable aroma perception of essential oils was reached and the flavour and aroma of the cheeses were negatively affected as compared with the control. Nevertheless, cheeses that were double-coated with chitosan containing oregano oil were the best evaluated in terms of aroma and flavour, while the other attributes had values which were similar to those of the control. This coating treatment practically inhibited fungal growth during the ripening period. Therefore, the application

of a double-coating based on chitosan and oregano essential oil is recommended, for cheeses where migration of compounds from essential oils are not objectionable.

Acknowledgements

The authors wish to acknowledge the financing of the project by the Program of Support for Research and Development (PAID-05-12) of the Universitat Politècnica de València.

References

- Aguirre, A., Borneo, A., & León, A. E. (2013). Antimicrobial, mechanical and barrier properties of triticale protein films incorporated with oregano essential oil. *Food Bioscence,* 1, 2-9.
- Bonilla, J., Talón, E., Atarés, L., Vargas, M., & Chiralt, A. (2013). Effect of the incorporation of antioxidants on physicochemical and antioxidant properties of wheat starch-chitosan films. *Journal of Food Engineering,* 118, 271-278.
- Chen, J. H., & Hotchkiss, J. H. (1993). Growth of *Listeria monocytogenes* and *Clostridium sporogenes* in cottage cheese in modified atmosphere packaging. *Journal of Dairy Science,* 76, 972-977.
- Cerqueira, M. A., Lima, A. M., Souza, B. W. S., Teixera, J. A., Moreira, R. A., & Vicente, A. A. (2009). Functional polysacharides as edible coating for cheese. *Journal Agricultural Food Chemistry,* 57 (4), 1456-1462.
- Cerqueira, M. A., Sousa-Gallagher, M. J., Macebo, I., Rodriguez-Aguilera, R., Souza, B. W. S., Teixeira, J. A., & Vicente, A. A. (2010). Use of galactomannan edible coating application and storage temperatura for prolonging shelf-life of “Regional” cheese. *Journal of Food Engineering,* 97, 87-94.
- CODEX STANDARD (2013) Codex General Standard for Cheese. Designation: CODEX STAN 283-1978.

- Conselleria d'Agricultura, Pesca i Alimentació (2008). *ORDE de 23 de desembre de 2008 per la qual publica la reglamentació de qualitat del formatge de cassoleta, el formatge blanquet, el formatge de la Nucia o de pastís, el formatge de tovalló i el formatge tronxon, per a la seua distinció amb la marca de qualitat CV.* [2008/15122].

- Conte, A., Gammariello, D., Di Giulio, S., Attanasio, M., & Del Nobile, M. A. (2009). Active coating and modified-atmosphere packaging to extend the shelf life of Fior di Latte cheese. *Jorunal of Dairy Science,* 92, 887-894.

- Duan, J., Park, S. I., Daeschel, M. A., & Zhao, Y. (2007). Antimicrobial chitosan-lysozyme (CL) films and coatings for enhancing microbial safety of mozzarella cheese. *Journal of Food Science,* 72 (9), M355-M362.

- Eck, A. (1990). Le fromage. Technique et Documentation (Lavoisier), París.

- El-Hofi, M., El-Tanboly, E-S., & Abd-Rabou, N. S. (2011). Industrial application of lipases in cheese making: a review. *International Journal of Food Safety,* 13, 293-302.

- Fajardo, P., Martins, J. T., Fuciños, C., Pastrana, L., Teixeira, J. A., & Vicente, A. A. (2010). Evaluation of chitosan-based edible film as carrier of natamycin to improve the storability of Saloio cheese. *Journal of Food Engineering,* 101, 349-356.

- Fedio, W. M., Ozimek, L., & Wolfe, F. H. (1994). Gas production during storage of Swiss cheese. *Milchwissenschaft*, 49, 3–8.

- Folkertsma, B., & Fox, P. F. (1992). Use of the Cd-ninhydrin reagent to assess proteolysis in cheese during ripening. *Journal of Dairy Research,* 59, 217-224.

- Gonzalez, Ch., Fuentes, C., Andrés, A., Chiralt, A., & Fito, P. (1999). Effectiveness of vacuum impregnation brining of Manchego-type curd. *International Dairy Journal*, 9, 143-148.

- Gripon, J. C. (1993). Mould-ripened cheeses. In: Fox PF, editor. Cheese: chemistry, physics and microbiology. 2. London: Chapman and Hall, 2, 111–136.

- Hocking, A. D. (2014). Spoilage Problems: Problems caused by fungi. In: Encyclopedia of Food Microbiology, 2nd edition. C. A. Batt and M.L. Tortorello (eds). *Elsevier*, 2, 471-481.

- Kampf, N., & Nussinovitch, A. (2000). Hydrocolloid coating of cheeses. *Food Hydrocolloids,* 14, 531-537.

- Lambert, R. J. W., Skandamis, P. N., Coote, P., & Nychas, G. J. E. (2001). A study of the minimum inhibitory concentration and mode of action of oregano essential oil, thymol and carvacrol. *Journal of Applied Microbiology,* 91, 453-462.

- Liewen, M. B., & Marth, E. H. (1985). Growth and inhibition of microorganisms in the presence of sorbic acid: a review. *Journal of Food Protection,* 48, 364-375.

- Mannheim, C. M., & Soffer, T. (1996). Shelf-life extension of cottage cheese by modified atmosphere packaging. *Lebensmittel.-Wissenschaft and Technology,* 29, 767–771.

- Mastromatteo, M., Conte, A., Faccia, M., Del Nobile, M. A., & Zambrini, A. V. (2013). Combined effect of active coating and modified atmosphere packaging on prolonging the shelf life low-moisture Mozzarella cheese. *Journal of Dairy Science,* 97, 36-45.

- Nuñez, M., García-Aser, C., Rodriguez-Martin, M. A., Medina, M., & Gaya, P. (1986). The effect of ripening and cooking temperatures on proteolysis and lipolysis in Manchego cheese. *Food Chemistry*, 21, 115-123.

- Owolarafe, O. K., Olabige, T. M., & Faborode, M. O. (2007). Macro-structural characterisation of palm fruit at different processing conditions. *Journal of Food Engineering,* 79, 31–36.

- Ramos, O. L., Pereira, J. O., Silva, S. I., Fernandes, J. C., Franco, M. I., Lopes da Silva, J. A., Pintado, M. E., & Malcata, F. X. (2012). Evaluation of antimicrobial edible coating from a whey protein isolate base to improve the shelf life of cheese. *Journal of Dairy Science,* 95 (11), 6282-6292.

- Robertson, G. L. (2006). Packaging of Dairy Products. In *Food Packaging: Principles and Practice*; Robertson, G. L., Ed.; CRC/Taylor and Francis: Boca Raton, FL, 400-415.

- Sánchez-González, L., González-Martínez, C., Chiralt, A., & Cháfer, M. (2010). Physical and antimicrobial properties of chitosan-tea tree essential oil composite films. *Journal of Food Engineering,* 98 (4), 443-452.

- UNE 87-004-79: análisis sensorial: guía para la instalación de una sala de cata. Aenor (1979).

- Var, I., Erginkaya, Z., Güven, M., & Kabak, B. (2006). Effects of antifungal agent and packaging material on microflora of Kashar cheese during storage period. *Food Control,* 17 (2), 132–136.
- Vivier, D., Compan, D., Moulin, G., & Glazy, P. (1996). Study of carbon dioxide release Feta cheese. *Food Research International,* 29 (2), 169-174.

IV. General Discussion

In the present Doctoral Thesis, different strategies to enhance the properties of starch based films are evaluated. In this section, a general discussion about influence of each one on the barrier and mechanical properties of the films as well as on their antimicrobial activity and biodegradation properties is done to evaluate the feasibility of these materials to be used in food packaging.

It is well known, that the main drawbacks of the starch materials are the poor mechanical and water barrier properties and the changes associated with the film ageing, which negatively affect to their mechanical behaviour.

A wide variety of commercial starches are available in the market and the selection of the proper raw material was needed. In this sense, the high amylose content in pea starch, in comparison with potato or cassava starch, confer to the films a greater rigidity and resistance to break and mechanical stability during the storage period, due to the fast crystallization of amylose, as compared with the delayed crystallization of amylopectin.

The first strategy followed to enhance the physical properties of pure pea starch based films was to blend it with other biodegradable polymer such as PVA. PVA is able to form highly transparent films with better mechanical resistance, non-affected by ageing, and barrier properties than pure starch films. Furthermore, its low cost (in comparison with other biodegradable plastics) makes this polymer a good option to be blended with pea starch.

Successfully, the first blend developed (2:1 S:PVA ratio) led to blend films with barrier properties closer to that of pure PVA films and a mechanical resistance, stretchability and rigidity intermediate between those of both pure polymers, and similar to commercial LPDE films probably due to the beneficial interactions established between both polymers (Figure 1a and 1b).

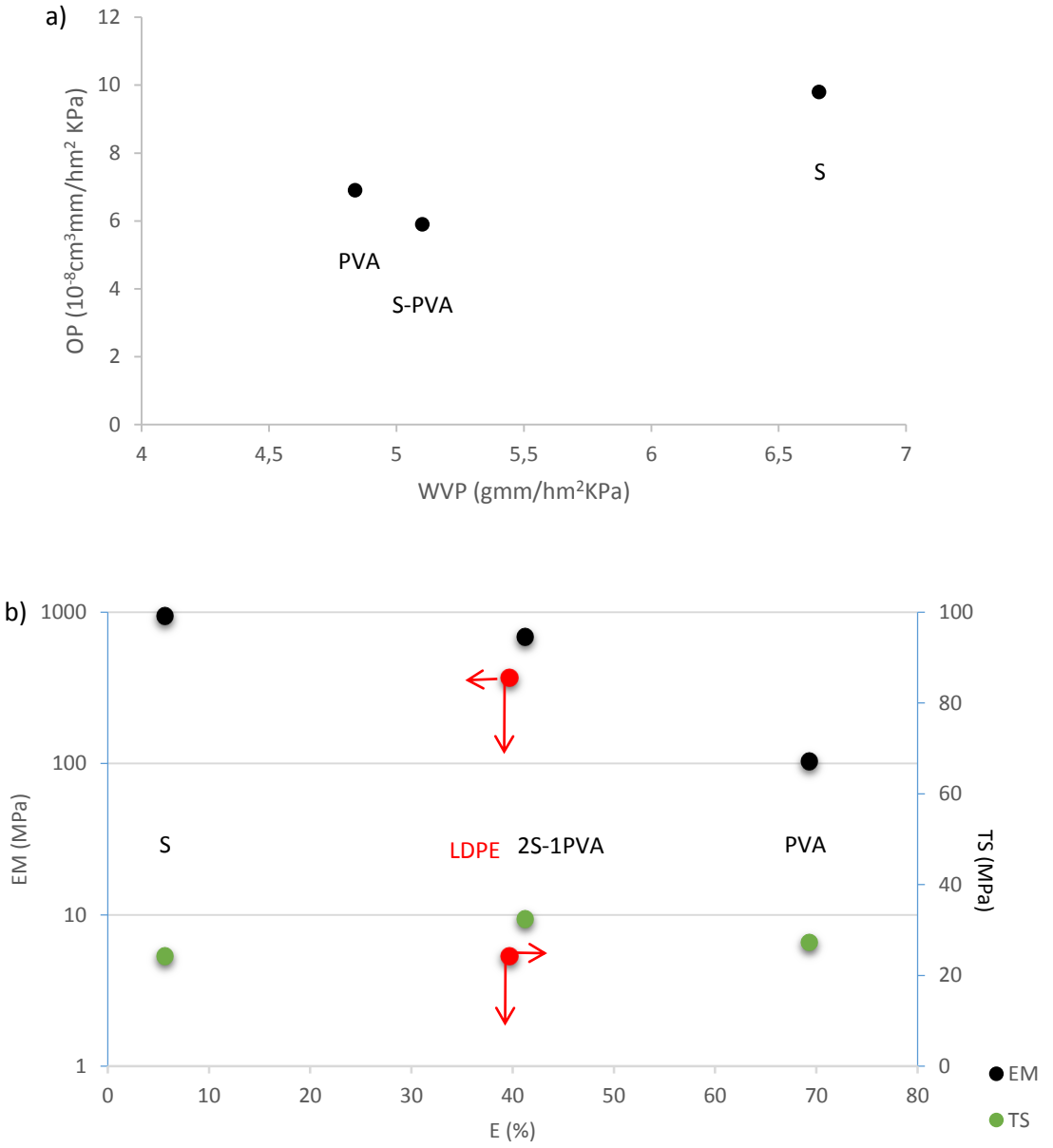

Figure 1. a) Oxygen (OP) and water vapour permeability (WVP) map and b) mechanical properties, elastic modulus (EM), tensile strength (TS) and percentage of elongation (E) of pure starch (S) and PVA films, and S-PVA blend films after 5 storage weeks.

As a consequence of these satisfactory results, the following step was to optimize the S-PVA ratio to improve the functionality of the S-PVA blend films. As can be observed in Figure 2a, the WVP of pure starch films was improved in all cases, but especially when using S:PVA ratios of 1:1 and 1:2. The differences in the WVP values of blend films were

related with the different hydrophilic nature of the polymers. In both, hydroxyl groups favoured water affinity but their distribution and density in the chains established relevant differences in the water sorption capacity and the mass transfer rate of water molecules (Cano *et al*. 2015).

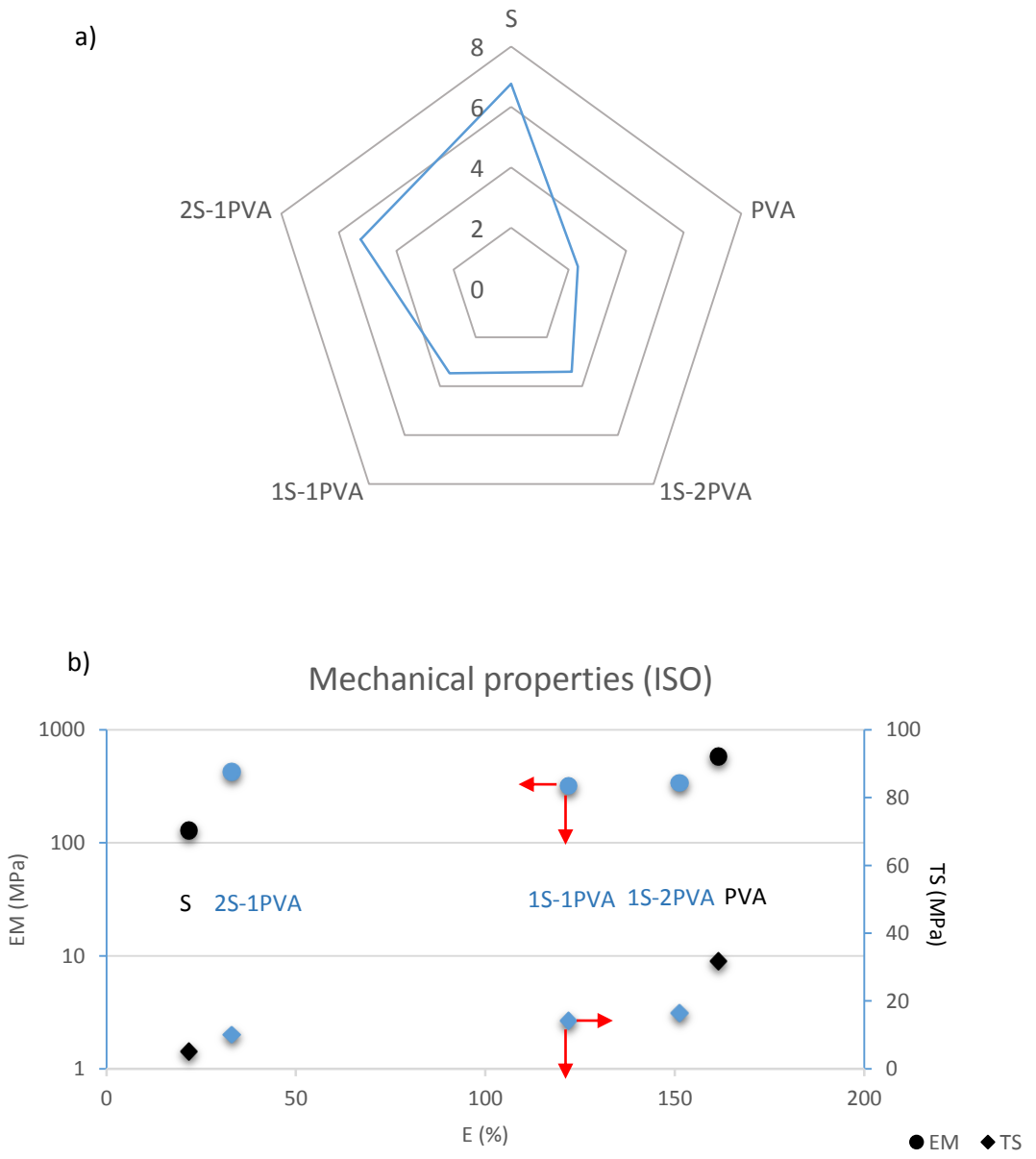

Figure 2. a) Water vapour permeability (WVP) and b) mechanical properties: elastic modulus (EM), tensile strength (TS) and percentage of elongation (E) of pure starch (S) and PVA films (black), and S-PVA blend films (S-PVA ratio of 1:2, 2:1 and 2:1, blue) after 5 storage weeks.

The TS and EM values of the blend films with the different ratio was very similar (Figure 2b) but the stretchability of the films dramatically increased when the PVA content rose in the blend (S-PVA ratios of 1:1 and 1:2). Thus, by blending S:PVA in a proper ratio (1:1 or 1:2) the water barrier and the mechanical behaviour of the film was significantly improved.

The second strategy followed to enhance the mechanical resistance of S:PVA films was the addition of reinforcing materials such as cellulose nanocrystals. Rice brand was also tested as a filler into the pure starch matrix, but its use was dismissed due to the poor obtained results. To this aim, S:PVA (1.2) blends were used.

Figure 3 shows the mechanical response of S-PVA films containing cellulose nanocrystals (CNCs) as filler material. As can be observed, the mechanical response of S-PVA was enhanced when the highest concentration of CNCs (5 %), giving rise to films more stretchable and stiffer, in comparison to the control matrix. These results confirm reinforcing properties of CNCs in the S-PVA films. Both strategies, blending PVA with starch and the addition of CNCs, led to films with enhanced mechanical properties, the polymer blending being the most effective.

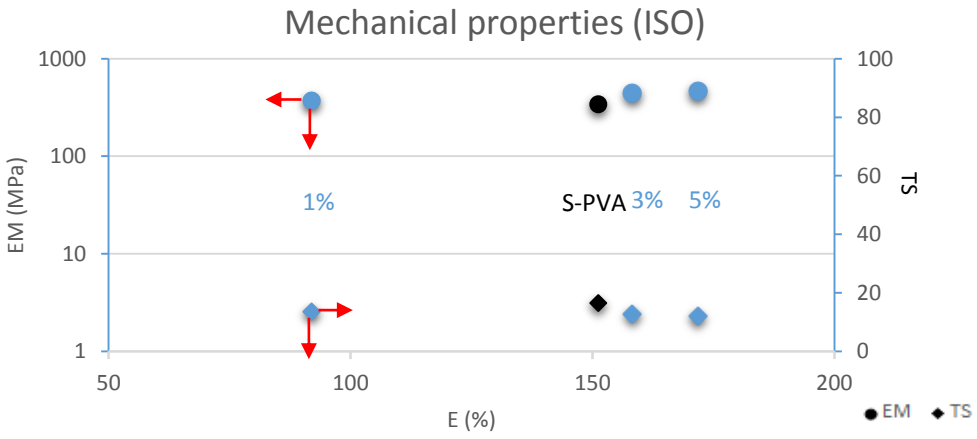

Figure 3. Elastic modulus (EM), tensile strength (TS) and percentage of elongation at break (E) of S-PVA (1:2 ratio) blend films (black) and composite films containing different amounts of cellulose nanocrystals (1, 3 and 5 % CNCs, blue) after 5 storage weeks.

In the second part of the thesis, the incorporation of natural active substances into biodegradable films as a current alternative to prevent food spoilage, extension of shelf-life, and maintenance of quality of foodstuff was evaluated. The objective was to add value to the S: PVA films by means of the incorporation of antimicrobial substances as neem oil, oregano essential oil and silver nanoparticles. S-PVA blend films with 2:1 ratio of the polymers was considered to fulfil the requirements established by FAO (2004) related with the use of PVA as food coating material.

The influence of the nature and concentration of the active antimicrobial substance on the physical and antimicrobial properties of the films, their disintegration and biodegradation behaviour was evaluated.

As concerns physical properties of the films both, barrier and mechanical properties were slightly affected by the incorporation of antimicrobial compound (Figure 4-a and 4-b). When using the higher antimicrobial oil content or a moderate amount of silver nanoparticles, a WVP was reduced. As shown Figure 4-b, the active compound incorporated into the S-PVA matrix also affected the mechanical behaviour of films. Films containing the highest oil concentrations showed the poorest mechanical response (the lowest tensile strength and deformability at break and EM) due to the presence of important structural discontinuities in the polymer network, reaching values of mechanical parameters close to pure S films.

The incorporation of the lowest oil concentrations and the presence of silver nanoparticles enhanced the films´ stretchability, while reduced rigidity and resistance to fracture, in line with a plasticizing effect associated to the interactions of these components with the polymer chains (Fabra *et al*., 2008; Rhim *et al*., 2013).

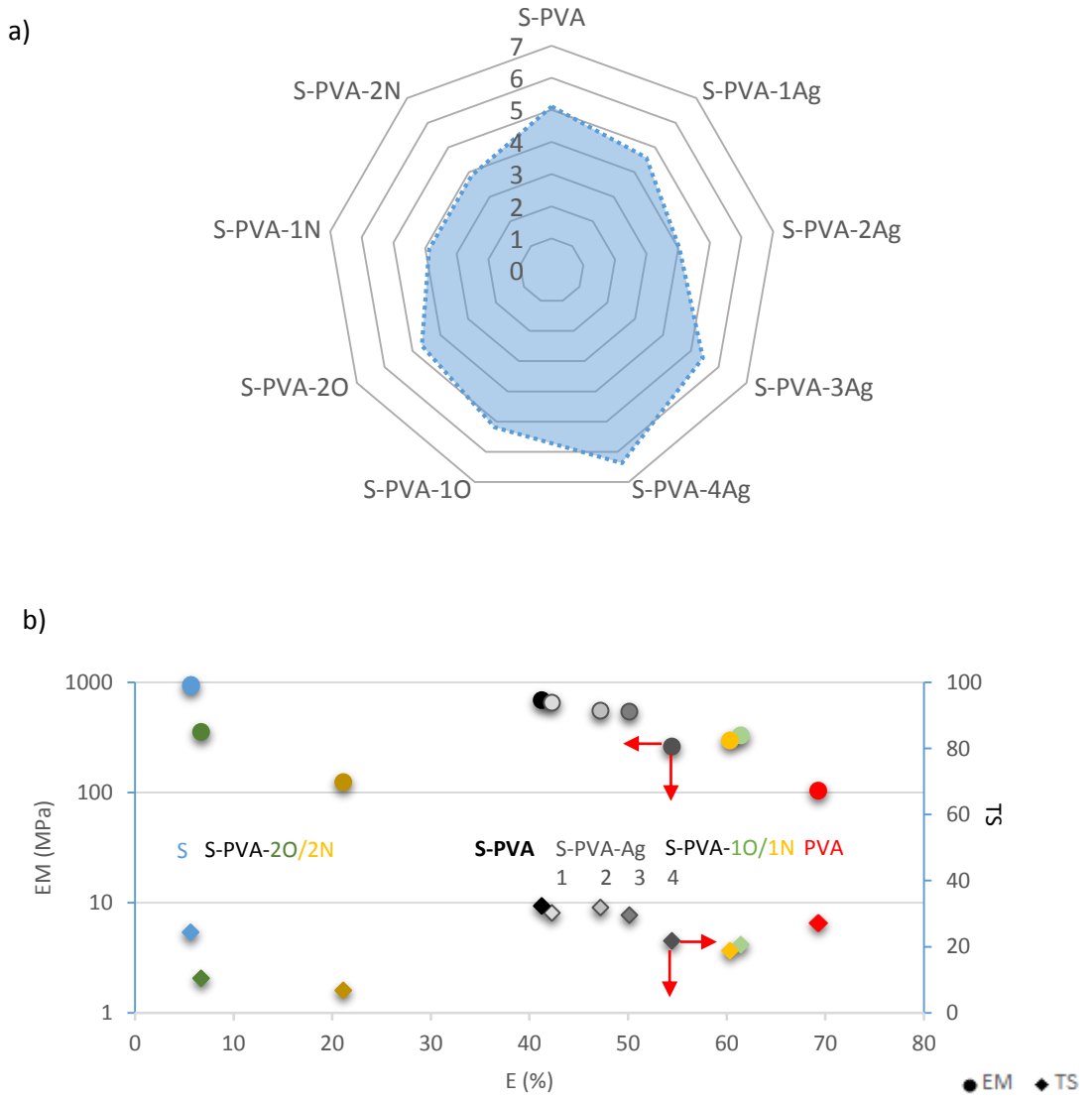

Figure 4. a) Water vapour permeability (WV) and b) mechanical properties, elastic modulus (EM), tensile strength (TS) and percentage of elongation (E), of pure starch and PVA films, S-PVA (2:1) blend films and composite films containing different amount of oregano essential oil (green points), neem oil (yellow points) and silver nanoparticles (grey points) at different concentration levels, after 5 storage weeks.

As concerns the antimicrobial effectiveness of the films, the inhibition of the microbial growth of *Aspergillus niger*, *Penicillium expansum*, *Listeria innocua* and *Escherichia coli* after 12 days in contact with the antimicrobial films is shown in Figure 5. As can be observed, the antimicrobial effectiveness (Log reduction with respect to the control film) depended on the type of the microorganism and the type and concentration of the active

substance. Films containing the highest oregano essential oil and silver concentrations exhibited a similar behaviour with a complete bactericidal and fungicidal activity against the tested microorganisms.

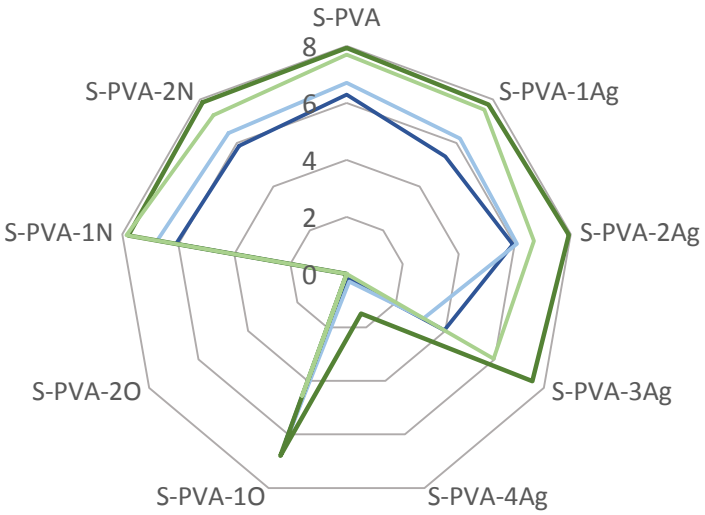

Figure 5. Microbial growth of *Aspergillus niger* (dark blue), *Penicillium expansum* (light blue), *Listeria innocua* (dark green) and *Escherichia coli* (light green) after 12 days in contact with S-PVA films containing or not different amounts of oregano essential oil (1 and 2 O), neem oil (1 and 2 N) and silver nanoparticles (1, 2, 3 and 4 AgNPs).

In Figure 6, the disintegration and biodegradability percentage values of the films after the composting period is summarized. As can be shown in the figure, there is not clear relationship between disintegration and biodegradability rates, for example, pure PVA did not disintegrate whereas a reasonable percentage of biodegradation was observed. The percentage of disintegration and biodegradability of S-PVA films reached intermediate values between those obtained for pure films (65 % and 100 %, respectively).

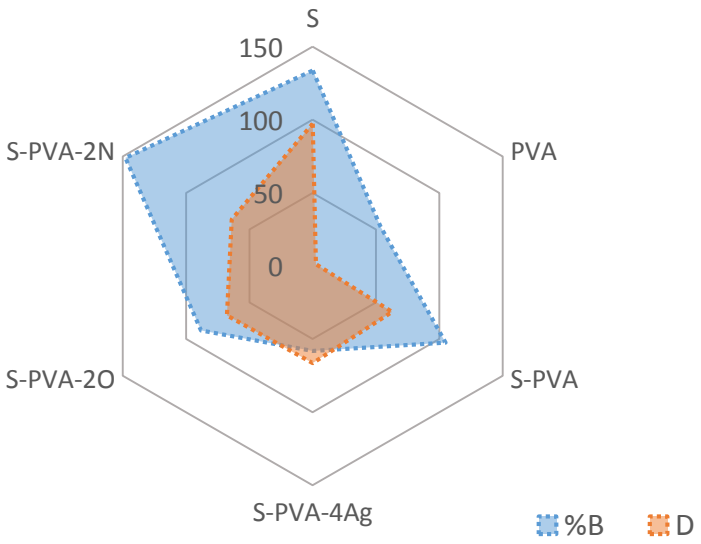

Figure 6. Disintegration (D) and biodegradation (B) percentage under composting controlled condition (57 ºC for 71 and 45 days for disintegration and biodegradation assay, respectively) of pure starch and PVA films, S-PVA (2:1) blend films and composite films containing the highest amount of oregano essential oil (2O), neem oil (2N) and silver nanoparticles (4AgNPs).

Whereas no differences were found on the disintegration behaviour of antimicrobial films with respect to the S-PVA blends, the biodegradation was slightly affected. The neem incorporation lead to easily biodegradable films and, on the contrary, films containing silver nanoparticles and oregano essential oil reached lower values. This suggests alterations in the compost inoculum in coherence with the antimicrobial effectiveness commented on above. In spite of these results, the biodegradation percentage of oil antimicrobial films reached values close to 90 % after 45 days of composting exposure, which is the minimum value recommended to consider the materials as biodegradables (Kale *et al*., 2007). Anyway, this recommended value was established for films submitted 90 days to the composting process. Only in films with the highest silver concentration, the biodegradation could be compromised, as they reached values of 60 % after 45 days under composting conditions. Experimental data after 90 days of composting are needed to complete the study. So, attending the obtained results,

it is possible to develop effective antimicrobial films in which the biodegradation process is not compromised.

Finally, a comparison on water vapour permeability and mechanical response between all biodegradable studied films and commercial LDPE, HDPE, PP and PET films has been done. Data of the commercial films used for comparisons were obtained from a commercial web page (Goodfellow). Figure 7 shows the water vapour permeability of both, the studied and commercial films. WVP values of commercial films ranged between 0.3 to 7.9 $gmmh^{-1}m^{-2}KPa^{-1}$, some of them exhibiting similar values to those of the developed blends. So, with a proper selection of the formulation, developed films could be used for different food packaging applications.

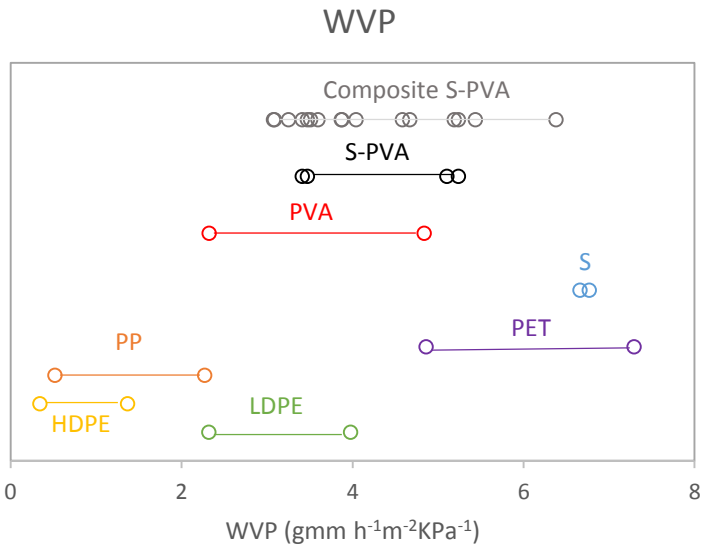

Figure 7. Range of water vapour permeability values for commercial PP, PET, LDPE and HDPE films and the biodegradable studied films.

In Figure 8, the mechanical response in terms of elastic modulus, tensile strength vs.: percentage of elongation can be observed for some commercial and developed biodegradable films. Most of the studied films behave similarly to the commercial ones in terms of the elastic modulus and percentage of elongation but exhibited lower

mechanical resistance (lower tensile strength values). Nevertheless, some blend films mechanically behave as commercial plastics taking into account their wide range of mechanical response.

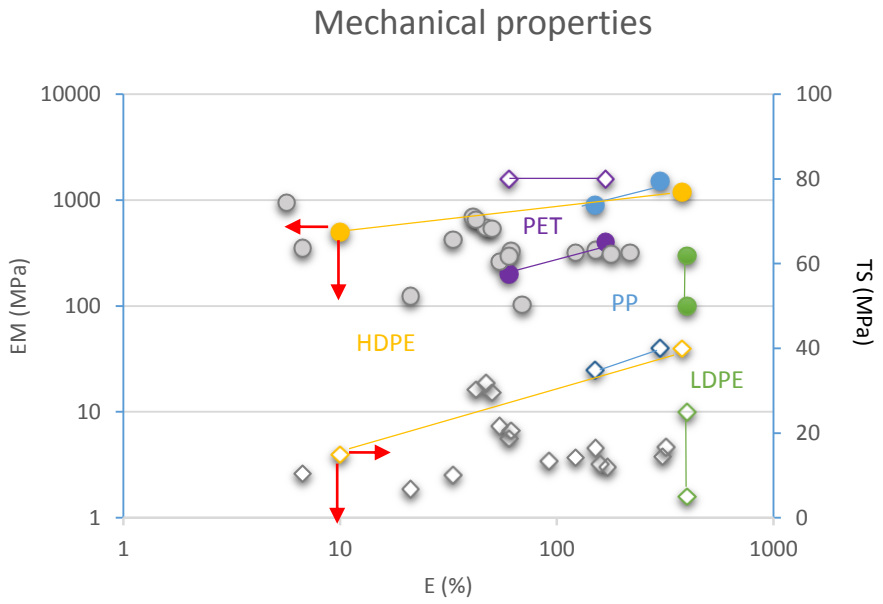

Figure 8. Mechanical properties: elastic modulus (EM) (full points) and tensile strength (TS) (empty points vs.: and percentage of elongation (E) for commercial PP (blue), PET (purple), LDPE (green) and HDPE (yellow) films and biodegradable studied films (grey).

In conclusion, the physical and functional properties of starch based films were significantly improved by blending the polymer with a proper amount of PVA and natural antimicrobials. This led not only to a biodegradable and active films, suitable as food packaging materials but also to antimicrobial coatings. The results were very promising, although the mechanical resistance of the developed films limits their use to some specific applications, for example for plastic bags, wraps or edible coatings and plastic containers for low-moisture food.

References

- Cano, A., Fortunati, E., Cháfer, M., Kenny, J. M., Chiralt, A., & González, C. (2015). Properties and ageing behaviour of pea starch films as affected by blend with poly(vinyl alcohol), *Food Hydrocolloid*, 48, 84-93.
- Fabra, M. J., Talens, P., & Chiralt, A. (2008). Tensile properties and water vapor permeability of sodium caseinate films containing oleic acid beeswax. *Journal of Food Engineering*, 85, 393-400.
- FAO (2004). Chemical and technical assessment of food additives (CTAs), 61 st JECFA (The Joint FAo/WHO Expertet Committee on Food Additives). Polyvinyl Alcohol (PVA).
- Kale, G., Kijchavengkul, T., Auras, R., Rubino, M., Selke, S. E., & Singh, S. P. (2007). Compostability of bioplastic packaging materials: an overview. Macromolecules Biosciece, 7, 255-277.
- Rhim, J. W., Wang, L. F., & Hong, S. I. (2013). Preparation and characterization of agar/silver nanoparticles composite films with antimicrobial activity. *Food Hydrocolloids*, 33, 327-335.
- http://www.goodfellow.com/E/Polyethylene-terephthalate.html (view on 07-25-2015).

V. Conclusions

- Properties of starch films were greatly affected by the amylose-amylopectin ratio. Amylose-rich films form amylose crystalline regions during film drying which give rise to stiffer, more resistant to fracture, but less stretchable films, with lower oxygen permeability and more water binding capacity. All the films develop throughout storage time, mainly due to water loss which leads to more compact matrices: stiffer, more resistant to fracture and less extensible, with lower oxygen permeability, but without changes in water vapour permeability. Rice bran with lower particle size ($D_{4,3}$= 57 μm) improved the elastic modulus of the films, especially in high amylose content films (pea starch), but reduced the film stretchability and worsened barrier properties, due to the enhancement of the water binding capacity of the films and the introduction of fibre discontinuities in the matrix. So, the hygroscopic character of the filler was a drawback to the improvement of the film properties. The reduction of the filler particle size is necessary to minimize the negative effect of large particles.

- The incorporation of PVA into pea starch blends implied the formation of interpenetrated networks of both incompatible polymers with the partial solubilisation of each one in the other polymer phase, depending on the polymer ratio. This has beneficial effects on the mechanical properties of the films, these becoming much more extensible and stable during storage. The water barrier properties were also improved by PVA blending at a S:PVA ratio of under 50 %, when films also reduced their water content as compared to the S films. The blends did not lead to a notable loss of transparency or gloss as compared to starch films and maintained their optical characteristics during storage, which did not occur in pure starch films. So, incorporating PVA to the S films at a ratio of around 1:1 represents a good strategy for improving the functionality of starch films without a notable increase in cost.

- The pea starch-PVA blend films showed phase separation and CNCs are distributed in both, starch rich phase and PVA rich phase. They are present as aggregates of

different sizes depending on their ratio in the film; the higher the ratio, the greater the aggregates, as deduced from the AFM analysis at surface level. No changes in water vapour permeability occurred due to the presence of CNCs, despite the increase in the hydrophilic nature of the films revealed by the overall migration values in polar and non-polar food simulants. Films with CNCs became slightly stiffer and more stretchable than control films, while crystallization of PVA was partially inhibited by CNC addition. The improvements conferred by CNCs in mechanical properties of pea starch-PVA blend films make them more adequate for food applications, especially for high fat foods, where overall migration values were very low.

- Composite films based on starch-PVA blends, containing potentially antimicrobial oils, exhibit antibacterial (*L. innocua* and *E. coli*) and antifungal (*A. niger* and *P. expansum*) properties when they contain oregano essential oil (O), whereas active neem oil did not impart these properties to the matrix. Antibacterial activity occurred at low O concentration (6.7 % in the dried matrix), while antifungal effect required higher doses of oil in the films. Incorporation of oils did not notably affect the water sorption capacity and water vapour barrier properties of S-PVA films, but reduced their transparency and gloss, especially at the highest concentration (22 % in the dried matrix). Mechanical performance of the S-PVA films was also modified by incorporation of oils but this was only relevant at the highest oil ratios. For the lowest oil concentration, mechanical properties of the S-PVA composites were in the range of those of some commercially available bags, becoming slightly more plasticized after 5 storage weeks. Among developed composite films, those containing 6.7 % of O exhibited the best physical properties, without significant differences with respect to the S-PVA matrix, while exhibit antibacterial activity. So, this represents a good alternative for food packaging applications.

- Starch-PVA based films embedding silver nanoparticles exhibited remarkable antibacterial activity against *Listeria innocua* and *Escherichia coli* and antifungal activity against *Aspergillus niger* and *Penicillium expansum,* which were significantly depended on the concentration of AgNPs in the film. This incorporation did not imply relevant changes in the physical properties of the films, except for their colour and transparency due to the fact that they were significantly turned to brown-yellowish and opaque, especially when the silver concentration in the films increased.

  The antimicrobial effectiveness of silver loaded films was limited by the release behaviour of silver from the films in contact with the agar plate, which seems to be reduced as compared to food simulants. Silver was completely delivered to aqueous simulants (including acidic one) within the firsts 60 minutes of contact. Nevertheless, when using a non-polar simulant, the release capacity of the films drastically decreased. The silver released into the food simulants widely exceeds the maximum permitted (60 mg/Kg simulant) in all cases, except when using the non-polar simulant (oleic acid). So, the use of the developed films as food packaging materials should be restricted to fat-rich foodstuff. Additional studies to optimize the release capacity of the films with moderate silver concentrations should be done, in order to reduce the burst release in contact with high aqueous environments and to comply with the current legislation.

- The incorporation of starch into PVA films improved significantly its disintegration and biodegradation behaviour in comparison with those with pure PVA. The addition of antimicrobial substances enhanced film disintegration, due to the introduction of structural discontinuities in the polymer network; the greater the antimicrobial content the more intense the effect. Likewise, antimicrobials affected the biodegradation profile of starch-PVA films, depending on the type of and concentration of the compounds. Neem and oregano essential oils slightly decreased the maximum

percentage of biodegradation without effect on the time needed to reach this maximum. However, silver species completely change the biodegradation profile of the films, slowing degradation rate and reducing the degradation extent, this suggesting a partial alteration of the compost inoculum. On the basis of the obtained results, it is possible to conclude that the used concentrations of antimicrobial oils did not apparently compromise degradation of active S-PVA film. Thus, these active compounds provided additional functional properties to the films at the same time that satisfy the new consumer demand for friendly environmental technologies. In the case of silver loaded films, silver concentrations low in the dried film are recommended to avoid serious alterations in the biodegradation process. In the future, in vivo eco-toxicity studies will be carried out in order to evaluate the possible negative biological effect exerted by the metabolites from the biodegradation of these antimicrobial films.

In conclusion, the physical and functional properties of starch based films were significantly improved by blending the polymer with a proper amount of PVA and natural antimicrobials. This led not only to a biodegradable and active films, suitable as food packaging materials but also to antimicrobial coatings. The results were very promising, although the mechanical resistance of the developed films limits their use to some specific applications, for example for plastic bags, wraps or edible coatings and plastic containers for low-moisture food.

On the other hand, chitosan-essential oil coatings prevent weight loss in semi-hard cheeses during ripening, while improving their microbial safety. As occurred in the samples treated with the antibiotic, lipolytic and proteolytic activity was reduced in coated cheeses, in line with the antimicrobial effect of essential oils and/or chitosan which, in turn, affected the enzymatic activity during ripening. An analysis of the impact of the essential oils on the cheese sensory attributes reveals that when three successive coating treatments were applied, the threshold for undesirable aroma perception of

essential oils was reached and the flavour and aroma of the cheeses were negatively affected as compared with the control. Nevertheless, cheeses that were double-coated with chitosan containing oregano oil were the best evaluated in terms of aroma and flavour, while the other attributes had values which were similar to those of the control. This coating treatment practically inhibited fungal growth during the ripening period. Therefore, the application of a double-coating based on chitosan and oregano essential oil is recommended, for cheeses where migration of compounds from essential oils are not objectionable.